DEVELOPMENT OF A SMART LIVESTOCK FARMING TOOL FOR IDENTIFYING ANIMAL GROWTH USING ARTIFICIAL INTELLIGENCE

A dissertation submitted by

Matthew J Tscharke, M Eng

For the Award of

Doctor of Philosophy

Engineering and Surveying • 2012

THE UNIVERSITY OF
SOUTHERN
QUEENSLAND

NCEA
NATIONAL CENTRE FOR ENGINEERING IN AGRICULTURE

THE UNIVERSITY OF
SOUTHERN
QUEENSLAND
AUSTRALIA

DEVELOPMENT OF A SMART LIVESTOCK FARMING TOOL FOR IDENTIFYING ANIMAL GROWTH USING ARTIFICIAL INTELLIGENCE

A Dissertation submitted by

Matthew J Tscharke, M Eng

For the Award of

Doctor of Philosophy

Engineering and Surveying • 2012

NCEA

NATIONAL CENTRE FOR ENGINEERING IN AGRICULTURE

ABSTRACT

Affordable tools with the ability to continuously monitor the growth rate of livestock animals are highly sought after by the livestock industries. This demand is driven by the potential for these tools to assist in improving animal welfare and production efficiency. In a rapidly growing population the demand for meat is escalating, especially in Asia, where the middle class is currently expanding. Meanwhile in the western world there is growing consumer concern surrounding animal husbandry, with certain organisations labelling some of the current husbandry practices cruel or sub-standard. The environmental impacts of livestock farming are also increasingly becoming scrutinised, pressuring researchers to find new methods to increase the efficiency of livestock nutrition, and improve health (disease prevention), reproductive and waste management practices. At the centre of these problems is the ever-changing individual animal as it continuously adapts to its surrounding environment and available resources.

Livestock growth is a fundamental measure which can be used for diagnostic purposes in these areas, therefore the main objective of this study was to develop a system to automatically determine the growth of individual and groups of livestock animals (pigs) using welfare friendly and non-invasive methods. A machine vision system was selected to undertake this weight estimation task, whereby pigs' body measurements are extracted from images and used to estimate their weight without physical interference.

Reviews prompted the development of a methodology to determine the weight-estimation equations as a function of not just the animals' body measurements but also their pose. Subsequently equations were generated from shapes that conformed closely to a specified reference template shape. Thus, to enhance precision during weight estimation the template shape was directly linked to the equation and pose validation aspects of the system. Filters were developed to provide recognition via the confirmation of the characteristic template shape and known body measurement and weight relationships. The shape filter ensured that 94% of weight estimates that passed through to output were within ±5 kg of the actual weight of the pig. Using the shape and limit filter in unison ensured that greater than 97% of the samples which passed had an weight estimate within ±5 kg of the actual weight of the pigs and 68% of the total number of samples were within ±2 kg. Statistical modelling was used to determine the importance of different body measurements in estimating weight. Subsequently a multivariate linear weight estimation equation was created to estimate pigs' weight using a stepwise selection of variables. The multivariate linear equation estimated 2% more sample weights within ±2 kg error and 3% less sample weights greater than ±5 kg error than the closest non-linear equation. Software was written to automatically recognise pigs inside the field of view (FOV) of the camera and to extract 16 body measurements from the pigs' body contours. Height was manually recorded from the back of a sample of pigs to determine its strength in weight estimation. Including the pig's height in the weight-estimation equation did improve predictive performance with a 7.34 % improvement in the number of samples estimated within ±2 kg of the pigs' actual weight compared to a multivariate equation without the height parameter. Although, this improvement was not significant enough to justify the additional practical development required to collect the height information automatically during the weight estimation process.

Both off-line simulation and on-farm experiments were undertaken using data collected from commercial facilities. During an off-line simulation, the shape and dimension filters were applied across a dataset containing over 20,000 frame samples of over 500 pigs. Gut fill was used as a guide to determine a practical error margin for measuring the weight of individual pigs across the course of a day. The machine vision system was found to operate within an acceptable error margin of 50 % of the gut fill according to the equation and average shape template used during off-line simulations. As on average pigs in the weight-range of 45 to 115 kg had their live body weight estimated to within 3.16 % and 2.20 % of their actual live body weight, respectively. For pigs less than 45 kg in weight the piGUI system operated, on average, to within 67% of the weight attributed to gut fill (between ±1.07 and ±1.49 kg error). During off-line simulations, the percentage mean-relative error obtained by the piGUI system was between 5.1 and 3.7% for pigs in the weaner to grower weight range (15 to 45 kg) and less than or equal to 2.5% for grower finisher pigs between 45 and 115 kg. Thus, on average, the system was able to estimate the pig's body mass with practical precision.

The system labelled 'piGUI' was installed in pens at commercial facilities which housed pigs in group-sizes of between 10 and 160 pigs. During testing, the system determined the average weight of groups of pigs on a daily basis, tracking the group's growth rate. In some trials, the pig's weights were also estimated along with the weight deviation of the group. During a 22 day trial period the system estimated the average weight of a group of finisher pigs within 2.1%, on the seven days when the actual group weight was recorded from an electronic scale. No information was passed between successive days by the system.

The diagnostic power of the piGUI system was also tested on-farm. A deflection away from the standard growth curve was recorded during two successive batches of grower pigs after reaching weights greater than ~45 kg. These growth deflections were believed to be caused by stress related directly or indirectly to temperature, as the summer temperatures reached over 38°C during these batches. The level of animal activity recorded by the system, the temperatures leading up to the deflection in growth and figures reported in literature support this theory.

The piGUI system was also tested to see whether it could estimate the weight of sows in their early stages of pregnancy and whether it could detect changes in the body measurements of individual sows before and after giving birth. A group of eleven sows between day 71 and day 82 of pregnancy had their group weight estimated to within 0.1 kg of their actual group weight. Eighty-two percent of their individual weights were estimated within a practical range of ±5 kg of their actual weight. The metric body measurements of two Large White × Landrace sows were also recovered by the vision system before and after giving birth. The widths and lengths of the sows' recorded by the vision system were consistent with those found in literature. Indicating that the device may be used to monitor sow weight and body morphology in future.

The developed device was also tested at various locations within the pen environment. Radio Frequency Identification (RFID) was integrated into the system to determine whether bias in group estimates could occur as a result of the sampling

region observed within the pen. A layout bias was discovered, caused by certain pigs visiting the FOV (containing the feeder) more frequently or for longer durations than others. Subsequently, feeding behaviour was determined using the RFID information collected and demand for the feeder was calculated for the pigs individually and as a group. The number of social interactions between pigs at the feeder was also determined, thus providing a method to identify social interaction and potentially the competitive nature of pigs automatically.

A comparative study was undertaken between a commercial system 'System-A' and the piGUI system. System-A failed to correctly estimate the group average weight of the finisher pigs in the trials. It was apparent that necessary conversions were not taking place within System-A's software to normalise the extracted body measurements to suit weight-estimation equation coefficients. It was found that, System-A's growth data would require a multiplication by a scalar factor to adjust the growth data to valid weight ranges. Code within the piGUI software performed the necessary conversions automatically during initialisation and was not burdened by this limitation. The piGUI system estimated the group average weight to within 2.1% on each of the seven days when the actual weight of the pigs were determined using the electronic scale. On these days, System-A reported group average weight estimates in excess of 16 kg error of the actual group average weight. It was clear that the distribution of weight data recorded daily by the piGUI system was far more concentrated around a mean estimate value than system-A.

The results of this PhD study demonstrate that the average weight of groups of pigs can be calculated with sufficient practical accuracy. The precision achieved during this study was better than reported in the literature and the precision of the system was also favourable compared to a commercially available system. Therefore the developed system can be used for practical purposes on commercial farms to determine the average weight and growth of groups of grower-finisher pigs.

CERTIFICATE OF DISSERTATION

This dissertation is submitted by Matthew J Tscharke (B. Eng - Mechanical) (Honours 2A) for the award of Doctor of Philosophy 2012 at the University of Southern Queensland, Faculty of Engineering and Surveying.

I certify that the ideas, experimental work, results, analyses, software and conclusions reported in this dissertation are entirely my own effort, except where otherwise acknowledged. I also certify that the work is original and has not been previously submitted for any other award, except where otherwise acknowledged.

ENDORSEMENT

Signature of Candidate	Date	Signature of Supervisor/s	Date
	11/7/12		11/7/12

PREFACE

This thesis presents PhD research carried out during the 2/2/09 to the 8/2/12 at both the University of South Australia and the National Centre for Engineering in Agriculture, University of Southern Queensland. Experiments were undertaken at three different commercial facilities during this time Rivalea, Corowa NSW, Riverhaven Enterprises, Morgan SA and PPPI, Roseworthy SA. Early development of this work was undertaken as part of a co-operative research centre program "Measuring feed intake and pig weights in commercial situations" under the subprogram "Practical and continuous measurement of feed intake and pig weight (2A-103)" which was funded by the PORK CRC and collaborative partners South Australian Research and Development Institute (SARDI) and Rivalea. This project was concluded in 2009, however, the PORK CRC continued funding the development of a system to estimate the weight of livestock (pigs) for the subsequent 3 years until early 2012.

This thesis presents the combined work from several published journal articles conference papers and submitted manuscripts to academic journals and industry organizations entitled;

1. **Tscharke, M.** & Banhazi, T. M. (2011). Review of methods to determine weight, size and composition of livestock from images. In *The Bi-annual Conference of the Australian Society of Engineering in Agriculture (SEAg 2011)*, 465-483. (Eds C. Saunders and T. Banhazi). Gold Coast, Australia: Australian Society of Engineering in Agriculture.

2. Banhazi, T. M. & **Tscharke, M**. (2011). Review of Image Analysis (IA) technologies for the Australian pig industry. Final report for APL. (54 Pages). Canberra, Australia

3. **Tscharke, M.** & Banhazi, T. M. (2011).Determining animal behaviour using machine vision and artificial intelligence. In *The Bi-annual Conference of the Australian Society of Engineering in Agriculture (SEAg 2011)*, 55 (Eds C. Saunders and T. Banhazi). Gold Coast, Australia: Australian Society of Engineering in Agriculture.

4. **Tscharke, M.** &Banhazi, T. M. (2011).Growth recorded automatically and continuously by a machine vision system for finisher pigs. In *The Bi-annual Conference of the Australian Society of Engineering in Agriculture (SEAg 2011)*, 454-464. (Eds C. Saunders and T. Banhazi). Gold Coast, Australia: Australian Society of Engineering in Agriculture.

5. Banhazi, T. M., **Tscharke, M.**, Ferdous, W. M., Saunders, C. &Lee, S.-H. (2011). Improved image analysis based system to reliably predict the live weight of pigs on farm: Preliminary results. *Australian Journal of Multi-disciplinary Engineering* 8 (2): 107-119.

6. Banhazi, T. M., **Tscharke, M.**, Ferdous, W. M., Saunders, C. &Lee, S.-H. (2009).Using image analysis and statistical modelling to achieve improved pig weight predictions. In *The Bi-annual Conference of the Australian Society*

of Engineering in Agriculture (SEAg 2009), p. CD publication. (Eds T. M. Banhazi and C. Saunders). Brisbane, Australia: Australian Society of Engineering in Agriculture.

7. Ferdous, W. **M., Tscharke**, M., Saunders, C., Lee, S.-H. &Banhazi, T. M. (2011).Digital image processing methods for the identification of pigs posture during weight estimation. In *5th European PLF Conference*, 422-432. Prague.

8. Banhazi, T. M., **Tscharke, M.**, Lewis, B. &Broek, D. (2009). Practical and continuous measurement of feed intake and pig weight. Final report for the PORK CRC. (108 pages). Adelaide, Australia.

9. Banhazi, T. M., Lehr, H., Black, J. L., Crabtree, H., Schofield, P., **Tscharke, M.** &Berckmans, D. (2011).Precision livestock farming: scientific concepts and commercial reality. In *ISAH conference proceedings*, p:137-143.

A patent has also been submitted:

Banhazi. T. and **Tscharke, M**. *Image analysis for size estimation*. **(Provisional patent application number: 61346310)**

During this time I attended four conferences on subjects directly related to this PhD study and made two oral and one poster presentation. During this PhD study I was also involved in the data collection and analysis of a sister component in the project (2A-103) involving the development of an apparatus to determine the dispensed weight of feed which is detailed in the following publication;

10. Banhazi, T. M., Lewis, B. **&Tscharke, M.** (2011). The development and commercialisation aspects of a practical feed intake measurement instrumentation to be used in livestock buildings. *Australian Journal of Multi-disciplinary Engineering* 8(2): 131-138.

AIMS AND THESIS OVERVIEW

The Chapters found in this thesis provide supporting evidence that relates to the general hypothesis of this PhD study which aims to determine whether the live weight of groups of livestock can be estimated reliably, efficiently, accurately and automatically using two dimensional image analysis techniques.

These chapters aim to answer the following key questions.

- What methodical approaches could be used to tackle this problem?
- What equipment could be considered in the system design?
- How can an animal be identified and tracked reliably within images?
- How accurately and reliably can an animal's weight be determined from its appearance in two dimensional images?

Two literature reviews form *Chapter 1* and *Chapter 2* of this thesis. Chapter 1 involves a comprehensive investigation into the methodologies other researchers have used to tackle the weight estimation problem. From all alternatives image analysis was found to be the most attractive technique to automate the weight estimation process. Subsequently studies using this technique are reviewed and the performance of a number of research based systems involving the weight estimation of several different livestock species is documented. The various modelling methods used to describe the relationship between weight and different body measurements are also determined. In the later part of Chapter 1 the image analysis techniques relevant to identifying and extracting semantic information of the animal out of the image for further analysis are presented, with specific attention given to techniques that complement the systems application environment. Review findings prompt further research related to the posture of the animal during weight estimation. As the animals posture has close ties to behavioural recognition Chapter 2 shifts focus slightly to review machine vision techniques and technologies used in the study of animal behaviour. No behavioural recognition software was available which could extract the required information of the animal out of images reliably. Consequently our own software development was warranted in this study. *Chapter 3* draws on the findings of Chapter 1 and Chapter 2 to identify weak points in existing methodologies for weight estimation using image analysis. Chapter 3 begins with a description of the task at hand, followed by a breakdown of the generic attributes of livestock-scales that provide insight into the various elements required in a livestock-scale design. Potential equipment and the working environment is then reviewed and equipment selection, configuration and installation positioning is justified. The individual software methods that were created in support of a scale's functioning elements are explained and illustrated. These methods identified a pig, its posture and determined its live weight from the body measurements extracted from images. For enhanced control, an integrated equation and shape builder was also formed. This builder configures and outputs a complementary shape and equation pair for weight estimation and shape validation during system operation. After integration, the combined segmentation, extraction, validation and estimation methods formed the 'piGUI' system which was used to test the hypothesis of the project. Simulated results of the performance of the piGUI system can be found at the end of Chapter 3. Various field trials were undertaken during system development. *Chapter 4* presents

the first on-farm trial undertaken at a small commercial research piggery housing finisher pigs. The ability of the piGUI system in estimating the live weight of finisher pigs was determined through validations performed both on-farm and off-line. In both validation trials the system estimated the average weight of groups of finisher pigs to practical levels. *Chapter 5* presents trail work undertaken to estimate the weight of grower pigs. Both off-line and on-farm trials at a large Australian commercial piggery were undertaken. In both trials the average weight of groups of grower pigs were estimated to practical levels by the system. The piGUI system's analytical power was also explored in this chapter, with hot summer temperatures appearing to adversely affect the activity level and growth of the grower pigs. In *Chapter 6* the system's ability to estimate the weight of sows' in early pregnancy is determined and the morphological changes recorded before and after giving birth are explored. The system estimated the average weight of a group of sows to practical levels. *Chapter 7* determined whether bias in group weight estimates could occur from certain pigs feeding more frequently and for longer durations than others. The system was installed above a feeder within a group of pigs' pen and Radio Frequency Identification (RFID) was integrated into the piGUI system to detect for any bias. Bias was identified from certain pig's body shapes and the sampling location of the device within the pen. *Chapter 8* contains a comparative study between two systems running in parallel; the piGUI system and an existing commercial image-based weighing system labelled 'System-A'. In *Chapter 9* conclusions are drawn from the results of each chapter and future improvements and directions are discussed. Technical detail can be found in the appendices when prompted.

ACKNOWLEDGEMENTS

Table of Contents

LIST OF FIGURES

XV

LIST OF TABLES

xix

Chapter 1

Review of Methods to Determine Weight, Size and Composition of Livestock from Images

Tscharke, M. & Banhazi, T. M. (2011). Review of methods to determine weight, size and composition of livestock from images. In *The Bi-annual Conference of the Australian Society of Engineering in Agriculture (SEAg 2011)*, 465-483. (Eds C. Saunders and T. Banhazi). Gold Coast, Australia: Australian Society of Engineering in Agriculture.

ABSTRACT

Technologies which can determine the weight and growth of livestock are reviewed. Limitations of the weighing task by these means are defined. Comparisons between the different techniques highlight the superiority of the non-contact vision-based method. Modelling techniques for weight estimation, size and composition are reviewed along with image segmentation and recognition methods. Conclusions identify that further work is required in regards to (i) estimating the weight and (ii) weight deviation of groups of livestock animals, (iii) estimating the weight of individual livestock animals and (iv) improving the design of livestock weighing methods to function in commercially realistic environments. Future direction also centres on enhancing automation, minimising invasive environmental control, maximising precision and repeatability during the recovery of body measurements and identifying and controlling the effect of any bias in weight estimation.

1.1 INTRODUCTION

In practice the most appropriate measures used to determine the nutritional requirements of livestock are live body weight and age relative to their surrounding environment (Whittemore and Schofield, 2000; National Research Council 1998). Therefore, to maintain and optimise the physical condition of livestock animals, feeding regimes must be structured based on a continuous assessment of their growth. Due to the promise of increased efficiency and subsequent production savings, mechanisms to facilitate control-loops of this nature have long been sought by livestock producers.

The largest cost involved in the production of pigs is feed cost which contributes to approximately 60-65% of the total production cost and accounts for 75-80% of the variable cost (Gillespie and Flanders, 2009). Consequently the way in which feed is managed can easily dictate the profitability of a farm. It is estimated that up to 10% of feed is wasted on-farms, with the majority of feed waste attributed to under or overfeeding the animals and poor feed management (Carr *et al.*, 2008). Overfeeding causes the animals to store the energy from the feed as fat, reducing the quality of the animals' carcass at slaughter and attracting penalties in the sale price. Underfeeding causes the animals to grow slowly, thus contributing to reduced production efficiency (Frost *et al.*, 1997; Korthals, 2001). A common behavioural tendency, which further contributes to over and under feeding, occurs when animals of varying weights are grouped together. In this scenario, smaller animals are more likely to be prevented from eating their appropriate ration by larger ones, which use competitive and sometimes aggressive actions to gain access to feeding spaces. It is, therefore, important to introduce management protocols that reduce the level of weight-variance found in groups of intensively housed pigs, as regular weight-based sorting of pigs into weight classes has proven to contribute to production savings via enhanced feed efficiency and product quality (Banhazi and Black, 2009; Korthals, 2001). Hence, by maintaining appropriate levels of feed for individual animals, savings can be made on feed, space, time, health and welfare.

However, before the correct ration can be allocated to a group of animals, their average weight must be determined. Conventionally, the weights of animals are not regularly recorded on individual and group-average bases. Furthermore, an unknown quantity of feed is generally fed to each animal (adlib feeding). Although this level of record keeping is suboptimal it is common practice as existing farm facilities, tools and resources are unable to acquire the required growth information in a cost effective manner (Frost *et al.*, 1997; White *et al.*, 2004; Black *et al.*, 2001).

Mechanical and electronic scales can be used to weigh the animals. However, a considerable amount of labour is required to move the animals through the scale, and to document and analyse the weight information recorded. It takes two farm workers approximately three to five minutes to weigh a heavy pig (Brandl and Jørgensen, 1996; Kollis *et al.*, 2007). Safety concerns also arise for the worker and animal during the manual handling process as injuries and stress may occur. Some studies show that up to 6% of reported livestock-related injuries to farm workers result from standing in close proximity to an animal (Criddle, 2001).

As a result of these practical limitations, the growth rate of successive batches of animals can only be approximated retrospectively based on the number of animals sent to market and the approximate feed consumed during the entire growth period. At this point it is too late to rectify growth problems experienced during the cycle. Hence, automating the growth measurement can help overcome these limitations.

During industrial processes objects are commonly inspected using a range of equipment and techniques in order to classify objects into different groups and to maintain certain standards such as those related to quality, safety and productivity. Often inspection processes are performed manually, and therefore rely on the intuition of skilled workers to manage the task or manage the machine undertaking the task. Long durations of concentration and interaction with a process can result in fatigue and drift from the task at hand. Subsequently errors in judgement can result. Therefore automating tasks of this nature can improve quality and productivity, as a machine can be managed to operate continuously and maintain a specific standard and reliable measurements.

Inspection tasks in the livestock industry focus on the animals and their activities. Arguably the most important inspection task within these industries is determining weight of the animal. For a number of reasons it is valuable to determine the weight of livestock as they grow. At the core of this reasoning is the livestock system's output; the condition of all of the animals the enterprise cares for. This measure is fundamental as it quantifies all inputs going into the production process. Subsequently the on-line feedback obtained during the process can be used to control and optimise management procedures (Kristensen, 2003; Parsons *et al.*, 2007). Growth is a prime indicator of animal condition, therefore successive weight measurements are required of both individual and groups of animals for quantification and optimisation to occur. Several suboptimal conditions can be identified and managed from measuring growth, such as (i) determining whether sorting is appropriate into smaller weight ranges to avoid competitive behaviour (ii) determining whether and when the animal is ready for market to maximise returns (Korthals, 2001), (iii) forecasting the likely requirements for feed, space (Petherick, 1983; Pastorelli *et al.*, 2006), and transport in the future, (iv) identifying weak or unwell animals by singling out animals which exhibit periods of poor growth (Maltz, 2010) and, (v) to monitor and analyse the animals' response to different feed and environmental scenarios to optimise and standardise the process (Green and Whittemore, 2005; Frost *et al.*, 1997; Doeschl-Wilson *et al.*, 2005; Whittemore and Schofield, 2000). Considerable value can be gained from refining these management processes (Niemi *et al.*, 2010). Due to the importance of these measures from a production and welfare perspective, techniques have been devised to assess the weight of livestock both on an individual and group basis. Progressively systems that measure the weight of livestock have evolved from inefficient, time-consuming and labour intensive methods to advanced methods designed to facilitate (i) higher levels of automation, (ii) increasingly accurate and semantic information and (iii) a safer working environment. Throughout this evolution several different types of scale have emerged which can be categorised into four different groups based on how they function during weight assessment. We identify which of these four weighing methods is best suited to undertake the weight estimation task and determine whether it can be improved and how. This statement forms the basis of the two main sections of this review.

The first section undertakes an in-depth look at the existing scales which can be used to automatically determine the weight of livestock automatically. The design considerations are presented, highlighting the positive and negative aspects of each of the weighing methods. The second section reviews research-based and commercially available machine vision systems that are used to estimate the weight of animals. The body measurements of several different species of animals are shown to have strong correlation to weight. The type and effectiveness of different equations in modelling weight using various body measurements are also determined. Segmentation and recognition techniques that are used to identify animals in images are also reviewed. Conclusions highlight the current limitations of this technology and provide insight into future research to enhance the method.

1.2   LIVESTOCK WEIGHING METHODS

Essentially four methods exist to obtain weight estimates of livestock animals automatically, (i) automated cage scales, (ii) foreleg and platform scales, (iii) vision-based scales and (iv) walk-through scales. The following section presents the function and obtainable precision of each of these methods.

An *automated cage scale* is comprised of a load cell or cells, a cage area and pneumatically, electronically or mechanically controlled gates. Sensors on the gates and inside the cage detect the presence of an animal and coordinate its confinement while weight assessment takes place. After a weight reading is obtained an adjacent set of gates are opened to release the animal. Advanced scales of this type can automatically sort animals by opening alternative release gates to direct an animal into an enclosure containing animals in its weight class (Weight Watcher™, Osborne Industries, Inc., Kansas, USA). In this process the weight of the animal is determined using load-cell(s) which are generally accurate to within ± 1 %. Some scale systems offer finer readings for different weight classes such as ± 100 g from 1 to 49 kg and ± 500 g from animals 50 to 150 kg. A single automatic cage scale can handle between 500 and 1500 animals depending on pen layout and the number of exit gates on the scale. If the scale can be transported easily it may be moved periodically between pens with the same layout to optimise the use of the scale and cater for additional groups of animals.

A *foreleg weigher* is alternative type of scale developed to obtain livestock live-weight continuously. A foreleg weigher consists of a small load-cell platform which makes a total weight estimate of the animal based on the weight of the animal's front legs. Foreleg weighers have been reported to estimate pig's weight to within 5% precision with 95% repeatability (Ramaekers *et al.*, 1995b). The weight 'state' of a pig using a foreleg weigher can be further refined using a Kalman filter (Williams *et al.*, 1996). Foreleg weighers have also been used to weigh cattle (Ramaekers *et al.*, 1995b). *Platform scales* measure the weight of the entire body of pigs using a load-cell device such as the ACCU-ARM® Weigh Race (Osborne Industries, Inc., Kansas, USA). A platform scale requires the animal to remain stationary during assessment. Platform type scales have also been used to automatically weigh poultry (Turner *et al.*, 1984b; Lott *et al.*, 1982) and cattle.

The weight of an animal can also be estimated based on the animal's body measurements as measured directly from the body of the animal using a flexible measuring tape called a tailors rule. In this weight estimation process a stockperson uses the animal's body measurements as variable inputs into a weight-estimation equation. From this concept steps have been taken to minimise the labour requirement for weight estimation based on the body measurements of the animal. An alternative and superior method based on the same concept is to extract the body measurements of the animals from video frames and use them to estimate the live weight of animals without making physical contact. We term this technique a *vision-based scale*. This method has proven to estimate the live weight of certain livestock animals to within 5% of their actual weight (Schofield, 1990). The assessment process requires the animal and its body measurements to be identified within the image frame so that the body measurements can be used in a weight-estimation equation to form a weight estimate. Minagawa *et al.* (2003) reported average mean error of 2.1% for individual pigs and 1.3% for group mean estimates using the pig's height and area as determined from images. Commercial systems for image-based weighing of pigs also exist and some report a maximum deviation of 3% for the group average weights of finishing pigs (Fancom; Hoelscher&Leuschner; InnoventTechnology).

Walk through scales estimate the animal's body weight while the animal is in motion (dynamically). This type of scale records the unique weight-signal over time which results from the animal's weight distribution across its feet as it moves across the load-cell platform of the scale. This signal-pattern is then used to identify the walking motion of a single animal, after which, an assessment of the relative load-cell reading(s) can take place to determine the weight (Cveticanin, 2003). An example of a walk-through weigher for dairy cows can be found in Filby *et al.* (1979) and for cattle in Martin *et al.* (1967). An alternative form of walkthrough dynamic scale was presented by Wang *et al.* (2008) who used a machine vision system to determine the live weight of pigs as they walked through a raceway. Several body measurements were extracted from video frames and then used in a weight-estimation equation to make an assessment of the pig's weight.

1.2.1 Adding Functionality and Value to Weighing Methods

Four different methods of automatic weighing have been presented above. Below is a summary of the advantages, disadvantages and additional practical potential of these methods.

A major benefit of automated cage scales is that they can be used to sort animals into enclosures of different weight ranges. There are several benefits of sorting animals into different weight classes, these include facilitating target diets for specific weight ranges, minimising tail biting and fighting and consequently mortality, identifying the number of market ready animals and adjusting feed accordingly. These characteristics of sorting devices can therefore lead to improvements in animal growth, feed management and welfare as well as feed and labour savings. An alternative function of a platform scale may be to determine whether the force distribution exerted on the weigh platform indicates the animal is protecting an injured leg.

Identification of weight from walkthrough scales relies on the identification of unique force-time patterns attributed to the animal walking over the load-cell platform. Correct recognition of a walking sequence pattern can effectively filter out other patterns such as those attributed to crowding on the scale or when there is only a small time between successive animals walking over the scale (Cveticanin, 2003). However notably, finer detail in walking-sequence patterns reveal the characteristic force-time patterns useful in the classification of gait (StepMetrix™, BouMatic, Madison, Wisconsin, USA). In addition, if points of impact between the animal and the platform can be identified on the horizontal plane then when using larger platforms multiple animals have potential to be classified and assessed for their weight.

Vision systems also present a range of potential functionality. As the system is appearance-based, additional code can be integrated into the system for the detection of certain behaviours such as fighting (Šustr et al., 2001) or tracking the movement of animals around their enclosure (Lind et al., 2005; McFarlane and Schofield, 1995). Vision-based scales automatically record various body measurements of the animals' bodies as they grow; alternative methods are unable to achieve this. Output from vision-based scales have been used to provide grounds for sorting animals which are similar to the tasks performed by automated cage-type scales (Hoelscher&Leuschner). The vision-based method also has the greatest future potential to contribute to individual animal identification due to advancements in the techniques for vision-based biometric-identification. The level of detail and semantic information is also likely to improve with the development of 3D vision systems capable of recording accurate reconstruction of the animal's body in 3D space (Wu et al., 2004). It has also been proposed that the identification of gender breed and body composition is attainable using vision-based methods based on the extraction of certain body measurements (White et al., 2004; Doeschl-Wilson et al., 2005; Fisher et al., 2003). An extension is using the system for body condition scoring (Bewley et al., 2008). The use of different vision-based sensors can also introduce additional functionality into the system. Although it is not feasible at this time for commercial applications, thermal imaging has potential to help determine an animal's temperament, thermal comfort and health as well as helping to simplify the segmentation process, all while maintaining the functionally attributed to image sensors that sense in RGB colour except appearance (Stajnko et al., 2008). Two dimensional vision systems also have the capability of viewing a large area and may be used to track individual animal movements and social interactions in future.

Determining the measurement equipment that is best suited for automatic weight estimation is governed by factors such as cost, functionality, practicality and accuracy. It is important for the cost of the device to remain low to help persuade farmers to adopt and justify technological advancements. In addition it is also necessary for the sensor to work in harsh environmental conditions where both moisture and dust are often unavoidable. These environmental considerations also provide additional reasoning to keep the equipment inexpensive in case damage occurs and a replacement is required. The sensor must also be accurate enough to ensure that the information gained is practical and comparable to measurements obtained using conventional methods (White et al., 2004).

The characteristics of the current methods used to automatically estimate livestock group-weight are summarised in Table 1. The vision-based weighing method is the preferred method given the very low level of contact between the scale, the operator and the animal, the very low level of additional infrastructure required for the scale to function and the very low safety risk posed towards animals and workers while the scale is in operation.

Table 1: Summary of Scale Selection Characteristics

Weigh Method	Level of Operator/Animal Contact	Level of Scale/Animal Contact	Level of Infrastructure Required	Safety Risk
Manual	VH[*]	VH	L	VH
Foreleg	VL	ML	L	L
Platform	VL	H	MH	L
Automatic Cage	ML	VH	VH	H
Vision	VL	VL	VL	VL
Walkthrough	L	H	H	ML
Walkthrough Vision	L	L	MH	L

[*] VL = very low, L = low, ML = medium to low, MH = medium to high, H = high, VH = very high

Level of Operator/Animal Contact refers to the requirement of stockpersons in the process. Notably the manual weigh method requires a very high level of animal handling skill. The walkthrough method would require some animal handling (low) to either train or persuade the animals to move through the raceway. The automated scale has been assigned a medium to low (ML) level due to the additional challenges involved in training the animals' to overcome any fear related to entering a confined area with moving parts.

Level of Scale/Animal Contact refers to the requirement for the scale to make direct contact with the animal. The most extreme cases are the automatic scale and manual method which require some form of confinement of the animal. An automated scale's gates are also often in direct contact with the animals. The raceway in the walkthrough type scales both encloses the animal and makes contact with the animal.

Level of Infrastructure Required refers to the level of additional infrastructure in direct contact with the animals which is required for the system to function correctly to obtain growth information. The vision system performs best in this category as it can be fixed to the roof of the building and therefore can make weight assessments without ever having direct with the animal and its environment. Depending on the level of co-operation of the animal, manual weight assessment method may be achieved without confining the animals, however, in general some confinement would be necessary of operator safety and to obtain the measurements in a timely manner. Walk through weighers and automated scales require fencing to channel the animals through the scale area adding to system cost and complexity.

Safety Risk refers to a combination of the risk of stress or injury on the operator or the animals during the weigh process. Essentially this measure is based on the Level of Operator/Animal Contact, Level of Scale/Animal Contact and Level of Infrastructure Required.

1.3   MACHINE VISION SYSTEMS FOR WEIGHT ESTIMATION

This following section covers the image analysis techniques and systems used in agricultural applications for weight estimation. In such a system a camera is

responsible for acquiring images of the animal and the software on a computer is responsible for controlling the acquisition, storage and analysis of image frames using a routine set of instructions. These instructions automatically recognise the animal within the image and extract one or more of the animal's body measurements to use as a predictor of weight in a weight-estimation equation.

1.3.1 Livestock Body Measurements and Their Correlation to Weight

The information gained from the study of vision-based and manual-based weight estimation methods (using a tailors rule) exemplify the underlying correlation between weight estimation and physical linear body measurements of the animal. These body measurements have been obtained manually (directly from the animal), estimated indirectly by machine vision systems in 2D (Schofield, 1990; Schofield *et al.*, 1999), 3D perspective (such as using a 2D side and 2D top view image of the animal) (Kmet *et al.*, 2000) and 3D stereo configurations (Wu *et al.*, 2004) to approximate the weight of several different species of livestock.

The body measurements have been extracted from images by either (i) using a printout image containing a reference object of known body measurements on the animal and taking the measurements manually (Phillips and Dawson, 1936), (ii) implementing an operator controlled process where instructions are imposed on a computer to control the identification of the animal's body and locate and extract the respective body measurements (Arias *et al.*, 2004; Minagawa *et al.*, 2003) and finally (iii) a machine controlled process where instructions are automatically imposed on a computer to control the identification of the animal's body and locate and extract the respective body measurements to estimate the growth of animals (Schofield *et al.*, 1999; Parsons *et al.*, 2007; Green *et al.*, 2003). These three extraction methods represent manual, semiautomatic and completely automatic processes.

The concept of using an animal's body measurements to estimate its weight has been applied to several livestock animals including cattle, buffalo, chickens, pigs, sheep, fish, horses and rabbits. The relationship extends to wildlife such as elephants (Hile *et al.*, 1997).

In cattle and buffalo these extracted body measurements include heart girth, wither height, hip width, hip height and body length. Other measures include age and condition related information such as the parity of the animal. In a study based on the direct manual-extraction of body measurements of Holstein Heifers, Heinrichs *et al.* (1992) determined that the highest coefficient of determination was between the heart girth and weight. Heart girth, wither height, hip width and body length also demonstrated high correlation $R^2 > 0.95$. Similarly a study of Holstein calves found that heart girth was also the highest correlating body measurement to weight. However, correlations were less pronounced between the different age groups studied R^2 0.72-0.77 (Wilson *et al.*, 1997). Dairy cows have been assessed for their weight based on their body measurements and parity with R^2 in the range of 0.80 to 0.89 (Enevoldsen and Kristensen, 1997). A coefficient of determination of 0.94 was found for Simmental heifers using the heart girth (Willeke and Dursch, 2002). There have also been several attempts to extract livestock body measurements using an indirect vision-based approach from different perspective views of the animal. Kmet *et al.* (2000) used three views (top side and end) of Simmental cattle to determine the

shoulder width, lumbar protuberance in the body width, rear thy area and the top-view body area. The R^2 relationship between weight and the various body measurements obtained was from 0.80-0.94. Different age classes of Simmental cattle have also been assessed for their wither height and hip height using thermal imaging techniques. Hip height (R^2 0.46-0.74) performed slightly better than wither height (R^2 0.43-0.66) across the growth period (Stajnko *et al.*, 2008). Minagawa (1994) used a stereo imaging method to recover the side surface of the Japanese shorthorn cattle to estimate their weight. Correlation coefficients for the five animals studied were r = 0.88, 0.81, 0.89 for weight estimates based on surface area, volume and projected area. External body measurements have been used to determine the weight of buffalo (Manik *et al.*, 1981; del Pilar *et al.*, 2002). The side-view surface area of Mediterranean buffalos have also proven to correlate well to weight with r = 0.90 using a light projection method and an image processing technique (Negretti *et al.*, 2007a). A vision system is also in development to determine the live weight and condition scoring of buffalo. Measured and modelled parameters include the animals wither height, rump height, body height, trunk, rump length and surface areas of the lateral profile (side view), of the profile of the hindquarters (end view) and of the lateral iliac tuberosity. The best performing parameters in respect to weight were the side view R^2 0.94 and end view R^2 0.92. Using these two parameters in a multiple regression equation obtained slightly better coefficient of determination R^2 0.96 (Negretti *et al.*, 2008).

Computer-assisted image analysis has also been used to quantify daily growth rates of broiler chickens. Weight based on the perimeter and area as viewed from above was estimated to 15 % and 10 % respectively (standard deviation of the residuals) De Wet *et al.* (2003). Similarly other studies report errors in the weight estimates of broilers between 0.04 and 16.47 % up to 35 days of age using image based techniques for the estimation Mollah *et al.* (2010).

The body measurements of fish have also been used to estimate their mass. Beddow and Ross (1996) estimate the mass of salmon to within ± 2 % error using manual measuring techniques. Image based estimation methods have been applied to blue fin tuna in commercial pens (Costa *et al.*, 2009). The total number of fish was estimated using a dual camera technique to 2.2 % and their mass was found to be within 50.6 % of the actual total weight which was an improvement on conventional methods which had 353.9 % error in estimates and the estimates provided by divers during the same study. Lines *et al.* (2001) found that the linear body measurements of salmon could be used to estimate their mass with a mean error of less than 0.5 % and these linear body measurements could be extracted automatically from stereo images with a mean error of less than 10 %. The mean mass measurement error was 18 % based on an off-line analysis of 60 images of 17 fish.

A large amount of work has been undertaken to estimate the live weight of pigs based on their body measurements. One of the first studies undertaken to determine the live weight of pigs from images involved a comparison between manually extracted body measurements and those obtained from images. The body measurements extracted from the images in the study were found to be very close to those extracted manually, with eight of the 11 measurements manually taken from the images measuring less than or equal to 1cm from the measure obtained from the surface of the animal (Phillips and Dawson, 1936). Similar findings between image-

based and physically taken measurements using conventional tools on different species of livestock can be found in Negretti and Bianconi (2004). Yeo and Smith (1977) and Pope and Moore (2002) used a girth measurement as a parameter to estimate the weight of sows to regulate their feed consumption. Vision-based systems have also been developed to obtain the body measurements of pigs non-invasively. Building on earlier research Schofield (1990) demonstrated that the live weight of pigs could be estimated from 2D images using the aid of a computer. This dramatically increased the efficiency of the method. The weight of three pigs weighing 75 kg, 52 kg and 30 kg were estimated using single images of each animal. The relative error in weight estimation was between 6.2 and 15.4%. These errors were minimised by averaging the estimates of several frames of each animal, resulting in a reduction in the relative error to between 2.5 and 6.3%. On average it was stated that using image analysis the weight of pigs could be estimated to within 5%. Later Minagawa and Ichikawa (1994) reported the correlation between the weight of two different breeds of pigs and several of their 2D image-extracted body measurements. The weights of 33 pigs weighing between 7 and 120 kg were estimated based on the average body measurements derived from 5 images of the animal as viewed from above. An image was only included in the analysis if the animal was standing with its body straight and its head was facing forward. The highest correlating body measurement was the central projected area with a coefficient of determination of $R^2 = 0.999$ and standard error of ± 0.9 kg followed by the orthogonal area $R^2 = 0.998$ (± 1.7 kg), length $R^2 = 0.998$ (± 4.4 kg) and mean width $R^2 = 0.988$ (± 4.0 kg). A study involving a larger group of pigs was undertaken by Brandl and Jørgensen (1996) which manually recorded the body measurements of 416 pigs (25 to 100 kg) of six different cross breeds from 2D images to determine their correlation to the weight of the animal. The study findings indicated that the body surface area as viewed from above was the strongest predictor of weight with $R^2 = 0.98$. Notably compared to Minagawa's study there was a difference in the way in which the area measurement was derived, as pilot testing had indicated that the head of the pig introduced errors into the area measurement from its motion. Consequently a trim above the front shoulder was performed and as thresholding proved to be sensitive to image disturbances the total area was derived from a manual trace of the pig's body (Brandl and Jørgensen, 1996). These studies proved that the body measurements of a pig (as perceived in images) could be manually and in some cases semi automatically extracted to form a basis of weight estimation. However, for practical purposes software and hardware developments were required to facilitate the automatic extraction and weight-analysis of these body measurements from streaming video (Brandl and Jørgensen, 1996; Minagawa and Ichikawa, 1994; Schofield, 1990). In effect these developments would generate a system which could perform online and continuous weight assessment without the need for physical contact with the animal and any manual labour determining the body measurements. There was a large amount of additional work required to facilitate this level of automation which was further limited by the technology of the day. Later Schofield et al. (1999) reported the development of a system at the Silsoe Research Institute (Wrest Park, Silsoe, Bedford, UK) which was able to provide group-weight assessment of pigs continuously without operator involvement. The system monitored the growth of three genetic strains of pigs to within 5% of their body weight for a total of 47 days as they grew from 47 to 90 kg. Further information on the system's performance in determining growth can be found in Marchant et al. (1999) and White et al. (2003). More recently Yang and Teng (2008) have

determined the live weight of pigs to 3.2% (mean relative area) using the side and top view of the pig from 2D images, although the level of automation is not clearly explained. A recent investigation into manually obtained measurements (physically and from 2D images) can be found in Zaragoza (2009). Preliminarily studies have also been undertaken to assess sheep for their live weight using vision-based methods (Burke *et al.*, 2004; Schofield *et al.*, 2005) and the live weight of lambs (Lambe *et al.*, 2008b). The concept has also been extended to rabbits and horses (Negretti *et al.*, 2007b).

1.3.2   Modelling Techniques to Estimate the Weight of Animals

Modelling methods used to estimate body weight include linear, power, quadratic, cubic, spline and artificial neural networks (ANNs). These methods are based on either single independent or multiple variables. Heinrichs *et al.* (1992) used several regression methods including linear quadratic and cubic effects on single independent variables. When considering multiple traits as independent variables the correlation between estimated and actual weights increased. Adding a second body measurement to the highest correlating measurement (heart girth of Holstein Heifers) increased the linear, quadratic, and cubic effects from R^2 0.95-0 .99. Similar findings were found when multiple regression modelling was applied to Holstein Calves (Wilson *et al.*, 1997) and dairy cows (Enevoldsen and Kristensen, 1997). Minagawa (1994) found the projected area, surface area and volume were best related to the side view of Japanese short horn cattle using a power function. Nonlinear modelling methods such as artificial neural networks (ANNs) have been used to estimate the weight of blue-fin tuna (Costa *et al.*, 2009), pigs (Wang *et al.*, 2008) and cattle (Arias *et al.*, 2004). In addition to further refine models, certain growth periods can been generalised by their own estimation equations Stajnko *et al.* (2008).

1.3.3   Body Composition, Scoring and Classification

The conventional method for determining the carcass composition of livestock is using ultrasound. McLaren *et al.* (1989) gives an account of the ability to forecast the carcass composition of pigs using ultrasonic measurement of back fat and loin eye area, to improve genetic selection or optimise selections for market. Correlations have been discovered between different body measurements and the fat and muscle content of the animal (composition). Ermias and Rege (2003) used various tail-based measures to determine the body fat of flat-tailed sheep for genetic selection. Vision-based techniques have also been used in a similar manner to determine the carcass characteristics of lambs (Lambe *et al.*, 2008a; Lambe *et al.*, 2009). The degree of fattening in buffalo has been estimated from body measurements extracted from images with a coefficient of determination of $R^2 = 0.85$ (Negretti *et al.*, 2008). An estimation of the value of various slaughter characteristics has also been achieved using vision-based methods on Simmental bulls (Kmet *et al.*, 2000). Cold carcass weight, live body weight, weight of meat in carcass and weight of meat in valuable cuts have obtained R^2 values of 0.7, 0.75, 0.65 and 0.64 respectively for the best performing body measurements extracted from images of bulls (Kmet *et al.*, 2000). Doeschl-Wilson *et al.* (2005) found that the measurements obtained from images of pigs "were useful in the estimation of muscle size, carcass conformation and composition" (Doeschl-Wilson *et al.*, 2005, p229). Wu *et al.* (2004), Tillett *et al.* (2004) and McFarlane *et al.* (2007) use a stereoscopic vision system consisting of

three pairs of cameras to recover the surface representation of a pig's body and determine any morphological body changes in respect to different diets. There is also potential to use the measurements obtained from vision-based techniques for body condition scoring (Bewley *et al.*, 2008), classification between different livestock species (Dunn *et al.*, 2003) and classification between genders and breeds of livestock (White *et al.*, 2004).

This research demonstrates the potential that machine vision systems have as an online condition assessment tool for livestock, as the body measurements they extract can be used to give an indication of an animal's value, body composition and health through growth variations and morphological changes in their body.

1.4   IDENTIFYING ANIMALS IN IMAGES

To identify an animal within an image, a method is required to determine image pixel values which represent the animal's appearance.

1.4.1   Segmentation Techniques

Essentially the segmentation method used can be categorised into a scene, shape, appearance or motion based technique. These techniques may also relate information between frames in a temporal manner. The following section presents the various techniques that have been used to separate the animal from the rest of the image within these categories.

Scene based segmentation can be an efficient and effective way of segmenting the target object from the background. Scene based techniques work on the principal that a background image is constantly maintained to maximise the difference between the background and any animal-object. This technique works under the assumption that if the animal-object is not part of the background then removing the background should only leave the animal-object in the image.

Scene based techniques can be broken into subcategories of background representation, classification, background updating and background initialisation (Moeslund *et al.*, 2006).

Background representation is a method where the image intensity, spatial properties and often temporal information are used to derive a representative template of the background (Elgammal *et al.*, 2002). An example of a basic background representation is chroma-keying which involves manipulation of the image scene environment (lighting and homogeneous background) such that the animal-object can be easily segmented due to the enhanced contrast between it and the known background colour. Dunn *et al.* (2003) used a chroma-keying technique to segment different species of animals from a blue background. An image can also be transformed into an alternate colour space to retain representation of different background features in the image such as shadows (Cucchiara *et al.*, 2001; Schreer *et al.*, 2002). Background classification involves the grouping of the data after segmentation takes place to eliminate the occurrence of false positives. False positives can occur during the subtraction process and are caused by a number of different factors such as large light changes (shadows), non-target objects or changes

to the cameras field of view (FOV) or scene. In a background initialisation method the background model is learned during an initialisation phase and can be considered static in that it does not change once initialised.

Background updating includes the background data in subsequent frames as a weighted combination of various measures. The simplest updating method is to store a template image of the background (updating the background) when no target object is present and then subtract this template image from future frames which contain the animal-object, leaving the animal-object as the difference. Kollis *et al.* (2007) use a similar updating method to determine an adaptive threshold value.

Mixture of Gaussians (MoG) or Gaussian Mixture Models (GMM) are reported as a robust and reliable technique used to segment a target object from the background in outdoor scenes without requiring any physical alteration to the scene or objects within the scene. In this segmentation technique every pixel has its feature information recorded across an image sequence (temporal information of each pixel is maintained). The various changes in the pixels are stored as one of K different features related to a pixel. Each K feature is represented by its own distribution and cluster (the modes of the background scene). The feature distributions are continuously updated online in an adaptive mixture model. The distributions are used to determine whether a pixel belongs to the background (or not) based on the incident pixels value in relation to the feature distributions. For example, the feature distribution is updated if a pixel is within 2.5 deviations from the distribution mean. If the pixel is not within the range of any of the distributions in the adaptive mixture model then the least significant distribution is overridden with the new distribution. Only two parameters were used in the process, alpha (α) a learning constant and T which is the assumed proportion of the data related to the background (Stauffer and Grimson, 1999). Zivkovic (2004) improves the Gaussian mixture model by creating an algorithm that automatically determines the number of distributions required to represent each pixel which results in a time saving and improved segmentation.

While mixtures of Gaussians are effective at maintaining appropriate segmentation in slowly changing scenes they have been known to have difficulty in identifying textures related to backgrounds that frequently change within the image scene. In order to minimise the effect of these characteristic variances during segmentation, various spatial-temporal techniques have been investigated. Zhong and Sclaroff (2003) devised a technique to segment objects away from dynamic textures or backgrounds which have repetitive patterns; a ship in waves for example. In their proposed system Kalman filter estimates the appearance of the dynamic texture and the foreground objects region and an autoregressive moving average model (ARMA) is used to segment the time varying background iteratively.

One well known *motion based* technique in the area of image processing is optical flow. This temporal technique determines the velocity of any movement between two or more images as a result of changes in the images' light patterns. The motion can be caused by a moving object or by movement of the camera itself. Different objects can be segmented based on their motion characteristics, as the rate of change of the objects direction, position and speed help with the identification of the object or its location within an image (Horn and Schunck, 1981). Several different optical flow methods have been developed, a quantitative comparison of nine techniques can be

found in Barron *et al.* (1994). One of the major benefits of using optical flow as a basis for segmenting and identifying objects is that small movements which might be hard to perceive in two body measurements can be identified; such as a ball rotating about its axis. In addition, the objects motion and its motion history can help with identification and tracking if the object becomes partially occluded by another object. However, the exact shape of the object may be hard to extract using this technique as the entire body may not always be in motion.

An *Active contour is a shape based* technique (also known as a snake) which involves morphologically displacing a contour (enclosed collection of points) overtime to follow a 2D shape contour in an image. The contour is active in the sense that it moves as it converges to the minimum energy, created by the magnitude of surrounding external and internal edge gradients located within the image search space that form the contour. Although active contours in their most basic form can successfully derive the correct shape of a deformable object and track it between successive frames they have the limitation of not knowing whether their location is correct or how they are deforming is correct as they have no inbuilt intelligence. They can easily drift and produce errors as a result. To prevent drift from occurring, information is required to validate the contour as the target shape. Point distribution models (PDM) and Finite Element Models (FEM) have been used individually and collectively to obtain more reliable information to form a basis for the active contours next move (Cootes and Taylor, 1995). Point distribution models determine the correct location of a point on a contour using a statistical based approach on a network of surrounding pixels. The PDM is trained in an off-line process. During training, points are applied in close proximity along target shapes over a large number of images. For example, if the model was being trained to detect people's hands for sign language recognition the points in the training set would surround the fingers and palm. The shape data located on and between adjacent points is required to be defined for a given hand signal such that it can describe any persons hand performing the action (Heap and Hogg, 1996). Processes that utilise this technique are often referred to as Active Shape Models (ASM) (Cootes *et al.*, 1995). Examples of tracking and recognition using ASM and PDM models can be found in Baumberg and Hogg (1994); Tillett *et al.* (2000); Sumpter *et al.* (1997); Marchant (1993); Onyango *et al.* (1995); Tillett (1991).

A threshold is commonly applied to the *spatial appearance* of an image to divide (classify) the image into two colour regions by allocating all pixel intensities above one intensity value (the threshold value) white (1) and all equal to or below the threshold value black (0) . The function of the threshold value is to divide the image into two regions such that the background image is represented by one colour and the foreground image containing the target object is another colour; effectively segmenting the target object. However, the segmentation of the object from the image depends greatly on the environment. If the environment such as the lighting and background is not controlled to suit the vision system's processes then is inevitable that the threshold value will begin to incorrectly divide the image when changes in lighting occur. To overcome this dependence, thresholding algorithms have been developed to automatically determine the threshold value using the information of the intensity within the image regions or the entire image globally. A good comparison of these thresholding methods can be found in Wu and Amin (2003). A simple and manual thresholding technique was used by Minagawa (1994)

and Wang *et al.* (2006) to derive the area of the pig from the image. Previously, Yang and Teng (2008) have used an adaptive thresolding technique based on the minimum found in a histogram of the image between the light (pig) and dark (background) regions in the image. De Wet *et al.* (2003) and Kollis *et al.* (2007) used adaptive thresholding and erosion and dilation filtering to minimise noise and redundant artefacts present in the background during and after binarization. Another appearance based segmentation technique is Active Appearance Modelling (AAM) which is an extension of active shape models (ASM). Active Appearance Models are a statistically based modelling method to match both the shape and appearance of a target object in a new image. Similar to ASM an AAM model first requires off-line training using a large number of sample images. During the training procedure landmark locations (coordinate points) are defined on the target object. These points are strategically chosen to adequately represent the spatial variance of the objects characteristics which are to be investigated, as a result the distribution of a set of shapes is found describing the objects shape and appearance (Cootes *et al.*, 1992). This training data represents a point distribution model (PDM) based on the derived principle components. The trained model is then applied within close proximity (good estimate) of the target object within the test images. The shape and appearance are found after a number of iterations searching the image (Cootes *et al.*, 1998).

Recognition techniques

A method is required to validate the object before during or after segmentation. One method applied to fish has been to identify the fish based on the 'crescent' or arc-shape created after subtracting two successive frames from one another within the fish enclosure. This arc shape (a result of movement of the fishes head) was found to be a suitable starting point for further validation for all fish within the tank regardless of size. Other reference points on the fishes' bodies were deemed to be inappropriate to use as identification cues as the swimming motion of the fish caused too much variance in these locations. Before the matching took place the entire body measurements of the fish were extracted using a point distribution model (PDM). This model was then cross-referenced to validate incident test-shape data (Lines *et al.*, 2001). Recognition in pigs has predominantly been based on their shape. Pig shapes have been outlined within the image using active contours where a continuous boundary morphologically deforms toward energies created by edges within the image (Marchant, 1993; Marchant and Schofield, 1993; Cootes and Taylor, 1992). In some studies pig presence was identified by the grey level of a central region of the image; as the pigs under observation were whiter in appearance in respect to their surroundings, an increase in intensity in this central image region indicated the presence of a pig. A search of the image recovered a shape using the snake technique. To validate the shape as a pig-shape the total area of the shape was determined along with the shapes width and length. For the shape to pass as a pig, the area, the ratio between the length and width and the ratio between the area of the front and rear section of the body of the animal was required to be within certain known physical limits based on known pig body measurements. If the shape passed this filtering stage the weight was determined based on the shapes area and recorded along with a time stamp. The shape has been validated by other means. For example Wang *et al.* (2008) used the asymmetry between the pig's left and right side of its body and only included those samples which had sides with areas within 15% of one

another. Binary pattern classifiers (Chan *et al.*, 1999), chain-code, s-phi curves (Dunn *et al.*, 2003) are other similar techniques used to match shape geometries.

1.5   DISCUSSION AND RECOMMENDATIONS

Four methods have been presented that continuously and automatically monitor the weight of livestock. The vision-based method had the greatest potential to overcome various practical limitations due to its non-invasiveness, ability to operate to practical accuracy, ability to determine animals' weights in parallel, enhanced safety due to no moving parts, manoeuvrability, maintainability and inherent and potential additional functionality. The ability of the vision-based method to determine the live weight of several different species of livestock animals was established. Majority of the systems demonstrated that they could work within practical accuracy and some proved to be more accurate than conventional methods. However, common trends in the limitations specific to vision-based methods were found in conclusions drawn from many authors. Predominately more attention in this field is required in the following areas (listed in order of significance):

System Automation: Only a few vision-based developments have reached the end goal of system capable of continuous and automatic operation. Many reports had the desire to further their work to facilitate complete automation (Arias *et al.*, 2004; Minagawa *et al.*, 2003; Wang *et al.*, 2006; Brandl and Jørgensen, 1996).

Two vision-based systems are available commercially. Hoelscher and Leuschner have developed a hybrid sorting device which constrains a pig and uses an image-based analysis of the pig's body to determine whether it has reached its market weight. Release gates are controlled accordingly to direct the animal to appropriate pens (Hoelscher&Leuschner). Vision-based systems which determine the average weight of groups of housed pigs are also available, however, these systems do not cater for individual animals and the large variability between the weight samples collected daily indicate that the filtering of erroneous data may require further development (Fancom; InnoventTechnology). The average weights of groups of finishing pigs are reported to have a maximum deviation of 3% using this system (Fancom). Notably if individual weights are precise enough the weight deviation within the groups of animals should be able to be recorded and subsequently used as an alert to the farmer of when it would be appropriate to sort the animals.

Repeatability in Measurements: Numerous authors highlight the fact that the pose of the animal was likely to have led to fluctuation in the obtained body measurements of the animal which in retrospect may have introduced error into weight estimates (Zaragoza, 2009). Those authors that did not remove the head and tail from the analysis experience additional challenges in repeating measurements (Mollah *et al.*, 2010; Minagawa and Ichikawa, 1994; Kollis *et al.*, 2007; Schofield, 1990; De Wet *et al.*, 2003; Wang *et al.*, 2006). An algorithm is required to automatically select the best images for weight estimation (Wang *et al.*, 2006) and generally a steady posture of the animal is required for analysis to take place (Stajnko *et al.*, 2008; Kmet *et al.*, 2000) to avoid variation in body measurements (De Wet *et al.*, 2003). Furthermore it has been argued that the measurements used to construct the weight estimation models may be of more worth than the final weight estimation value as these measurements can be used to record genetic and composition characteristics among

other classifications (Whittemore *et al.*, 2001; White *et al.*, 2004). Therefore precise measurements are of added importance.

Environmental control: Although several authors use structured lighting this approach may not always be practical in a commercial setting. It was interesting to note few authors have attempted to exploit the benefits of spectroscopic analysis to identify the characteristic reflectance of light off of the surface of the livestock animals. Notably if appropriate this reflectance may be useful in determining a suitable optical filter to place over the imaging sensor to suppress background artefacts and assist in segmentation (De Wet *et al.*, 2003). The colour and cleanliness of the animals also pose problems when distinguishing based on appearance. Movement of the animal through artificial environments or to a structured area also facilitated additional levels of control (Minagawa and Ichikawa, 1994; Stajnko *et al.*, 2008). However, these arrangements in some cases were probably outside the bounds of commercial reality due to equipment costs and labour cost involved in moving the animals.

Bias and fine tuning: The bias in measurement toward individuals within groups of animals can be overcome using Radio Frequency Identification (RFID). However, for many livestock species this is currently not feasible on a per-animal basis. However, there is potential for individual animals to be identified through images and vision-based tracking in future. Additional causes of bias may result as a consequence of the time of day when the livestock are assessed. For example, broilers may be "significantly heavier in the evening than in the morning" (De Wet *et al.*, 2003, p 530). The process or system layout may also cause bias (Lines *et al.*, 2001). Thus, in-depth validation should be undertaken. Some fine tuning of parameters may also be required to categorise different weight classes or body types into different estimation equations or recognition routines. Other parameters such as age may be required to further refine estimates (Ramaekers *et al.*, 1995b; Brandl and Jørgensen, 1996).

A large amount of work spanning the four previously mentioned categories is still required in this research area to realize the full potential of weight estimation using vision-based techniques.

Chapter 2

A Review of Methods to Determine Animal Behaviour Using Machine Vision and Artificial Intelligence

Banhazi, T. M. & **Tscharke, M**. (2011). Review of Image Analysis (IA) technologies for the Australian pig industry. Final report for APL. (54 Pages). Canberra, Australia

Tscharke, M. & Banhazi, T. M. (2011).Determining animal behaviour using machine vision and artificial intelligence. In *The Bi-annual Conference of the Australian Society of Engineering in Agriculture (SEAg 2011)*, 55 (Eds C. Saunders and T. Banhazi). Gold Coast, Australia: Australian Society of Engineering in Agriculture.

ABSTRACT

Although animal behaviour is a widely studied field, a vast amount is still unknown. This is mainly due to the difficulties encountered when manually identifying the complex underlying behavioural patterns which occur between animals and their environment. Often behavioural assessment relies heavily on the intuition of the observer which varies considerably between assessors. Animal behaviour studies are becoming more prevalent in the livestock industry as consumer opinion increasingly influences production processes. However, increasing the frequency of livestock monitoring is difficult to achieve. This is due to the high costs involved in manually documenting and determining, individual behaviour, social interaction and the health condition of large numbers of animals. Hence, this review investigates the recognition qualities and potential that machine vision systems have in monitoring the behaviour of animals. A review of commercially available and research-based behaviour monitoring systems was undertaken. Findings indicate that there are currently no recognition systems which can reliably determine complex behaviour of livestock in commercially realistic environments. Thus further research and development in this area is warranted to overcome the inconsistencies and costs that are associated with human observation in behavioural recognition tasks.

2.1 LIVESTOCK BEHAVIOUR AND VISION SYSTEMS

Measuring and assessing the behaviour of livestock is important as it can be used to indicate welfare status. Behaviour is formed from an animal's continuous interaction with its environment (Figure 1). Animals use behaviour to respond to internal stimuli (physiological) such as hunger or external stimuli such as climate. If the goal of the behaviour is not or cannot be achieved the animal may change its behaviour or physiological response.
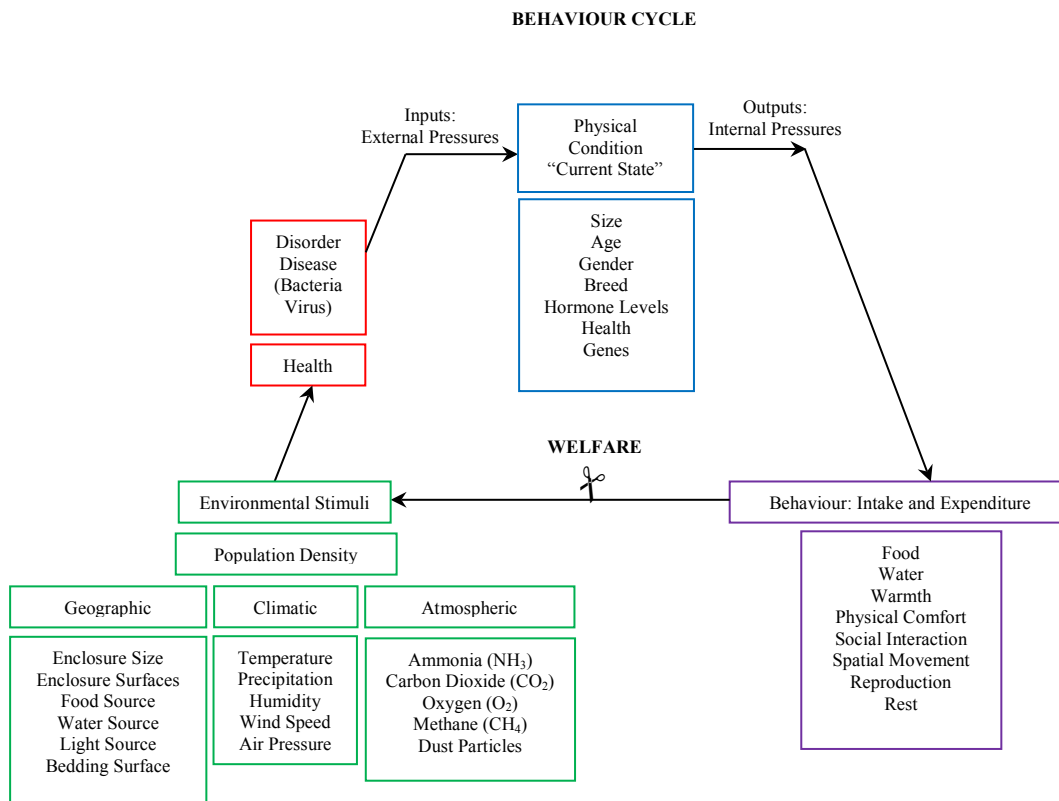
BEHAVIOUR CYCLE

Figure 1: Behaviour Cycle

There is potential for welfare problems to arise when there are inadequate environmental triggers to support the behavioural needs of livestock.

It has been argued that the husbandry methods used in intensive livestock production have resulted in the deprivation of some naturally occurring behaviours (Fraser, 1983). Such information is often misconstrued by the public. However, regardless of public opinion, producers have a strong interest in maintaining the welfare of their livestock from both economic and ethical perspectives; as proactive welfare management often has a positive effect on the farm's production efficiency and the quality and marketability of the end product. However, the observation processes currently used to measure livestock behaviour are subjective, as farm workers perform the welfare assessment. There are also high labour costs involved in monitoring animal behaviour which can further influence the amount of attention an individual animal receives. Consequently, behavioural measurements are open for interpretation and may be overlooked.

To overcome these issues, tools that can objectively assess the behaviour and welfare status of livestock species accurately, repeatedly and continuously are required. Ideally an autonomous system is required that:

(i)   Can recognise the onset of welfare related problems (mimics the intelligence of a trained welfare inspector) and
(ii) Has the ability to monitor and recognise these behaviours continuously

Machine vision systems are a device suitable for undertaking this task as they are (i) automatic and (ii) have the potential to quantitatively assess animal behaviour under a predetermined process that will not change greatly (Noldus *et al.*, 2001). For these reasons, vision systems have replaced 'human inspectors' in many inspection tasks in food-related industries (Brosnan and Sun, 2004). In recent times, research surrounding developing tools for the automatic identification of animal behaviour has gained interest.

Researchers have identified similarities between behaviour recognition and the principles that are used to recognise speech. Conceptually, these principles are useful to help describe how behaviour can be quantitatively assessed using a machine vision system. Bregler (1997) introduced the concept that in the study of behaviour a "*movemes*" could be treated as being similar in function to a "*phoneme*" (a sound) and a gesture (composed of a sequential combination of *movemes*) could be comparable to a word (a sequential combination of sounds). This concept can be extended to include the sequence of several words (a sentence) which is analogous with visually defined activities and behaviours. For example, identifying the activity of someone 'throwing darts' would involve the identification of the dart board, the motion and the orientation of the thrower's hand, arm, body and the dart in the direction of the board. In this example the path of behaviour can be followed if the components (dart, hand) can be tracked and recorded and broken down into smaller components with adequate levels of detail. The reaction with the environment can be observed as the position that the dart lands on the board. This constitutes the end result of the sentence or interpretation of the goal-driven behaviour. The reaction can be labelled as the result ('throwing a bulls eye'). Furthermore, by analysing the tracked observations and results of many 'reactions' one may be able to begin to forecast the reaction in a similar manner to how people often finish one another's sentences. The thrower may have only just released the dart but it may still be possible to predict what result is likely to occur based on various observed features, such as the dart's trajectory and speed at the time it is released from the hand, in relation to past observations.

As the above example demonstrates, behaviour recognition systems are required to automatically collect and recognise behaviour-related features which describe the target object(s) at each time step. These features need to be modelled in sequence and within the constraints that characterise the behaviour. Surrounding objects may also be recognised to help label certain behaviours.

As human beings, we intuitively come to learn and understand what we are looking at in an image from the world around us. However, a computer only sees an image in its most primitive sense; as a matrix of stored values. The content within the image is meaningless to the computer unless we give the computer instructions to determine

the underlying meaning from the image values. Johansson (1975) introduced the idea of moving light displays (MLD) to describe the visual motion of bodies in the 'computer's' world. For a better perspective the reader can think of an animal in an image as a moving light display; a collection of small moving lights (pixels).

The process to locate a moving light display within an image is known as segmentation, where the target object's light values are separated from the background light-values to form two separate groups of values representing the target object and background scene. Software is required to manipulate the image matrix to perform this classification automatically so that only the meaningful visual data representing the target object is left for further analysis. The system also needs to be structured such that it provides direction toward a predetermined outcome, such as monitoring certain behaviours. At the same time the system must compensate for variances caused by unwanted changes in light across the image. These variances in light can be caused in local sections of the image from shadows, other non-target objects and reflections, or alternatively, globally over entire image from illumination changes to the scene. Fortunately, the image can be manipulated to compensate for these variances using various hardware and image analysis techniques. These techniques may become essential if the vision system is required to operate outdoors in random environments where any physical control or removal of the causes of these variances is impractical.

The purpose of this review is to demonstrate whether machine vision systems can be used to:

(i) Objectively and automatically determine animal behaviour in commercial environments (especially those surrounding the pose of the animal) and to (ii) Identify any undesirable behaviour

A vision system is made up of hardware (camera, computer) and software components (intelligence). These components are programmed to communicate with one another similar to that of the communication between the eyes and brain. The eyes provide information to the brain which interprets the information to automatically make decisions or help make decisions in a recognition process.

2.2   THE RECOGNITION PROCESS

A vision system's behaviour recognition procedure can be broken into four main stages: (i) initialisation, (ii) tracking, (iii) pose estimation and (iv) recognition (Moeslund and Granum, 2001) (See Figure 2).

Data → Model Constraints

Initialisation ↔ Calibration

Software → Software Variables

Camera System Variables

Hardware

Tracking ↔ Segmentation → Object or Feature

Background

Pose Estimation ↔ Predictive Model
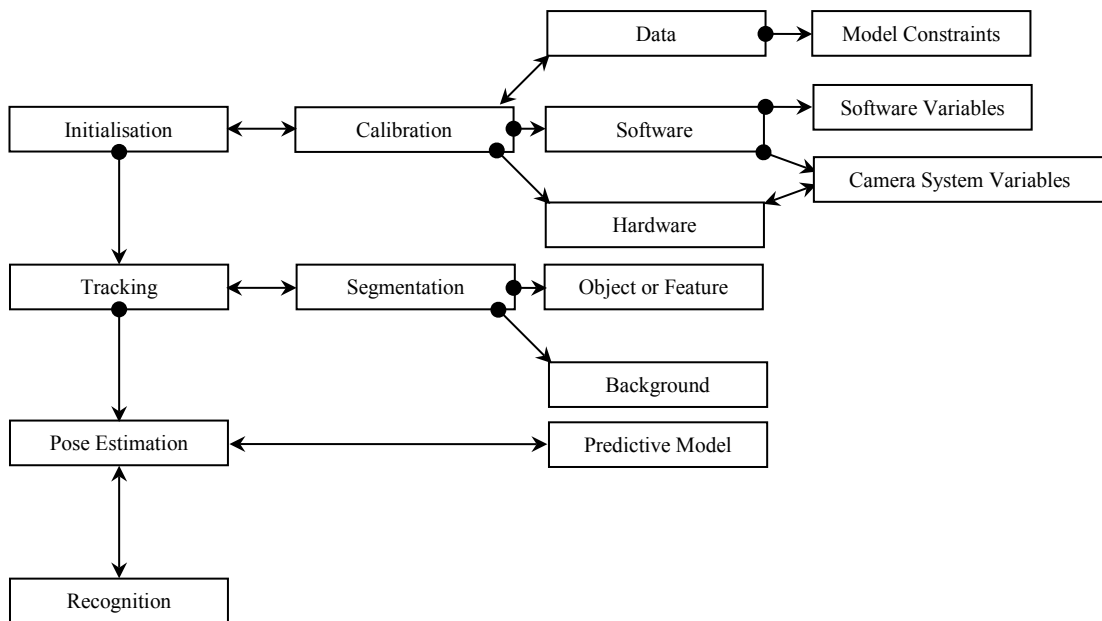
Recognition

Figure 2: The Recognition Process

Initialisation is a setup stage where the foundation for further processing is achieved. Reference to the information gained in the initialisation stage makes it easier for the system to interpret the scene in subsequent processes. This stage can be further broken up into software, hardware and data calibration components, all of which assist in obtaining an appropriate representation of the image scene and the information within it. *Tracking* involves the identification of feature(s) within the scene and segmenting (separating) them from the remainder or the image so that they can be analysed further. Tracking techniques create associations between successive image frames using some form of measure found within the image. *Pose Estimation* is a stage that aims to describe or identify the orientation of the target object within an image scene. The body pose can be identified as a combination of the orientation (angles and body measurements) of several components (limbs), or as a whole. *Recognition* is the correct labelling and identification of a pose or a sequence of poses as a given action or gesture.

2.2.1   Initialisation

Initialisation can involve tasks carried out before (off-line) or after (online) the vision system becomes active. In essence, each task of the initialisation stage will involve some form of calibration. Hardware such as the room lighting and camera settings (such as exposure, focus and contrast) may need to be calibrated to application-specific levels. This is done to optimise the integrity of the image for further processing and is usually carried out off-line, however, some instruments enable online adjustment of these features. Examples of these are cameras with built-in 'automatic focus' which can automatically adjust the focal length between the lens and the imaging sensor to obtain a clear image and cameras with built-in 'automatic exposure' which can maintain a suitable dynamic range within the resultant image by controlling the amount of light incident onto the imaging sensor.

Like hardware, software must also be initialised. Software initialisation requires the calibration and optimisation of variables within the software to enable the tracking and recognition processes to function seamlessly.

Finally the data describing the target object is required to be collected and calibrated. This can be performed either off-line where a detailed model of the target object is pre-defined (known as a model based on *a priori* knowledge). Or alternatively online where there is no *a priori* information available (model free) and the model for the target object is learnt and built over time from tracking, clustering and classifying the object features in successive images. The off-line models include information describing the physical and kinematic constraints of the object. These models are either continuously referred to in a matching process by the software component (direct model), or are used to identify a pose for further learning (indirect model). If properly applied, *a priori* models have an advantage over model free systems as they can be used to minimise the solution space through the effective use of their predefined constraints (Moeslund *et al.*, 2006). Data such as image distortion coefficients and other model-related referencing variables may also be included in the off-line data (Lind *et al.*, 2005).

As the initialisation stage encompasses the main structure of the system, the way in which these components are configured with one another has a large influence in the overall performance of the system. The selection of the descriptive features associated with the object also plays a vital role.

2.2.2   Features and Cues Selection

This section discusses the features that can be extracted from images which have special meaning (i.e. are semantic). Only features associated with images acquired in the visible spectrum are considered here, however, various other features can be identified from image sensors sensitive to other bands in the electromagnetic spectrum.

It is desirable for a tracking system to have access to the descriptive 'feature' information of the target object so that it can be reliably validated and re-located after analysis. However, the computational cost and efficiency of the feature extraction processes need to be practical in respect to the application. Each feature is also required to be found reliably to prevent errors in subsequent estimation or recognition stages. Therefore only features that reliably and efficiently describe the target object should be selected.

Features can be classed as temporal, spatial, valued, or textural. Examples of temporal features found across images are velocity and acceleration which can be determined over time when motion occurs. Spatial features are point(s), edge(s) or shapes of various size and body measurements. Value features are image-specific values such as colour information acquired from an image colour space. Textural features are a group or range of features such as colours, intensities, edges, points and shapes which can be combined into a textural feature or template. A feature can also derive its own characteristic distribution over time. In general, the data describing each feature contains information that is redundant and can be represented in a more efficient and compressed format. An explanation of techniques such as PCA that can be used to convert the feature data into a more efficient representation can be found in Appendix A.

For the remainder of this chapter, a 'feature set' will indicate a collection of image derived features which describe an object within an image. Furthermore, as an animal's behaviour is likely to be the result of an environmental stimulus or goal-driven need, the concept of 'features' should not be restricted to only those features directly related to the target object. For example, a nocturnal animal will exhibit very different behaviour depending on whether its environment is 'light' or 'dark'; so here illumination is the stimulant. Therefore, illumination may be an important external-variable and necessary to adequately defining the behaviour in this example. Other external variables such as temperature, air quality, and the location of feed and drinking stations can also be considered features which explain the current conditions. After the image-related feature set is chosen certain techniques must be applied to effectively identify, segment and track them in and across each image frame.

2.2.3 Tracking

The process of tracking involves the combination of two processes (i) segmentation and (ii) temporal correspondence. *Segmentation* involves the process of extracting target feature(s) from images. Thus a 'feature set' describing the object and any other conditions will be the result of the segmentation process. *Temporal correspondence* refers to the process of associating (linking) one or more features in an image frame to adjacent frames by continuously collecting and referring to prior feature information. The correspondence can also be described as spatial-temporal indicating that there are space and time body measurements factored in during the tracking process. This process can dramatically improve the chance and speed in relocating the feature(s) of interest in subsequent frames and therefore helps with the overall efficiency of the segmentation process.

Four classes of techniques are used to recover the 'feature set' from the image in the segmentation and temporal correspondence processes. These are (i) scene-based, (ii) motion-based, (iii) shape-based and (iv) appearance-based techniques. Scene based techniques aim to describe the background scene so that any object entering it can be easily segmented when the background scene is removed. Scene based techniques include subtraction methods and Mixtures of Gaussians (MoG). In a subtraction method the pixels' values in subsequent frames are subtracted from one another resulting in an image containing the 'new' information relative to the assumed static background. A MoG approach learns to recognise the image background overtime using a series of adaptive distributions to describe the background. The background model is then used to identify regions that are not highly correlated to the derived background model which indicates that they are a foreground object and could potentially be the target object (Stauffer and Grimson, 1999).

Motion based techniques use temporal correspondence between frames to determine the movements of objects within scenes. The velocity and acceleration (optical flow) of the 'movement' of light representing the target object within the image can be found. This movement can be characteristic of some form of behaviour. For example, boxers fighting in a ring will have periods of fast moments which indicate attacking moves and slow movements during defensive moves or when planning attack. These fighting motions have been studied in rodents through manual observation (Pellis and Pellis, 1987).

Shape based techniques strive to recover unique dimensional attributes of the target object(s) from edges and points located within the image. Active Shape Models (ASM) is an example of a shape based method used to find shape information within the image. The model can locate shapes based on reference to previously defined shape information on the target object. Appearance based techniques utilise the image colour properties such as intensity, saturation and hue to form a basis to segment the image (Cootes and Taylor, 1992). Similar to ASM are Active Appearance models (AAM) which can locate appearance features based on reference to previously defined appearance information of the target object (Cootes *et al.*, 1998).

These four classes of techniques can be used in any sequence. As an example, a scene based technique may be used to segment an object, then a shape and appearance based technique can be used to describe it. In another example, an appearance based technique can be used to find certain colours in an image followed by a shape based technique to describe the boundaries of the colour region(s). These four classes can also be used in combination to form textures. An example is appearance-shape textures which can be derived using a combination of space and appearance techniques. Blob analysis utilises an appearance-shape texture method as the image values and their respective spatial positioning are used in combination to provide grounds for segmentation (Wren *et al.*, 1997b). Generally vision systems use a combination of the results from one or more of these techniques to arrive at feature set which describes the object(s). Generally before a technique is applied to extract a feature set from an image(s), the image values are manipulated to assist with the feature extraction in a process known as enhancement some enhancement methods and edge detection methods can be found in Appendix F.

2.2.4 Pose Estimation and Recognition

The following sections deal with the 'brains' of the system: how to estimate pose(s) and recognise behaviour based on an extracted feature set. Here pose estimation is the successful identification of the subject, its orientation, position and/or current movement (a *movemes*); determining the correspondence between a feature set and a pose. The recognition phase is the correct identification or labelling of a sequential combination of poses using a cross-reference to previously obtained data. Similar processes are used when recognising behaviour from a sequence of poses and when estimating a pose from a given 'feature set'.

2.2.4.1 *Behavioural Modelling Methods*

One of three different data storage and retrieval methods can be programmed into a vision system to derive a target object's feature set(s) or to use an existing stored feature set(s) for validation. These three methods which structure the data-flow are model free, direct and indirect methods. Here the word 'model' refers to the characteristic distributions (clusters or groups) that represent dissimilar feature sets (the data which describes the observations). Systems that do not use prior knowledge, build their recognition database (feature set groupings or clusters) online while the system is running. They are *model free* at initialisation. These systems are widely researched and their application in artificial surveillance is promising as

systems that operate *model free* can effectively learn and categorise anything systematically. Hence, they are commonly called 'machine-learning systems'. However, there is one limitation for a model free system; intuition. As external intelligence is required to correctly label or interpret the discovered data clusters for a particular pose/behaviour (see Figure 3).
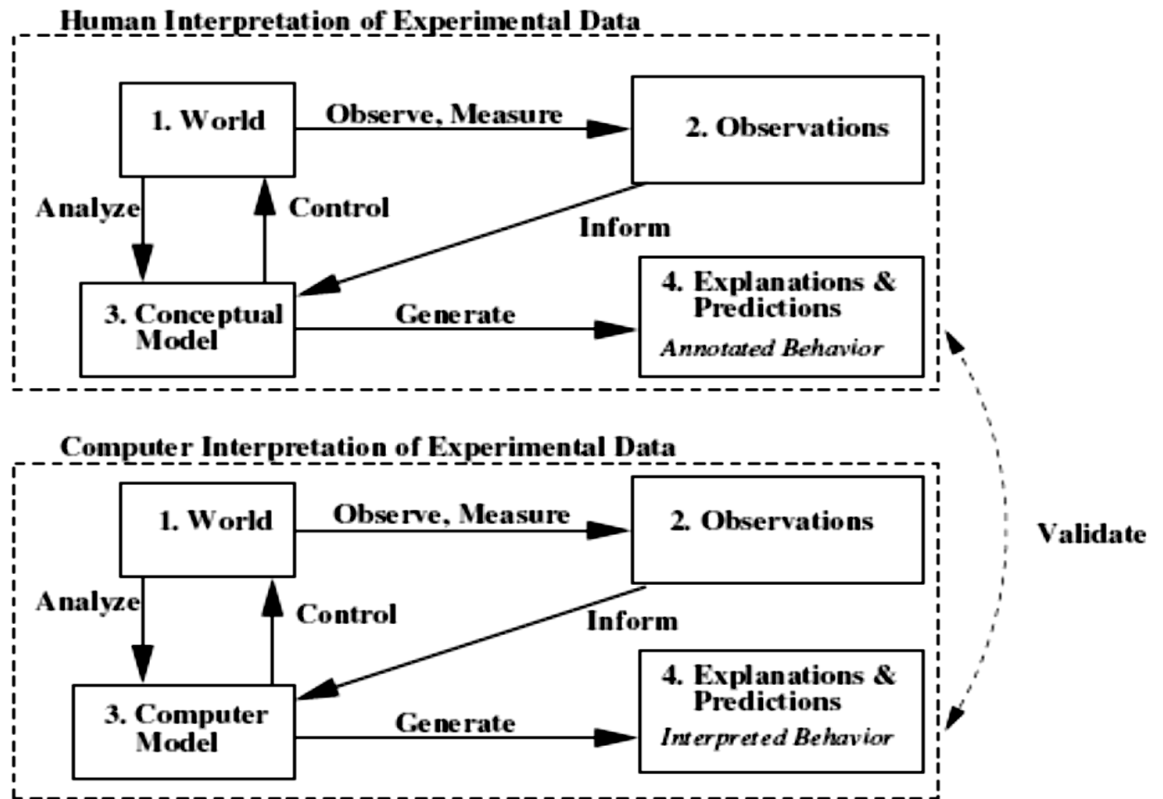
Figure 3: The Validation Process: Comparing a Computer and a Human's Interpretation of a Behaviour from Xue and Henderson (2006)

Alternatively, to minimise the solution search-space, a *direct* data-retrieval method can be adopted which uses previously stored knowledge such as the kinematic and dimensional characteristics of the target object. The feature set(s) of the target object are collected, modelled and labelled before initialisation so that specific information can be retrieved for goodness of fit between a new observation and the existing labelled observations. However, the restriction of a method that directly cross-references to a database is that it cannot adapt, the system is only as good as the constraint data representing the target object in its predefined model. Assume for example that an animal is involved in a fight and sustains an injury which severely affects its gait. As a result, the kinematic movement and perceived shape of the animal is distorted. If the referenced data distributions are not flexible enough to correctly respond to problems like this, identifying the behaviour of the animal (in this case, walking) may be unrecognisable. For this reason an *indirect* method can be used which is a combination of both model free and direct methods.

An indirect method self-learns in a similar manner to the model free method only with constraints which restrict the adaptation of the model. The updates to the model only occur when the observed feature set is highly correlated to a cluster representing a built-in feature set. New clusters can form when there is significant evidence to

support the proposal that a new cluster exists. Therefore, this method can be used to help confirm the integrity of the initial *a priori* model distribution(s) and labelling over time. However, if not done correctly the indirect model can update and compound the reference data (and thus models) with errors if false positives are frequently introduced into the model. The balance between whether the system updates its model (or not) is known as the *plasticity* of the system. This balance is based on how well the observed feature data relates to the existing model. The control and flexibility in the indirect data storage and retrieval method make it well suited for 'recognition type' vision systems that observe deformable bodies which continuously change.

If a method other than model free is chosen, then information on the target object needs to be collected to form the feature sets. This *a priori* data can be collected in one of the three following ways:

(i) Actively by attaching sensors to the subject
(ii) Passively by observing the subject using a sensor device such as a video camera
(iii) Using markers, which involves a combination of active and passive techniques

More detail of these data collection methods can be found in Appendix B. Once sufficient information of the target object has been acquired, the underlying definition of the behaviour(s) or poses under investigation must be described and programmed into a computer readable model. This model is categorised using three techniques known as (i) clustering, (ii) classification and (iii) training.

A basic recursive training process containing classification and clustering stages is illustrated in Figure 4. Condition 1 refers to a classification stage. At this point the system cross-references between the stored model and the incoming features set and a calculation is made that determines whether or not the feature set belongs to one of the distributions (or clusters) defined within the model. If the feature set does belong to one of the predefined distributions then the distribution's meaning or label is used for the output. If it does not then Condition 2 (a clustering routine) is executed which deals with the adaptation of the model. In the clustering stage, the incident feature set is cross-referenced between all other (previously stored) feature sets which did not have a significant relationship with any of the distributions in the model. If a group of stored feature sets share significant similarities and have accumulated to reach a defined threshold level then the group's distribution can be integrated into the model and can appear in the next classification stage. This recursive process where the data is categorised is known as training. Some common forms of clustering and classification algorithms are discussed in Appendix B.

The clustering and classification stage will result in the information being structurally represented so that the computer can make an association with the incoming feature set extracted from the image. However, before a feature set is either classified or clustered, it must be scaled appropriately to represent the data efficiently and effectively.
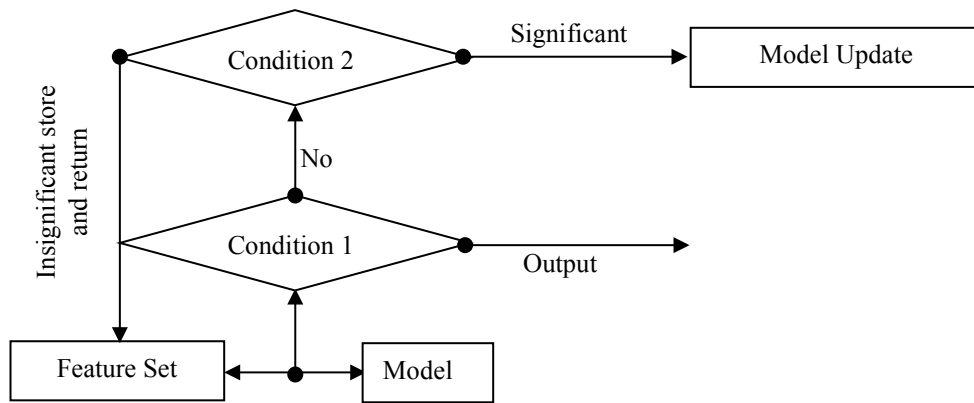
Figure 4: Supervision: A Classification and Clustering Process

There are two types of scale relevant to identifying behaviour. These are spatial and temporal scale. Objects can vary in size and shape (spatial) and the size and shape of objects can vary over a random period of time (temporal). The modelled distributions are required to be normalised into scales which can easily translate to, or represent, checkpoints states during an observed physical action. For example, it may take a child less than a second to sit down but it may take and elderly person half a minute. How can a system intuitively interpret this as the same action? In a spatial example, a person walking away from a camera will continuously have a decreasing amount of pixels associated to his or her body. How can a system interpret this as the same object across all frames?

In both cases a single method is required to facilitate these changes of scale within the image and across the image sequence. A basic system that neglects temporal scale altogether can be considered 'static' as correlations between new observations and prior data references are only made within the scene at the current time step. Here matching is performed to identify only the desired final pose, like an observation in a photograph. This process is often called template matching where the segmentation, pose estimation and behaviour recognition are found simultaneously. However, using such a system severely limits the ability to forecast behaviour as it does not take advantage of the prior sequence of actions leading into the final interpretation and physiological reasoning behind the behaviour.

Several different methods are used overcome the problems associated with temporal and spatial scale in and across images. In general, these methods are based on dynamic Bayesian networks (DBN). A DBN is a data structure that supports different 'states'. The states within the DBN are defined by training a collection of feature sets corresponding to a sequence of behaviour. So, if the system observes a behaviour that has been included in the DBN before initialisation or during adaptation, we can expect a feature set found within an image of the behaviour to have a strong correlation to a predefined state within the DBN. A state does not have to be an exact match but just the closest match above a given threshold. The match is based on conditional probability. A DBN can be thought of conceptually as a path which defines the behaviour. The feature set is used to determine the location (the state) of the subject on the behaviour path. Once the position on the path is found, the system can transition between adjacent states based on the fit between the feature set and the DBN. Monitoring the timing and frequency of transition patterns between states can

be used to track, recognise and forecast a given behaviour. Techniques for modelling behavioural scale can be found in Appendix A.

2.2.5   Commercially Available Vision Systems that Determine Behaviour

Commercially available behaviour monitoring systems have been developed for both humans and animals. Two different types of behavioural vision systems are presented in this section. First, a motion capture system is presented which is an example of a system that can be used to record the biomechanical model (*a priori* data) for a particular behaviour. The second system presented recognises and quantifies the behaviour based on streaming video. This section concludes with a description of the state of the art in human-based behaviour monitoring applications which has the potential to be transferable to the behavioural assessment of any living organism.

2.2.6   Biomechanical Recording Systems

Several companies pride themselves on the ability to geometrically record and reconstruct models of certain body postures based on motion capture using vision systems. These systems provide a tool for determining the underlying prior constraint data describing the biomechanical model for a given sequence of movement by an animal. These systems do not recognise and identify the behaviour, they only record the behaviour so the information (body measurements, angles, timing) recorded can be used for building the model of the target object and subsequently used as a reference by the vision system. The information found using these systems still needs to be programmed into an automatic and computer readable model to form the artificial intelligence of an automated vision system.

Vicon Systems (Vicon 2010) has a range of systems for life sciences animation and engineering that have the ability to record and reconstruct models of human and animal movement. They have systems which can record behaviours in 2D, 3D with the use of markers (active) and in 3D without the assistance of any markers (passive). Landmarks (kinematic reference points) on the body surface can be user-defined when using the passive system to highlight certain body movements. Tolerances of 0.01 mm can be achieved for the reconstructed body surface mesh. The kinematic model is captured in 3D using a system composed of up to 10 cameras. The system is capable of presenting real-time 3D information such as joint angles. Some Vicon systems can achieve frame rates between 1 and 2000 fps. The company also provides systems designed for the capture of animals biometric information (Vicon, 2010). All kinematic data is transferable to third party software packages such as Matlab and Labview for further analysis in the form of a C3D file. Vicon systems have been used to record the biomechanical function of animals for later off-line analysis in numerous research projects on animals including pigs (Liu *et al.*, 2007; Herring *et al.*, 1993).

2.2.7   Behaviour Recognition Systems

The majority of the behaviour recognition systems that are currently commercially available can only generate and analyse behaviours that involve the spatial tracking of the animal over time. A large percentage of the systems are designed for

laboratory type experiments in simplified and controlled environments. These controlled environments assist in the segmentation task of separating the animal from the background. Given the small size of the animals, the experimental enclosure can be easily constructed, controlled and maintained. Structured lighting can be applied easily and the integrated image processing techniques can be relatively simple. However, behavioural recognition systems become far more complex when they are required to assess large or multiple animals outside the comfortable setting of a laboratory such as in commercial farm environments.

Difficulties in commercial farm environments were experienced by a number of authors (Lind *et al.*, 2005; Šustr *et al.*, 2001). The main reason for the increase in complexity is due to the animals' housing environment. Not only is there variation between housing layouts, but environmental factors such as temperature and air quality are harder to control. These factors can also cause certain animal behaviours; such as coughing in relation to air quality for example. Of the systems presented in this section, only one had the potential to determine more complex behaviour based outside of the recorded spatial co-ordinates of the animal in the enclosure. Robust and generic system designs are unavailable. Behaviours such as grooming and fighting must be manually defined within the system and the operator must either prompt the system to record these complex behaviours when the behaviour is taking place, or they must be identified off-line after the experiment is completed. In most systems a stimulant (such as the movement of doors, light changes, shock and sounds) can be automatically inferred into the test subject's environment. Because the techniques used by these companies are similar, a general introduction and description with highlights are presented.

2.2.7.1 *Animal Surveillance and Tracking Systems*

Behaviour recognition systems can be classified into either laboratory or field-type implementations. Laboratory type implementations allow for the additional expenditure on control (building, enclosure or environmental alterations) that may not be feasible to operate in commercially realistic environments. Field-type implementations are flexible and can be integrated into existing commercial environments (which are variable) with little or no control required. Furthermore, the type of behaviour assessed by the system can be categorised into either tracking or pose related behaviour, where tracking relates to the co-ordinate position of the animal relative to its surroundings and pose relates to is actual physical actions.

In general, the commercially available systems found during the review had the objective to record the spatial movement of a laboratory animal performing a set task. Observational tests carried out using vision systems included tracking the rodent through various maze types to analyse the animal's behaviour when subject to certain environmental conditions. Other vision systems recorded fear conditioning experiments, light-dark-testing, tail suspensions, swim tests and novel object recognition. Recorded variables included, time resting, time moving, entry to a zone, time in a zone, locomotive speed, distance travelled, contact between different coloured animals and condition-place-preference. The systems generally export data output into Microsoft Office Excel (Microsoft Corporation, Redmond, WA, United States) and facilitate a visual output of the tracking plot. In most tracking systems presented here, the animals were identified and tracked by their geometric centre

after segmentation. A description of the main features of some commercially available systems follows.

The *Video Mot2* (TSE Systems GmbH, Bad Homburg, Germany) system can track and record the position of an animal over time in a controlled environment. The system can support up to 6 cameras per computer. Each camera image can be divided by the operator into an unlimited number of image sections (arenas) which are the boundaries for an experiment involving either one or two animals. The system can also be configured for day and night recording. The animal in the experiment can trigger the collection of data based on predefined positions or zones within the image arena defined by the user. For example, the animals can start or pause the experiment by moving between different locations inside the image (TSE-Systems, 2010).

Actimetrics (2010) has four vision systems *Freeze Frame*, *Water Maze*, *Limelight* and *Big Brother* (ActiMetrics, Wilmette IL, USA) which are all marketed at different testing environments. *Freeze Frame* is a fear conditioning software which is used to determine the animal's motion when it is subject to a fear provoking stimulant such as loud noise or uncomfortable environment. This motion recognition system can detect the movement of limbs (grooming, sniffing turning and rearing) when an animal (mouse or rat) is stationary, however, it has no ability to recognise, label or record these movements. *Water Maze* has a project planning component where the user can enter an experimental design before running an experiment. The system then notifies the user which animals should be introduced into to the experiment, and the timing of their introduction. The animal's movement can be used to trigger different recording properties of the experiment in a similar way to the TSE system mentioned above. An algorithm compensates for lighting changes and shadows within the image. The *Limelight* system can track up to four arenas at once using one camera. Complex behaviours are manually labelled or scored (offline or online) by an operator. A novel feature of the *Limelight* system is the ability to monitor body length which indicates different stretch-attend behaviours caused by changes in the body length of the test animal. For example from the camera's top view, the body length will be shorter when the animal is in a rearing position (sitting). Over the course of the experiment, the body lengths are divided into short, medium or long body lengths manually. These three data clusters are then used to cross examine the spatial locations in which the animals are situated at the time the change in body length occurs, and to identify any relevant patterns. The *Big Brother system* is a system which is capable of tracking a large number of laboratory animals from above in open field type tests (in the laboratory). Each camera's image can be divided into 50 sections to define the boundaries of 50 arenas containing a rodent to be tracked. Thus, four cameras can be used to track the movement of up to 200 animals (Actimetrics, 2010).

Med Associates Inc (2010) also has a range of systems for monitoring lab animals. A fear conditioning and tracking system which utilises video recorded of the near infrared spectrum, an open field video tracking system with test enclosure, and a water maze and video tracking software designed to determine the path co-ordinates undertaken by the animal and other motion variables that occur during a Water Maze test.

Qubit Systems Inc (2010) has two video systems. The *QUATTRO* (Qubit Systems Inc., Kingston ON, Canada) system can track animals in three dimensions using two cameras (top and side view). The system determines and tracks the animal's geometric centre. A mask (image-based filter) is applied to remove false positives improving identification. Another one of Qubit's products called *Video Tracking Software*, can track an animal in a range of the different observation type tests previously listed. Qubit Systems, Inc also offers a system called *DanioTrack,* which can determine the tracking information of multiple danio (zebra fish) in one arena from pre-recorded video (Qubit Systems Inc, 2010).

Biobserve (2010) has four vision systems. The *Trackit2D* (BIOBSERVE GmbH, Augustin, Germany) system uses a pan-tilt-zoom (PTZ) camera to automatically follow the object and keep it within the boundaries of the image. *Trackit 3D* uses the top and side view of the animal's arena to obtain the x, y and z co-ordinates of the test subject. The system can be used to track fish species in a tank. The *Viewer* system tracks the centroid, nose and the tail of mice and rats. Additional movement can be identified using these three points such as the animal moving its head from side to side (head wagging), stretching and freezing (when the animal stops abruptly). The *Forced Swim Test* or FST system is designed to observe the reaction of an animal from the side view when it is placed in water. The system automatically determines whether the animal is struggling, swimming or floating by measuring its position between predefined zones on the surface of the water (Biobserve, 2010).

Noldus (2010) has a wide range of products targeting animal and human behaviour. The *Observer XT* (Noldus Information Technology BV, Wageningen, Netherlands) software can be used to organise a behavioural assessment during an experiment or observation trial. The user pre-configures and defines the behavioural actions to be witnessed and recorded during a given experiment. The user then manually documents the behaviour as it takes place from either streaming video or pre-recorded video files. The software organises the data so that results of certain behaviours can be easily accessed by querying the acquired data. *EthoVision® XT* is a vision system which can track the nose point, centroid and tail base of a laboratory animal. From these three points the body elongation can also be found. *Catwalk XT* is a novel system to analyse the gait of mice (Deumens *et al.*, 2007). The mice walk over a LED illuminated glass plate which reflects the light of all points within the glass plate except for where the animal is in direct contact. The feet of the animal can be observed and are automatically classified by the system. The tail or other parts of the animal's body which are not required in the analysis can to be removed manually by the operator (Noldus, 2010).

IBM's smart surveillance solution (S3) is a commercially available surveillance software package for tracking humans. The system simultaneously monitors different levels of surveillance. For example, the system can be used to track a car, its number plate, and its occupants in the parking space surrounding a building. Lower level cameras monitor the entry and exit points of the building and provide a means of facial and appearance recognition. Using this surveillance framework the movements of the car's occupants can be tracked in a time line from when their vehicle arrives to when it leaves. The system is structured to be able to accept queries to classify events. For example, someone or a vehicle remaining in the camera view for an extended period of time could be considered loitering or abandoned so a query can

be set to sift through all events bounded by this criterion. Other search criteria consider the target-object type, size, image-region, and appearance (Chiao-Fe *et al.*, 2005).

2.3 RESEARCH BASED VISION SYSTEMS THAT DETERMINE BEHAVIOUR

There are many applications of vision systems in agriculture and other industries which essentially fit within three broad research categories of surveillance applications, control applications and analysis applications (Moeslund *et al.*, 2006). The following section presents various research projects using machine vision systems to determine animal and human behaviour.

A number of vision systems have been created specifically for animal production. Most applications are designed to reduce animal handling and improve efficiency in comparison to traditional methods. Some examples are systems which survey the linear or angular body measurements of livestock such as cattle and pigs for sorting or weight estimation (Banhazi *et al.*, 2009b; Schofield *et al.*, 1999; Schofield *et al.*, 2002; Brandl and Jørgensen, 1996). A vision-based control application was demonstrated by Wouters *et al.* (1990) who applied imagining techniques to housed piglets. The application used the spatial behavioural characteristics of piglets as observed in images to determine parameters to control the thermal comfort level of their housing. More recently a number of authors (Xin, 1999; Shao and Xin, 2008; Xin and Shao, 2002) created a similar system, also basing their control system on the resting behaviour of the pigs found using a vision system. In an effort to determine the behaviour of pigs in relation to their housing requirements, researchers have created and simulated models of pigs' behaviour based on spatial-temporal information recorded of live pigs (Stricklin *et al.*, 1998; Gonyou *et al.*, 1997).

Another example of a control application can be found in Sumpter *et al.* (1997) where a 'robotic sheep dog' was developed to herd a group of ducks. In the study a vision system was used to control the path of the robot by determining the location of the robot in respect to the ducks. A behavioural simulation model was built based on parameters acquired from observing the behaviour of the ducks. Vaughan *et al.* (2000, p 117) later reported the success of the 'robotic sheep dog' project in both the simulation and real world applications, concluding that the "methodology is appropriate for future animal-interactive robotics experiments" and that uncomplicated mathematical models could be used to model basic flock behaviour.

Vision systems have also been designed to function as tools to analyse complex biomechanical movements of humans and animals in research and clinical applications. An example is gait analysis which often includes muscle movement and force generation (Bharatkumar *et al.*, 1994; Chen and Lee, 1992; Rohr and Systeme, 1997; Little and Boyd, 1998; Aydin *et al.*, 2010; Favreau *et al.*, 2006). Gait analysis has been used in the development of sports simulation models to improve the athletic performance of both humans and animals. The objective measurement of complex biomechanical movements such as gait should increase the accuracy of measurement by eliminating human error and thus facilitate the conduct of experiments, by automating data capture and collation.

Locomotor activity of the animal has also been determined though the observation of body parts other than a direct observation of the legs. Burghardt *et al.* (2004) and Burghardt and Calic (2006) devised an image processing technique to determine in the loco-motor behaviour of wild lions based on head posture and facial recognition.

Numerous experiments in psychology and pharmacology, involving visual observation of the interaction between humans and machines, and animals and objects can be found in literature.

A large number of analysis methods also focus on animal tracking. In the poultry industry, researchers used a vision system to detect and track broiler chickens to identify the birds interacting with the drinker and feeder (Sergeant *et al.*, 1998). Kato *et al.* (1996) used a vision system in an aquatic environment to track and record the position and velocity of fish in a tank and successfully identified the left and right turning behaviour of the fish. In a similar manner, Cangar *et al.* (2008) determined the spatial movement of a cow in a barn using a vision system. Measures of walking trajectory, distance walked, orientation of the main axis, body width/length ratio, hip length and back area were recorded. Eating, drinking, standing and lying behaviours were derived from the continuous monitoring of these variables in relation to its enclosure.

EthoVision, a generic behavioural assessment software, has been described in the literature (Noldus *et al.*, 2002). The software has been used to study insects in various applications such as the time taken for cockroaches to reach the odour bait and the behavioural interaction between other insects including wasps, aphids, ticks, beetles, flies, and spiders (Noldus *et al.*, 2001).

Šustr *et al.* (2001) used the EthoVision system and their own software to create a hybrid system to enable them to study the interactions of pigs during pre and post weaning. The study focused on behaviours related to contact such as fighting. Markings were made on the pigs and identified by the system to track the pig's movements. Like Šustr, Lind *et al.* (2005) developed a basic vision system to overcome some of the limitations of the EthoVision software in tracking the movements of pigs. Their study involved the administration of apomorphine to minipigs to observe and record the locomotor behaviour of the subject. Perner (2001) used a side viewing angle to successfully track the movement of pigs based on motion parameters and time.

Vision systems have also been developed to determine when an animal's welfare is compromised based on certain behavioural characteristics. Duarte *et al.* (2009) identified the behaviours or activity of flat fish 'taking off' and 'surface swimming' as a preliminary measure of their welfare. Branson and Belongie (2005) also developed a vision system to monitor the behaviours of multiple mice from a side view, to give an indication of the animals' welfare through various activities. Complex behaviours such as grooming frequency and basic postures such as stretch, sit and walk were identified. Systems have also been designed to monitor herds to detect their behaviour during milking (Kaihilahti *et al.*, 2007).

Identification of multiple animals within the field of view presents additional challenges as multiple regions within the image containing individual animals need to be identified and analysed. Tweed and Calway (2002) demonstrated the ability to identify and track multiple birds (during flight) using image processing techniques. Kalafatic *et al.* (2001) tracked multiple mice in a laboratory setting using a contour tracking technique that was based on the animals' movements.

A large number of vision systems are targeted at specific human-behaviour applications. One such example is given by How-Lung *et al.* (2006) who developed a system which can monitor people in an aquatic environment. The application acts as a virtual life guard for a swimming pool. As their system was aimed at preventing drowning, they monitored the surface of the pool for people acting in distress.

Several large-scale multilevel surveillance research projects are also being undertaken in an effort to enhance the safety of the general public. The HERMES system (Human Expressive graphic Representation of Motion and their Evaluation in Sequences) is a blanket system designed to track people using pan-tilt-zoom (PTZ) cameras. The system has three levels of recognition. Level one identifies the object or 'agent' which can be done from a long distance. The system then automatically instructs the camera to zoom in on the agent to perform another level of analysis. At the next stage the agent is classified based on its posture or movement. For example, the system determines whether agent is a car or human. If further detailed information can be acquired from the agent, such as a face, a third level is used to identify the face and/or facial expression. The system is structured to learn and has the ability to recognise the movement patterns and shape for certain silhouette postures (HERMES, 2009). The W^4 project has similar aims and objectives to the HERMES project (Haritaoglu *et al.*, 2000). Wren *et al.* (1997a) created a system called '*Pfinder*' (People finder) an improved derivative of the ALIVE system (Maes *et al.*, 1997) which can identify the head, hands and body of a person in real time using a camera with a fixed view. It is suggested that the system could potentially be used to track vehicles and animals.

2.4 FUTURE RESEARCH POSSIBILITIES

A system which can identify complex behaviours in and between animals, such as fighting, is not currently commercially-available. Given the techniques used, the performance of the commercial systems reviewed would be questionable if applied outside the laboratory environment. Therefore, a vision system would need to be designed to monitor both simple tracking and complex behaviours in a commercial farm environment. For example, a significant amount of information can be gained by simply determining the pose of an animal. For instance, if a sow can be automatically and reliably identified in a standing posture the result can lead into two useful surveillance applications. When the sow is not standing it must be lying down or sitting, therefore by detecting when the sow is not standing one can assume that is beginning to lie down. This transition can be used to activate a control system to prevent her crushing her piglets (Weary *et al.*, 1996). Using the same identification scheme, one can log the time taken in a standing pose in addition to the general activity of the sow or gilt which can be used for oestrus detection during their interaction with boars (Cornou, 2006; Ostersen *et al.*, 2010). It may also be possible to detect when a sow is on heat from the distinct lack of motion (freezing), pricking of its ears and the arching of its back, which shortens the perceived length of the animal. This form of automated oestrus-detection system could result in up to 30% labour-cost savings by both minimising the manual labour required to facilitate the interaction between the sow and boar(s) and the non-productive days (Freson *et al.*, 1998).

The potential to identify welfare-compromised animals through other motion characteristics or spatial characteristics can also be explored. Systems that identify dead animals or animals with poor mobility can be developed by tracking the movement of the animals around the pen (Tillett *et al.*, 1997). Animals with poor mobility or dead animals can also be found by averaging the image over time and observing the animals which have greatest presence in the background image. The mobility or condition of the animal may be achieved by a gait analysis as performed by a vision system (von Wachenfelt *et al.*, 2010; Favreau *et al.*, 2006; Aydin *et al.*, 2010).

Tracking the animal around its enclosure can also lead to the discovery of other important behaviours such as the time taken at the feeder or drinker and help to optimise the animal's requirements, such as the number of feed stations or space requirements. The behavioural activity around certain parts of the enclosure has the potential to assist with disease prevention. For example, an outbreak of diarrhoea can be traced back to excessive water consumption of individual animals (Pedersen and Madsen, 2001). A system that identifies sufficient space requirements based on the posture or activity of the animals is also a possible application area (Ekkel *et al.*, 2003).

Stressors or threats can be recognised from animals' freezing and abrupt lack of motion in the image. Tail biting in groups of pigs or wounds from animals fighting can be identified in images based on blood colour information. Single tail biting events are suggested to be strong indicators of a larger outbreak approaching and therefore, if identified early enough may provide sufficient information to implement management strategies to control the problem (Statham *et al.*, 2009). Fighting behaviour may also be detected from various motion characteristics (Pellis, 1988).

Thermal infrared cameras give an indication of the thermal comfort of an animal which can be based on a particular body reference region. For example, Andersen *et al.* (2008) determined that a pig's ear temperature relates to its thermal comfort and behaviour. An infrared vision system can potentially be used to determine the required thermal level for input into the environmental control system in a similar manner to what was demonstrated previously by Shao and Xin (2008) and Wouters *et al.* (1990). The difference would be that the control would be based using the actual temperatures of the individual animals not on their spatial characteristics.

Potentially, the same system could also be used to monitor the animal's health (through variations in temperature) and its relationship to its behaviour, as IR imaging has been used for the detection of disease and flu symptoms (Gariepy *et al.*, 1989; Rainwater-Lovett *et al.*, 2009; Schaefer *et al.*, 2007; Stewart *et al.*, 2007; Banhazi *et al.*, 2009a). This would also immensely improve traceability. Ng and Acharya (2009) described how Thermal IR was used during the 2003 SARS out break to identify people who might have been carrying the H5N1 virus. The same concept can potentially be undertaken at piggeries to identify an outbreak or localise animals or groups of animals with flu or disease like symptoms based on their temperature profile.

Temperature may also be related to types of behaviour. For example, fighting animals may have increased temperatures. Monitoring temperature could help with the identification of fighting behaviour (Pedersen *et al.*, 1998).

Temperature has also shown a correlation to the level of pen fouling as pigs may choose to lay on surfaces that are zoned for excreting to satisfy their thermal comfort (Aarnink *et al.*, 2006). In addition, inflammation around wounds may also be able to be identified from heat characteristics giving some indication of fighting, tail biting or injury to the hoofs (FLIR, 2010). Another advantage of using thermal IR is that segmentation of the animal from the resulting images is relatively straight forward if the surrounding temperature is not similar to animal temperature. This segmentation benefit could also be used to document when and where the animal excretes within its enclosure. Despite these benefits, the major problem with Thermal IR video cameras is that their expense which limits their application on farms. However, in future as they become cheaper and operate at higher resolutions, they will be the preferred choice for most applications (Banhazi *et al.*, 2009a).

2.5 CONCLUSION

An animal welfare is the primary reason for its behaviour to be monitored. Hence, the main focus is to identify behaviours that lead up to the event that causes an animal's welfare to be compromised. In particular, the behaviours which may result in long-term adverse effects need to be targeted. To achieve this, first tools to assess animal welfare are required (Smulders *et al.*, 2006). Machine vision systems are able to facilitate this assessment and overcome problems related the level of individual animal attention, labour and welfare assessment. It is possible for a machine vision system to recognise the critical points in an observed behavioural sequence that indicates welfare problem. At one end of the scale the basic motion derived behaviours such as freezing (no-motion) and an animal's movements relative to its environment can be tracked using relatively straight forward techniques. At the other end of the scale are complex behaviours which require more demanding reconstruction, validation and adaptation of models to document behaviour in detail.

Numerous experiments in psychology and pharmacology, involving visual observation of the interaction between humans and machines, and animals and objects were found in the literature. It was found that using vision systems to automatically track or monitor moving objects, such as laboratory animals in research projects, is becoming more common. The majority of commercially available behaviour recognition systems, analysed behaviours that occurred in relation to an animal's spatial position within its enclosure over time. In general, these systems were designed for laboratory-type experiments. Given the small size of the animals, the variables associated with the construction and control of the experimental enclosure could be managed with relative ease. For example, structured lighting could be applied to simplify image processing techniques. However, application of this technology to monitor the health, welfare or production of commercial livestock on farms is a relatively new concept. No commercially available behaviour monitoring system was found that recognised complex behaviours in humans besides a facial recognition system by Noldus (2010) which could identify several facial expressions of humans. However, some research papers did demonstrate the ability to reconstruct relatively complex body movements from

images and then recognise them. Behaviour recognition systems in commercial farm environments require more complex controls and sophisticated algorithms to be useful, as they need to assess large animals, large groups of animals and operate in dirty and often corrosive environments with non-uniform lighting. For these reasons, a number of authors experienced difficulties implementing behaviour recognition systems in commercial farms. Systems which can identify complex behaviours in and between animals are not currently commercially available. Given the techniques used, the performance of the commercial systems reviewed would be questionable if applied outside the laboratory environment. Therefore, further development is required to realize the full potential of vision-based techniques in monitoring and recognising the complex behaviour of livestock in commercial farm environments.

Chapter 3

Methodology: Linking Body Pose and Weight Estimation

Banhazi. T. and **Tscharke, M**. *Image analysis for size estimation*. **(Provisional patent application number: 61346310)**

ABSTRACT

The preceding two review chapters have provided background understanding and a knowledge base to shape the project's direction. The review undertaken in the first chapter concluded that more work is required to further minimise the error of (i) group average daily weight estimates, (ii) individual animal weight estimates, (iii) group weight deviation and enhancing the robustness of the apparatus to function in commercially realistic environments. Development tasks were also required to focus on enhancing automation, minimising invasive environmental control, maximising precision and repeatability during body measurement recovery and identifying and controlling the effect of any bias in estimation.

The review undertaken in *Chapter 2* delved into the behavioural side of the problem, highlighting techniques for pose recognition that are applicable during weight estimation, and detailing the potential behavioural monitoring applications which may be integrated into the software in the future. No commercial system was available to recover the pig's body from images, so techniques were required to be developed, however, this knowledge base provided a starting point for the development of techniques found in this methodology chapter.

This chapter begins with a description of the task at hand, followed by a breakdown of the generic attributes of livestock-scales; providing insight into the various functional elements required in a livestock-scale design. Potential equipment and the working environment is then reviewed and equipment selection, configuration and installation positioning is justified. The individual software methods that were created in support of a scale's functional elements are explained and illustrated.

These methods identified a pig, its posture and determined its live weight from the body measurements extracted from images. During the development of the system the relationship between pose and weight became a focal point as the pose of the animal needed to be well defined and automatically recognisable to minimise uncertainty in body measurements. Consequently filtering techniques were created. After integration, these combined methods formed the PiGUI system which was used to test the hypothesis of the study. Simulated results can be found at the end of this chapter.

3.1 AN INITIAL ASSESSMENT OF THE STATE OF THE ART

A commercially available vision system was tested for its ability to determine the growth of grower and finisher pigs (refer to *Chapter 8 Comparison between PiGUI and a Commercial System*). The problems encountered during trials using the commercial system prompted the system development found in this study. The weight information acquired from the commercial system was not within the 5% precision stated by the software vendor. The system was also not easy to use, calibrate and understand. This raised concerns about its implementation at farm level where technical skills may be limited. Reported weight estimates of the commercial system can be found in Table 60 in *Chapter 8*. The development processes documented in this thesis overcome various limitations in respect to those experienced during testing of the commercially available system.

This study aims to develop a system that can collect a daily sample to represent the daily pen average weight for a population of housed pigs as industry has identified this as being important (Cambell pers. comm.).

3.2 THE TASK AT HAND

The previous review chapters have given insight into the processes necessary to undertake the weight estimation task. However, no formal taxonomy has been created to describe this process. Consequently, a hierarchical approach to the weight estimation process is now defined based on the review findings. The process is as shown in Figure 5 and is a revised version of the taxonomy outlined by Moeslund *et al.* (2006) for human motion capture and analysis to include weight estimation.

The four processes which combine and integrate the hardware, software and data components into the complete vision system to estimate weight are: (i) *initialisation*, (ii) *tracking*, (iii) *pose estimation*, and (iv) *weight estimation* (Figure 5).
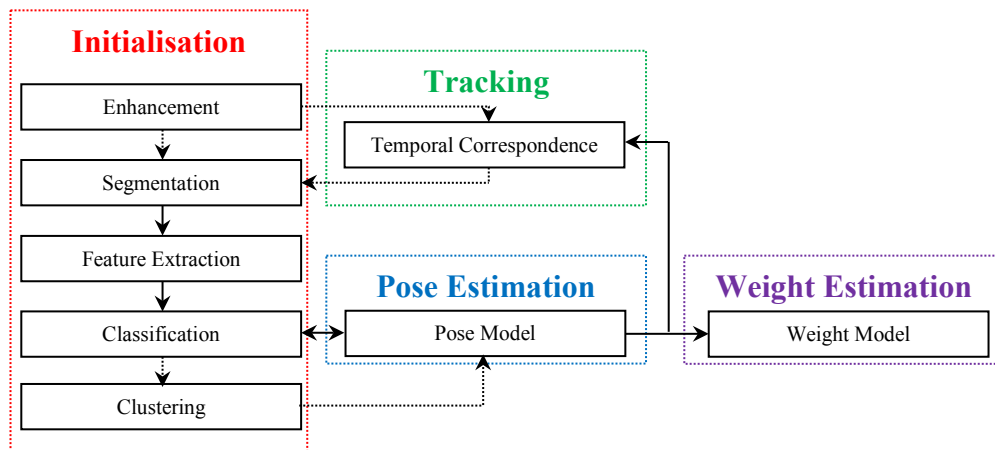
Figure 5: The Process Involved in Estimating an Animal's Weight from Images

These methods can be created and linked together to perform a weight estimation task using vision-based techniques and artificial intelligence. Of these methods, the core components are segmentation classification and the weight estimation models. These three critical stages underline the processes that (i) retrieve the associated animal information from the image along with at least one of its body measurements,

(ii) validate that it is an animal and (iii) perform the weight estimate using a weight-estimation equation. The other methods reinforce the performance of these three fundamental processes.

3.3   SCALE DESIGN CONSIDERATIONS

There are certain functional elements which need to be considered when designing or choosing an appropriate method to undertake the automatic weighing of livestock. The following section breaks down a scale's main function into the smaller functional elements necessary for it to operate correctly within the pen environment. The various design flaws and strengths of theses lower level functions of the four livestock weighing methods presented in *Chapter 1* are discussed and considered in the subsequent project development. The potential causes of weight-related error (bias) from various elements are also highlighted.

3.3.1   A Breakdown of the Scale and its Interaction with Livestock

This section presents a breakdown of interaction between the animal and scale into smaller functional elements. The different essential functional elements which the scale exploits in order to automatically obtain the animal's weight are emphasised.

Occlusion handling is a term given to indicate how well a scale system can prevent two animals interfering with a single sample weight estimate. Through design, one can handle occlusion either passively or actively. Passive occlusion handling involves identifying and removing the occurrence of occlusion in an estimate or sample. Passive methods are generally a software related filter assisting in the removal of errors post-assessment. In a vision-based scale, this is the ability to distinguish between two separate animals that are in contact or obscuring one another from the camera. In a load-cell-based scale, it is the ability to discriminate between the force-time pattern of an individual animal when more than one animal is present on the scale.

Active occlusion handling involves putting procedures in place to prevent occlusion occurring before weight assessment in an effort to automatically single out animals during weight assessment. An automatic cage scale uses the sensors on its gates to control occlusion in an active sense, as do the barriers which can be installed at the feeder. Generally, active methods act as a hardware filter pre-weight-assessment and consequently increase the invasiveness of the method due to physical changes to the animals' environment.

Another design consideration stems from the fact that an animal may not use the weighing device correctly as a result of its *body position.* For example, an animal may not have all its weight on the platform during assessment on a load-cell type scale. Foreleg weighers rely heavily on the way the animal positions itself at the feeder and consequently the distribution of its body weight on its front legs and the platform. An animal that sits to feed or fails to place both hooves on the scale correctly will produce erroneous weight estimates. A vision-based scale may also experience limitations related to body pose as it may require the animal's pose to be quantitative so body measurements can be referenced and repeated to form reliable weight estimates.

Problems also occur when an animal is completely on the weighing device during assessment. Hence, animal behaviour may cause the device to function incorrectly. For example, an animal may jump or bounce on a load-cell type scale (exerting an uneven force), and cause errors in weight samples. This scenario may increase the *sample variation,* which is a term indicating the variation in weight estimates taken from the animal during a weight assessment. The steady state read is the mean value of this variation. A similar effect can occur during weight estimation using a vision system, where partial segmentation of the animal from the image, incorrect extraction of body measurements from the animal's body contour, or movement in posture can cause a fluctuation in weight estimates.

Closely linked to the sample variation is the *sampling period* which is time duration that satisfies the correct function of the weighing device. For example, the length of time to either let the load-cell scale reach a steady weight reading, or the amount of time required to obtain a steady vision-based estimate with sufficient confidence to support its integrity and validity. The sampling period may also depend on the speed at which an animal walks such as during a weight-assessment on a walkthrough scale.

The weighing device may also not zero (tare) correctly before the next animal enters, resulting in a *re-zero error.* In a 2D vision system the (re-zero) calibration relies on the installation height between the camera lens and ground. If the height of waste build-up on the ground becomes excessive, cleaning of the pen space is required to effectively re-zero the instrument. Re-zero on a load-cell type scale occurs when the instrument reaches a steady state within a certain deviation from its initial reading. If the scale maintains a reading outside this deviation, a re-zero error will cause systematic errors.

Prevention of access to the scale or behaviour of the animals towards the scale may cause *bottle necking.* Automated cage-type scales may experience bottle necking if an animal chooses to lay (or sleep) on the scale or a power failure or gate fault occurs. Bias may occur if an animal chooses to lie on the scale over a long period, as during this time the weight sampling of other animals is prevented. Bottle necking may compromise the animal's welfare in a negative flow arrangement if the animal is obstructed from food, water or other stimulant for prolonged periods. Walkthrough scales suffer from the similar congestive problems. Bottle necking may also occur if barriers are used to restrict the access to the feeder to a single animal as certain animals may dominate the feed space. This scenario may also cause bias in measurements and adversely affect animals feeding behaviour (Schofield *et al.*, 1999). Notably this bias may also occur without the barriers in place, constituting a *layout* related *bias*.

Training is directly related to the behaviour of the animal and the invasiveness of the instrument. It is a measure of the willingness of the animal to use the scale regularly. Those systems set up around a feeder or drinker require little or no training as the animal is generally oblivious to the assessment process. Automated cage-type scales generally require training to help the animals understand that the scale is a thoroughfare and to overcome the fear of confinement within the scale during weight assessment.

Identification relates to the individual identification of animals. None of the methods are able to identify individual animals. All methods require radio frequency identification to pair sample estimates with individual animals so that individual weight estimates can be obtained.

Frequency, capacity and service: Frequency refers to the period of time the device requires to take a sample or make an estimate. *Capacity* refers to the number of weight assessments possible by the device at one time. *Service* refers to the number of animals one device can handle. The vision-based scale can view a large area and potentially perform the weight assessment of multiple animals from a single frame making it far superior in its scalability compared to other methods which can only facilitate the measurement of one animal at a time. However, the service of a vision system is limited by the number of feed spaces or the size of the pen space it observes. In certain layouts some animals may religiously use feeders or pen spaces which are outside the view of the camera, which could potentially cause a bias in group weight estimates. Platform type scales located at the feeder such as the ACCU-ARM® Weigh Race cannot service large numbers of animals as one system can only facilitate 12-15 pigs. Therefore, facilitating the multiple feeder spaces encountered in large group sizes is not feasible. Automated cage scales can service large group sizes of up to 500 animals effectively, however, they have limited scalability as they can only assess a single animal at a time. Cage scales may also be limited in terms of frequency if using the scale is optional for the animals.

Manoeuvrability refers to how easily the device can be moved by farm staff to a new location. The major benefit of a vision-based scale is that it can be effectively placed at any location without the need for additional infrastructure or any physical contact between the scale and the animal. A vision system is the only automated system to have this level of flexibility as the unit-weight of a vision system and its peripheral mounting equipment are considerably less (or negligible) in comparison to the weight and size of the alternatives. Some smaller load cell-type scales have wheels to assist with transportation, however, once placed at their destination they are often required to be fixed to the ground to prevent movement over time.

Safety relates to the level of risk the device poses to the animals and farm workers. Additional stress or injury can occur from machine controlled gates which have limited intelligence to constrain the animal correctly and do not have intelligence to sympathise with animals should they become trapped. An automated cage scale may in some cases, also cause negative disruptions to the animals' routines and feeding behaviour due to bottle necking. Vision systems have no moving parts so there is negligible safety risk to operators or animals during system operation.

Determining the bodyweight of livestock using manual methods is dangerous and physically demanding. Animals which have not been manually handled or exposed to new environments or confined spaces before, are likely to show some level of resistance, become stressed, and begin to exhibit defensive behaviours which may compromise worker or animal safety. For these reasons, and the inefficiency involved in weighing a large number of animals, the weight assessment of animals using this technique is undesirable. Studies report that 6% of livestock related trauma cases were caused by simply standing in close proximity to a livestock animal

46

(Criddle, 2001). Mechanization of agricultural processes have also been attributed to increases in injury in the agricultural industry (Erkal *et al.*, 2008). Therefore, systems developed for agricultural purposes should always keep safety as a high priority.

Maintainability relates to the level of maintenance required to ensure the device functions correctly. Load-cell type scales are more susceptible to damage as they are in direct contact with the animal and its environment. The physical presence of the scale in the pen also causes it to be a target for misuse by the animals. In addition, the scale and surroundings require frequent cleaning to prevent any measurement errors arising from the build-up of manure (White *et al.*, 2004). The benefit of a foreleg weigher is that it requires less frequent cleaning compared to an automatic cage scale and the animal is not required to be confined during weighing (Ramaekers *et al.*, 1995b). The vision system may require periodic cleaning of the lens if an air curtain is not present. An insect deterrent could also be used to prevent insects from landing on the lens and equipment. Certain mechanised systems may also require routine inspection. For example, daily observations may be required to prevent any adverse effects caused by bottle necking in a negative-flow cage-type system as animals are forced to use the scale as a thoroughfare.

The growth of (i) individual animals and (ii) the growth of animals as a group can be obtained from a continuous and automatic weighing process. However, as all automated weighing techniques rely on the cooperation of the animal to initiate the assessment, it is not possible to guarantee that a weight assessment of each animal will occur each day. Consequently, various forms of *estimation bias* may occur in a daily group-average estimate as a result of:

- Certain animals re-visiting the scale area more than others and remaining in the scale for longer durations
- Missed weight recordings due to multiple animals in the scale area causing errors
- Missed weight recordings due to certain animals not visiting the scale area
- Large daily weight fluctuations from excessive fouling, health or nutrition problems
- Manual removal of sick or market ready animals from the pen

Identification bias may occur in a vision-based scale as certain animals may be filtered out of analysis or sampled more frequently during the filtering process. For example, Lines *et al.* (2001) noted that the error handling used to identify and pass image information for mass estimation has the potential to cause bias if favouritism is inadvertently given to a particular fish of certain characteristics (such as size or shape) within the population. Other contributing factors related to identification bias include the gender of the animal and the variability in body type as some animals have larger shoulders where as others have larger posteriors (Baxter, 1984; Ramaekers *et al.*, 1995b). Consequently, different filters accommodating different classes of body type or appearances may be required as there is evidence that specific estimation equations are required for different breeds of animals (Brandl and Jørgensen, 1996; White *et al.*, 2003).

3.3.2 Scale Positioning and Behavioural Interaction

The design considerations presented in the previous section have highlighted how important it is to consider the interaction between animals and the scale within their environment, as this may have a major effect on how well or often weight sampling will occur. Therefore, in the early stages of development a behavioural assessment should be undertaken between a proposed automated livestock handling or monitoring tool and the animal. Frameworks coordinating the design of automated management tools have been formed to assist with the efficient development and implementation of systems to eradicate pest species in Australia (Bengsen *et al.*, 2008). The underlying principles of such frameworks can be adopted to accelerate the automation of livestock handling and monitoring processes. A fundamental property of the framework is extensive knowledge of the behaviour of the animal, as the animal must be a willing participant in what will be an automatic process. Thus, the behaviour of the animal needs to be considered in the design stage, as it may provide opportunity to simplify solutions. For example, some designs exploit a unique physical ability or instinct of an animal to assist in its capture. In such a system, strategic placement of the apparatus in the animal's environment may also maximise the likelihood of the animal's behaviour occurring.

A second and equally important stage in the framework is discovering or obtaining detailed biometrics of the animal which can again lend itself to many opportunities in the system's design as a form of validation or identification from unique physical constraint(s). Weight, body measurements, sound and appearance all assist in the correct identification and validation of different species. For example, Dunn *et al.* (2003) demonstrated how several different species of animals were classified using a visual inspection of their shape. A third and fundamentally important stage which can easily be overlooked is determining the perception of the technology in the public arena and how the system may impact or appear to impact the welfare of the animal(s) adversely.

Fortunately, in livestock production the automation process is somewhat simplified as the animals environment can generally be controlled to better accommodate their needs and basic instinctive behaviours, such as those that arise from the need for food and water, can be exploited to assist in gathering data automatically. A systems-based account of the requirements of an integrated livestock management system can be found in Wathes *et al.* (2001). The four different automated systems described in *Chapter 1* either strategically manipulate the layout of the enclosure or use an existing feature within it to automate the weighing process. Although the vision-based scale, foreleg weigher and the platform race are not restricted to the feeding and drinking space, they can effectively automate the sampling process by exploiting the need for the animal to feed or drink at these locations each day (illustrated in Figure 6 (a) and (c)). Often the feeder is the desired choice as it has been found that a pig will spend four times longer at the feeder than the drinker (Ramaekers *et al.*, 1995a). Feed barriers, also known as stalls, may be installed at these locations to restrict access to the feeder and drinker to a single animal (Figure 6 (a)). These barriers prevent additional animals from affecting the instrument during a weight reading and fighting between animals over access to feed, which also affects weight reading.
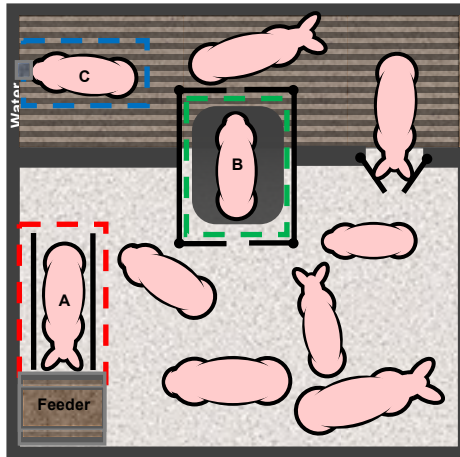
Figure 6: Examples of Different Weighing System Layouts/Locations in Piggeries Feeding Stall (Feed Barriers) (A), Walkthrough/Automatic Cage (B), Drinker (C)

Walkthrough scales and automatic cage scales require adjustment to the enclosure in order to channel the animals through the instrument (illustrated in Figure 6 (b)). There are two different types of layouts for automated scales of this type; positive and negative flow. A negative flow system is strategically placed within a network of smaller pens or paddock sections to provide a single thoroughfare between feed, water, space or other stimulant. Alternatively, in a positive flow system, animals can always access feed and water, and choose whether or not to pass through the scale (Donkersgoed, 2004). However, the thoroughfare may be shut periodically to train the animals to use the scale or to obtain more precise individual or group weight estimates on particular days (Donkersgoed, 2004).

These layout and behavioural considerations are important as the interactive behaviour between the animal and scale can contribute to bias (Chedad *et al.*, 2000; Stacey *et al.*, 2004). Animal curiosity, physical limitations or territorial behaviour may have an adverse effect. Turner *et al.* (1984a) and Mollah *et al.* (2010) discuss these factors in their scale design as the shape and location of their scale within the environment needed to cater for various physical limitations of the animals to provide automatic, daily, unbiased weight estimates.

3.3.3   Practical Precision of the Weight Estimation Task

In addition to the design considerations, the variability associated with the body weight and size of livestock was reviewed to determine what level of accuracy could be considered practical precision.

3.3.3.1   *The Effect of Gut Fill*

Gut fill was used as a guide to determine a practical error margin for measuring the weight of individual pigs across the course of a day. The amount of an animal's total body weight which is made up of food, digesta and faeces is known as its gut fill (GF) and is responsible for the majority of the animals day-to-day weight variance. Here two levels are considered: (i) where the gut is assumed to be the healthy mean weight (live body weight LBW) and (ii) empty (empty body weight EBW) where the digestive systems is empty. Therefore, an acceptable range of error in an individual weight measurement can be half of the gut- fill (the weight difference between LBW

49

and EBW (De Lange *et al.*, 2003)); assuming the animal always has access to food and water. The digestive systems and gut-fill of several different livestock species have been modelled, however, some ambiguity remains as to what percentage the gut-fill is relative to the LBW. This is understandable considering the many input variables involved in the calculation of gut fill such as animal breed, digestive time, conversion efficiency, diet and age which contribute to the density, duration and amount of storable waste able to be treated by an animal's digestive system at any given time. For example, the gut-fill of pigs was attributed to be approximately 6% of the pigs' LBW by (Boisen *et al.*, 2000) and 5% by Agricultural Research Council (ARC) (1981) and Stranks *et al.* (1988). Alternatively, pigs at 20 and 100 kg LBW have been shown to demonstrate GF from 9% to 4.5% respectively by both Whittemore *et al.* (1988) and Lorschy *et al.* (1997). A predictive equation for gut-fill is provided by De Lange *et al.* (2003) derived from Whittemore *et al.* (1988) and Lorschy *et al.* (1997) :

$$GF = 0.277 \times LBW^{0.612}$$

Therefore the error bounds for estimating the weight of pigs (ΔW) can be given by:

$$\Delta W = 0.5 \times GF = 0.1385 \times LBW^{0.612}$$

And, one could reasonably expect that two LBW weight samples of the same animal taken at separate times within a 24hr period should be within ΔW of one another. Some errors for different weighing methods relative to LBW are shown in Table 2 in respect to error posed by 50% gut fill (second row of Table 2).

Table 2: Allowable Error in Individual Weight Estimates Based on the Predictive Gut Fill Equation Presented by De Lange *et al.* (2003)

LBW (kg)	20.0	40.0	60.0	80.0	100.0	120.0	140.0
GF Error ΔW (kg)	0.9	1.3	1.7	2.0	2.3	2.6	2.9
Scale Error ΔW (kg) ±1%	0.2	0.4	0.6	0.8	1.0	1.2	1.4
Vision ΔW (kg) 2.1% (mean)	0.4	0.8	1.3	1.7	2.1	2.5	2.9
Foreleg ΔW (kg) >5%	1	2	3	4	5	6	7
Proportion of GF Error to LBW (%)	4.5	3.3	2.8	2.5	2.3	2.2	2.1

According to De Lange's equation, as animals grow the proportion of their gut fill to LBW weight decreases and thus contributes to a smaller variation in total weight. This can be observed in the last row of Table 2. Consequently, as the LBW increases, the precision in weight estimation also needs to increase. Generally scales that utilise load-cell technology can estimate the weight of an animal to ±1% accuracy. Given the variability of weight due to gut fill, these load-cell type scales perform well within what can be deemed acceptable error (Table 2). This level of precision may even be considered of little relevance in pig production due to the fact that an animal's weight can fluctuate dramatically within a short period of time (Brandl and Jørgensen, 1996). Some semiautomatic vision-based weighing devices have been able to perform to 2.1% mean error which is also within the error bounds attributed to gut-fill in the 20 to 140 kg weight-range (Minagawa *et al.*, 2003).

To give a preliminary indication of how quickly the weight of groups of animals may vary, a small observational study was performed. Three groups of animals were moved to a clean pen area for a 40 minute period. No feed was available during this

time. After moving the animals back to their enclosure the solid waste was collected and weighed to the nearest half kilogram. It was found that over this small time frame 0.47 kg per animal was lost for the first group containing 15 animals with an initial average weight of 97.10 ± 4.77 kg. Group 2 containing another 15 animals had a weight loss of 0.57 kg per animal with an initial group average weight of 95.23 ± 4.44 kg and the last group of 11 animals had a 0.41 kg loss in weight per animal with an initial average group weight of 85.05 ± 6.26 kg. It is important to note that the weight of liquid waste was not obtained during the test which would have further contributed to the amount of weight loss. The proportion of each animal's contribution to the total waste was also not documented. Therefore, it is not known whether individual animals contributed a significant amount of the total waste collected.

Table 3: Weight Loss from Solid Waste of Three Groups of Finisher Pigs over a 40 Minute Period

No. Pigs	Group Average Weight (kg)	Waste (kg)	kg Loss / pig
15	95.23	8.5	0.57 (0.6%)
15	97.1	7	0.47 (0.5%)
11	85.05	4.5	0.41 (0.5%)

A group of 17 smaller pigs with an average weight of 28.8 kg were also weighed twice within a 40 minute period. During this time the collective weight lost per pig was 0.7% of their starting weight as shown in Table 4.

Table 4: Weight Loss of a Group of 17 Grower Pigs over a 40 Minute Period

No. Pigs	Group Average Weight (kg)	kg Loss / pig
17	28.79	0.21 (0.7%)

These figures indicate the GF does alter weight within a short period of 40 minutes by solid waste alone. Therefore, it was plausible that given a longer duration for the test the weight loss attributed to gut fill would have reached the levels defined by De Lange's equation, however, weight levels are less likely to occur closer to EBW. As a guide half of the total GF as given by De Lange's equation has been used to define the expected level of precision of a device performing the assessment of individual animals over the course of a day. Ideally weight estimates will fall within this range given an animal's actual LBW.

3.3.3.2 *Potential Morphological Effect on Precision*

A critical component of the identification of an animal is its shape and appearance. It is well known that each animal will vary geometrically depending on its genetic history (White *et al.*, 2004). However, a not so obvious fact is that the environmental conditions to which the animal is exposed may cause immediate variation to its geometry during its growth cycle. Allen (1877) and Bergmann (1847) created two separate rules based on a similar underlying theory that the climatic conditions to which an animal is exposed, will morphologically alter its appearance. Allen's rule was based around the observation that animals exposed to colder climates had a reduction in the size of their extremities compared to that of animals exposed to warmer climates. The underlying rational for the rules are that in a colder climate an animal will adapt such that it has a smaller surface area to conserve energy so that it is less susceptible to a reduction in heat transfer. The inverse is also true where, in

warmer climates, animals will adapt by growing longer appendages to create more surface area to dissipate heat. Bergmann's rule follows a similar sentiment, along with the proposal that the temperature also slows the sexual maturity of the animal, resulting in a prolonged growth period to reach full maturity. Although the physical change related to size is most relevant in this study, other forms of adaptation have also been observed in order to acclimatize the body such as insulation in the form of hair, fur, and tissue density.

To assess the validity of these rules, Weaver and Ingram (1969) conducted a study on a litter of large white pigs which were divided into two separate climates (5°C and 35°C) to determine whether any morphological changes would be experienced during their growth. There were apparent differences in the body shape between the animals housed in the 5°C and 35°C enclosures. Although the animals shared similar growth in terms of weight, the animals housed in the 5°C climate were shorter, stockier and had shorter tails and smaller ears (effectively half the surface area). For comparative purposes, an image of a pig from the 5°C and 35°C housing are shown in Figure 7 from Weaver's study.

Figure 7: Morphology in Pig Growth when Exposed to Extreme Temperatures
35°C Conditions (Left) and 5°C Conditions (Right) from Weaver and Ingram (1969)

Due to Australia's harsh and variable climate and the fact that pigs cannot regulate their thermal comfort easily (as pigs cannot sweat), most piggeries have some form climate control within their buildings or shelters, such as shade, sprayers or air-conditioning. Therefore, it is believed that the morphological effect in the controlled experiment presented above would not occur to this extreme in practice, however, it may have some effect (such as seasonal variation in body geometry), so it is worthwhile noting.

3.4   CAMERA SELECTION

The elements and installation aspects that will help make the developed system function automatically and appropriately have been determined. Limitations related to precision have also been discussed. Therefore the data capture device can be selected with these and the following considerations in mind: (i) spectral band recorded, (ii) camera configuration and (iii) installation environment.

There are various types of sensor which can be used in this application. Selection and justification of the most appropriate type of apparatus to obtain the information is now discussed. Potential sensor configurations include 2D, 3D perspective, 3D stereo. The potential recording environment conditions include day, night and thermal conditions, and the intensity recorded includes black and white, colour, NIR, IR, UV and thermal.

3.4.1 Spectrum Sensed

An image is often thought of as a sensor based re-construction of incident light (irradiance) in the visible range, however, there are many different frequency ranges which are sensed to create an image (see Figure 8). The common wavelength ranges which use the sun's irradiation to form images are visible light (VIS 400-700nm), ultra violet (UV 200-400nm) and Infrared (IR 700nm-1mm) of which Near Infrared (NIR 700-1400nm) is used (Figure 8). The sensors which operate in the visible spectrum have been used to grade and assess based on colour, appearance, body measurements and mass in both agricultural and manufacturing industries. Examples in agricultural industries are meat grading and inspection, fruit grading, animal tracking and behavioural studies (Bull, 1993; Brosnan and Sun, 2002; Chao *et al.*, 2002; Chao *et al.*, 2000; Stajnko *et al.*, 2004; Dusenbery, 1985; Harmsen and Koenderink, 2009; Shao *et al.*, 1998; Shao and Xin, 2008).

A disadvantage of using vision equipment that operates in the visible spectrum is that the lighting arrangement of the scene is often uncontrollable and may inhibit the function of the system if not properly designed or compensated for by using some form of environmental control. Spectral band-pass filters can be placed in front of the imaging sensor to restrict the observable wavelengths to a specified range. This technique can be used to identify an object of a certain colour by filtering out wavelengths of light from all other bands. Most cameras have an infrared (IR) cut-off filter which reflects near infrared (NIR) light away from the sensor such that the light in the IR range does not impact the visual appearance of the image to the human eye. However, NIR imaging can be used to an advantage during the day and night. During the day NIR can be used to help segment objects which have different textural qualities but the same colour. During the night sensors sensitive to NIR can generate images effectively with the help of illuminators. However, as pigs are generally asleep and are not active at night, the benefit of using NIR and structured lighting, day or night, for weight estimation purposes is negligible. There is more merit in having this additional equipment to record feeding behaviour in low light conditions such as in the morning and afternoon or occasionally during the night. Having additional equipment will also reduce the reliability of the system due to additional parts and increases the system's installation and maintenance requirements. If structured lighting were to be used it would be desirable to use a wavelength that would not affect the animals. There is still debate as to the colour range in which pigs are believed to be able to see (Lomas *et al.*, 1998). Pigs are believed to have the basis for dichromatic colour vision with each of the two cones having an average maximum sensitivity of 439 nm and 556 nm (Neitz and Jacobs, 1989).

Other devices record images from radiation produced from the source directly. For example, sensors that acquire thermal infrared (IR 1400nm to 1mm) use radiated heat

from objects to form images (thermograph). These images also contain feature information on the temperature of the target object. This technology has been explored in livestock applications. For example, Stajnko *et al.* (2008) assessed different age classes of Simmental cattle for parameters that could be used to determine their live weight using thermal imaging techniques. Thermal imaging was used to overcome segmentation issues using RGB images surrounding the non-homogeneous nature of the cattle's appearance (brown, red and white). The environment was controlled to some extent by placing the bull in cold-concrete surroundings (Stajnko *et al.*, 2008). Schaefer and Tong (2000) determined that the thermal radiation emitted from livestock can also be used to estimate the animals composition. Such technology may also be more applicable to the weight estimation of sheep where the fleece would otherwise distort weight estimates when based on visual appearance alone.

Alternative imaging techniques include X-ray, Computer Tomography (CT), Positron Emission Tomography (PET) and Magnetic Resonance Imaging (MRI) which are created by absorbing the radiation which passes through the object. These are used for precise diagnosis of the organism while stationary or sedated. These methods can provide an accurate means for modelling *a priori* data such as body measurements both internally and externally. For example, MRI, CT and X-ray are known to be powerful tools for the estimation of muscle and fat tissue in pigs and sheep (Vangen and Jopson, 1996; Mitchell *et al.*, 2002; Kvame and Vangen, 2006).
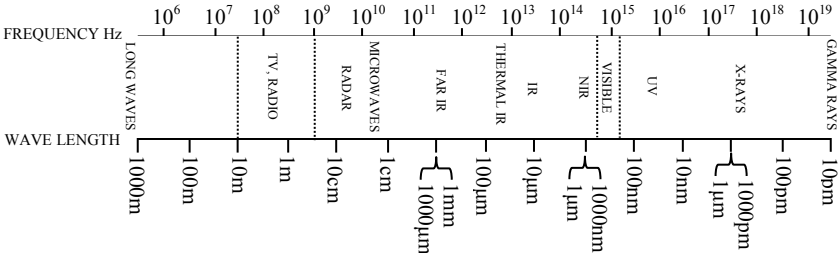
Figure 8: Electro-Magnetic Spectrum

3.4.2   Perspective View and Configuration

In addition to the selection of the image sensor device, the camera configuration and its installation location must also be considered. There are predominately three methods, (i) 2D, (ii) 3D perspective or (iii) 3D stereo, which can acquire information from an animal's body through an image. These three methods come under the broader study area of photogrammetrics.

Conceptually, a 2D image of a pig is a single plane record of the actual physical body of the animal in a static pose. From different viewing angles the shape and appearance of the pig (in an image) will appear completely different. Each one of these 2D observations is a compressed representation of the animal's body which describes a certain proportion of the entire body. An accumulated set of observations covering all perspectives of the animal can be used to 'virtually' illustrate the animal in three body measurements (Wu *et al.*, 2004). The number of different animal poses that can be recorded by these means is extensive. Consequently, in the interest of

efficiency, the camera configuration chosen in this study needs to only accommodate a range of this body and pose information which enables weight estimates to be determined to practical levels of accuracy for both individual pigs and groups of pigs.

Although it does record the most detailed representation of the animal, a 3D stereo reconstruction requires a larger quantity of data storage and imaging equipment and thus also increases demand on the processor and peripheral computer equipment. In addition, as the extracted body measurements of an animal depend on its posture, a weight-estimation equation built from the body measurements taken from multiple cameras (or cameras in motion) will require the animal to maintain a suitable pose for all the camera's perspectives to prevent missed weigh events or motion-based time delay errors.

The top and side views (3D perspective) have been used in several machine vision applications in this area. Yang and Teng (2008) use a side and top view of the pig to determine the live weight of pigs. This is arguably a poor design choice as, in practice, a side view will increase the requirement for infrastructure, maintenance, and decrease the likelihood of a weight assessment event taking place.

In order to obtain accurate measurements of the animal's body from a 2D perspective side-view, the distance the camera is away from the animal needs to be determined or the animal must be positioned parallel to the lens of the camera at a known distance (refer to Section *3.5.3 Projecting Extracted Pixel Dimensions to Metric at Ground Level*). This distance can be recovered using a laser telemeter (Tasdemir *et al.*, 2011; Negretti *et al.*, 2007a) however, such equipment is likely to come at an additional cost as well as make the system more complex and sensitive during calibration. To overcome these calibration issues a barrier may be used to keep each animal a fixed distance from the camera during a weight-assessment from the side view. This configuration is inherently prone to issues, however, as the vision system will be in close or direct contact with the barrier, the animals' and the animals' environment and therefore would undoubtedly demand frequent cleaning, be more susceptible to damage and potentially nullify its non-invasive quality. Another inherent problem associated with the side-view is occlusion caused by animals obscuring one another from the cameras view.

The 2D top view has also been used to extract the body measurements of pigs from images by many authors (Schofield, 1990). Refer to Section *1.3.1 Livestock Body Measurements and Their Correlation to Weight* for more examples. The top view is the preferred perspective to acquire the body measurements of the animal for the following reasons: (i) more than one animal can be assessed in a single image, (ii) the distance of the animal's body measurements are always relative to the ground, (iii) the background surrounding individual animals is less likely to contain other animals and therefore provides better contrast between the animal and background (enhancing the chance of correct segmentation), (iv) the background is more likely to be uniform as issues presented by direct solar radiance and surrounding objects are minimised as the camera is facing downward (v) the system does not have to come in close proximity with the animal and its surroundings, (vi) the system is more likely to observe the animals in a pose suitable for weight estimation as varying body measurements caused by articulated joints (legs) are hidden from view, (vii) the

animals can be tracked relative to their location within the pen and finally (viii) the entire enclosure or a region of interest within the enclosure can be observed without obstruction. The main limitation of the 2D top view is that the height of the animal is required (or could potentially be estimated) to obtain an approximation of the animals real-world body measurements. Where weight estimation is concerned, the effect that height has on weight estimation precision also needs to be established and, if required, potential 2D height recovery techniques need to be reviewed.

3.4.3 Hardware Selection

Ideally, the chosen imaging device would be a camera device operating in the thermal infrared band due to the potential ability to determine aliments of the animal as well as assisting in segmentation. However, due to the high cost of thermal imaging equipment its use on-farm is currently not feasible as short to midterm replacement is likely. However, the algorithms developed to extract and interpret the pig-related information present in the images will be similar regardless of imaging device. Therefore the essence of this research does not need to be constrained by the image format presented by the chosen imaging device, as the method created to automatically extract and interpret the information within the images can be applied to images acquired from other imaging devices (such as thermal) in future with minor modification.

The main benefit of using a 3D stereo configuration is that it virtually recreates the surface of the animal and thus the height information and other dimensional information can be recovered precisely. However, there are several reasons why a 3D configuration may not result in the optimum solution. Reasons include increased system cost, increased processing burden, further complication of processing tasks, increased storage requirements, increased infrastructure and calibration, potential to decrease the system's non-invasive nature (may require a stall) and inability to assess multiple animals at the same time.

Therefore, to avoid potential over-complication of the system, first the weight estimation potential of a 2D configuration should be revised to determine whether results can be achieved reliably, within practical accuracy and comparable to conventional weighing method such as those obtained from electronic livestock scales.

By fixing a 2D camera system's view to observe the animal from above, the observed scene is greatly simplified which results in four flow-on benefits: (i) a number of the body measurements of the animal become hidden and therefore less information is required to describe it, (ii) these hidden body measurements are the most variable (such as the legs) which ensures that the observed body measurements will be easier to repeat while the animal is standing, (iii) consequently less data storage and processing is required, and (iv) there is less chance of pigs obscuring one another from the camera. However, this fixed viewing constraint comes at the cost of losing some body information. A task for this study is to determine whether this lost body information is necessary to achieve practical precision in weight estimates for both groups and individual animals.

Historically, most estimation equations are based on measurements taken physically from the animal's body and work on the basis that the animal is an approximation of a cylinder and thus a length and girth measurement is required. However, a fixed two dimensional vision system can only observe one perspective and therefore is not able to determine the girth measurement taken around the circumference of the main axis of the body behind the front legs. Therefore, in this study the animal's width becomes an approximation of the girth measurement and the area of the animals back is an approximation of the animal's three dimensional body; a compressed representation of the 3D object. To obtain the approximate real world body measurements of a pig using the 2D system an actual or estimated height measurement will be required. The camera should also have a wide angle lens and where possible have onboard post processing to correct for off-angle effects (image distortion) such that it can observe a large pen area from a small height with a high resolution.

3.5 OVERVIEW OF THE SYSTEM DEVELOPMENT PROCESS

This section provides an executive summary of the software development undertaken in this PhD and forms the remainder of this methodology chapter.

Datasets were collected and analysed off-line to: (i) define the strength of the various body measurement(s) in respect to estimating weight (*3.6.1 Modelling*), (ii) build and validate the weight estimation models (*3.6.1.1 Modelling the Weight-Estimation Equation*) and to (iii) construct the body measurement (*3.5.4 Filtering the Extracted Body Measurements for Weight Validation*) and shape filters (*3.5.5 Filtering the Shape for Pig Recognition and Pose Validation*).

Many of the methods used to extract the data from videos in order to build the weight estimation models were subsequently used in the online version of the software. Matlab with image acquisition and processing toolboxes was the chosen IDE to create the software (MathWorks, Inc., Natick, MA). In Matlab, function files (m-files) encapsulate code-instructions, including those instructions required to acquire images from the camera, create a graphical user interface, perform operations on the image matrix and to write the extracted information result to text file. The image-matrix operations developed had the specific functions to: (i) segment, (ii) extract, (iii) convert, (iv) track and validate the (v) shape and (vi) body measurements of a pig within the image.

The segmentation operations were required to first separate the animal-related information from the background information within the image and then to prepare the animal-information for feature extraction (see Section *3.5.1 Segmentation Development*). These functions followed with the feature extraction operations responsible for determining points of reference along the animal's body contour and extracting the corresponding body measurements (see *3.5.2 Feature Extraction Development*). A conversion stage then undertook the task of converting the recovered body measurements from pixels to millimetres to approximate the real world body measurements of the pigs and to free equation coefficients from projection errors related to installation height (see Section *3.5.3 Projecting Extracted Pixel Dimensions to Metric at Ground Level*).

Filtering functions were then produced to regulate the system's input and output based on perceived shape and measurements relative to weight (see Section *3.5.4 Filtering the Extracted Body Measurements for Weight Validation* and Section *3.5.5 Filtering the Shape for Pig Recognition and Pose Validation*).

Finally, a tracking stage determined the appearance-based attributes of the pig within the image to assist with the recognition and subsequent re-location of the pig between image frames (see Section *3.6.6 Determining the Appearance-Based Attributes of Pigs for Tracking*).

These functions were integrated to form the piGUI system.

The following sections discuss these functional elements of the piGUI system in greater detail. The effect that these functions have on weight estimation is presented when appropriate in Section *3.6 Simulation Results* in the later part of this chapter, followed by the chapter conclusions.

3.5.1 Segmentation Development

Early segmentation attempts for the basic prototype system were based on the articles Kollis *et al.* (2007) and Wang *et al.* (2008) and involved the segmentation of the animals using thresholding techniques.

Thresholding segmentation attempts progressed from manually selected thresholding, to adaptive thresholding of the entire image and then to localised thresholding of various image subsections (Otsu, 1979). Thresholding is a technique adopted for its simplicity and because others had used it in the same application area. However, this technique proved to be cumbersome. The problems associated with these thresholding techniques reflect those encountered by Brandl and Jørgensen (1996) who decided to manually trace the contour of the pig's body after the selection of manual thresholding did not find the precise contour of the pig's body. Dirt on the pig's back, poor contrast between the pig's body and background often lead to poorly defined contours and incorrect association between the animal's back and the background. An additional classification routine was also required to identify and remove non-pig objects that remained in the resulting image after thresholding. It became apparent that this technique required controlled lighting and environmental control such as providing a black background and clean animals for it to work reliably. These factors indicated that the thresholding segmentation technique was not well suited to a commercial environment for the purpose of weight estimation. Segmentation development focused on gradient-based techniques which had potential to find the precise outline of the pig's body inside the image.

3.5.1.1 *Using the Image Gradient to Determine the Frames that Contain a Pig*

Prior to segmentation, a processing task was created to determine when a pig was likely to be present within the image. This task needed to quickly assess each image (accept or reject it) so that: (i) time was not wasted assessing images which had little chance of obtaining the correct information and that (ii) the processing time did not inhibit the flow of the incoming data stream and introduce the need for buffering. Thus a fast filtering process was required to make this discrimination between frames

so that the real-time capabilities of the application were not compromised and information throughput was maximised.

Investigating the intensity surrounding the animal brought about a new method to identify the animal named "the cross hair method". This low level filtering method targeted large steps in intensity which indicated a transition between a foreground object and background object. The cross hair method aimed to reduce the processing time by observing the intensities at four line segments of the image shown as the different colours in Figure 9.
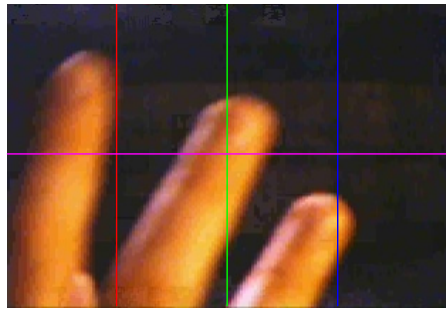
Red = Section 1 (Front),
Green = Section 2 (Middle),
Blue = Section 3 (Rear),
Magenta = Section 4 (Length)

Figure 9: Example Image of the Cross Hair Method
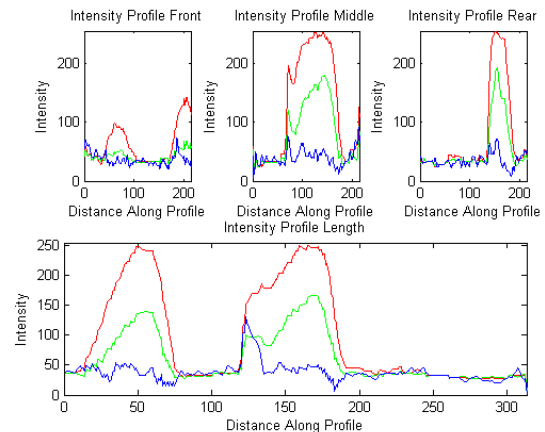
Figure 10: Pixel Intensity Profile Along the Line Segments of Figure 9

Figure 10 shows the output of the intensities of the various sections of Figure 9. The magenta line in Figure 9 begins in the background and the RGB intensities increase as the magenta line crosses the fingers. Comparing this magenta line directly with the 'intensity profile length' in the bottom of Figure 10, the two fingers can be clearly observed as jumps in intensity (red is dominant).

This can be used to identify the pig's presence in the field of view of the camera. The following Figure 11 is an image of the background directly before a pig walks into the cameras field of view (FOV). This frame may also be used to subtract the proceeding good frame of the pig. The histograms and intensity profiles are shown in Figure 12. As expected the intensities are all very low referring to the darkness of the image.
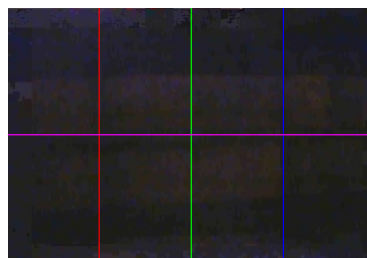
Figure 11: Background Image of the Cross Hair Method

59
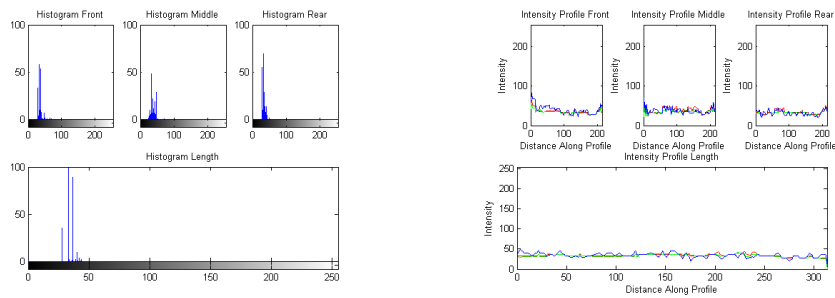
Figure 12: Histogram and Pixel Intensity Profiles of the Line Segments of Figure 11

Figure 13 shows a pig entering the FOV. The rear image section represented by the blue line has peaked and the respective histogram (Figure 13 (b) top right) also indicates that there are high intensity pixels present. The image section represented by the magenta line (length) has also peaked indicating that some portion of the pig was in the middle of the frame. The progression of the pig across image can be monitored using this method, by analysing the position of the peak across the image's x-axis (distance along profile: see bottom of Figure 13 (c)).

| (a) | (b) | (c) |
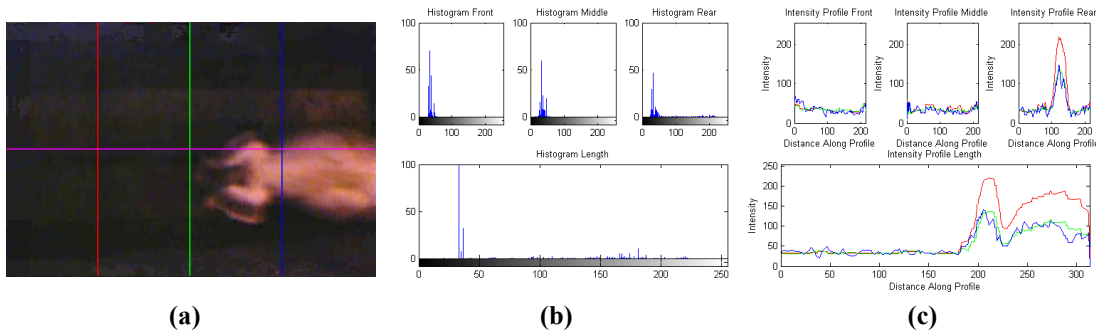
**Figure 13: (a) Pig Entering the FOV; (b) Histograms of the Line Segments in (a);
(c) Pixel Intensity Profiles of the Line Segments in (a)**

Once the pig was entirely within the FOV (Figure 14) the approximate width of the pig could be recorded by determining the step up and down in intensity along the green line section in the middle of the image (Figure 14 (c) top middle). The midpoint of this width was identified and an image section relative to the x-axis of the image was acquired through this point. The approximate length was determined by identifying the step up and down intensity along this line (Figure 14 (c) bottom). A ratio between the length and width was then calculated to determine whether the image was likely to hold a pig shape, prompting further analysis. The half brown pig shown in Figure 13 and 14 is similar in colour to the background, highlighting some of the complexities involved in the identification and segmentation task. The profile of the length (magenta line) shows the intensity drop off dramatically in the brown coloured half of the pig (Figure 14 (c) bottom).

60

(a)   **(b)**   **(c)**
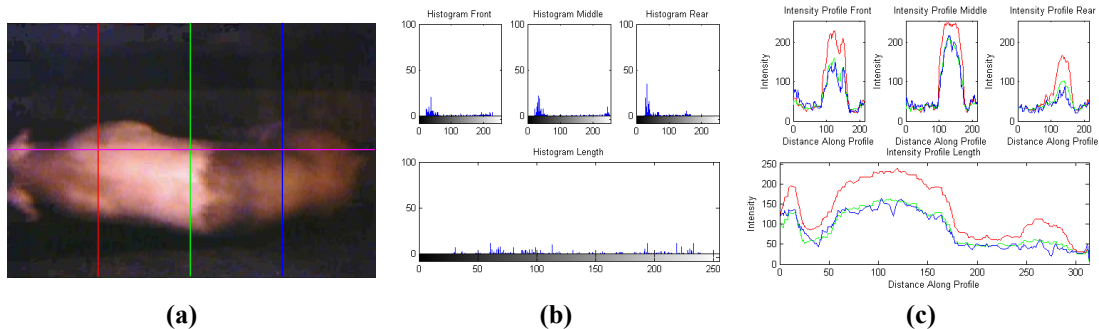
Figure 14: (a) Pig Inside the FOV; (b) Histograms of the Line Segments in (a);
(c) Pixel Intensity Profiles of the Line Segments in (a)

This task was effective at identifying the pig when it was in the FOV of the camera and gave an early indication of the size of the pig, where size was determined by finding the distances between edge points representing the transition between a foreground (pig) and background pixels along the width and length sections. Further investigation of this method led to the development of the algorithm used to obtain the complete shape of the animals contour (presented in the following section).

61

3.5.1.2 The Final Segmentation Method

The software process undertaken to extract the contour of pigs after the system is commissioned is shown in Figure 15 below. Figure 15 also contains references to Figures found later in this section that illustrate various stages in the process.

Function (Image, Trim %, Filter Size)
Create array for the filters movement
Determine the size of the image
Determine the middle of the image — Figure 18
Determine the gradient along the middle section of the image
Determine the maximum gradient along the section
Store the co-ordinate
Minimise the gradient values around the first maximum
Find the second maximum gradient along the section
Store and sort the co-ordinates — Figure 19
Check and make sure that the starting co-ordinates of the filters are within the image body
Create memory space for the top and bottom arrays
Assign the starting points for the filters — Figure 20
Execute a loop that increments from the middle of the image outward
Check and make sure that the starting position of the filter is within the image body
Determine the gradient within the four filters
Record the co-ordinate point of the maximum gradient in the respective filter array — Figure 21
Concatenate the recorded points to form the top and bottom — Figure 23
Determine the orientation of the object using the midline — Figure 24
Trim the curve taking into consideration the orientation of the object and the Trim % — Figure 25
Assign an artificial curve to either end which takes into consideration the orientation of the object and encloses the shape
Create a spline curve based on a number of evenly spaced points taken from contour of the enclosed shape — Figure 26

Figure 15: Flow Diagram of Operations Undertaken to Recover the Pig's Body Contour

The image gradient locates boundary information between objects in the image. The gradient image of the image in Figure 16 is shown in Figure 17.

Figure 16: Original Image of a Pig's Body
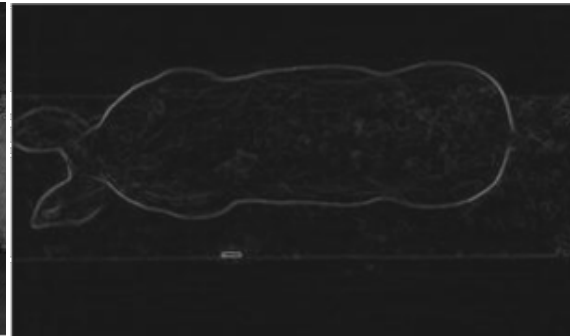
Figure 17: Image Gradient of a Pig's Body

The method extracts the image intensity values of a midline within the image running perpendicular to the length of the pig (Figure 18). The gradient of the image is calculated along this section (shown in Figure 19 as the black line). The green line in Figure 19 indicates the intensity values along the section shown in Figure 18 (scaled between 0 and 1). Two starting edge points are found either side of the animal. The location of these points are indicated by the red stars in (Figure 19 and Figure 20). Two filters are located at the 'Top' starting point and two at the 'Bottom' starting point.
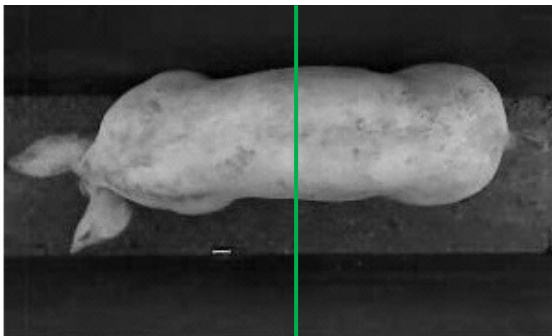
Figure 18: Assessment of the Middle Portion of the Pig
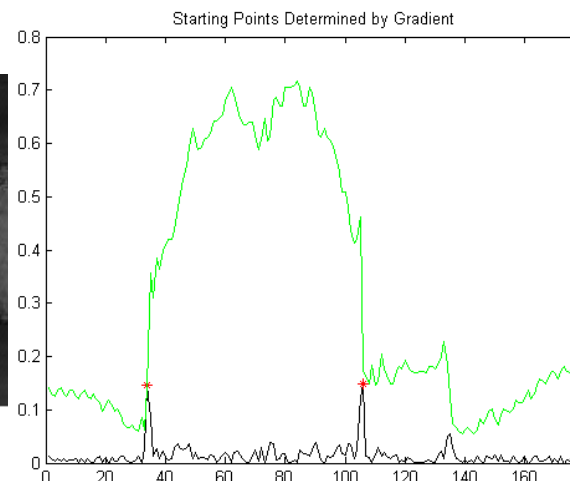
Figure 19: Locating Starting Points Along the Edge of the Pig's Body

Each filter is continuously incremented outwards by one column sequentially and in different directions shown by the red dashed arrows in Figure 20.
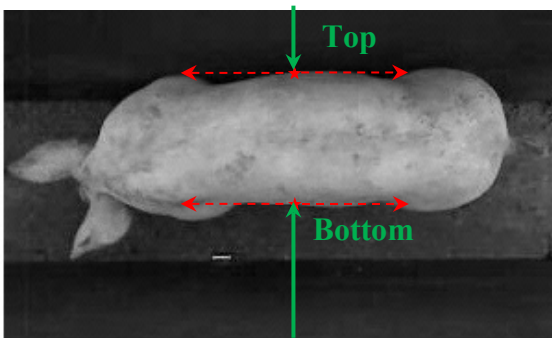
Figure 20: Top and Bottom Starting Points
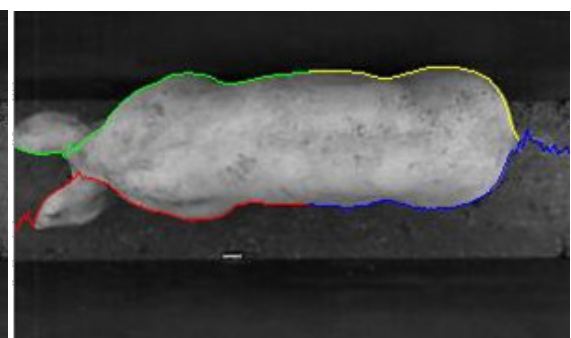
Figure 21: Flow of Four Localised Gradient Detection Filters

63

The filter (7x1 green) and its movements with respect to the edge gradient are demonstrated in Figure 22. At stage 'A' (starting point) column 'B' is searched for the location of the maximum gradient using the same position as the filter in stage 'A'. The maximum gradient point in stage 'B' is then identified as one point below the existing maximum gradient point at stage 'A'. Consequently the filter is then moved down one space for stage 'C'. Meanwhile the movement from the starting point 'A' and the maximum gradient co-ordinate is recorded for stage 'B'. The filters move incrementally in this fashion until the edges of the image are reached. Figure 21 illustrates the complete traced path of the four filters movements. The filter can be set to different size or shape and work in the same manner as long as it is incremented through the image or for a set number of iterations.
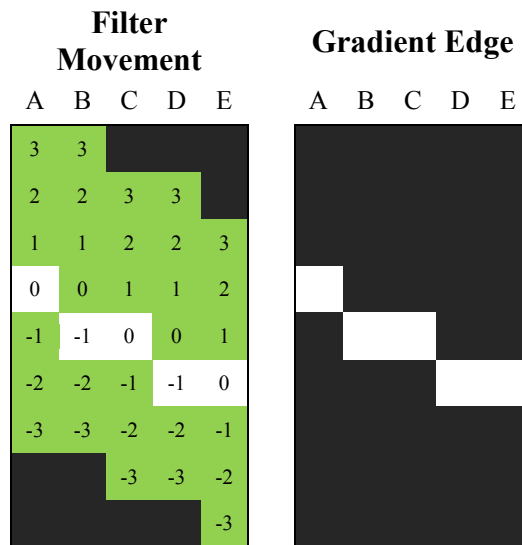
Figure 22: 7x1 Filter Movement in Respect to Located Maximum Gradient in the Image Columns A→E

After the contour is located it is then trimmed to ensure that the variance caused by the movement of the pig's head does not impact the measurements taken from the body (Figure 23, Figure 24 and Figure 25). For more detail refer to Section *3.5.1.4 The Trimming Method to Remove the Head and Tail*.
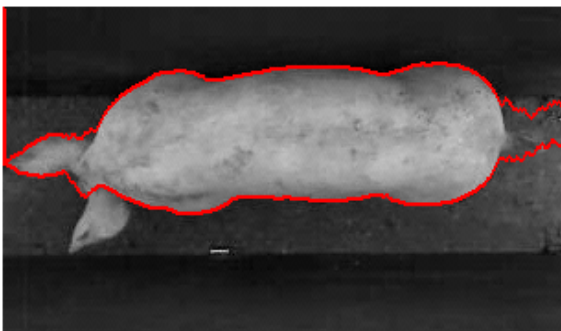
Figure 23: The Body Contour Recovered after Gradient Detection
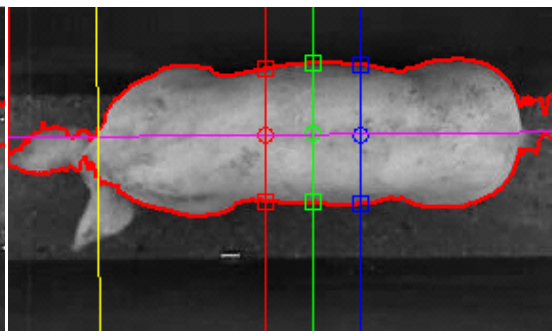
Figure 24: Determining the Orientation of the Pig's Body
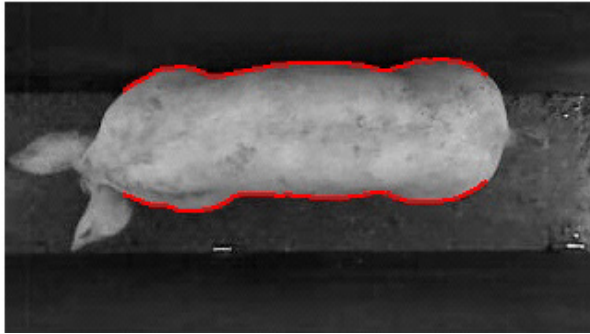
Figure 25: The Body Contour After Trimming the Operation

A curve is created to join the end points of the Top and Bottom contour to enclose the body shape. At this point the contour still may be affected by fluctuations caused by the filter in the detection of the gradient. A spline curve is then fitted to a sample of the original points to remove or smooth-out any outlying points, thus reducing the chance of extracting erroneous measurements from the contour (Figure 26).
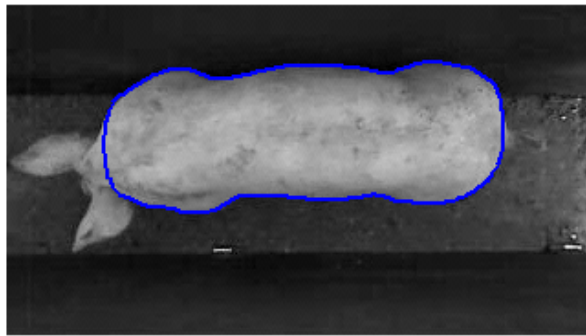
Figure 26: The Final Body Contour: An Enclosed Spline Curve

An investigation into how the calculation of the gradient within the filter effected the selection of contour points is found in following section.

3.5.1.3   *Calculating the Gradient of the Body Contour*

The gradient calculation performed within the filter neighbourhood directly affected the point selected as a contour point. Therefore, testing was undertaken to determine the best method to calculate the gradient within the filter neighbourhood (illustrated in Figure 22). Gradient operations, both in the negative and positive x, y directions were undertaken (Figure 27). Incorporating the gradient in the x direction proved to cause errors as can be seen in Figure 27 (a) and (d). This was due to the fact that the animal was horizontal in respect to the main axis of the image and gradients calculated within the neighbourhood in the x direction were less likely to reference the boundary gradient between the animal and the background.

(a)   (b)

(c)   (d)
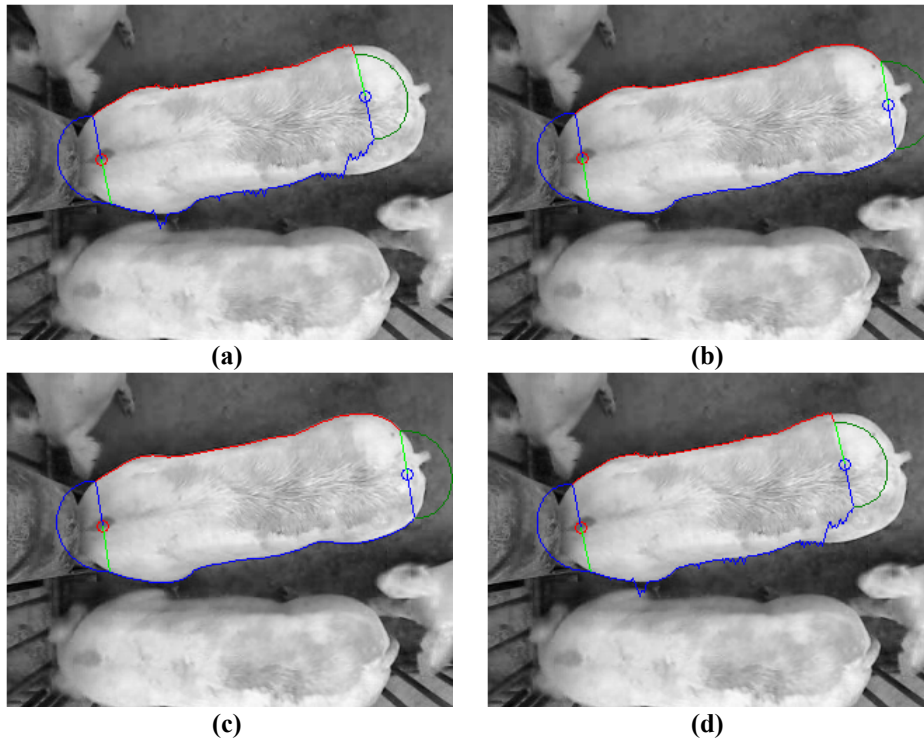
Figure 27: Determining the Appropriate Gradient Calculation within the Filters

The gradient operations in the y direction Figure 27 (b) and (c) were more desirable given the orientation of the camera installation within the pen environment. These gradient operations in the y direction were assessed further. It was noted that the rising or falling edge of the calculated gradient would directly affect the point selection. This resulted in of all points in either of the Top or Bottom array being offset by one pixel, which was undesirable. The effect can be seen in Figure 28 (a) and (b) where the gradient is offset into the actual body of the animal. If not accounted for, the Top and Bottom array may have a 1 pixel error along the entire length of the animal.
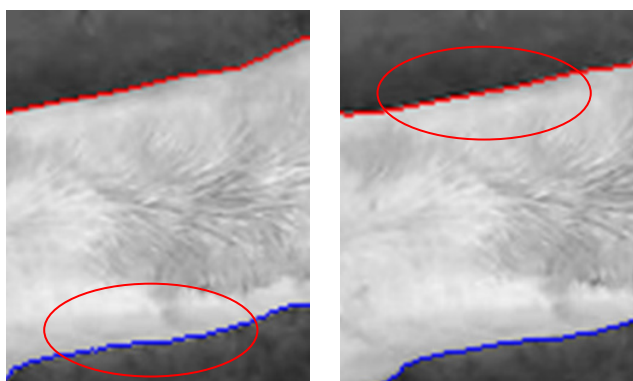
Figure 28: The Contour Incorrectly Identified Using a Single Gradient Calculation on Both Sides of the Pig's Body

Subsequently, a combination of the operations shown Figure 27 (b) (for the Top contour) and (c) (for the Bottom contour) were used to determine the edge gradient as they enabled the highest precision in representing the true edge of the contour surrounding the animal. These operations were formed by selecting the points

66

located at the falling edge of the gradient on either side of the animal. The result is shown in Figure 29.
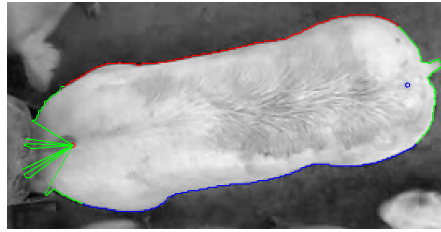
Figure 29: Final Method Used to Determine the Contour from the Gradient

After the Top and Bottom lines of the contour of the pig were recovered, a trimming operation was performed.

3.5.1.4   The Trimming Method to Remove the Head and Tail

Pilot testing had indicated that head of the animal introduced larger variance in area assessment due to its frequent motion. The removal of the head and tail was also undertaken by other authors for the same reason (Brandl and Jørgensen, 1996; Schofield, 1990; Wang *et al.*, 2008). Despite this fact, other researchers have chosen to keep the head as part of the analysis (Minagawa, 1997).

Originally the head trimming task was performed using a technique described by Wang *et al.* (2008). In Wang's method the binary image of a pig was rotated to the horizontal plane before summating the pixels along the image's x-axis. The resulting curve from the summation of the pixels along the x-axis can be seen in Figure 30. A minimum reference point (the neck) could be found from this array and used to remove the pixels (associated with the head) from further analysis (Figure 30).
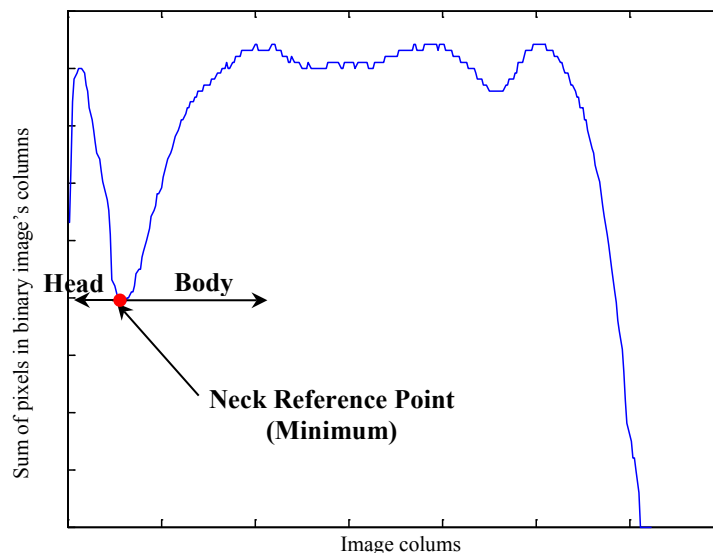
Figure 30: Using the Summated Columns of the Pig's Body Contour to Trim the Head Based on a Method Found in Wang *et al.* (2008)

This trimming method did work in some scenarios when the pig was completely straight. However, as soon as the pig's posture changed, the procedure to identify the trimming point became problematic. The vertical trim resulted in some ambiguity

when trying to reference a repeatable trim point on successive frames as the neck of the animal and the head posture resulted in different neck thicknesses and different reference points. This variability in the trimming operation had a direct effect on the body area and would, therefore, impact the variability of weight estimates (as the area is regarded in literature as the best predictor of weight). In addition, the trimming method would ideally not require a complete image rotation and could be performed regardless of the orientation of the animal. For these reasons Wang's method was modified extensively.

Development focused on defining suitable and reliable reference points along the contour for trimming to occur. Information, gathered during the contour trace, was used to overcome these rotation and variability issues. Once the Top and Bottom line of the contour were discovered the midline between these two sets of points was determined (see Figure 31 (a)). The slope of this midline was also determined as the orientation of the animal within the image. If one were to rotate the image, this slope could be used to get the animal positioned along the horizontal axis. However, to avoid time wasting the slope of the midline was used to shift the points in the Top and Bottom arrays such that they were aligned adjacent to one another at the angle of the line perpendicular to the midline (see Figure 31 (b)). Therefore, by determining the distance between adjacent points in the Top and Bottom array, a width profile could be built similar to that shown in Figure 30 only rotating the image was not required. The head and tail portions were then trimmed.

This trimming process first involved determining a trimming width value. To find this value the three widths were found at sections along the summated profile of the contour. These three widths were then averaged and multiplied by 85% to form the trimming width (shown in Figure 24). This process to determine the trimming width ensured that the trimming method was adaptable to different weight ranges and sizes of pigs. This trimming width was then passed over the width profile and the first points at either end of the width array less than the trimming width were identified. The information on either side of these two points was removed; effectively cropping the head and tail of the pig. After the trim operation, the shape was enclosed.

(a)   **(b)**
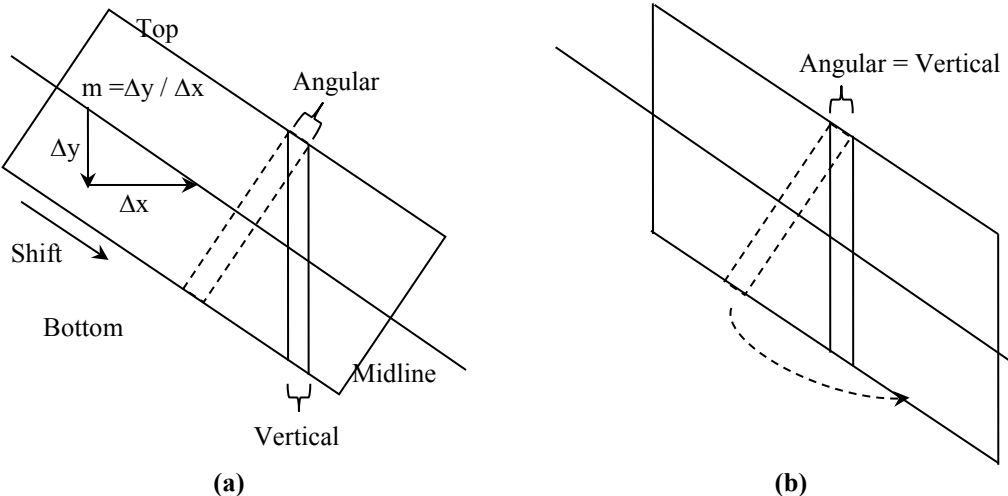
Figure 31: Determining the Width Profile without Rotating the Body Contour
(a) Before and (b) After Performing a Shift Operation to Align Angular Body Co-ordinates to the Horizontal Plane

3.5.1.5 *The Stitching Method to Enclose the Contour Shape*

To provide continuity, the shape needed to be closed after the trim operation. Originally the contour points at the front and rear sections of curve were constructed using polynomial fitting. However, the fit created variance in the area measurement (see Figure 32). Consequently, alternatives were explored.
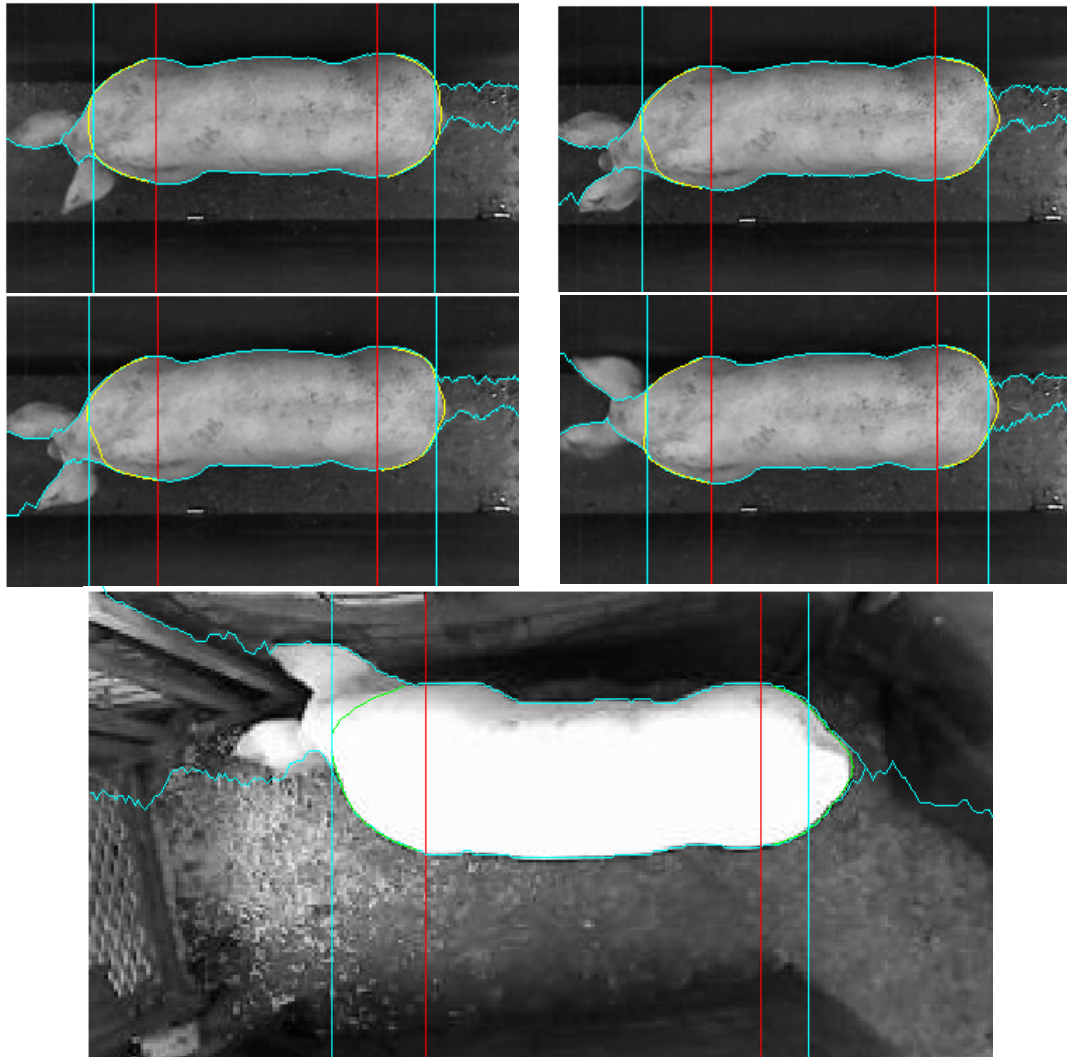
Figure 32: Constructing and Fitting Polynomial Curves to Enclose the Ends of the Body Contour

The first alternative was to simply create an artificial curve (arc of an eclipse) that connected the Top and Bottom curves. This resulted in a complete contour with less variance due to a similar curve being created each frame. However, problems occurred in the construction of this arc when the animal was orientated in a direction other than horizontal. This issue was subsequently overcome by aligning the curve to the main axis of the animal's body using the orientation information found during the trimming process.

Another method was developed to determine the precise contour of the rear. An arc and two 'o' points (one blue and one red) can be observed in Figure 33 at either end of the pig indicating the starting point of the search algorithm. This method involved

creating an array of values along a line between the arc and the 'o' points at every iteration. These 'o' points are the midpoints between the Top and Bottom arrays' end points. The function performs in a similar manner to a wind-screen wiper where a filter is rotated across the ends of the pig; recording the maximum gradient along each line segment from the 'o' point to the arc as it rotates. The result is a more precise contour of the rear of the pig (Figure 33). In addition the variability in the contour's ends could be used to distinguish the end containing the pig's head.

(a)

(b)   (c)

(d)
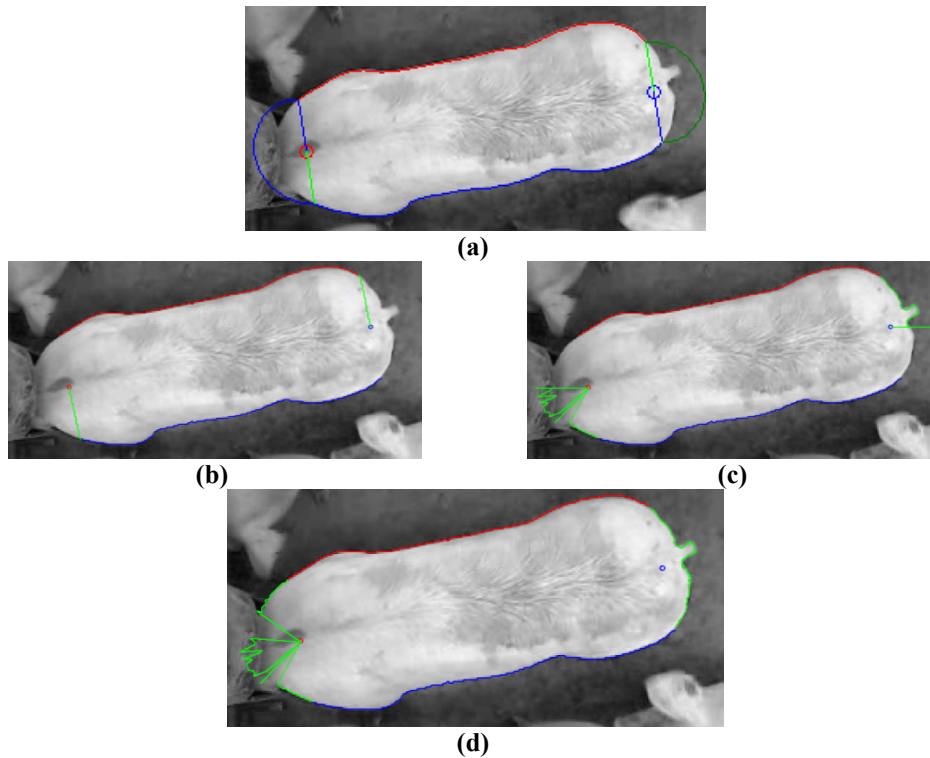
Figure 33: Performing a Trace to Determine the Curves at the Ends of the Body Contour
(a) Front and Rear Arc Search Paths; (b) Start; (c) Half Way; (d) Completed Search

Although this method found the precise edge points of the rear of the pig, it was too slow for integration into the system. The remaining presence of the tail also required additional operations to remove it. However, this algorithm does have potential to replace the existing method of finding the contour in future by seeding points inside the boundary of suspected animals within image and performing a 360 degrees trace in the same manner. In this fashion, multiple pigs in a single image might be found and have their weight estimated simultaneously. In spite of this, the artificial curve was used to enclose the shape in this study due to its efficiency. After enclosing the ends of the contour, a spline curve was fitted to the contour to smooth out any abnormalities. The contour was then ready to have its measurements determined.

3.5.2   Feature Extraction Development

The feature extraction stage involved developing a method to determine points of reference along the animal's body contour. These reference points were related to the body measurements, which were required to be recovered automatically using the software. The contour of the pig is the enclosed shape, derived from the edge of the pig's body (transition between the pig and the background) excluding the tail and the head as viewed from above.

Figure 34 shows the 16 body measurements on the contour of the pig which were targeted during feature extraction development. The majority of these body measurements coincide with those recovered by the system presented in White *et al.* (2004). However, body measurements ML_{Rho}, FML_a, RML_a, mWF_a and mWR_a have not been associated with any similar study found in literature. Note that the 'a' denoted in mWF_a and mWR_a indicates that that the measurement can be found at any angle.

Dimension			Key	
L_1	MWF_a		M	Max
L_2	mWF_a		m	Min
L_3	$MWMid_a$		W	Width
L_4	mWR_a		L	Length
L_5	MWR_a		F	Front
L_6	MidL		R	Rear
L_7	ML		Mid	Middle
L_8	FML_a		A	Area
L_9	RML_a		a	angular
A_1	AF_c		c	curvature
A_2	$AMid_c$		T_2	Spline
A_3	AR_c		Rho	centroid
A_4	AT_2			
L_{10}	WF_c			
L_{11}	WR_c			
L_{12}	ML_{Rho}			
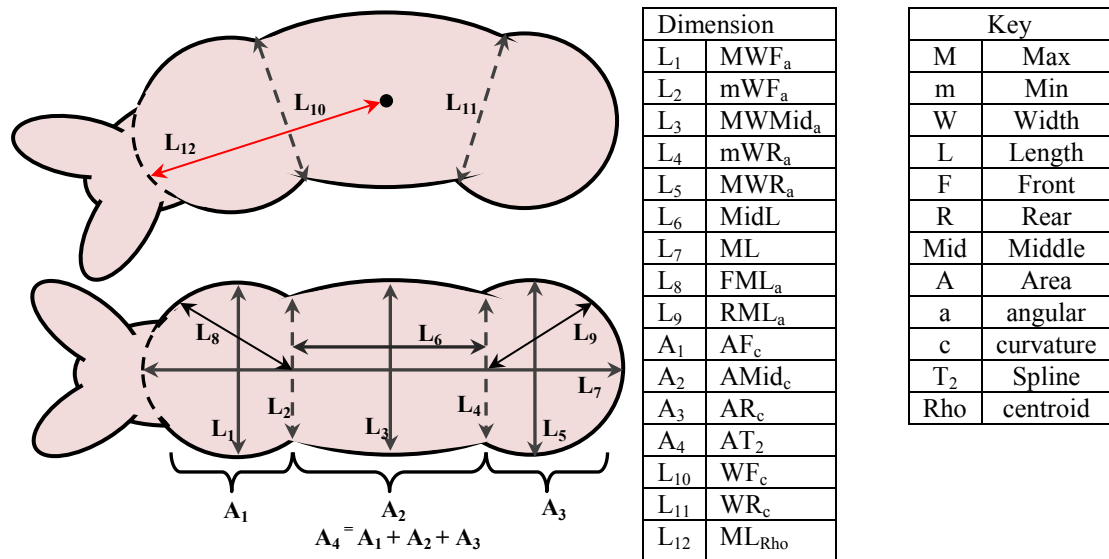
Figure 34: The Body Measurements Extracted from the Pig's Body Contour

The body measurements WF_c and WR_c in Figure 34 refer to the widths that link the points directly behind the front legs and in front of the hind legs respectively. These body measurements are often different from the minimum widths recorded (mWF_a, mWR_a) due to the pose of the animal. The subscript 'c' indicates that WF_c and WR_c are derived from points of curvature rather than global minima or maxima like other width and length measurements. The ML_{Rho} measure is the maximum distance from any point on the contour to the shapes centroid. Body measurements FML_a and RML_a were calculated for pose discrimination purposes as their angles could potentially indicate the degree of bending of the animal and their magnitude could potentially determine whether the head and tail trimming operation was performed satisfactorily. FML_a and RML_a are the maximum distance between the midpoint of mWFa and the contour of the front section and the midpoint of the mWRa and the contour of the rear section, respectively.

A major aim of this study was to devise the methods required to automatically and repeatedly identify the reference points that correspond to the body measurements shown along the pig's contour in Figure 34.

Additional body measurements might need to be recovered to enhance precision. For example, it has been stated that incorporating a height parameter in the weight estimation equation will reduce the mean relative weight estimation error of individual animals (Minagawa *et al.*, 1997). However, deciding to incorporate a height measurement needs to be well justified as an animal's height differs over its curved back-area relative to its posture. This makes the pig's height difficult to

reference correctly using both manual and automatic techniques. Including height as a variable in the weight-estimation equation will further complicate the system and may contribute to errors or missed weigh events if the height measurement is unavailable or not referenced correctly every time sampling of other body measurements takes place. However, in contrast, a height related error may also occur if two animals (one with long legs and one with short legs) have the same weight as they will both produce different pixel areas relative to how close they are to the camera. Therefore, the height of the animal may be a critical parameter worth perusing to correct for such a scenario. To overcome this issue, the role height has in the estimation of weight needs to be investigated in this study. Section *3.6.1.3* later in this chapter is dedicated to this topic.

3.5.2.1 *Extracting Vertical Body Measurements*

Initially, the width-array was divided into three sections to determine various body measurements of the pig's contour (shown in Figure 35). The first section of the width-array was searched for a minimum value, corresponding to the trimming point (refer to Figure 30 of the width array in Section *3.5.1.4 The Trimming Method to Remove the Head and Tail*). The other divisions were used to find minima and maxima along the body contour. First the array was halved and a minimum was found either side of the halfway point using a gradient-based approach. These were the positions at which the minimum width front (mWF) and the minimum width rear (mWR) were found. The maximum point between the two minimum points was recorded as the maximum width middle (MWMid) and the maximum points found on the exterior side of the minimums were the maximum width front (MWF) and the maximum width rear (MWR). The length was simply the length of the array after performing the trim.
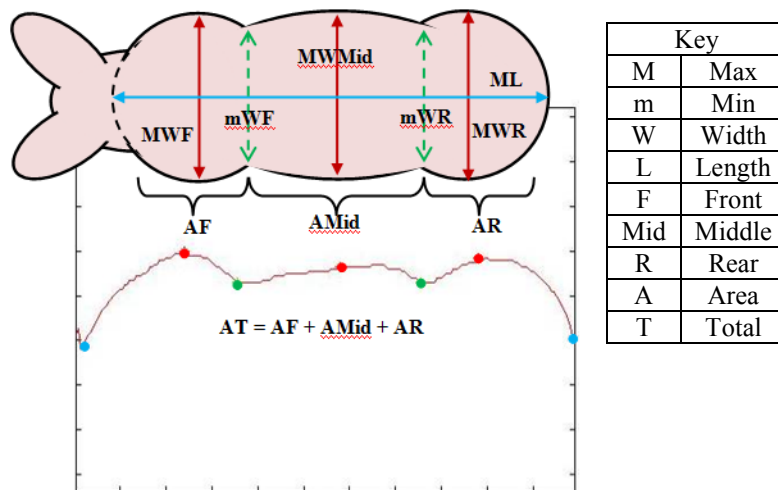
Figure 35: Original Verticle Measurments Extracted

The resulting vertical measurements of the widths are illustrated on a pig in Figure 36 below.
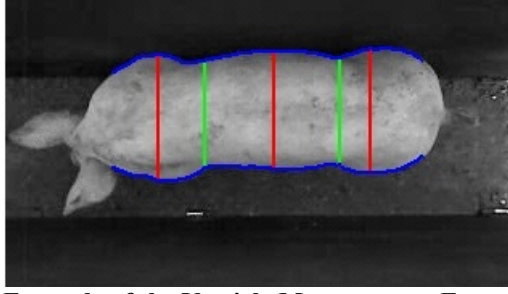
Figure 36: An Example of the Verticle Measurments Extracted from a Pig's Body

Although this method performed reasonably well, it was limited to extracting the measurements along the vertical and horizontal plane of the image. Consequently, the true body measurements were not recorded correctly, as in most instances the pig's posture was not completely straight and symmetrical. For this reason, methods to extract the angular measurements from the body of the pig needed to be developed.

3.5.2.2   The Final Method Used to Extract Body Measurements

Work was undertaken to devise a method that could determine the precise measurements of the pig's body contour. This required the automatic identification of pairs of reference points on the pigs' contours to repeat the various width and length measurements. The contour of the pig's body had been recovered during the segmentation process (described in Section *3.5.1.2 The Final Segmentation Method*). Therefore, the measurements that needed to be extracted were within the pairs of points bounded by the contour shape. Thus the problem was approached holistically, where all of the point to point distances (Euclidean distance) between the points on the curve were calculated using Pythagoras theorem (Equation 1).

$$
\begin{bmatrix} d_{1,1} & d_{1,2} & \cdots & d_{1,n} \\ d_{2,1} & d_{2,2} & \cdots & d_{2,n} \\ \vdots & \vdots & \ddots & \vdots \\ d_{n,1} & d_{n,2} & \cdots & d_{n,n} \end{bmatrix}
$$

$$
= \left\{ \left(\begin{bmatrix} x_{1,1} & x_{1,2} & \cdots & x_{1,n} \\ x_{2,1} & x_{2,2} & \cdots & x_{2,n} \\ \vdots & \vdots & \ddots & \vdots \\ x_{n,1} & x_{n,2} & \cdots & x_{n,n} \end{bmatrix} - \begin{bmatrix} x_{1,1} & x_{2,1} & \cdots & x_{n,1} \\ x_{1,2} & x_{2,2} & \cdots & x_{n,2} \\ \vdots & \vdots & \ddots & \vdots \\ x_{1,n} & x_{2,n} & \cdots & x_{n,n} \end{bmatrix} \right)^2 \right.
$$

$$
\left. + \left(\begin{bmatrix} y_{1,1} & y_{1,2} & \cdots & y_{1,n} \\ y_{2,1} & y_{2,2} & \cdots & y_{2,n} \\ \vdots & \vdots & \ddots & \vdots \\ y_{n,1} & y_{n,2} & \cdots & y_{n,n} \end{bmatrix} - \begin{bmatrix} y_{1,1} & y_{2,1} & \cdots & y_{n,1} \\ y_{1,2} & y_{2,2} & \cdots & y_{n,2} \\ \vdots & \vdots & \ddots & \vdots \\ y_{1,n} & y_{2,n} & \cdots & y_{n,n} \end{bmatrix} \right)^2 \right\}^{\frac{1}{2}}
$$

Equation 1: Using Pythagoras Theorem to Construct a Euclidean Distance Matrix

The resulting matrix stored all possible distances between any two points on the pig's body. Two views of the resulting distance matrix are presented in Figure 37 (a) and (b). The width profile can be observed within the distance matrix Figure 37 (a).

| (a) | (b) |
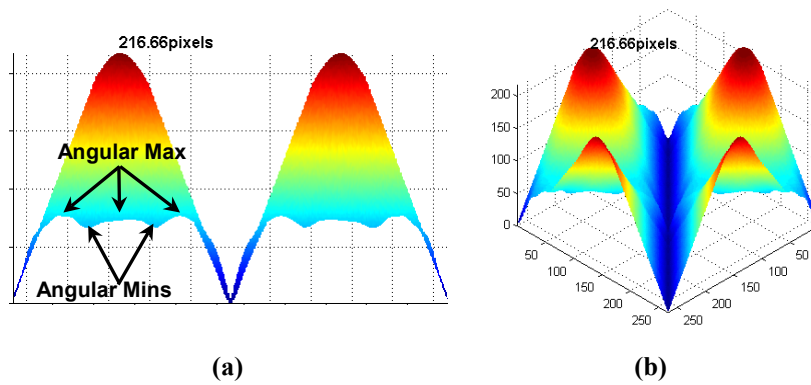
Figure 37: Looking Down the Main Diagonal (a) and Angular View Down the Main Diagonal (b) of the Euclidean Distance Matrix of the Body Contour (Z-axis point-to-point distance in pixels)

The various body measurements presented in Section *3.5.2 Feature Extraction Development* needed to be found and extracted from this matrix. The matrix is organised such that the main diagonal is a zero vector (the distance of a point to the same point) and, as the diagonals are analysed away from this starting point, the distance between points within the contour array is also incremented. Subsequently, the matrix can be indexed to refer to the points on the contour that created any given distance. For example, Figure 38 (a) shows the original contour used to create a distance matrix. The two red stars in Figure 38 (b) were found by referencing the point in the matrix surface corresponding to the maximum distance between any two points on the contour. Hence, this distance is the maximum peak in the matrix surface and refers to the maximum length of the animal's body. Using this method the various body measurements of the pig's contour can be found regardless of its angular orientation.

| (a) | (b) |
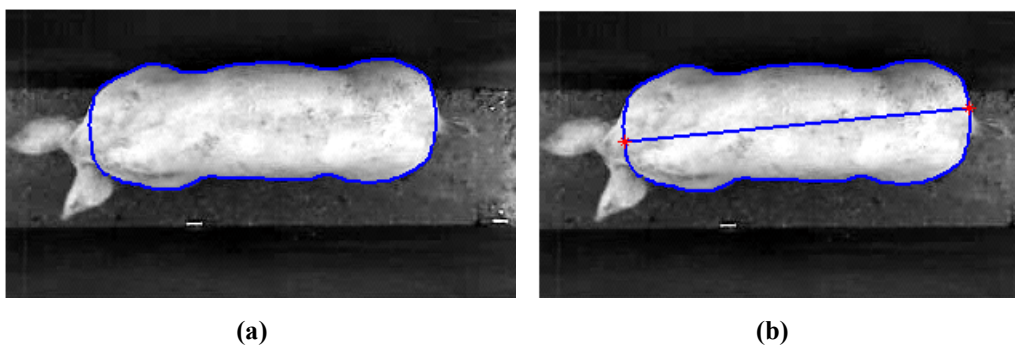
Figure 38: Original Body Contour (a) and Maximum Angular Length (b)

Additional methods were required to determine the points (distances) on the matrix surface that represented the pig's other (key) body measurements reliably (refer to Figure 34 for a list of extracted body measurements).

3.5.2.2.1 *Initial Method to Find the Points of Curvature on the Pig's Body Contour*

The next two distances determined from the matrix surface corresponded to the minimum widths (mWF_a and mWR_a). These measurements were chosen because they lay at minima within the Euclidean distance matrix and therefore there was no ambiguity in determining their location precisely. Initially these measurements were determined by first locating points in the distance matrix surface that were in close proximity to the minima (WF_c and WR_c) and then searching surrounding area for the

74

true minima (mWF$_a$ and mWR$_a$). The distance matrix was not used to determine the measurements WF$_c$ and WR$_c$. Instead the curvature of the contour shape was assessed to determine the reference points.

To determine WF$_c$ and WR$_c$ the contour array was first broken into two halves based on the points which corresponded to the maximum angular length. These two halves were then halved again so that four sections could be assessed independently. These sections are illustrated in Figure 39 (a). The red star in Figure 39 (a) is the starting point of the contour array and the two black stars indicate from where the four coloured sections are derived.

| (a) | (b) |
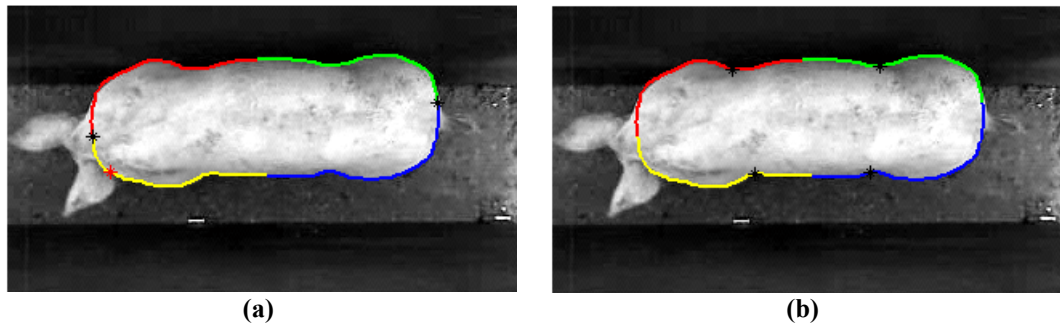
Figure 39: (a) Divisions of the Body Contour; (b) Identifying Points of Minimum Curvature

Each of the four segments were then analysed to find the points of minimum curvature. The points of minimum curvature were found using (Equation 2) and are shown as black stars in Figure 39 (b) on the pig's contour. For more information on determining curvature see (Pressley, 2010). The y'' in Equation 2 denotes the second derivative of the Cartesian y co-ordinate, likewise x' is the first derivative of the x co-ordinate.

$$kappa = \frac{x'y'' - y'x''}{(x'^2 + y'^2)^{\frac{3}{2}}}$$

Equation 2: Curvature Equation

The black stars in Figure 39 (b) coincide with the endpoints of the widths WF$_c$ and WR$_c$. These endpoints were then used to calculate the body measurements (distance) of WF$_c$ and WR$_c$. As these endpoints lay on the contour, the resulting distance calculated for WF$_c$ and WR$_c$ was represented within the distance matrix. Therefore, the location of WF$_c$ and WR$_c$ could be found in distance matrix by either indexing the endpoints or searching for it for the matching distances. Figure 40 displays the top view of the distance matrix with the located end points of the minimum curvature (WF$_c$ and WR$_c$) represented by black dots.
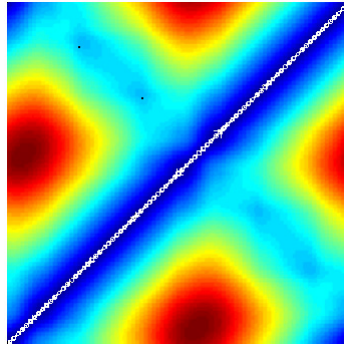
Figure 40: Top View of the Euclidean Distance Matrix of the Body Contour Points of Minimum Curvature Marked as Black Dots

3.5.2.2.2 *Finding the Minimum Widths of the Pig's Body*

Two slices were taken out of the distance matrix around these two points. An example of the front and rear slices of the distance matrix surrounding the WF_c and WR_c points are displayed in Figure 41 (a) and (b) respectively; Dark blue refers to smaller distance values corresponding to the minima. These points lie within close proximity to the angular minimums presented in the side view of the distance matrix in Figure 37 (a).

| (a) | (b) |
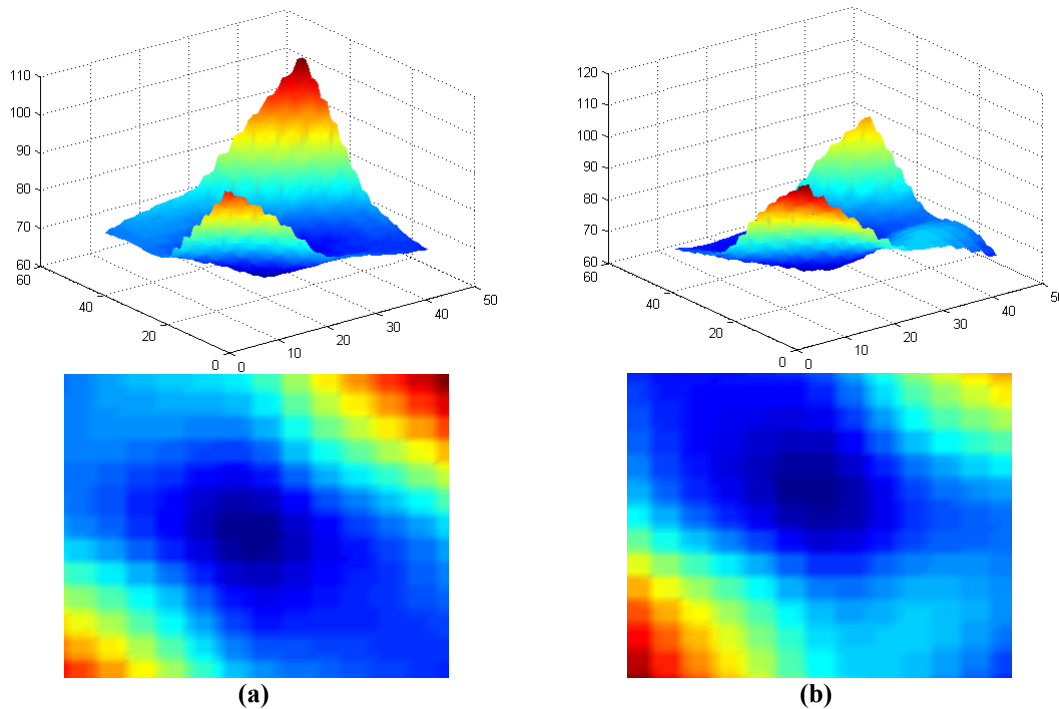
Figure 41: Slices of the Euclidean Distance Matrix that Contain the Absolute Angular Minimums
(a) Front and (b) Rear

The mWF_a measurement was found by searching the front slice Figure 41 (a) for its minimum value. The procedure was then repeated for the mWR_a measurement. Figure 42 shows the WF_c and WR_c measurements (red lines) in respect to the mWF_a and mWR_a measurements (light blue).
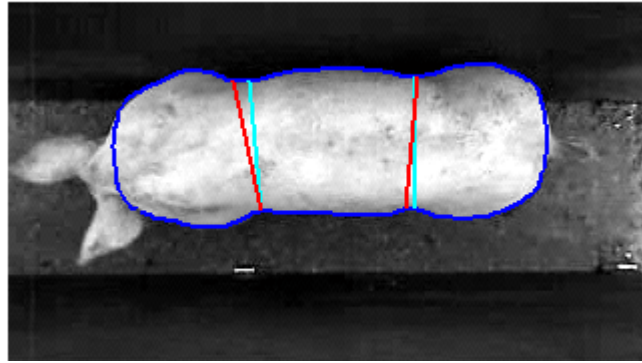
Figure 42: The Curvature Width Measurements WF$_c$ and WR$_c$ (Red) and Minimum Width Measurements mWF$_a$ and mWR$_a$ (Light Blue)

WF$_c$ and WR$_c$ are then used to break the pig's body contour into three area sections; AF$_c$, AMid$_c$ and AR$_c$. These are different than the area sections that would result if the pig was divided into sections based on the body measurements mWF$_a$ and mWR$_a$.

3.5.2.2.3   Finding the Maximum Widths of the Pig's Body

As mWF$_a$ and mWR$_a$ are referenced reliably during the process they were chosen as reliable starting points to determine the other angular measurements; MWF$_a$, MWMid$_a$ and MWR$_a$. Notably, recovering these widths reliably is slightly more complicated as the magnitude of the width recovered is dictated by the angle at which it is referenced.

To determine the widths, first the distances were extracted along a line section running through the minima (mWF$_a$ and mWR$_a$) of the Euclidian Matrix (refer to the black line in Figure 43).
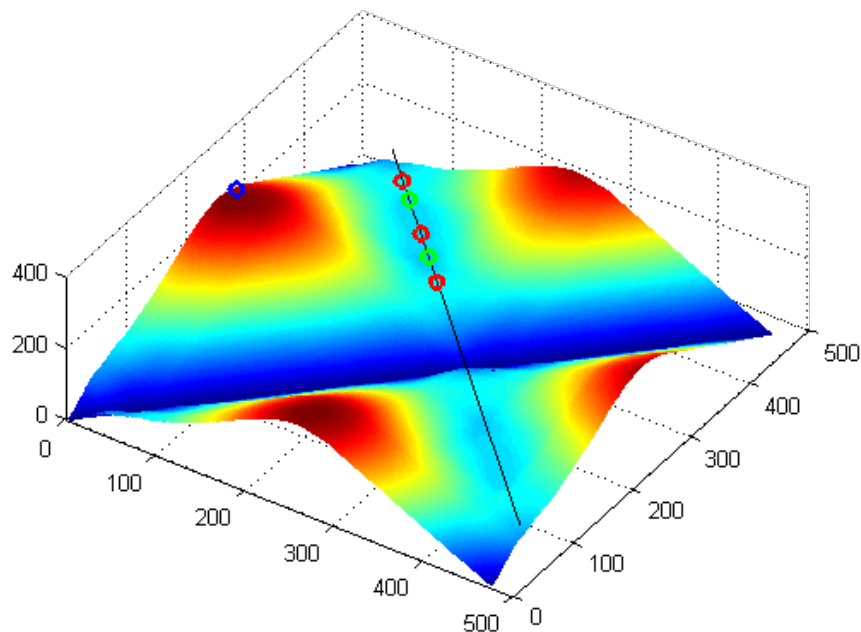
Figure 43: The Location of Extracted Body Measurements within the Matrix Maximum Length (Blue 'o'), Maximum Widths (Red 'o') and Minimum Widths (Green 'o').

77

The extracted information along the line is illustrated Figure 44 (some cropping is performed automatically). The widths (distances) of this line section were analysed further for the MWF_a, $MWMid_a$ and MWR_a measurements. As the minimums were known, the width profile was could be broken into three sections. In a similar manner to the process performed earlier using the vertical measurements, each of these sections was assessed to recover one of the maximums MWF_a, $MWMid_a$ and MWR_a. These maximum locations are illustrated as the red circles in Figure 44 on the width profile and along the black line in the distance matrix Figure 43.
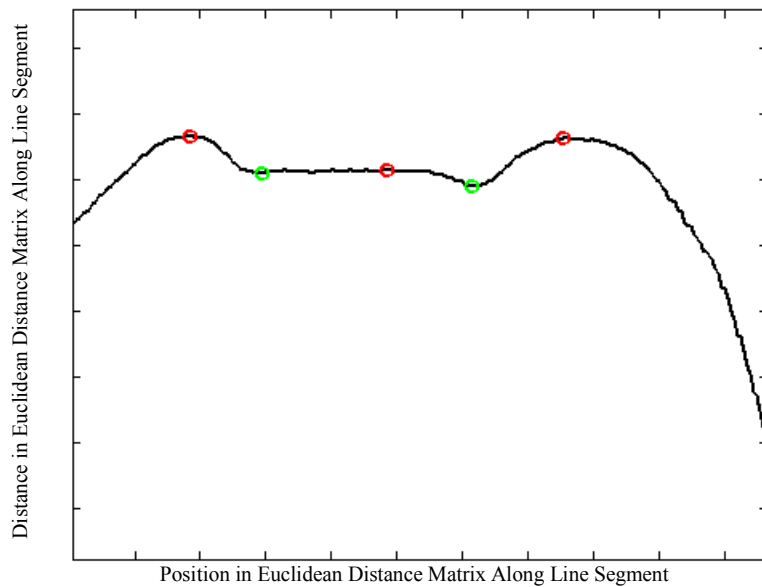
Figure 44: Distances Found Between Points on the Pig's Body Contour as Extracted Along the Line Segment of the Euclidean Distance Matrix

The four remaining measurements to be determined were the front length angular (FML_a), middle length angular (MidL), the rear length angular (RML_a) and ML_{Rho}. These measurements were calculated to give some indication of the animal's body posture. For example, if the body is stretched or compressed. The MidL measurement was found by first determining the mid-points of WF_c and WR_c. The distance between these two mid points became the MidL measurement. The FML_a and RML_a measurement was determined by constructing a spline curve around the front and rear section of the pig's body and determining the maximum distance from it and the midpoint. The ML_{Rho} measurement was found by averaging the x and y co-ordinates of the contour to obtain the centroid of the shape and then finding the furthest distance from the centroid to any point on the contour. More details on how this measurement was determined can be found in Section *3.5.5 Filtering the Shape for Pig Recognition and Pose Validation*. A sequence of frames illustrating the extracted body measurements is shown in Figure 45. Table 5 documents the size in pixels of the extracted body measurements (ML_{Rho} is not included).
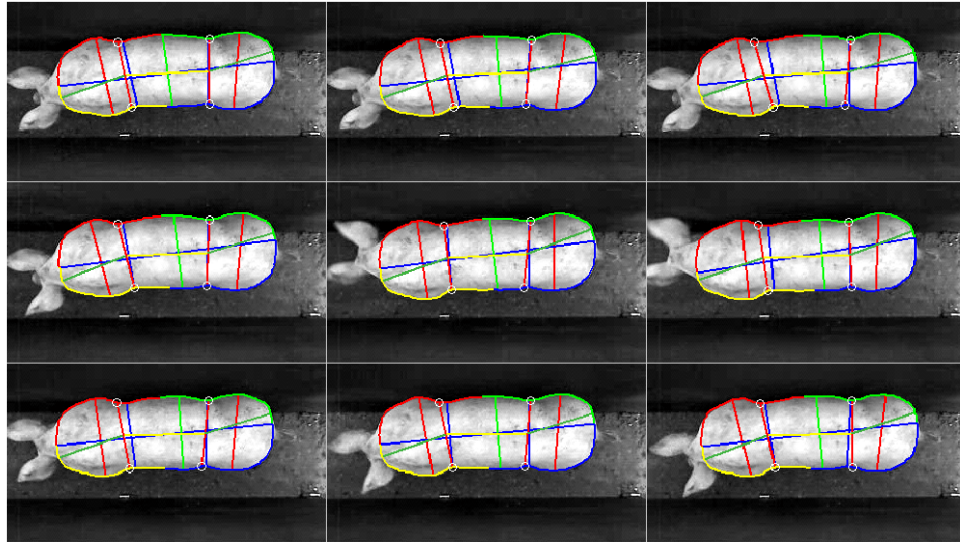
Figure 45: Sequence of Frames with the 15 Extracted Body Measurements Overlaid on the Pig's Body

Table 5: The 15 Body Measurements Recorded from the Video Sequence in Figure 45

Value	AF_c*	$AMid_c$	AR_c	AT_2	WF_c	WR_c	ML	FML_a	$MidL$	RML_a	mWF_a	$MWMid_a$	mWR_a	MWF_a	MWR_a
1	4586	5549	4375	14511	66.9	65.8	217.7	67.8	85.1	66.2	66.1	72.3	65.5	76.6	78.6
2	4623	5181	4605	14409	65.8	65.2	218.4	68.5	82.1	68.9	64.9	71.1	65.0	77.0	78.2
3	4537	5226	4611	14375	67.1	65.8	219.1	66.9	84.6	69.0	65.1	71.7	65.6	77.1	78.3
4	4683	5181	4589	14454	66.8	66.0	218.1	68.5	82.2	68.7	66.4	73.7	66.0	77.1	78.9
5	4732	5315	4604	14652	64.9	67.7	217.1	69.5	79.7	69.3	64.8	72.1	66.6	76.9	79.8
6	4625	5837	4399	14861	66.9	65.2	221.2	68.1	87.5	67.1	64.4	71.4	65.1	77.1	79.6
7	4615	5399	4592	14606	67.1	67.1	217.4	67.7	82.1	68.9	65.1	73.9	66.2	76.6	78.8
8	4602	5412	4573	14588	67.1	66.6	216.7	67.2	82.1	68.5	65.5	73.4	66.0	77.1	79.5
9	4586	5600	4392	14579	66.0	67.1	216.9	67.3	85.1	66.1	65.3	73.5	66.6	77.2	78.9
AVE	4621	5411	4527	14560	66.5	66.3	218.0	67.9	83.4	68.1	65.3	72.6	65.8	77.0	78.9
STD	57	219	104	147	0.77	0.91	1.41	0.83	2.37	1.27	0.64	1.07	0.59	0.24	0.59
CoV	0.012	0.041	0.023	0.010	0.012	0.014	0.006	0.012	0.028	0.019	0.010	0.015	0.009	0.003	0.007

*All measurements in pixels, AVE = average, STD = deviation

3.5.2.2.4   Final Method Used to Find the Minimum Widths of the Pig's Body

At this stage of the development there was still a critical processing step which was causing a problem in many frames. This problem was due to the necessity of finding the correct points of curvature (close to the true minimum) so that the correct width measurements could be obtained. In some animal postures these points of curvature were very difficult to automatically recognise as these points are subject to a wide level of variance as the animal moves. An alternative method was undertaken to eliminate the dependency on the points of curvature (WF_c and WR_c) to find the minima.

To prevent dependency on the points of curvature, the minima had to be referenced from the distance matrix directly. The proposed method was to determine a line section similar to that shown in Figure 43 and use the distance information from this line segment to find the locations which were likely to be in close proximity to the minima (mWF_a and mWR_a) in a similar manner to what was done using the points of WF_c and WR_c.

To achieve this, each diagonal section of the distance matrix (starting at the main diagonal and ending at the corner) was analysed for its variance and minimum value. The minimum value of each diagonal section is plotted over the distance matrix in

Figure 46 as a black line. It can be seen that part of the line that intersects the axis of the matrix that needs to be sampled.
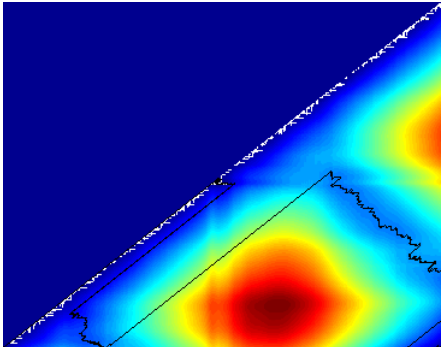
Figure 46: Minimum Value along Each Diagonal of the Euclidean Distance Matrix

As distance values along each diagonal are an equal index-spacing away from adjacent points (this spacing increments by one for each diagonal from the main diagonal). The variance within each of these diagonal sections is the variability (in distance) of each point to an adjacent point an equal distance away in the contour array. The highest variability can be found when both small and large distances are found along a diagonal. This occurs between the two peaks of the maximum point to point distances; as can be seen between the red sections of Figure 46. By thresholding the minimum array (black line in the Figure 46) with a limit on variance (var<0.05) the section of the minimum line that needs to be sampled can be determined; where the minimum and maximum body measurements of the contour are located (Figure 47).
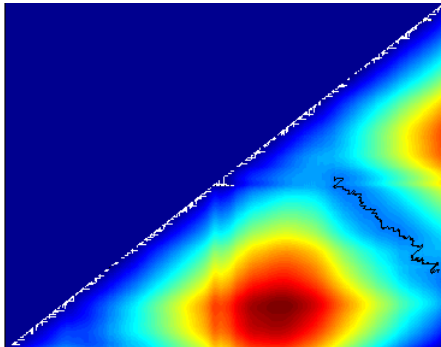
Figure 47: Remaining Array of Minimum Values after Applying a Threshold Based on Variance along Each Diagonal

Using a least squares approach a line approximation was derived from the remaining section of the minimum line section as seen in Figure 48.
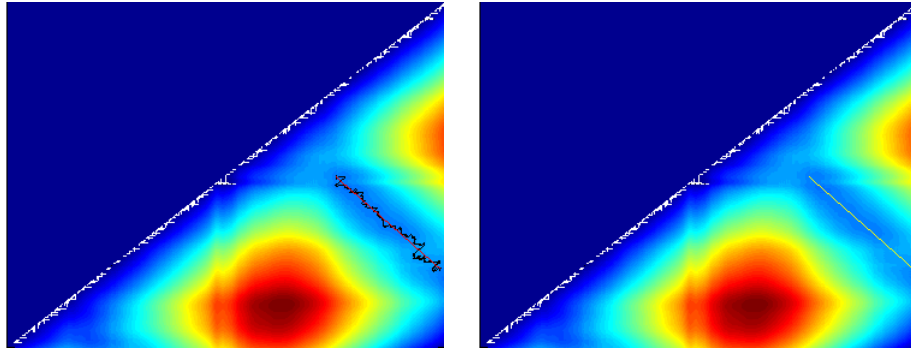
Figure 48: The Least Squares Line of the Co-ordinates of the Array of Minimum Values

The distance measurements were then extracted from the matrix along this line. The resulting array is shown in Figure 49. The array has been broken into two sections to locate the minimums (red and green circle in Figure 49) which will be in close proximity to the actual true minimums within the distance matrix.
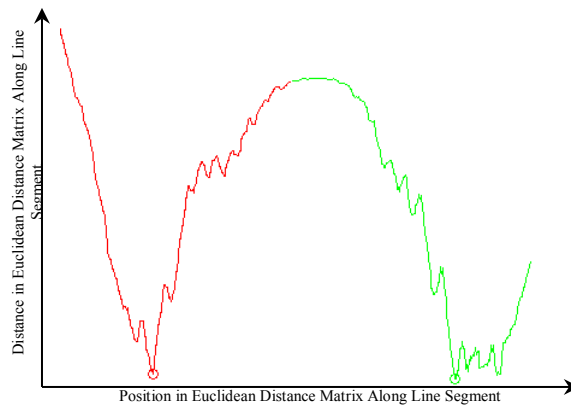
Figure 49: The Distances Extracted along the Least Squares Line Section

The areas of the distance matrix surrounding these minimums are searched in the same manner as shown earlier in Section *3.5.2.2.2 Finding the Minimum Widths of the Pig's Body*. Figure 50 shows the location of the points of the initial minimums found along the line segment as the red and green 'o'. The red and green dots represents the true location of the minimums (mWF_a and mWR_a) located nearby.
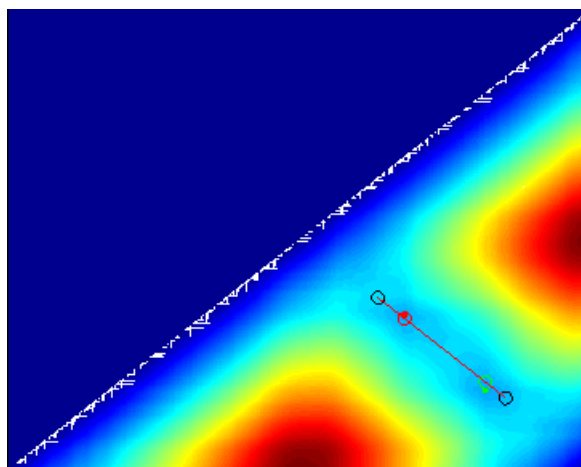
Figure 50: Final Method Used to Find the Measurements, mWF_a and mWR_a

81

3.5.2.2.5 Final Method Used to Find the Points of Curvature on the Pig's Body Contour

An alternative and more reliable method was developed to determine the points of curvature such that the locomotion of the animal might be detected. The contour was first broken up into sections as demonstrated by Figure 39 (a). These sections were then broken down further into eighths (Figure 51) such that a point of curvature lay somewhere along each of the contour segments.
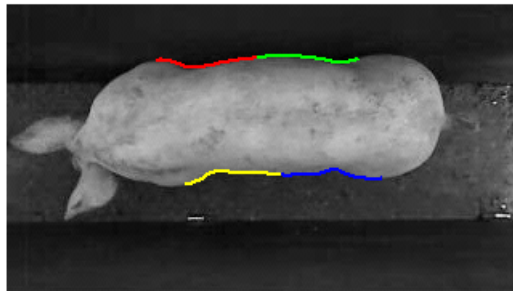
Figure 51: Sections of the Contour Used to Determine the Maximum and Minimum Points of Curvature

To determine each of the points of curvature, a line was created joining the end points of each segment Figure 52. These line segments have the same amount of elements as the contour section. The line was then used as a reference axis such that each point on the contour was some distance away from it. The point of curvature was then found by determining whether the segment was on the top or bottom of the contour and then finding the maximum distance or minimum distance away respectively. A plot of the distance between the contour and each of the four line segments can be seen in Figure 52.
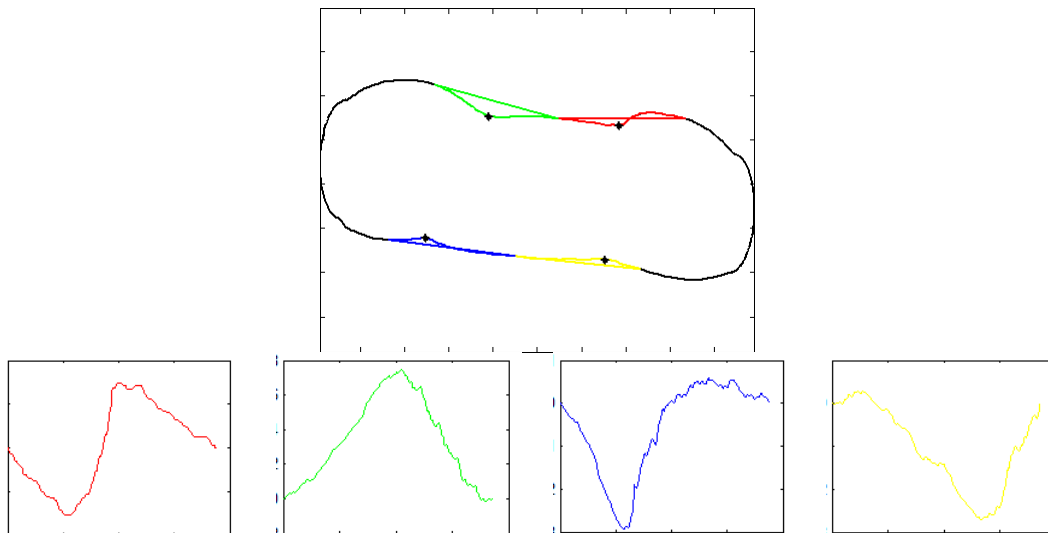
Figure 52: Final Method Used to determine the Maximum and Minimum Points of Curvature

These extraction methods were used to obtain the 16 pig body measurements from within the image. However, these methods were systematic and did not have the ability to determine the integrity of the contour shape from which the body measurements were extracted. Therefore, filtering methods were required to validate both the segmented contour and its extracted body measurements. However, before

82

this filtering took place, the body measurements extracted needed to be converted to millimetres at ground level to standardise input for the weight-estimation equation and filtering operations.

3.5.3 Projecting Extracted Pixel Dimensions to Metric at Ground Level

The raw body measurements extracted from the image are originally found as pixel lengths or pixel areas. However, it is important to recover the actual body measurements of the animal in a metric measurement for a better understanding of its body measurements and to build estimation equations appropriately. A combination of factors surrounding: (i) the installation height between the camera and the object (animal or ground), (ii) the field of view of the lens and sensor assembly and the (iii) cameras resolution setting, are required to perform the conversion from pixels to metric measurements. The conversion method between pixels and metric adopted by the system in now discussed.

Figure 53 illustrates a typical installation, where the height of the camera $h_{w_{camera}}$ is known (from lens to ground) and the height of the pig $h_{w_{pig}}$ is unknown.
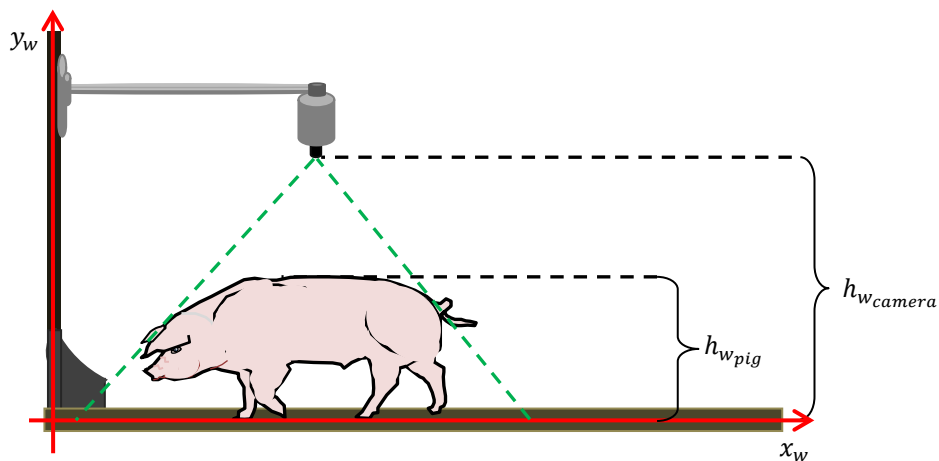
Figure 53: Basic Diagram of a Typical Installation of the System

When $h_{w_{camera}}$ is known, the characteristics of the field of view and sensor size of the camera can be used to determine the pixel to millimetre relationship at ground level. The specific characteristics that are required for the conversion are the sensor size $l \times w$ and the focal length (f) of the camera lens and sensor assembly. The focal length of the camera used in this study was $f = 3.7\ mm$ and the sensor size was 1/3.2", meaning the height and width of the sensor was $l = 3.416\ mm$ and $w = 4.536\ mm$ respectively. Using these parameters, the field of view could be determined using simple calculations to determine the angles a_w, a_d and a_h illustrated in Figure 54.

83
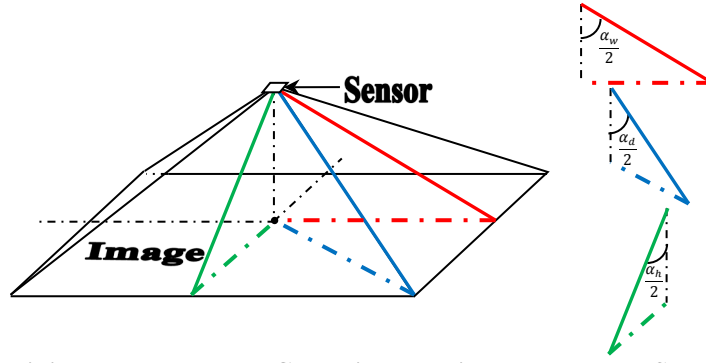
Figure 54: Determining the Real World Co-ordinates Using the Lens and Sensor Characteristics

Calculations of these angles for the camera used in this study are shown in Table 6.

Table 6: Equations Used to Determine the Angles of the Cameras Field of View

$$\alpha_w = 2arctan\left(\frac{w}{2f}\right) = 2arctan\left(\frac{4.536}{2 \times 3.7}\right) = 63.01434319$$

$$\alpha_h = 2arctan\left(\frac{h}{2f}\right) = 2arctan\left(\frac{3.416}{2 \times 3.7}\right) = 49.55813687$$

$$\alpha_d = 2arctan\left(\frac{d}{2f}\right) = 2arctan\left(\frac{\sqrt{3.416^2 + 4.536^2}}{2 \times 3.7}\right) = 75.00186484$$

As the actual sensor size of the camera used in this study was not given by the camera manufacturer a simple test was performed to recover it. The camera was orientated so that its sensor was facing parallel to a wall. Markers were then placed on the wall such that they could be observed at the corners of the resultant image. The angles of the lens could then be derived from the distance between the markers in the resulting images and the working distance between the camera and the wall. The equations presented in Table 6 were then rearranged to determine l and w. Tables containing standard sensors sizes were then used to determine the actual sensor size, and lens angles based on closest match to l and w.

These angles could then be used to determine the pixel to millimetre ratio at ground level for any resolution setting or installation height. For example, if the camera system is installed at a height of 2 m and set to UXGA resolution (1600x1200 pixels) then the number of millimetres that each pixel represents at ground level can be determined using simple trigonometry with the field of view angles $(\frac{\alpha_w}{2}$ or $\frac{\alpha_h}{2})$. Figure 55 illustrates how to calculate the distance of the image width at ground level in this scenario.

$$x = 2\tan\left(\frac{\alpha_w}{2}\right)$$
$$x = 2\tan(31.507) = 1.2259m$$

Multiplying x by 2 to get the entire image width at ground level

Image width $= 2x = 2.4519$m
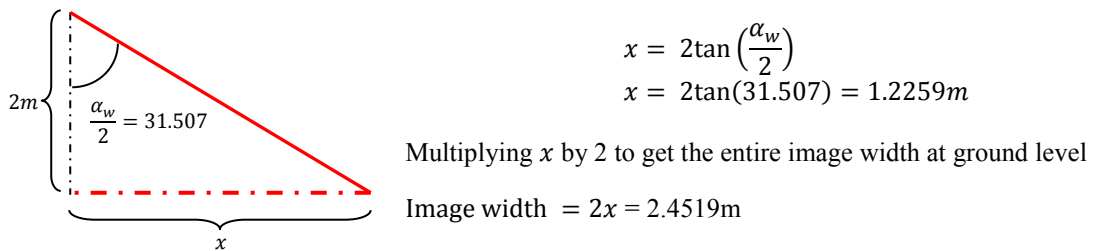
Figure 55: Calculating the Real World Image Dimensions at Ground Level

Using this information, the pixel to millimetre ratio can be determined as 2451.9 mm / 1600 pixels = 1.5324 mm / pixel. Hence every pixel represents 1.532 mm at ground level at an installation height of 2 m when using UXGA resolution using this particular camera. In the same manner, a conversion can be carried out across any selected resolution as long as the installation height is given.

This conversion process is very important, as it can be used to standardise the space for equation input in this study, meaning that weight-estimation equations can retain the same coefficients regardless of installation height or selected resolution. This is possible as the camera observes growth (from above) relative to ground level. Thus body measurements in pixels can always be converted to metric at ground level using the procedure discussed above. Therefore, by creating equations at the ground reference plane and converting the obtained pixel body measurements to metric at this plane, the equation coefficients will always relate to the correct input body measurements. It is believed that this conversion feature was incorrectly implemented into the commercial system's software tested in *Chapter 8 Comparison between PiGUI and a Commercial System*.

However, it is important to note that the converted body measurements do not relate to the real world body measurements of the animal in millimetres, but are the size of the animal in millimetres relative to the ground. To obtain the actual real world body measurements of the animal the same principal is used. If the approximate height of the animal is known, then the same millimetre to pixel conversion can be performed over a distance that is the installation height minus the estimated height of the pig. This then results in a pixel conversion that will approximate the actual real-world body measurements of the animal. To achieve this, however, a height estimate or height measurement of the pig is required. Several methods have been used to recover the height of the animal. These techniques include:

- Using multiple cameras (stereo or 3D camera configuration) to recover depth from images
- Using a single camera techniques such as light striping
- Using a side view image
- Using a single camera in motion to build stereo pairs
- Using markings on the pig of known body measurements
- Calculating the focal distance between two regions within the image (animals-back area and the background) to be estimated (Fear and Herz, 2008)

Notably, the height measurement is only approximate as it is difficult to measure precisely due to the curved surface of the pig's back. To avoid system over-complication, the role height plays in weight estimation was revised (see Section *3.6.1.3 The Effect of Height as a Variable Input into the Weight-Estimation Equation* later in this chapter).

3.5.4   Filtering the Extracted Body Measurements for Weight Validation

The body measurement extraction methods presented in Section *3.5.2 Feature Extraction Development* were applied to a large number of video frames to determine the body measurements of pigs. Although the extraction methods were effective at finding the body measurements from the contour, they did not have intelligence to

determine whether the body measurements that they extracted were obtained correctly from the contour of a pig. Subsequently, a filtering procedure was required to perform this validation task.

This involved modelling a curve for each body measurement in respect to weight. The curve of each body measurement could then be used to validate the weight of an animal. An example of the model-curve between weight and the area body measurement AT_2 is shown in Figure 56.

A software program (named limits) was written to construct the filter's constraints so that the filter could be easily fine-tuned (shown in Figure 56). To begin the process, the data of sample video frame weights and their respective (extracted) body measurements were stored in a table. This data table was then referenced by the limits software when the user chose to apply confidence limits to any given weight and body-measurement relationship. The software user has the option to select a confidence limit value from 1% to 99% for each weight and body measurement model. A 1% confidence limit indicates that 1% of the data are captured within the upper and lower limit of the modelled relationship, while setting the confidence limits to 99% will ensure that 99% of the data are captured within the upper and lower limit of the modelled relationship. These two settings indicate the strictest and loosest settings for filtering the dataset respectively. When the Save button is pressed the upper and lower limits are saved to a table which is later referenced by the main program during operation.

The resulting filter makes the decision to include or exclude contours for weight output based on their extracted body measurements in respect to their estimated weight. For example, if a contour produces a weight estimate during normal operation of the piGUI system then the limits validation function (filter) will be called. This function first determines the body measurements extracted from the contour that have been selected for filtering using the limits software. These body measurements are then compared with the limiting range specified for each body measurement's weight estimate. The weight is outputted if the extracted body measurement(s) fall within the limiting range provided and disregarded otherwise. The performance of the filter is documented in Section *3.6.4 The Dimension Limiting Filter*.
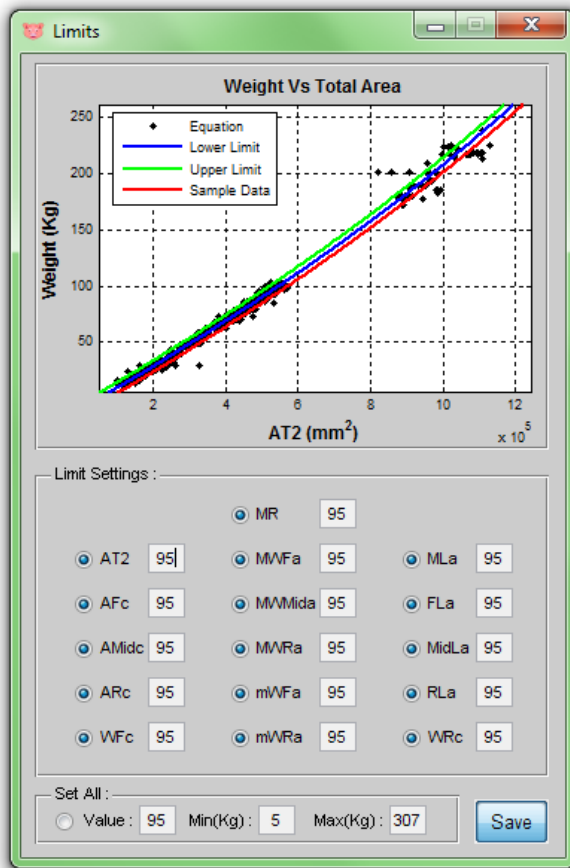
Figure 56: Setting the Confidence Limits on Body Measurement Data for Validating each Body Measurement

Many thousands of contours were successfully identified as a pig using this limiting method. However, there were inconsistencies in the poses of the animals which passed though the limiting filter and, on occasion, a false positive would occur (see Figure 76). The limiting filter was also applied late in the processing loop, immediately before weight output, so redundant data identified at this late stage caused undesirable disruptions to processing time. Due to these limitations another filter was created that could determine the integrity of the contour sample to remove redundant information early in the process. As a result a new filtering method was investigated surrounding the segmented shape.

3.5.5 Filtering the Shape for Pig Recognition and Pose Validation

The literature survey found numerous authors who stated that the variability in the animal's body pose was likely to have led to errors in the extracted body measurements, causing errors in the resulting weight estimates. Therefore, an effort was made to create a method which could identify an animal within the image when it was in a specific pose. This method would enable the body measurements to be referenced and repeated reliably during the extraction stage and consequently a higher-level of control could be maintained in respect to the body measurements that were passed into the weight-estimation equation.

3.5.5.1 *Building the Average Pose Based on a Template Shape*

87

The shape filtering method began by first selecting a frame of a pig that was in the desired pose; standing with its head and body straight and its legs obscured from the camera. The contour was then recovered from this pose to form the initial template. An example is given in Figure 57. The Cartesian co-ordinates of the contour were converted into polar co-ordinates such that the contour could be reconstructed from an angular vector THETAt (Figure 58 (b)) and a magnitude vector RHOt (Figure 58 (a)). These vectors were then extrapolated so that they both had 1500 points. The procedure used to recover a reference contour from an image can be found in Appendix C.
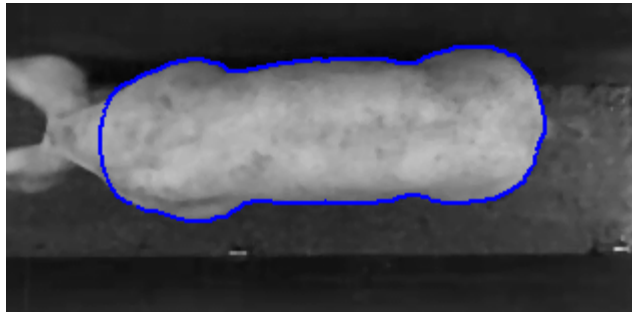
Figure 57: The Specified Template Shape of a Pig's Body Pose

The characteristic appearance of the angle and magnitude vectors of the template shape (and pose) are shown in Figure 58 in respect to the shape's centroid.

(a)   (b)
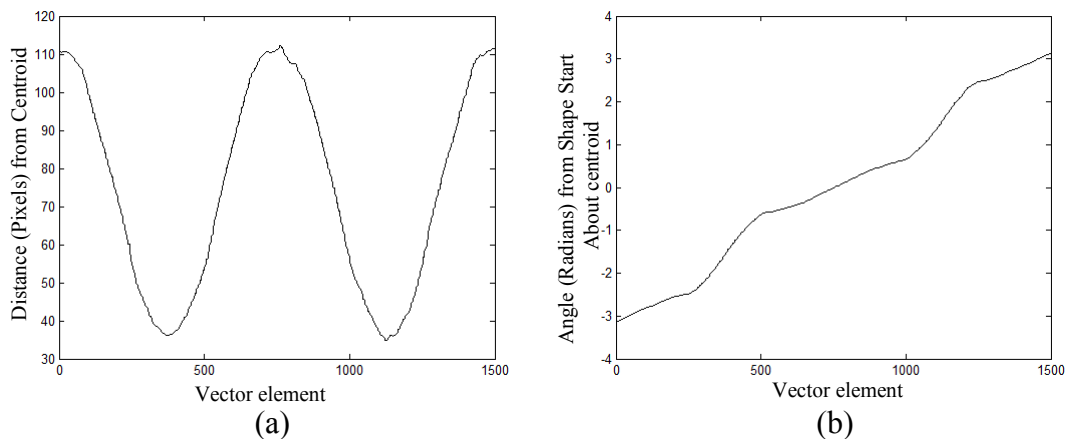
Figure 58: The Characteristic Profile of the Polar Co-ordinates of the Template Shape (a) The Magnitude of the Contour Points (RHOt); (b) The Angles of the Contour Points (THETAt) (radians)

The vectors of the template shape could be compared against the vectors of other body contours to determine their fit against one another. However, the magnitude was required to be normalised first so that the comparison could be carried out for different sized animals over a range of weights. This involved determining the greatest magnitude within the magnitude vector and then dividing the magnitude vector by this value. The result ensured that the largest magnitude within the vector was 1. Once the reference contour and a sample contour were in this format they could be compared directly.

To perform this comparison, a convolution between the template shape magnitude vector (RHOt) and the sample vector (RHOs) was undertaken. This involved recursively shifting RHOs over RHOt and recording the difference between the two

vectors. After the RHOt vector had completely passed over the RHOs vector the stored matrix of differences was evaluated to determine where the minimum difference between the two vectors had occurred. This evaluation involved finding minimum absolute variance within the matrix and the iteration in which it occurred. This iteration indicated when the alignment of the two contours magnitudes was closest. An identical shift operation was performed on the angle vector so that the angles were also in the best possible alignment. Figure 59 to 61 illustrate this process. Figure 59 shows two different segmented pig contours that are in similar postures but orientated at different angles. Figure 60 shows the blue contour in alignment with the red contour as result of finding the minimum absolute variance within the difference matrix created during the convolution. Figure 61 illustrates the two contours after they have both been normalised. There is a noticeable similarity between the shapes of the different sized and weight pigs after this step.
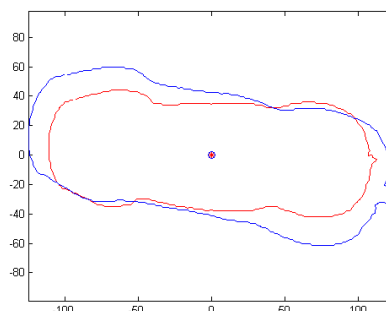
Figure 59: Comparing the Contours of Different Pigs
Template shape (RHOt, Red), Contour Sample in (RHOs, Blue)
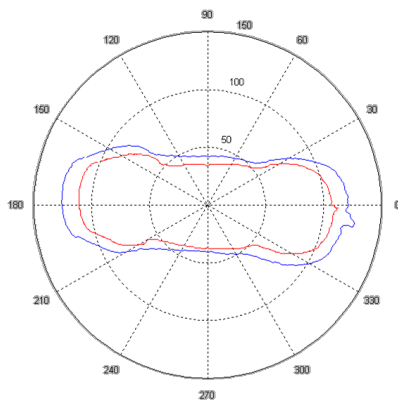
Figure 60: Aligning the Contours   **Figure 61: Scaling the Contours**
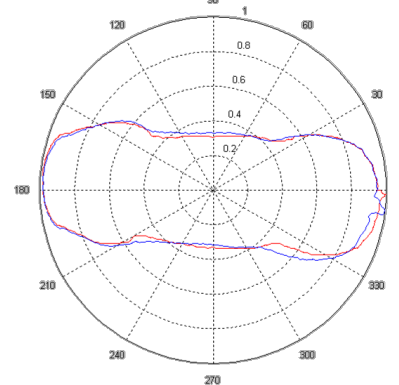
The difference between the best fit between the reference contour and a sample contour was recorded as the residual (Figure 62). This residual could then be used to discriminate between two shapes. Various calculations indicating the fit between the two shapes could be made based on this residual. Examples are the sum or absolute of the residual error, sum of squared error (SSE), the variance, the correlation coefficient (r) or the coefficient of determination (R^2).
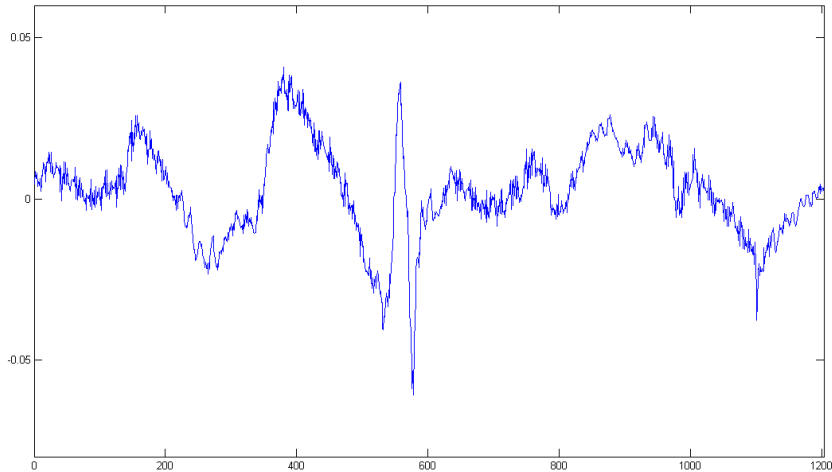
Figure 62: The Residual Difference Between the Sample and the Template shape

3.5.5.2 *Testing the Residual as a Basis for Shape Filtering*

To test the residual as a basis for shape filtering, the comparison between the magnitude and the angle was carried out across a small collection of 700 contour samples in respect to the template shape. Figure 63 shows the variance of these samples' residuals in respect to the template shape. In Figure 63 the variance has been sorted from minimum variance (best fit to RHOt) to maximum variance, (worst fit to RHOt) over all the 700 samples. Alternatively two other sorting methods could have been used in a similar manner: (i) using the angle vectors or a (ii) combination of the both the angle and magnitude vectors.
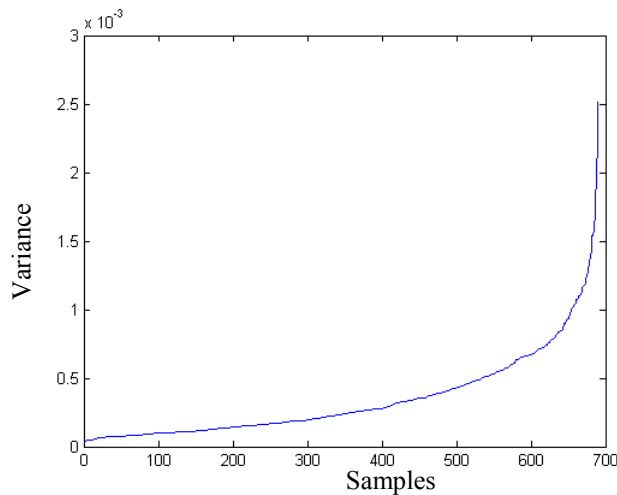
Figure 63: Sorting Contour Samples Based on the Absolute Variance of the Residual between the Sample and Template Shape

After sorting the samples, a gradual increase in variance can be observed (see Figure 63). The samples on the far right of this figure indicate the most poorly fitted contours and have the highest pose-related error from the template shape pose. To give a preliminary indication of how well this method might determine the pose related to the template shape, the first and last samples in the sort array

90

(corresponding to best and worst poses) were identified. These two samples are shown in Figure 64 (a) and (b).

(a) **(b)**
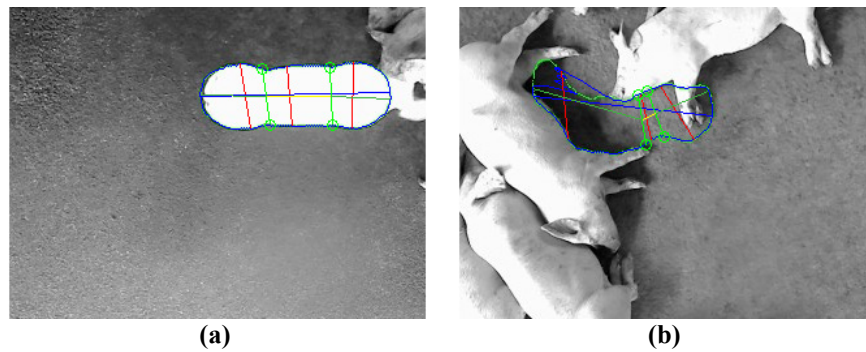
Figure 64: Using the Absolute Variance of the Residuals to Determine the (a) Best and (b) Worst Fitting Contours to the Template Shape

Figure 64 (a) is of a pig in an almost perfect posture as defined using the template shape earlier. The body measurements have also been recovered correctly. In contrast, Figure 64 (b) is not even the contour of a pig and should have been rejected. Figure 65 shows the clear differences between the magnitude and angle of the template shape and the sample contour shown in Figure 64 (b).
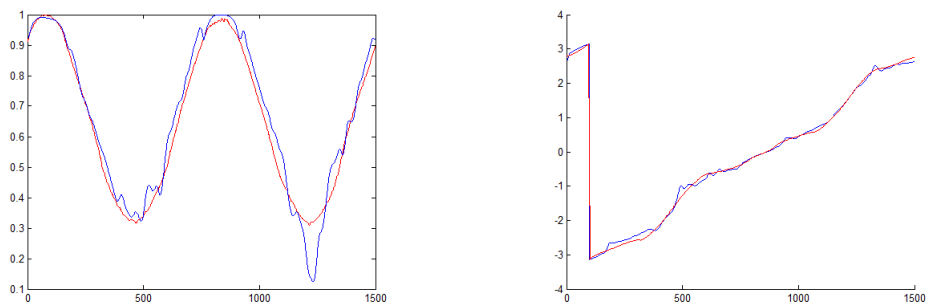
Figure 65: Using the Template Shape to Identify Errors in Contours
The Contour Sample in Figure 64 (b), Shown in Blue and the Template Shape Shown in Red

It would be inappropriate to base the shape filtering component of the system on a single template shape as abnormalities may be associated with it. Consequently, the sample contours which fitted closely to the template shape were grouped together and combined to form an average template shape. This was a simple process, as all angles and magnitudes of the contour samples had 1500 points and were in alignment and scaled appropriately. Subsequently, the average template shape could be formed by averaging the angle and magnitude vectors on a point by point basis for the group of selected samples.

This process was carried out over a dataset containing over 750 videos of 586 pigs with weights between 12.5 and 306 kg. In total 22419 contours (THETA and RHO vectors) were recovered from the frames of these videos after segmentation.

The average shape created from all these 22419 THETA and RHO vectors is shown in Figure 66. Considering that during the segmentation process the system was free to collect shapes with only basic constraints, the resulting shape has surprisingly maintained an appearance resemblant of a pig contour. This is likely to be the result

91

of the tracking procedure described later in Section *3.6.6* which managed to locate the pig in the majority of frames.
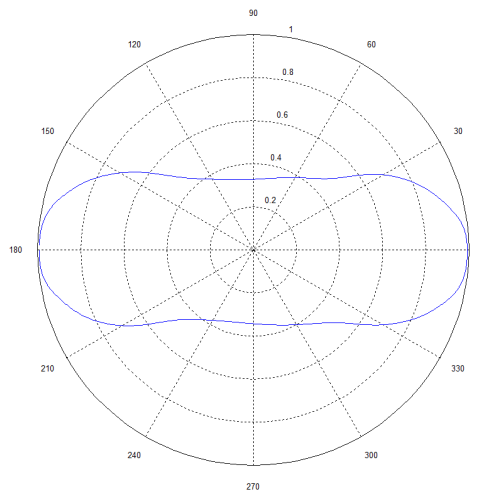
Figure 66: Average Shape of All 22419 Samples

However, the averaged shape, in Figure 66, is built from many erroneous contours which should be removed. To determine the contour samples which should be included or excluded in the average template shape, the fit to the template shape was used. In the following example an R^2 fit between the contours was used. This involved first calculating the sum of squares of the residual between the template shape and each sample (SSE) and the sum of squares of the regression (SSR) between the average value of the template shape and each sample. Using this information the R^2 fit of the 22419 shapes to the template shape was determined. Figure 67 below shows the worst two fitting contour vectors as decided (after sorting) based on the magnitude Figure 67 (a) and angles Figure 67 (b) respectively.
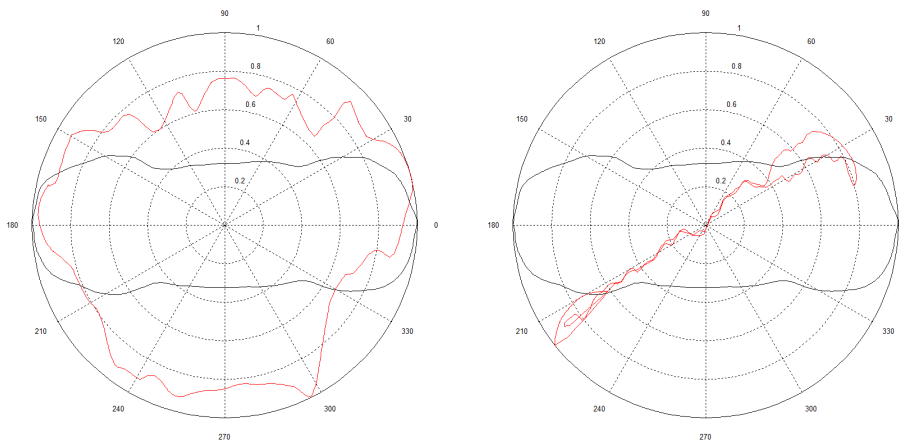
(a) RHOs (R^2 =0.36)   (b) THETAs (R^2 = 0.24)

Figure 67: The (a) Worst Fitting Rho and (b) Theta Vectors to the Template Shape (Black) Out of All 22419 Contour Samples

In contrast, Figure 68 (a) shows the best fitting contour based on sorting the R^2 of the magnitude and the angle (Figure 68 (b)) vectors separately. Both sorting methods have resulted in the selection of sample contours which closely resemble the pose of the pig in the template shape. A similar result was achieved earlier using the variance of the residual and sorting based on magnitude, highlighting that different methods can be used to determine the fit (or rank) of the samples.

92
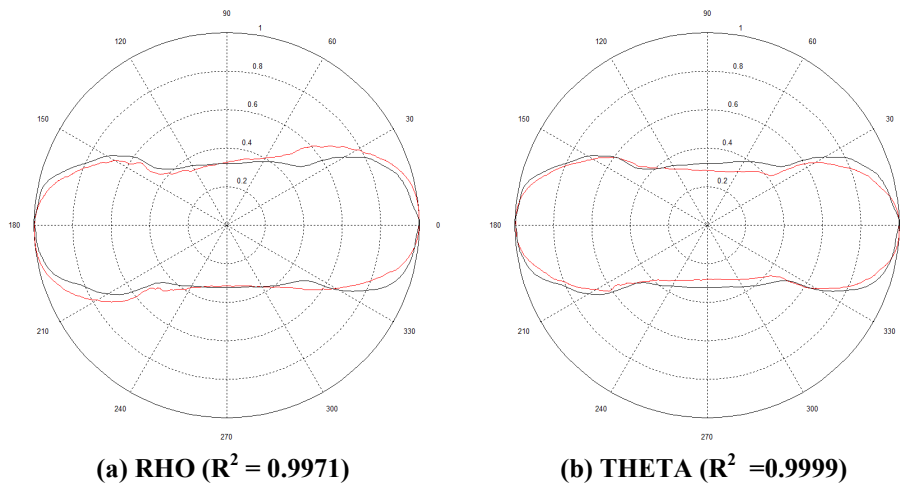
(a) RHO (R^2 = 0.9971)   **(b) THETA (R^2 =0.9999)**

Figure 68: Best Fitting Rho (a) and Theta (b) Vectors to the Template Shape from All 22419 Contour Samples

The magnitude and angular R^2 fit between all the 22419 contour samples is shown Figure 69 in order of best to worst fit.
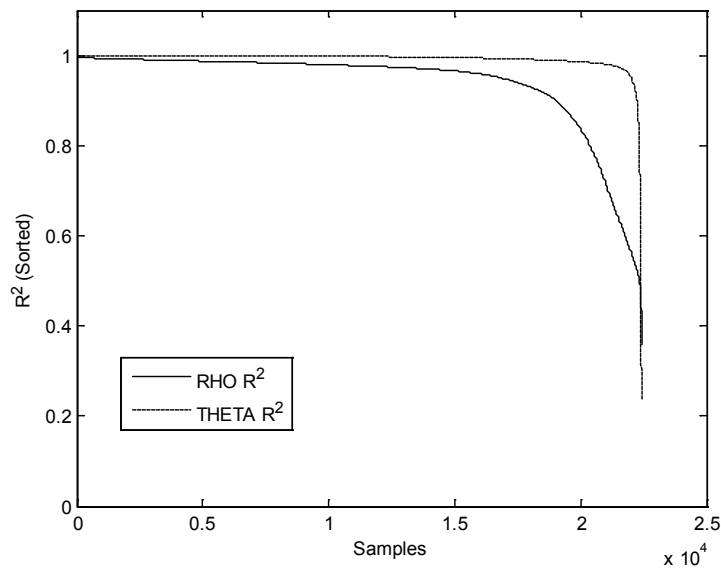
Figure 69: All 22419 Contour Samples Sorted in Order of Highest to Lowest R^2 Based on Theta and Rho

Figure 69 indicates that the angle vectors of the contour shapes correlate highly over majority of the dataset. Thus a small negative deflection in the angular fit from the template shape indicates a potentially large change in shape. The R^2 value for the angle vector will drop if there is a delay in the angular progression around the sample contour in relation to the template shape. For example, if the angle slows down, stops or reverses (as Figure 67 (b) demonstrates) as it indicates that the contour has been sampled sub-optimally from the image. The variation about the average deviates more dramatically for the magnitude vector in Figure 69 indicating that a small deflection in the R^2 fit of the magnitude will result in a more modest change in shape.

Therefore, those samples to the left of Figure 69 are candidates for contour selection to form the average template shape as they fit the closest to the template shape pose.

93

3.5.5.3 *Forming the Average Template Shape*

Two methods were used to determine how many of the contour samples should be used to build the average template shape. These were: (i) organising the shapes into order of fit using either the variance, SSE or R^2 and determining a cut-off value or (ii) determining those samples which had all points lye within a certain deviation of the template shape. A flow diagram documenting these different processes is shown later in Figure 77.

3.5.5.3.1 *Method 1: Determining the Average Template Shape Iteratively*

The first method involved progressively including a new sample contour into the average template shape. At each iteration a new average template shape was formed and compared with the previous average template shape. As sample contours were introduced into the average shape the difference between successive average template shapes tended to zero. After the first nine contours the absolute difference between the current and preceding average template shape was 0.0011. After the inclusion of the top 1136 fitting magnitude and 6899 angle vectors the difference between the current and preceding average template shape was less than 1×10^{-7} based on an R^2 sort. At this point the magnitude and angular vector components of the average template shape was only changing a small amount so it could be approximated as zero. These vectors were then average and used to build a new average template shape as shown in Figure 70 below.
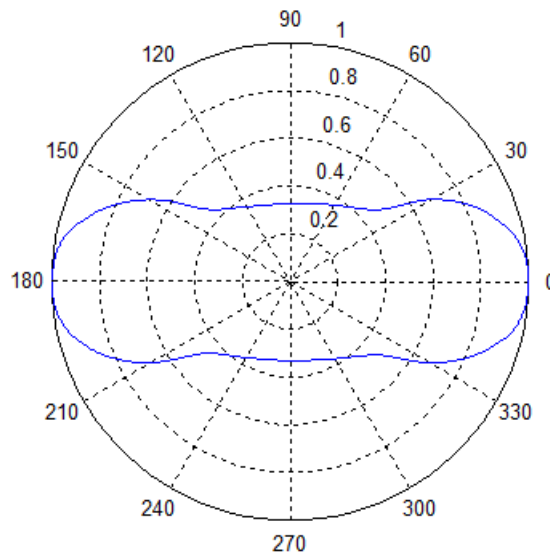
Figure 70: The Average Template Shape Iteratively Built from the Best Fitting Contour Shapes

3.5.5.3.2 *Method 2: Determining the Average Template Shape on a Point by Point Basis*

The second method involved the comparison between the contour samples and template shape's magnitude and angular vectors on a point by point basis. In this method the template shape's vectors formed a base reference to which a deviation-based limiting range was applied. This is illustrated in Figure 71.

(a)   (b)
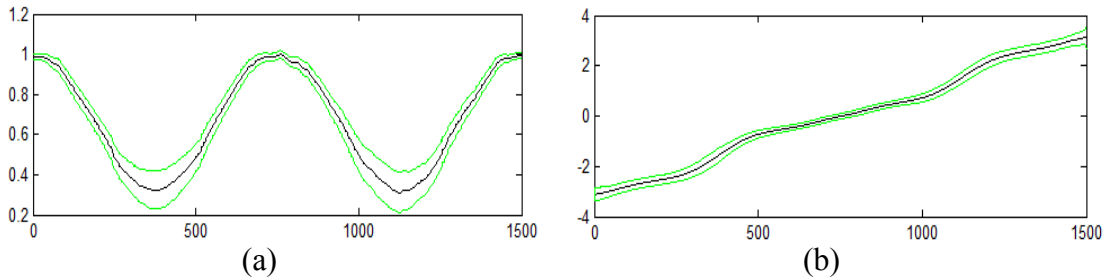
Figure 71: The (a) Magnitude and (b) Angle Vectors with Deviation Limits

The standard deviation of the 22419 contour samples was determined for both the magnitude and angle vectors. The initial filtering limit was set at 1.3 times this standard deviation. Subsequently, all the 22419 sample contours were compared with the reference vectors and limiting range to see whether all the contours' points passed within these deviation limits. This is illustrated in Figure 72.

(a)   (b)
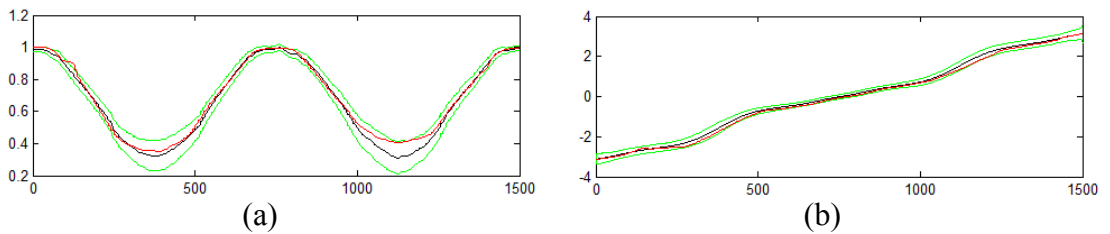
Figure 72: Determining the Number of Contour Points (Red) within the Deviation Limits (Green)

The samples which had all their 1500 points pass within these limits were selected for use in the following stage of the average template shape building process. This next stage involved determining the mean and deviation of the samples that passed. The filtering limit was then set to 2.5 times the calculated deviation of the selected samples. Those samples which passed through this secondary filtering process were averaged to form the final average template shape (shown in Figure 73). A total of 1229 magnitude and 6927 angle vectors were used to build the contour shape. The deviation figures of 1.3 and 2.5 were determined by observing the predictive response (precision and number of good quality weight estimates) of the built shape. A table containing the results from different variations of deviation rejection bounds for filtering and modelling the weight-estimation equation can be found in Section *3.6.3 Adjusting the Bounds of the Shape Filter*.

95
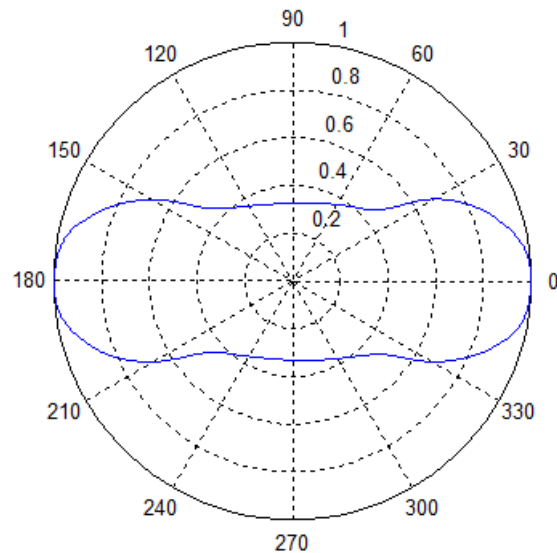
Figure 73: The Average Template Shape Built from the Contours which had the Highest Rate of Points Passing within a Certain Deviation of the Template Shape

These methods both produced a similar average template shape from a similar number of samples. However, the second method was chosen for reasons explained later in Section *3.6.1.2.1 Ranking and Selecting Estimates Based on their Contour Shape*. To avoid the likelihood of the average template shape having a bias toward a particular weight range, the animal weights of the sample contours that were used to build the average template shape were revised.

3.5.5.4 Determining the Weight Distribution of Samples Used to Create the Average Template Shape

The preferential order in which certain pigs made up the average template shape was determined so that the weight range of the animals that had derived the average shape could be assessed further. There were 1229 magnitude and 6927 angle vectors which contributed to the average template shape. These samples represented frames from 503 of the 703 videos and 416 of the 586 pigs, as 87 pigs had a second video which had at least one frame used to help build the average template shape. It was of interest to see what the weight distribution was for the pig shapes used to build the average template shape to avoid the likelihood of any bias to particular weight ranges. Figure 74 shows the frequency of the animal weights included in the average template shape based on the videos that had frames which contributed to the contour.

96
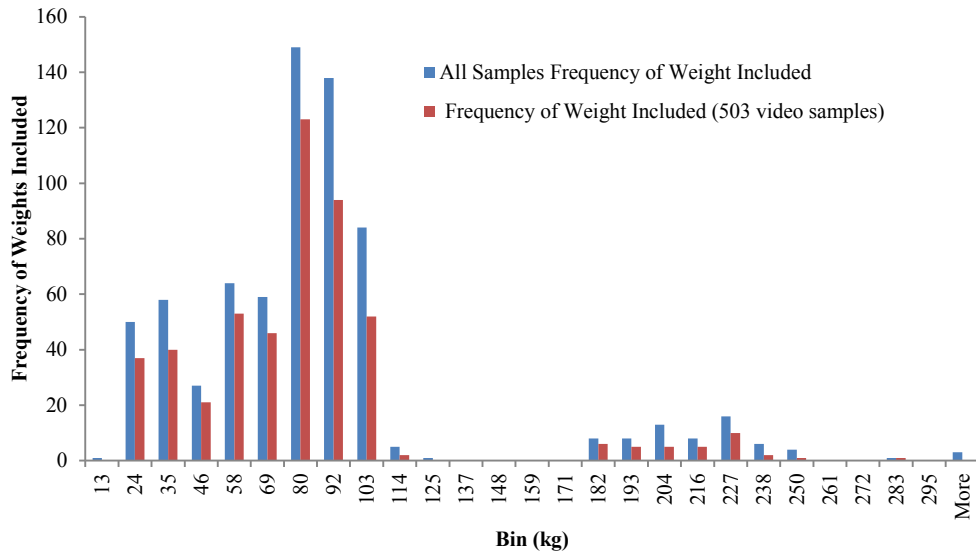
Figure 74: Frequency of Pig Weights Included in the Average Template Shape

The weights of the animal contours used to build the average template shape are a reflection of the number videos available for analysis in each weight category (refer to Figure 74). This suggests that there has been no contour-weight-related bias in the selection of sample contours into the average template shape during the building process. Table 7 shows the percentage of available videos within each weight category that were used to build the average template shape.

Table 7: Frequency of Pig Weights Included into the Average Template Shape

Weight Range (kg)	All	Included	%
0-13	1	0	0
13-24	50	37	74
24-35	58	40	69
35-46	27	21	78
46-58	64	53	83
58-69	59	46	78
69-80	149	123	83
80-92	138	94	68
92-103	84	52	62
103-114	5	2	40
114-125	1	0	0
125-137	0	0	0
137-148	0	0	0
148-159	0	0	0
159-171	0	0	0
171-182	8	6	75
182-193	8	5	63
193-204	13	5	38
204-216	8	5	63
216-227	16	10	63
227-238	6	2	33
238-250	4	1	25
250-261	0	0	0
261-272	0	0	0
272-283	1	1	100
283-295	0	0	0
295-More	3	0	0

Table 7 further demonstrates that it is unlikely that favouritism or a bias may exist towards a specific weight as between 60% and 83% of sample videos had at least one sample included in the equation, within each weight category between 13 and 103 kg. The other categories vary, however, this is suspected to be a result of the limited availability of data (less than 20 videos) in these categories. Noticeably, a more conclusive dataset for pigs less than 13 kg and greater than 103 kg could be

97

collected, however, pigs in this weight range are outside the scope of this study as the apparatus focuses on pigs in their grower and finisher phase from 30 to 120 kg. What is reassuring, is that the contour vectors of every weight range have been incorporated into the average template shape from 13 to 277 kg and majority of these (92.6%) come from pigs in their grower or finisher phase; the target weight range. This indicates that the filter should be suitable to recognise pigs across this weight range.

This average template shape formed the base for the shape filter which was subsequently used in the model building process.

3.5.6 Modelling

This section presents the model development from the first dataset obtained during the late stages of the CRC project through to the finalised dataset obtained and used during this PhD study to construct the weight-estimation equation. Nomenclatures for the abbreviations found in this section are shown below in
Table 8.

Table 8: Nomenclature for Abbreviations used for Equation Building and Selection

DF_e	Degrees of freedom for the error, used in the calculation of R^2_{adj}
DF_r	Degrees of freedom for the regression
S_{Se}	Sum of squares error (of residuals) – the closer to zero the smaller the random error component and thus indicating it is more useful for prediction
S_{Sreg}	Sum of Squares Regression
p_i	Equation Coefficient
F	F-Statistic for mean testing the final model versus no model
R^2	The proportion of variance accounted for by the model
S_{ey}	Root Mean Square Error – an estimation of the standard deviation of the random component in the data, the closer to zero the smaller the random error component indicating it is more useful for prediction.
S_{eb}	The standard error value for the constant p_2
S_{en}	The standard error values for the coefficients

3.5.6.1 *Extracted Body Measurements and their Correlation to Weight: Early Findings*

The initial assessment was undertaken on a dataset consisting of a collection of 177 video segments of a random number of pigs. A corresponding CSV file with the animals' actual weights and six extracted body measurements also formed part of the dataset. These extracted body measurements were obtained from the videos using a vision system that was not part of this development. The body measurements included total body area (PixelArea,), area of Gut (GutArea), the diameter of the front and rear sections (ForeDia and RumpDia), the Body Length and the Maximum body width. The statistics of the different body measurements are presented in
Table 9.

Table 9: Statistics of Dataset Obtained from the Original Vision System Developed in the CRC Project

Statistic	PixelArea	RumpDia	ForeDia	BodyLength	MaxWidth	GutArea
p_1	1.31E-03	0.34	0.43	0.16	0.36	-1.84E-07
S_{en}	3.40E-05	0.01	0.02	8.30E-03	7.70E-03	2.20E-07
R^2	0.28	0.27	0.21	0.12	0.35	3.96E-04

F	1521.26	1455.87	726.49	347.69	2141.61	0.70
S_{Sreg}	104880.49	101574.38	28972.69	15639.45	132750.62	31.56
p_2	7.81	4.15	-6.76	6.25	-0.75	33.78
S_{eb}	0.77	0.89	1.51	1.48	0.84	0.16
S_{ey}	8.30	8.35	6.32	6.71	7.87	6.74
DF_e	4006.00	4006.00	2672.00	2668.00	4006.00	1755.00
DF_r	1	1	1	1	1	1
S_{se}	276187.23	279493.34	106560.81	120010.40	248317.10	79621.20

The statistics in Table 9 indicate that the linear least squares fit between weight and the body measurements are poor. There are two possible causes for these poor relationships: (i) the body measurements were recovered precisely and the data collected is a true representation of the variability between the weight and each of the body measurements relationship or (ii) the body measurements were recovered inaccurately and the variability is a result of careless errors occurring during image analysis by the apparatus. Drawing on the findings of the literature survey, it can be identified that the latter of these two causes is likely to be the reason behind these poor relationships as several authors have demonstrated high correlation between some of these body measurements such as pixel area (Minagawa and Ichikawa, 1994; Schofield, 1990). Figure 75 below exemplifies this fact by showing the erratic spread of the max width records ($R^2 = 0.35$) taken from the dataset. Despite the large number of outliers, a solid cluster of data can be seen which potentially describes the underlying relationship between the extracted maximum width measurement and weight.
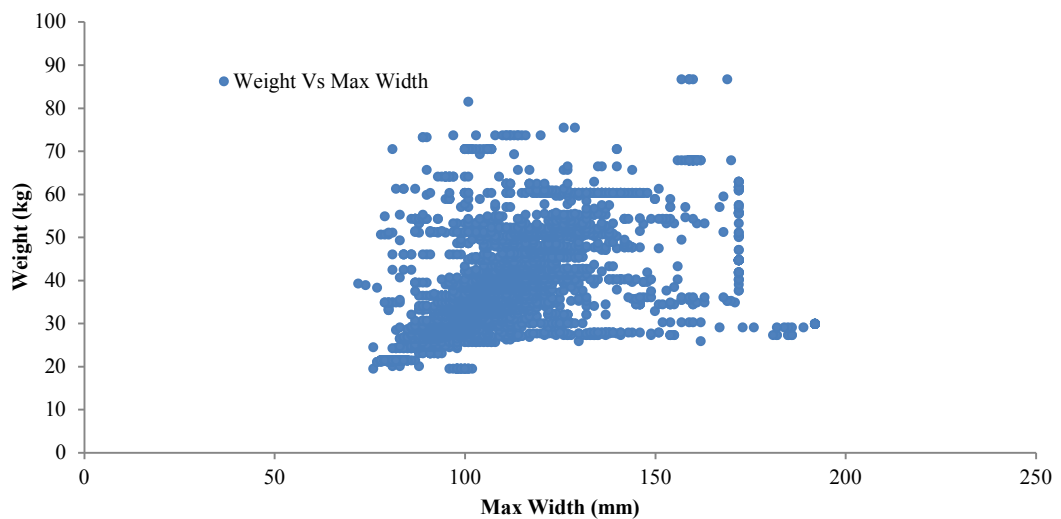
Figure 75: Variation in the Maximum Width Measurement as Recorded by the Original Vision System Developed in the CRC Project

Although the equations derived from this dataset are not likely to be conclusive, a small test was undertaken to determine the weight estimation ability of the body measurements extracted using the CRC Project vision system. This could then be used as a benchmark for the work undertaken in this study. The p_1 and p_2 values in Table 9 are the coefficients of the linear equation for each of the extracted body measurements (see Equation 3).

$$f(x) = xp_1 + p_2, \text{ where } x = \textbf{PixelArea}, \textbf{RumpDia} \dots \textbf{ect}$$

Equation 3: Linear Equation Used to Estimate Weight

These equations were built using half the acquired data located in the CSV file. The other half of the data samples were used to test the equations. Not all body measurement vectors had the same number of elements. It was believed that this was due to certain body measurements being excluded during the analysis when they were not extracted correctly. The number of data pairs (weight and body measurements) used to building and test the equations is shown in Table 10.

Table 10: Division of Data Used for Modelling and Testing the Data Obtained from the Original Vision System Developed in the CRC Project

	PixelArea	RumpDia	ForeDia	BodyLength	MaxWidth	GutArea
Modelling	4008	4008	2674	2670	4008	1757
Testing	4008	4008	2674	2670	4008	1757

The tests results were presented in seven weight error categories indicating various levels of estimation precision. The weight error in Table 11 is the absolute error between the actual weight obtained from the electronic livestock scale and the vision systems weight estimate (W_{est}). The categories shown in the first column of Table 11 contain the number and percentage of weight estimates which occurred within the seven precision ranges

Table 11: Weight Estimation Performance of Equations Derived from the Data Obtained from the Original Vision System Developed in the CRC Project

Error Category (kg)	PixelArea	RumpDia	ForeDia	BodyLength	MaxWidth	GutArea
$w_{est} < 0.5$ kg	423 (11)[*]	347 (9)	244 (9)	247 (9)	409 (10)	156 (9)
0.5 kg $\leq w_{est} < 1$kg	408 (10)	339 (8)	229 (9)	229 (9)	362 (9)	132 (8)
1 kg $\leq w_{est} < 2$ kg	655 (16)	652 (16)	458 (17)	408 (15)	837 (21)	179 (10)
2 kg $\leq w_{est} < 3$ kg	553 (14)	499 (12)	439 (16)	453 (17)	564 (14)	239 (14)
3 kg $\leq w_{est} < 4$ kg	496 (12)	442 (11)	382 (14)	365 (14)	491 (12)	242 (14)
4 kg $\leq w_{est} < 5$ kg	272 (7)	371 (9)	283 (11)	273 (10)	334 (8)	97 (6)
$w_{est} \geq 5$ kg	1201 (30)	1358(34)	639 (24)	695 (26)	1011 (25)	712(41)
Total Samples	4008	4008	2674	2670	4008	1757
$w_{est} < 2$ kg	1486(37)	1338(33)	931(35)	884(33)	1608(40)	467(27)

[*]Count (Percent)

The results from the CRC Project dataset indicated that the CRC Project system had the potential to estimate individual animal weights within ±2 kg approximately 40% of the time if the derived weight-estimation equation was used during online operation (refer to MaxWidth in Table 11). The large number of estimates that were greater than or equal to ±5 kg (> 24%) reinforces the point made earlier that there is a large amount variability in the extracted measurements that formed the dataset; a direct cause of poor weight estimates.

3.5.6.2 *The Start of the Vision System Development: CRC PhD Study*

The current benchmark for estimating the weight of both individual and groups of animals was set using the results of the previous Section (*3.5.6.1 Extracted Body Measurements and their Correlation to Weight: Early Findings*), trial results with a commercially available system (see *Chapter 8 Comparison between PiGUI and a Commercial System*) and figures as reported in literature.

An early attempt was made to extract information from the videos within the CRC Project dataset. Although majority of the images were poor quality, those that were

salvageable (such as when the pig was moving slowly beneath the camera and under relatively uniform illumination) were analysed. Primitive versions of the extraction methods presented earlier were used to process the videos and extract the body measurements to form the basis of the first estimation model.

Using these methods, twelve measurements were extracted: Max Length (ML), Max Width (MW), Max Width Front (MWF), Max Width Middle(MWM), Max Width Rear (MWR), Minimum Width Front (mWF), Minimum Width Rear (mWR), Area Front (AF), Area Middle (AM), Area Rear (AR), Skeleton Length (SL) and Total Area (AT). In total, 159 pigs were analysed from the 177 videos within the dataset. The 12 body measurements extracted from each pig across the video frames were averaged out to form a single 1x12 vector. These 159 sample vectors were broken in half for modelling (n_m = 80) and half for testing (n_t = 79) to determine each of the body measurements' ability to estimate weight. The exception was the skeleton length which only returned 148 samples (n_m = n_t = 74) as, on occasion, it was not referenced correctly during processing and as a result was sometimes discarded.

The results of the initial methods used to extract body measurements of the pigs from images are shown in Table 12. The absolute error between the actual weight and the weight estimates (W_{est}) of the individual animals were grouped into the same seven error categories as presented previously.

Table 12: Off-line Estimation Performance of Equations Derived from Early Image Analysis Techniques Developed in this PhD Study

Error Category (kg)	ML	MW	MWF	MWM	MWR	mWF	mWR	AF	AM	AR	AT	SL
$w_{est} < 0.5$ kg	12(15)*	9(11)	14(18)	10(13)	14(18)	13(16)	8(10)	10(13)	8(10)	9(11)	17(22)	6(8)
0.5 kg $\leq$ $w_{est} < 1$ kg	12(15)	14(18)	10(13)	11(14)	13(16)	9(11)	13(16)	5(6)	7(9)	6(8)	17(22)	4(5)
1 kg $\leq w_{est} < 2$ kg	20(25)	27(34)	21(27)	20(25)	20(25)	20(25)	19(24)	14(18)	16(20)	11(14)	23(29)	9(12)
2 kg $\leq w_{est} < 3$ kg	12(15)	14(18)	15(19)	19(24)	14(18)	20(25)	17(22)	12(15)	19(24)	18(23)	9(11)	10(14)
3 kg $\leq w_{est} < 4$ kg	10(13)	11(14)	8(10)	10(13)	7(9)	10(13)	7(9)	6(8)	13(16)	16(20)	12(15)	15(20)
4 kg $\leq w_{est} < 5$ kg	5(6)	2(3)	6(8)	4 (5)	7(9)	4(5)	8(10)	5(6)	4 (5)	6(8)	1(1)	7(9)
$w_{est} \geq 5$ kg	8(10)	2(3)	5(6)	5(6)	4(5)	3(4)	7(9)	27(34)	12(15)	13(16)	0(0)	23(31)
Total Samples	79	79	79	79	79	79	79	79	79	79	79	74
$w_{est} < 2$ kg	44(56)	50(63)	45(57)	41(52)	47(60)	42(53)	40(51)	29(37)	31(39)	26(33)	57(72)	19(26)

*Count (Percent)

Table 13 shows the statistics for each of the derived equations for the 12 body measurements extracted from the CRC Project dataset.

Table 13: Statistics and of the Goodness of Fit for the 12 Body Measurements Extracted from the CRC Project Dataset

Statistic	ML	MW	MWF	MWM	MWR	mWF	mWR	AF	AM	AR	AT	SL
p_1	2.65E-01	4.75E-01	4.91E-01	4.12E-01	4.70E-01	5.02E-01	0.42	1.43E-03	1.38E-03	2.94E-03	1.35E-03	6.65E-02
S_{en}	1.95E-02	2.48E-02	3.31E-02	3.04E-02	2.91E-02	3.10E-02	0.03	3.44E-04	1.57E-04	3.50E-04	5.70E-05	3.52E-02
R^2	0.71	0.83	0.74	0.71	0.77	0.77	0.68	0.18	0.50	0.48	0.88	0.05
F	185.76	367.65	220.50	184.25	259.68	261.18	165.90	17.17	77.24	70.50	564.62	3.58
S_{Sreg}	1499.50	1753.77	1572.09	1495.91	1635.98	1638.12	1448.70	386.83	1062.17	1013.80	1866.53	96.57
p_2	-39.49	-15.75	-15.80	-8.03	-12.62	-13.13	-3.74	22.07	18.95	11.28	-0.46	20.45
S_{eb}	5.30	2.54	3.28	3.02	2.83	2.85	2.85	2.61	1.62	2.58	1.41	6.53
S_{ey}	2.84	2.18	2.67	2.85	2.51	2.50	2.96	4.75	3.71	3.79	1.82	5.19
DF_e	77.00	77.00	77.00	77.00	77.00	77.00	77.00	77.00	77.00	77.00	77.00	72.00
DF_r	1	1	1	1	1	1	1	1	1	1	1	1
S_{se}	621.57	367.30	548.99	625.16	485.10	482.95	672.37	1734.25	1058.91	1107.27	254.55	1943.11

These early extraction techniques demonstrated an increase in precision compared to those used previously in the CRC Project development. For example, the PixelArea previously had a coefficient of determination of 0.28 whereas the equivalent measurement (AT) extracted using the developed techniques was higher at 0.88 (refer to Table 13 and Table 9). According to the test-set the Area measurement (AT) could be used to estimate the weight of individual pigs within ±2 kg approximately 72% of the cases with negligible errors ($w_{est} \geq \pm 5$ kg).

There were two likely reasons that this enhancement occurred. The first was that the previous method was automated, and had very little supervision except for what had been written into the software to control the extraction of the pig's body measurements. In contrast, the body measurements recovered using the developed extraction techniques were found under supervised circumstances and in most cases each of the sample body measurements recovered had been validated to ensure that they had been taken in close proximity to their actual location. The second reason is that the results of the analysis found in Table 12 and Table 13 were based on pigs weighing between 20 and 45 kg. This lower weight range was the result of the limited availability of video frames of larger pigs (>45 kg) where their body was entirely in the FOV of the camera. As a consequence, the task of correctly extracting the body measurements of these larger pigs became much more complicated and, as a result, they were excluded from the analysis. Therefore, when comparing the two datasets, it is possible that the increase in precision within the second analysis is due to the resulting equations being better suited to a specified weight range.

Comparatively, the two analyses on the CRC Project dataset suggested the obvious scenario: that as variability in determining the extracted body measurements decreases, the ability to estimate weight more precisely will increase. Consequently, it appeared that the poor weight estimates (40% < ±2 kg and 25% ≥ ±5 kg) from the previously developed CRC Project system was a result of the incorrect extraction of the body measurements from the image.

Therefore, the system development needed to be based around three aspects to work towards the optimum solution. These were that: (i) the weight-estimation equation needed to be built from information that was as error free as possible (to optimise the estimation model), (ii) performance benefits may occur by applying different weight-estimation equations to different weight ranges and (iii) the level of control needed to be increased such that the body measurements were automatically referenced and extracted correctly. These three areas would complement one another making subsequent weight estimates more reliable.

3.5.6.3 *The Results from the New Dataset*

Although there was limited practical use of the original CRC Project dataset, it contributed to the understanding of acceptable conditions to make a weight-assessment, and what needed to be done to enhance the chance of correct segmentation. As the image is the foundation of the analysis that follows, the videos collected were required to have a good dynamic range to maintain adequate contrast between the animal's contour and its surroundings.

There were also three other considerations to take into account while collecting the new dataset. First, so each pig's body measurements could be referenced and extracted in respect to one another, each video sample should contain frames of the pig entirely in the field of view and should also be in a stationary pose to avoid any motion blur. Second, more appropriate data on pigs weighing more than 45 kg and up to 120 kg was required. Third, critical information that was not recorded along with the new dataset such as the camera's sensor height from the ground (working distance) as well as other specific characteristics of the camera such as the focal length needed to be documented.

The new dataset was collected inside a commercial facility with a camera that enhanced the collected video quality (Logitech Quickcam Pro 9000, Logitech, Quarry Bay, Hong Kong).

Development surrounded two of the key aspects mentioned in the previous section. These were that: (i) to optimise the estimation model, it should be built from information that was as error free as possible and (ii) that an increased level of control was required so that the body measurements could be automatically referenced and extracted correctly and subsequently the amount of data available to the model could be maximised.

The extraction process was again supervised to ensure that the weight and body measurements would be modelled correctly. Thus body measurement data were only included in the model when it was observed to have been referenced correctly. The weights of the pigs included in the new dataset were between 9 and 137 kg to cover the grower-finisher stage. The extraction and trimming method had also been revised. Now rotation of the image to the horizontal was not required before extracting the body measurements. Furthermore, the body measurements could be extracted regardless of the angular orientation of the pig (instead of the vertical measurements, refer to *3.5.2.1 Extracting Vertical Body Measurements*).

The goodness of fit of both the angular and vertical based measurements obtained using the new dataset can be seen in Table 14 in order of lowest to highest R^2.

Table 14: The Goodness of Fit between Vertical Body Measurements and Angular Based Body Measurements (Linear Regression)

Weight Vs.	p_1	S_{en}	R^2	F	S_{Sreg}	S_{eb}	S_{ev}	DF_e	DF_r	S_{Se}
AT_2	7.14E-03	1.08E-04	0.984	4335.80	54418.88	1.13	3.54	72	1	903.68
AT1	7.16E-03	1.09E-04	0.983	4288.64	54409.11	1.14	3.56	72	1	913.45
AT	7.48E-03	1.23E-04	0.981	3712.95	54270.17	1.22	3.82	72	1	1052.39
AMX_a	1.14E-02	2.25E-04	0.973	2596.67	53829.97	1.46	4.55	72	1	1492.59
MWR_a	2.10	5.48E-02	0.953	1464.77	52730.60	3.41	6.00	72	1	2591.95
MWM	2.55	7.15E-02	0.946	1269.16	52352.57	4.04	6.42	72	1	2969.99
MW	2.12	6.21E-02	0.942	1167.97	52110.20	3.86	6.68	72	1	3212.35
MWR	2.08	6.08E-02	0.942	1167.08	52107.89	3.75	6.68	72	1	3214.66
mWR_a	2.35	8.05E-02	0.922	849.29	50999.02	4.00	7.75	72	1	4323.53
mWF	2.34	8.30E-02	0.917	798.06	50744.46	4.33	7.97	72	1	4578.09
MWF	2.19	7.90E-02	0.915	771.09	50598.03	4.60	8.10	72	1	4724.53
mWF_a	2.34	8.47E-02	0.914	761.23	50542.08	4.35	8.15	72	1	4780.47
mWR	2.39	8.92E-02	0.909	717.15	50275.07	4.57	8.37	72	1	5047.49
ML	0.77	2.88E-02	0.908	710.01	50228.97	4.92	8.41	72	1	5093.59
MWF_a	2.18	8.29E-02	0.906	693.46	50118.88	4.85	8.50	72	1	5203.67
AR_a	1.85E-02	7.50E-04	0.894	609.18	49475.05	2.78	9.01	72	1	5847.50
ARX_a	3.20E-02	1.56E-03	0.854	419.96	47225.88	3.24	10.60	72	1	8096.67

AFX$_a$	3.22E-02	1.67E-03	0.837	370.45	46319.83	3.24	11.18	72	1	9002.72
AR	1.55E-02	8.50E-04	0.821	331.02	45439.02	3.25	11.72	72	1	9883.53
AF$_a$	1.61E-02	1.05E-03	0.764	232.48	42240.44	3.97	13.48	72	1	13082.12
AF	1.99E-02	1.52E-03	0.704	171.13	38939.47	4.82	15.08	72	1	16383.08
AM	1.55E-02	1.27E-03	0.674	148.95	37294.83	4.20	15.82	72	1	18027.72
MidL	0.96	1.55E-01	0.348	38.34	19224.63	8.44	22.39	72	1	36097.93

The majority of the body measurements extracted have a strong correlation to weight with relatively small random error components (refer to Table 14). Using the new dataset and enhanced extraction techniques, the goodness-of-fit has increased between the weight-body measurement models compared to those presented using the previous dataset. For example, the AT$_2$ measurement (area) had a higher coefficient of determination of 0.98 (compared to 0.28 and 0.88 previously) indicating that there was now a good linear fit between the respective body measurements and the weight of the pigs. As this extraction process was supervised (semi-automatic) we know that the model coefficients derived from this dataset should have less error. However, the RMSE slightly increased. This increase was believed to be the result of the equation being generalised over a wider weight range. To indicate whether or not this was the case, the weight range was segmented and modelled in two, three and four categories to see whether estimation performance could be enhanced by targeting different equations to specific weight ranges. In this test, the first division (Division 1) was one equation between 9 and 137 kg, Division 2 was two equations with weight ranges of < 60 and ≥ 60 kg, Division 3 was three equations, (< 45, 45 ≤ x < 90 and ≥ 90 kg) and Division 4 was four equations (< 30, 30 ≤ x < 60, 60 ≤ x < 90 and ≥ 90 kg).

Using the AT$_2$ measurement as an example, Table 15 demonstrates that Division 4 (assigning four different weight-estimation equations to four weight ranges) increases estimation performance marginally by 4% in comparison to one single generalised equation across all weights (Division 1). This indicated that the relationship was possibly non-linear.

Table 15: Estimation Performance of Linear Equations Tailored for Specific Weight Ranges

Error Category (kg)	Division 1	Division 2	Division 3	Division 4
w_{est} < 0.5 kg	14(19)[*]	8(11)	13(18)	14(19)
0.5 kg ≤ w_{est} < 1kg	5(7)	9(12)	6(8)	9(12)
1 kg ≤ w_{est} < 2 kg	17(23)	21(28)	19 (26)	16(22)
2 kg ≤ w_{est} < 3 kg	12(16)	15(20)	10(14)	17(23)
3 kg ≤ w_{est} < 4 kg	10(14)	6(8)	11(15)	4(5)
4 kg ≤ w_{est} < 5 kg	7(9)	9(12)	6(8)	5(7)
w_{est} ≥ 5 kg	9(12)	6(8)	9(12)	9(12)
Total Samples	74	74	74	74
w_{est} < 2 kg	36(49)	38(51)	38(51)	39(53)

[*]Count (Percent)

These results were also compared to the results obtained from the previous dataset. Notably, 19% fewer samples had been recorded within ±2 kg (53%) compared to the analysis of the previous dataset (72%). In fact the result was closer to the 40% that was the projected estimate obtained from the benchmark formed by the original dataset. A possible reason for the reduction in precision was that the results from the analysis shown in Table 15 were determined from a wider weight range (between 9 and 137 kg). Therefore for comparative purposes the dataset was cropped such that it

obtained only the results of the pigs that were between 0 and 45 kg. The results are presented in Table 16 for the various equation divisions.

Table 16: Estimation Performance of Linear Equations Tailored for Specific Weight Ranges for Pigs between 0 and 45 kg

Error Category (kg)	Division 1	Division 2	Division 3	Division 4
$w_{est} < 0.5$ kg	7(30)*	6(26)	6(26)	7(30)
0.5 kg $\leq w_{est} < 1$kg	2(9)	2(9)	3(13)	4(17)
1 kg $\leq w_{est} < 2$ kg	8(35)	10(43)	9(39)	6(26)
2 kg $\leq w_{est} < 3$ kg	1(4)	2(9)	2(9)	3(13)
3 kg $\leq w_{est} < 4$ kg	2(9)	1(4)	1(4)	1(4)
4 kg $\leq w_{est} < 5$ kg	0(0)	0(0)	0(0)	0(0)
$w_{est} \geq 5$ kg	3(13)	2(9)	2(9)	2(9)
Total Samples	23	23	23	23
$w_{est} < 2$ kg	17(74)	18(78)	18(78)	17(74)

*Count (Percent)

Table 16 shows that the percentage of estimates within ±2 kg for pigs weighing between 9 and 45 kg was between 74 and 78 %; which is much closer to the 72% found during the previous analysis. Therefore, the system appeared to be ~25% more likely to estimate the weight of a pig in the range of 9 to 45 kg to within ±2 kg of its actual weight than a pig weighing greater than 45 kg. A possible reason for this is that as the animals grow their shape encounters greater variability, suggesting that they are more uniform in appearance when they are younger.

3.5.6.4 *Benchmarking the Early Prototype*

Variables were selected in a stepwise manner to form a multiple regression equation based on their estimation performance during testing (see Section *3.6.1.1.3 Multivariate Linear Model*). At this stage, some parameters were also intuitively selected or rejected on the basis of how often they could be successfully extracted from the images. The resulting equation was built using a combination of the AT_2, MWF_a MWM_a, MWR_a, mWF_a, and mWR_a measurements and was incorporated in to a prototype system for testing.

Prior estimation performance (in the tables above) was determined from data that were recovered from images processed semi-automatically in a supervised process. The body measurements were only included in the model if they had been referenced and extracted correctly from the image. However, during operation, it is not feasible to perform this discrimination semi-automatically (such as using a human observer). To overcome this problem an artificial supervision method was required. A limit filtering procedure was incorporated into the code that determined whether a proposed weight estimate was valid given the size of the pig's extracted body measurements (see Section *3.5.4 Filtering the Extracted Body Measurements for Weight Validation*).

To form the prototype system the segmentation, extraction, equation and limit filtering processes were all incorporated and integrated into software. The prototype was then benchmarked to see what stage the development was at. The system was setup at a commercial piggery (PPPI, University of Adelaide, Roseworthy campus) and 5 pens of between 10 and 19 animals were observed. The objective was to determine the group-weight average of all pigs in each pen and the system's ability to determine the weight of individual pigs in a commercial setting. The pigs were first herded from their pen into the scale area before being individually directed underneath the camera. After a weight estimate was recorded by the system, the pig

was persuaded into a nearby electronic weigh-scale where its actual weight was recorded. The limits were set in the software to 95% confidence intervals meaning that if the supervised method used to configure the dataset was repeated 100 times, 95 of the results would reside within the given interval. Hence, the limits were used to supervise the process automatically.

In total, 98 sample weights from sixty-nine pigs were collected. Weight assessment of some pigs occurred more than once due to the automatic nature of the system and the inability to distinguish between identities. Thus, each of the 98 sample weights were formed by averaging weight estimates obtained over a number of video frames collected of each animal as it stood beneath the camera. A total of 306 image frames had successfully passed the limiting filter which formed the 98 sample weights in this manner.

The average weight calculated by the prototype system for each of the four groups is shown in Table 17. Note, the pigs from pen one were weighed twice with two different confidence interval settings.

Table 17: Testing the First System Prototype

PEN	# Pigs	# Pigs Sampled	AVE (kg)	Vision AVE (kg)	Error (kg)	STD (kg)	Error STD
PEN 1 (99%)	10	10	84.6	85.7	1.1	6.4	6.8
PEN 1 (95%)	10	7	84.1	84.0	-0.1	6.3	4.8
PEN 2	9	8	97.7	91.1	-6.6[*]	4.6	19.4
PEN 3	11	11	75.2	77.0	-1.8	3.5	3.1
PEN 4	19	18	72.3	73.5	1.2	6.7	6.9
PEN 5	11	11	80.0	83.3	3.3	4.4	4.0

[*]Caused by an error where an object was identified that was not a pig, AVE = average, STD = deviation

The results demonstrated that the average error of the system was 2.82 kg. It was discovered that the incorrect identification and weight assessment of an object that was not a pig caused a large proportion of this error. An example image of this error is shown in Figure 76(a) along with a typical image used to perform a weight assessment (b).
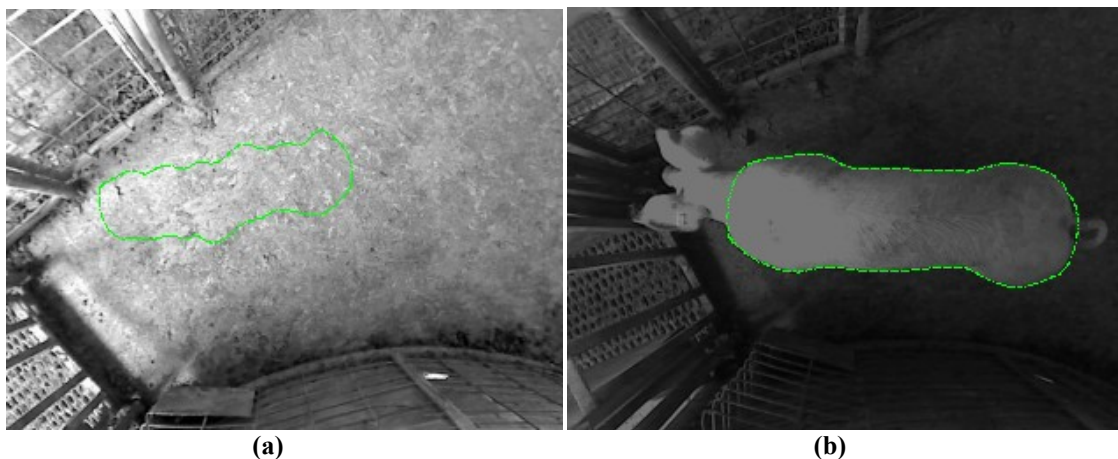
(a)   (b)
Figure 76: Images Collected from Testing the First Prototype
(a) A False Positive; (b) The Correct Capture of the Pig's Body Contour

Table 18 shows the same data only with the errors removed. As a result of the removal of the errors the group-average error drops to 1.67 kg.

Table 18: Results with Erroneous Contours and False Positives Removed from the Group Weight Estimate

Average (kg)	Vision Average (kg)*	Error (kg)
84.6	84.53	-0.07
84.1	84	-0.1
97.72	96.6	-1.13
75.23	77.04	-1.81
72.32	74.27	1.95
80	83.27	3.27

*With errors removed

It was clear that the limiting process was working, however, the errors that passed through were having a large effect on the overall precision of the system during the experiment. In spite of this fact, the testing conditions potentially exaggerated this error as in practice the system will be setup above the pen and allowed to run continuously. Therefore, the system will have considerably more time and data available to form group average estimates than the short minute interval per animal used to collect the data in the test. Thus, the longer sampling period may minimise the effect of this type of error.

The system's ability to determine individual weights was also revised during the test. Identities were determined by pairing the time stamps recorded during weight estimation to those recorded when the animal's actual weight was obtained.
Table 19 shows the performance of the system in determining individual animal's weights.

Table 19: The Precision of Individual Weight Estimates Made During Testing of the First Prototype

Error Category (kg)	Count (%)
$w_{est} < 0.5$ kg	12(12)
0.5 kg $\leq w_{est} < 1$kg	10(10)
1 kg $\leq w_{est} < 2$ kg	18(18)
2 kg $\leq w_{est} < 3$ kg	14(14)
3 kg $\leq w_{est} < 4$ kg	4(3)
4 kg $\leq w_{est} < 5$ kg	13(13)
$w_{est} \geq 5$ kg	26(27)
Total Samples	98
$w_{est} < 2$ kg	40(41)

The system generated 41% of the estimates within ±2 kg of the pig's actual weight and 27% of the estimates had error greater than ±5 kg. Notably these two figures bare a close resemblance to the theoretical performance of the benchmark (40% < ±2 kg and 25% ≥ ±5 kg) described in Section *3.5.6.2 The Start of the Vision System Development: CRC PhD Study*.

The three outcomes of the test were that: (i) the system was estimating the weight of individual animals on a similar level to the projected performance of the benchmark, (ii) the current average error of the system was 2.82 kg when calculating group weight estimates and (iii) the calculation of both group average weight and individual weights could be improved as errors were still making their way into the dataset and making large contributions to the overall error. Hence, further refinement of the filtering process was required.

Consequently, work focused on creating a method to recognise the animals pose(s) to overcome the distorted individual pig weight estimates associated with the contour not being extracted or identified correctly. It was also realised that if the variation in extracted body measurements could be minimised based on pose automatically, then the predictive quality of each of the body measurements and the individual weight estimates might be improved as well.

3.5.7   Final Model Building Method: Linking the Pose Filter to the Weight-Estimation Equation

More information was required in order to gain a uniform understanding of the pigs' body shapes to form grounds for discrimination. Over 750 videos were collected of 586 pigs with weights ranging from 12.5 to 306 kg. Of these videos, 703 were used to build the shape model. Software was written to automatically identify the pig in each image frame, and rotate it to the horizontal before extracting the body measurements from it. As there was not a real-time constraint on extracting the dimensional data during model building, the code was modified such that the reliability of recognition was enhanced. In total, 22419 contours were recovered from the videos. The methodology described in earlier was then applied to filter the shape data and build the weight and pose model (see Section *3.5.5 Filtering the Shape for Pig Recognition and Pose Validation*). Using this method, the body measurements extracted from a certain pose become the basis in forming the weight estimation equation, and thus the resulting estimation equation and template shape form a set to be used together to estimate the weight of pigs. Thus, weight assessments have greater potential to be enhanced and controlled as the weight-estimation equation is a function of a shape.

A flow diagram of the shape and equation model building process can be seen in Figure 77.

Data_2010_PhD

Function Start

1. Select a template contour for initial reference pose

2. Convolute template across all contour data and collect residuals

3. Sort residuals based on number of points passing within the set deviation from the template reference shape

⊕

3. Sort residuals from highest to lowest based on a measure (R^2, SSE, Absolute Variance)

5. Select the contours which have had all (or a high percentage) of points pass between the set deviation from the template reference shape

5. Iteratively include contours into an average shape and determine when its change is approximately zero

6. Determine the mean and standard deviation of the selected contours

7. Select the contours which have had all (or a high percentage) of points pass between the set deviation from the average template contour built

8. Determine the mean and standard deviation of the selected contours and store the final average template contour

→ **For online shape-filtering**

9. Halve the selected samples for testing and equation building

10. Create equations based on the body measurements extracted from these samples (stepwise multivariate linear,

→ **For online weight estimation**

11. Validate equations and shape using test set

12. Evaluate the results; check the precision and check the weight range covered by the equation due to the shape filter

Figure 77: The Process Used to Build the Template Shape and Weight-Estimation Equation

Reasons why this method may be beneficial are:

(i)   It is efficient in terms of data storage as fewer (yet more accurate) weight assessment samples will be carried out daily (only a single accurate estimate per pig is required to make a very accurate daily group average (rather that collecting many more suboptimal images to form an average))

(ii)   Reduces processing load as the system spends more time searching for quality data rather than extracting body measurements from images that will have little positive effect on the resultant weight estimate and averages. The pose recognition filter can discriminate (accept or reject) the data early in the process, immediately after segmentation,

(iii)   Is more accurate than referencing body measurements from a pig that is in a largely unknown posture.

109

(iv)   Has an adaptable methodology which can be used to generate equations for different poses, pig shapes, breeds of pigs and potentially different species. With some modification the same methodology could be used for data acquired from alternate camera configurations such as 3D, by using the animal's surface rather than its contour.

3.6 SIMULATION RESULTS

3.6.1 Modelling

The magnitude and angle vectors used to form the average template shape were selected from the dataset in the manner described in Figure 77 in the previous section. However, as the average template shape was built from a combination of magnitude and angle vectors sourced independent of one another, there were a different number of magnitude vectors and angle vectors. Some of which were associated with the same sample. For example, the magnitude and angle of a particular sample may have been used in the build. Therefore, the position (or index) of these vectors within the dataset was determined for both components and only unique index values were determined to avoid duplication.

In total 7276 of the magnitude and angle vectors were unique. The extracted body measurements of these 7276 vectors were used to construct the weight-estimation equation. Some of the 7276 vectors did not have a corresponding height (284) or area measurement (11), so for comparative purposes these were excluded, leaving 6981 weight and body measurement(s) pairs. The samples that had no area (177) or height (1348) information were also removed from the larger dataset (22419) leaving 20894 complete contour/body measurement vectors of information.

Those of the 20894 sample contours which passed the filter had their body measurement(s) modelled in respect to weight. An example is shown in Figure 89 which is the result after shape filtering for the ML_{Rho} measurement. Another example of how these relationships were found in respect to the entire dataset can be found later in Section *3.6.2.1 Testing the Template as a Shape Filter*.

Several types of fit were tested on the filtered data. The majority of the body measurements in respect to weight were best represented by a curve, particularly at weights above 120 kg and less than 30 kg (as the ML_{Rho} measurement demonstrates in Figure 78).
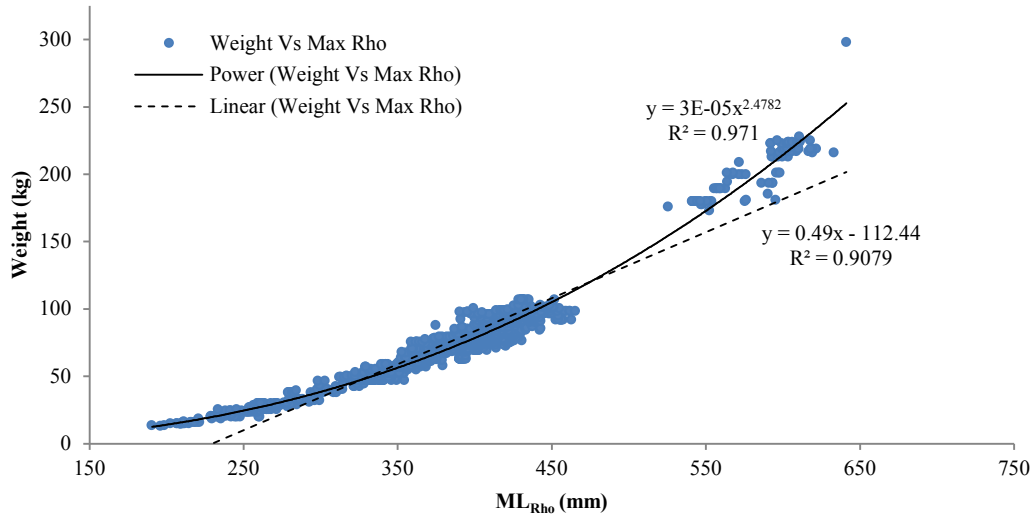
Figure 78: The Weight vs. ML_{Rho} Relationship

This relationship was not exponential as the natural logarithm of the dependant (y) variable (weight) did not yield a straight line when compared to the independent (x) variable of the measurement. It was also apparent that it was not purely linear either as Figure 78 illustrates. It was determined that a power relationship best represented the relationship between each body measurement and the animal's weight. This relationship coincides with the findings of Minagawa and Ichikawa (1994) and Brandl and Jørgensen (1996). The only contradictions were the body measurements MidL and $AMid_c$ that demonstrated a slightly better fit as a linear equation rather than a power equation, and although some of the body measurements were approximately linear such as AT_2 (refer to Figure 79) it was noted that a linear model might find it difficult to estimate the weight of pigs at the lower (< 30 kg) and upper (> 120 kg) portions of the relationship correctly.

In this case two or three linear models could be assigned to respective weight ranges as shown in Table 16 in Section *3.5.6.3 The Results from the New Dataset*. Note that these body measurements are not a real world representation of the actual metric body measurements of the pig; they are the metric body measurements relative to the ground level. The body measurements are required in this format to create a generic estimation model based on the installation height and camera parameters (refer to Section *3.5.3 Projecting Extracted Pixel Dimensions to Metric at Ground Level*).

111
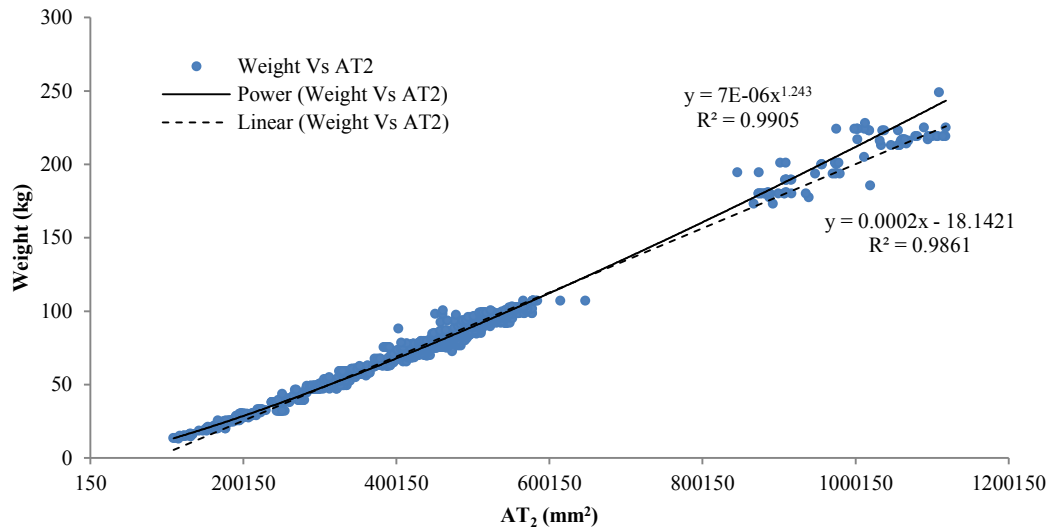
Figure 79: The Weight vs. AT_2 Relationship

3.6.1.1 Modelling the Weight-Estimation Equation

Initially the weight-estimation equation modelled using sample contours and averaged body measurements obtained from 477 videos. The linear fits applied to the 16 body measurements extracted from these videos are shown in Table 20 in order of R^2.

Table 20: The Goodness of Fit between Angular Based Measurements (Linear Regression)

Weight Vs.	p_1	S_{en}	R^2	F	SS_{reg}	p_2	S_{eb}	S_{ey}	DF_e	DF_r	S_{Se}
AT_2	2.20E-04	1.18E-06	0.986	34660.11	876371.15	-18.46	0.55	5.03	475	1	12010.24
$AMid_c$	5.81E-04	5.43E-06	0.960	11461.88	853030.33	-15.95	0.94	8.63	475	1	35351.06
AR_c	6.70E-04	6.56E-06	0.956	10425.99	849671.05	-13.47	0.96	9.03	475	1	38710.35
AF_c	6.68E-04	7.58E-06	0.942	7769.87	837200.35	-16.43	1.14	10.38	475	1	51181.05
WR_c	0.51	6.02E-03	0.938	7185.97	833299.46	-93.68	2.05	10.77	475	1	55081.93
mWF_a	0.50	5.99E-03	0.935	6861.63	830864.34	-95.95	2.13	11.00	475	1	57517.05
WF_c	0.48	5.85E-03	0.934	6726.31	829783.52	-95.13	2.14	11.11	475	1	58597.87
$MWMid_a$	0.50	6.31E-03	0.929	6231.50	825460.15	-110.84	2.41	11.51	475	1	62921.24
mWR_a	0.51	6.81E-03	0.922	5584.10	818737.18	-97.46	2.38	12.11	475	1	69644.21
MWF_a	0.41	6.31E-03	0.901	4315.52	800294.71	-93.19	2.64	13.62	475	1	88086.69
ML_{Rho}	0.31	4.86E-03	0.898	4168.20	797499.90	-109.21	2.93	13.83	475	1	90881.50
ML	0.16	2.43E-03	0.898	4160.94	797357.47	-109.02	2.92	13.84	475	1	91023.92
MWR_a	0.43	6.86E-03	0.891	3898.21	791889.18	-98.27	2.85	14.25	475	1	96492.21
RML_a	0.43	8.15E-03	0.856	2823.72	760458.83	-86.52	3.13	16.41	475	1	127922.56
Height	3.82	7.32E-02	0.852	2723.71	756458.97	-150.54	4.39	16.67	475	1	131922.42
MidL	0.43	8.92E-03	0.831	2327.85	737826.90	-105.16	3.83	17.80	475	1	150554.49
FML_a	0.44	9.96E-03	0.803	1930.60	712965.02	-93.07	3.93	19.22	475	1	175416.37

As each body measurement was not linear in respect to weight, non-linear multiple regression was required to create the best representation of the weight as a function of the extracted body measurements over the complete weight range. However, linear multiple regression still remained a viable option for the model in this study as the relationship was close to linear in the grower finisher phase (between 30 and 120 kg).

3.6.1.1.1 Linear Model

Graphical output was used to document the effect that the average template shape had on weight estimation performance (see Figure 80). An explanation of the graph follows for the linear case where no average template shape had been used to sort the contour samples. Samples are arranged in ascending weight. The x-axis of Figure 80 refers to the 20894 samples of the dataset. Each point along the x-axis represents a

sample consisting of a shape and the body measurements extracted from that shape. An equation has been applied to each sample's body measurement(s) to estimate a weight. On the y-axis is the cumulative error category. Each sample has estimated a weight within one of these seven error categories. As samples are introduced (from left to right) each sample's weight estimate will contribute to a certain error category which is represented by an increment in the y direction for that error categories line. Using this plot it is easy to observe the proportion of samples within each error category.
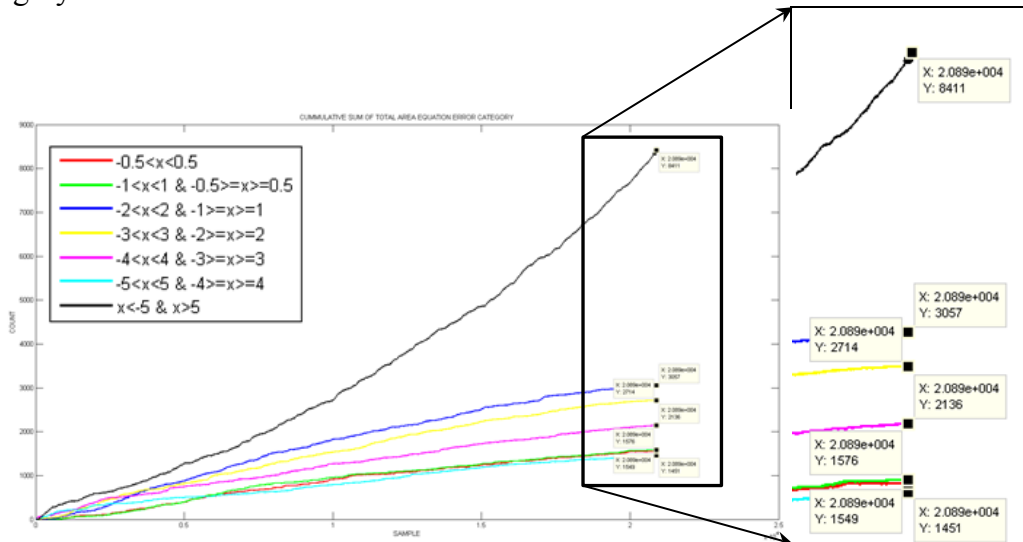
Figure 80: Cumulative Weight Estimate Error of Contour Samples Using a Linear Model

If a vertical line is overlayed anywhere across the x-axis (intercepting the cumulative counts of each error category), the point on the x-axis indicates the number of samples tested at that point. Furthermore, the point(s) at which the vertical line intersects the line of each cumulative error category is the relative proportion of the x number of samples which contain that error.

For example, Figure 80 shows markers on the counts of each error proportion when the last of the 20894 samples has been included. The y proportions, when added become 20894 and therefore an accumulative percent of the error in each category can be determined. For example 7.41% (1549/20894) of the total samples had an estimation error within ±0.5 kg of the actual weight for the linear (AT_2 area) equation used. Re-running the code with a different equation will yield a different result. It can be observed that the error category greater than ±5 kg (black line) grows steadily from the inclusion of the first sample at the far left of Figure 80 after a steep increase in errors at the beginning. This is most probably because the samples have been sorted in weight from lightest to heaviest pigs and the lightest pigs (< 30 kg) are possibly more prone to result in weight estimation error due to the fit of the linear model.

3.6.1.1.2 Non-Linear Model: Power Equation

As Figure 79 and Figure 78 have previously shown that a power equation better represents the relationship between weight and body measurements. Figure 80 was regenerated to see the effect when using a power equation (see Figure 81).

113
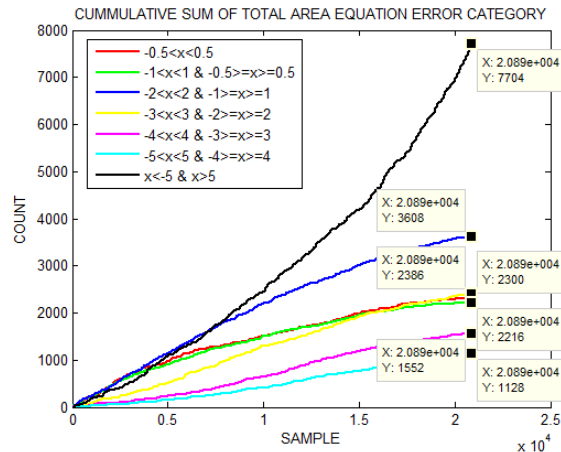
Figure 81: Cumulative Weight Estimate Error of Contour Samples Using a Power Model

This power equation was built with half of the best fitting contours to the single original template (Figure 80). The power equation was then reproduced using the top samples derived from the averaged template shape. Figure 81 shows an improvement from the linear model as there has been a 3.38% (707 samples) reduction in the number of estimates greater than ±5 kg and a 9.29% (1942 samples) increase in the number of samples in the error category less than ±2 kg compared to the original linear model estimate. The smaller error categories (±1 kg < and < ±0.5 kg) have performed moderately better (~3% each). Noticeably, the jump in estimates greater than ±5 kg at the low weight ranges has also been suppressed (black line to the left of Figure 80 and Figure 81). What is also interesting is that the error greater than ±5 kg increases in a slightly curved manner with respect to weight (as samples are sorted in ascending weight). This possibly reflects previous results that demonstrated that is easier to estimate the weight of smaller animals more precisely (although they may be harder to capture).

3.6.1.1.3 Multivariate Linear Model

In an attempt to improve the estimation potential, multivariate linear regression was undertaken on the body measurements. This involved a stepwise selection of terms using the *stepwisefit* function in Matlab's statistical toolbox (MathWorks, Inc., Natick, MA). This function adds and removes terms based on their statistical significance. The power of the model is compared as each term is included or excluded based on the p-value of an F-statistic. For a term to enter the model it had to have the minimum p-value of available terms and had to be within the entrance tolerance of 0.05. While the model is being built if the p-value of a term exceeds the exit tolerance of 0.10 then the term is removed.

Various models were built and tested in this manner:

  M1. A model was built using intuitively selected variables of the 16 extracted body measurements
  M2. A model was built using a stepwise selection of the 16 extracted body measurements
  M3. A model was built using a stepwise selection of the 16 extracted body measurements and 11 angles

114

M4. A model was built using a stepwise selection of the 16 extracted body measurements and the 120 paired interactions between them
M5. A model was built using a stepwise selection of the 16 extracted body measurements and 11 angles and the 351 paired interactions between them

These five different model building methods were applied to: (i) half the extracted body measurements of the 6981 individual samples and to (ii) the average body measurements of each animal in the 477 videos. Details of the coefficients and the term names can be found in Appendix D. The other half of the data were used to test the methods and models. Output is shown in Table 21.

Table 21: Comparison of Results between 5 Different Modelling Methods

Error Category (kg)	Individual Data Count (%)					Averaged Data Count (%)				
	M1	M2	M3	M4	M5	M1	M2	M3	M4	M5
$w_{est} < 0.5$ kg	596 (17)	580 (17)	611 (18)	608 (17)	628 (18)	36 (15)	32 (13)	41 (17)	38 (16)	43 (18)
0.5 kg $\leq w_{est} < 1$kg	570 (16)	577 (17)	608 (17)	609 (17)	622 (18)	43 (18)	33 (14)	36 (15)	39 (16)	31 (13)
1 kg $\leq w_{est} < 2$ kg	905 (26)	931 (27)	924 (26)	946 (27)	911 (26)	60 (25)	71 (30)	70 (29)	55 (23)	56 (24)
2 kg $\leq w_{est} < 3$ kg	534 (15)	543 (16)	561 (16)	609 (17)	604 (17)	34 (14)	31 (13)	28 (12)	35 (15)	34 (14)
3 kg $\leq w_{est} < 4$ kg	357 (10)	347 (10)	331 (9)	337 (10)	332 (10)	20 (8)	23 (10)	25 (11)	31 (13)	19 (8)
4 kg $\leq w_{est} < 5$ kg	231 (7)	238 (7)	209 (6)	152 (4)	175 (5)	12 (5)	14 (6)	11 (5)	12 (5)	20 (8)
$w_{est} \geq 5$ kg	297 (9)	274 (8)	246 (7)	229 (7)	218 (6)	33 (14)	34 (14)	27 (11)	28 (12)	35 (15)
Total Samples	3490	3490	3490	3490	3490	238	238	238	238	238
$w_{est} < 2$ kg	2071(59)	2088(60)	2143(61)	2163(62)	2161(62)	139(58)	136(57)	147(62)	132(55)	130(55)

Table 21 indicates that if the software is programmed to generate a weight estimate for every recovered contour, then Model 4 or 5 should be used to model the relationship. If the software is programmed to collect and average the body measurements over a short period of time then Model 3 should be chosen to build the model. Overall, the models based on individual data have provided the best precision ($w_{est} \geq \pm 5$kg $<10\%$) and Model 5 is the most desirable choice to integrate into the system and generate weight estimates. This model was applied over the entire 20894 sample dataset. The result is shown in Figure 82.
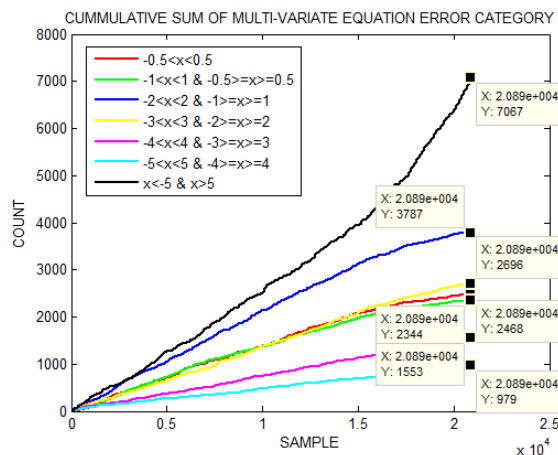
Figure 82: Cumulative Weight Estimate Error of Contour Samples Using the Multivariate Model (Method 5)

3.6.1.2 Selecting the Weight-Estimation Equation

Comparative results from the linear, power and multivariate equations are shown in Table 22.

Table 22: Comparison of Performance between Linear, Non-Linear (Power) and Multivariate Equations

Error Category (kg)	Multivariate	Non-Linear	Linear
$w_{est} < 0.5$ kg	2468(12)[*]	2300(11)	1549(7)
0.5 kg $\leq w_{est} < 1$ kg	2344(11)	2216(11)	1576(8)
1 kg $\leq w_{est} < 2$ kg	3787(18)	3608(17)	3057(15)
2 kg $\leq w_{est} < 3$ kg	2696(13)	2386(11)	2714(13)
3 kg $\leq w_{est} < 4$ kg	1553(7)	1552(7)	2136(10)
4 kg $\leq w_{est} < 5$ kg	979(5)	1128(5)	1451(7)
$w_{est} \geq 5$ kg	7067(34)	7704(37)	8411(40)
Total Samples	20894	20894	20894
$w_{est} < 2$ kg	8599(41)	8124(39)	6182(30)

[*]Count (Percent)

Table 22 shows the superior performance of the multivariate equation in comparison to the non-linear and linear models. Most improvement has been observed in the greater than ±5 kg category with the multivariate model recording 637 (3%) fewer samples than the non-linear model. The number of samples within ±2 kg of the actual weights predicted by the nonlinear and multivariate is around 40% which is similar to the results obtained previously. The 34% of sample greater than ±5 kg reflects the fact that one in every three contours included could not be used for weight estimation and need to be removed. This is not surprising considering that the automated extraction process had only negligible constraints on what shapes and body measurements were recorded in the database. The next section demonstrates the results after applying filtering methods to suppress these erroneous samples.

3.6.1.2.1 Ranking and Selecting Estimates Based on their Contour Shape

The previous figures and tables have highlighted the effect between weight estimates and the samples. For example, Figure 80 previously demonstrated that error will be included at a near constant rate if the fit of the contour-sample to the average template shape is not known. However, these figures have been ranked in order of ascending weight (ordered from left to right) and do not take into consideration the shape of the pose of the animal used to obtain the estimate. The previous figure (Figure 81: non-linear power equation) was regenerated after including the shape filter so that the samples were re-arranged in order of R^2 from best to worst fit to the average template shape. The cumulative errors of these shape-sorted samples are shown in Figure 83 for three different sorting methods.

(a) R^2 **Sort Based on Rho**

(b) R^2 **Sort Based on Theta**
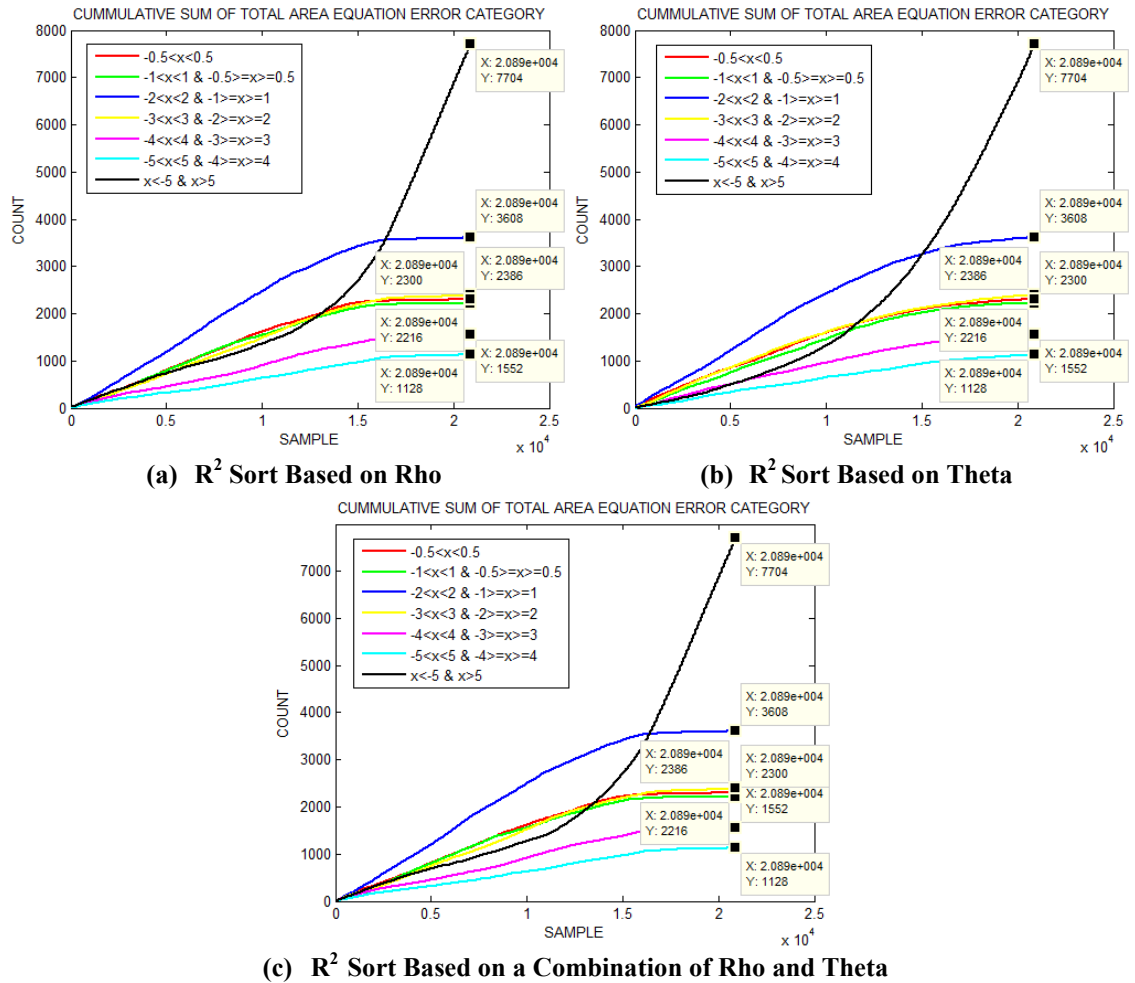
(c) R^2 **Sort Based on a Combination of Rho and Theta**
Figure 83: Cumulative Weight Estimate Error of Contour Samples Using the Power Model after Sorting the Contour Samples Based on R^2 Fit (Left to Right) to the Average Template Shape

The various sorting methods presented in Figure 83 visually show how conformation of pose can be used to suppress the error rate during weight estimation. This can be seen to the left of Figure 83 where the error category greater than ±5 kg depresses while the quantity of estimates within ±2 kg error increases. The samples to the left are, therefore, less likely to contain error and can be selected for weight estimation output with greater confidence. Essentially this cumulative sum of errors graph indicates the potential rate at which erroneous samples can be removed for a given template shape and equation pair after filtering (sorting). These results are based on sorting and modelling based on Method 1 in Section *3.5.5.3.1*. However, a secondary approach to filtering the shapes was also undertaken and involved determining those samples which had all their points pass within a certain deviation of the average template shape (see Section *3.5.5.3.2* for the alternative method). In this method the samples were then sorted based on the number of points which passed through the filter bounds. The identical power based area equation was used.
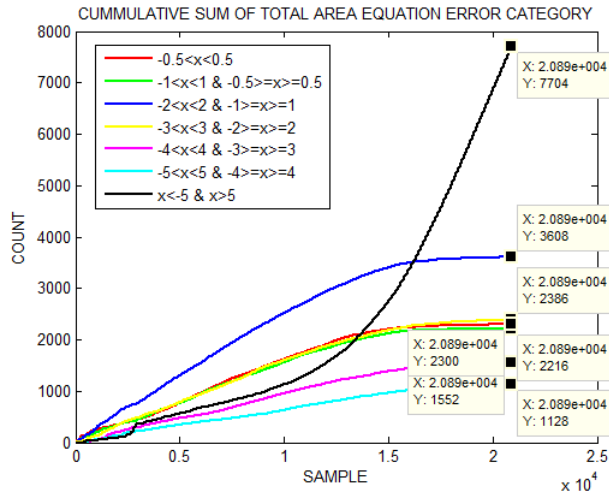
Figure 84: Sorting Contour Samples Based on the Number of Points that Passed the within a Certain Deviation of the Average Template Shape

Figure 84 illustrates a desirable deflection in both the less than ±2 kg and greater than ±5 kg error categories for the first 2500 samples (the samples that had all point pass within the filter bounds). It can be observed that the weight estimation error rate increases as samples are introduced to the cumulative sum (from left to right) which coincides with samples that had fewer points pass within the limits of the average template shape. This deflecting effect can be improved further by enhancing the estimation potential or determining the uniqueness of those samples which have error greater than ±5 kg and attempting to remove them.

Figure 85 illustrates the weight estimation results after applying the multivariate equation (see Section *3.6.1.1.3 Multivariate Linear Model*) to the dataset and sorting based on both R^2 (Figure 85 (a)) and the number of points passing within a certain deviation of the template average shape (Figure 85 (b)).

(a)

(b)
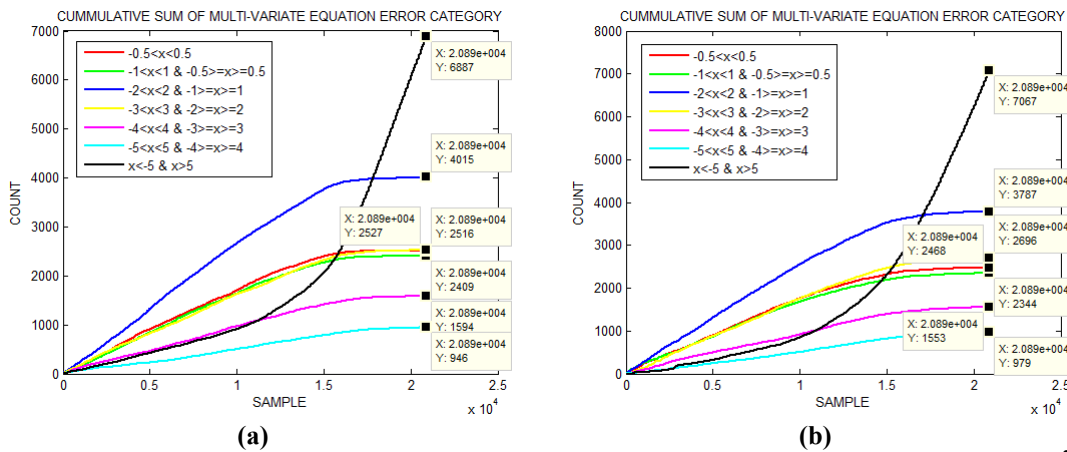
Figure 85: Weight Estimation Results Using a Multivariate Model and Sorting Based on (a) R^2 and (b) the Number of Points Passing within a Certain Deviation of the Average Template Shape

118

Table 23: The Differences between Sorting Methods to Determine Samples Appropriate for Weight Estimation.

Error Category (kg)	Multivariate R^2 Sort	Multivariate Deviation Sort
w_{est} < 0.5 kg	2516(12)[*]	2468(12)
0.5 kg $\leq w_{est}$ < 1kg	2409(12)	2344(11)
1 kg $\leq w_{est}$ < 2 kg	4015(19)	3787(18)
2 kg $\leq w_{est}$ < 3 kg	2527(12)	2696(13)
3 kg $\leq w_{est}$ < 4 kg	1594(8)	1553(7)
4 kg $\leq w_{est}$ < 5 kg	946(5)	979(5)
$w_{est} \geq$ 5 kg	6887(33)	7067(34)
Total Samples	20894	20894
w_{est} < 2 kg	8940(43)	8599(41)

[*]Count (Percent)

Table 23 shows the results generated by the equations built with the subset of body measurements related to the contours which had strong coefficient of determination (Table 23, column 2) or had all their points pass within a certain deviation of the template shape (Table 23, column 3). The same body measurement variables were used to build the equation for both methods, however, each method was responsible for choosing the samples to build the equation and the average template shape (under minor constraint). The equation was built using half of these selected samples for both methods and tested using the other half. The test results for the selected samples are shown in Table 24.

Table 24: Contour Samples Appropriate for Weight Estimation: Results between Two Methods

Method	R^2		Passed Deviation	
Error Category (kg)	Count	%	Count	%
w_{est} < 0.5 kg	652	17.99	628	18.77
0.5 kg $\leq w_{est}$ < 1kg	591	17.82	622	17.02
1 kg $\leq w_{est}$ < 2 kg	939	26.10	911	27.04
2 kg $\leq w_{est}$ < 3 kg	550	17.31	604	15.84
3 kg $\leq w_{est}$ < 4 kg	314	9.51	332	9.04
4 kg $\leq w_{est}$ < 5 kg	193	5.01	175	5.56
$w_{est} \geq$ 5 kg	234	6.25	218	6.74
Total Samples	3473	100.00	3490	100.00
w_{est} < 2 kg	2182	61.92	2161	62.83

Both methods chose a similar number of samples to build the equation and yielded similar results within the test-set. However, this is only a small observation in respect to the entire dataset, and only holds partial value in the strength of the derived shapes overall filtering and estimation potential. With reference to Figure 85 the error rate and the number of samples within each error category is different between the two methods. These are different because different shapes were used to build the equation and different methods and average shapes were used to sort (filter) the data in order from least to most chance of error. Overall, the first method (based on a R^2 sort) has fewer error-counts greater than ±5 kg compared to the second method, which is desirable. However, the second method based on the points passing within a certain deviation of the average template shape, actually performs better at filtering out the erroneous samples for the first 1000 samples, as Figure 86 and Table 25 demonstrate.
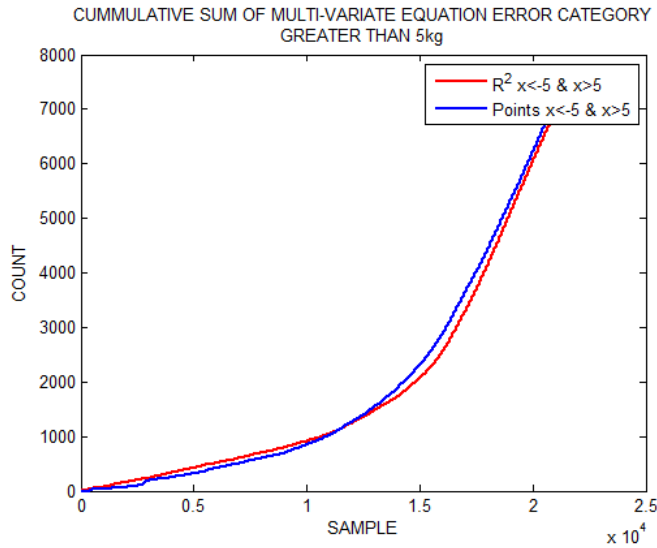
Figure 86: Comparing the Cumulative Weight Estimate Error greater than ±5 kg for the Two Sorting Methods

Table 25 below shows the comparative results over the first 3500 samples after applying both sorting methods separately over the entire dataset.

Table 25: Weight Estimate Error of the Two Methods after Sorting the Entire Dataset (Observation at 3500 Samples)

Method	R^2		Passed Deviation	
Error Category (kg)	Count	%	Count	%
$w_{est} < 0.5$ kg	641	18.31	625	17.86
0.5 kg $\leq w_{est} < 1$kg	575	16.43	622	17.77
1 kg $\leq w_{est} < 2$ kg	882	25.20	900	25.71
2 kg $\leq w_{est} < 3$ kg	603	17.23	612	17.49
3 kg $\leq w_{est} < 4$ kg	347	9.91	361	10.31
4 kg $\leq w_{est} < 5$ kg	169	4.83	162	4.63
$w_{est} \geq 5$ kg	283	8.09	218	6.23
Total Samples	3500	100.00	3500	100.00
$w_{est} < 2$ kg	2098	59.94	2147	61.34

Method 2 performs better in both the greater than ±5 kg and less than ±2 kg categories compared to Method 1. These results also indicate that shape has a direct influence on the estimation performance, as building a weight estimation-equation and filtering data based on a particular contour can enhance the precision of weight estimates and the correct validation of weight estimates for output.

3.6.1.3 The Effect of Height as a Variable Input into the Weight-Estimation Equation

Previously the multivariate equation has not used height as a parameter. However, as height was recorded manually from the back of the animals during the data collection, its effect on the overall performance of the predictive response could be determined to justify the inclusion of any additional software or hardware to extract its value. The same multivariate equation (as previously used) was used to generate estimation output for the entire dataset twice, without height as a parameter and with height as a parameter. The cumulative sums of error categories for the estimates are shown in Figure 87 ; a positive effect can be observed when height is used as a parameter.

120
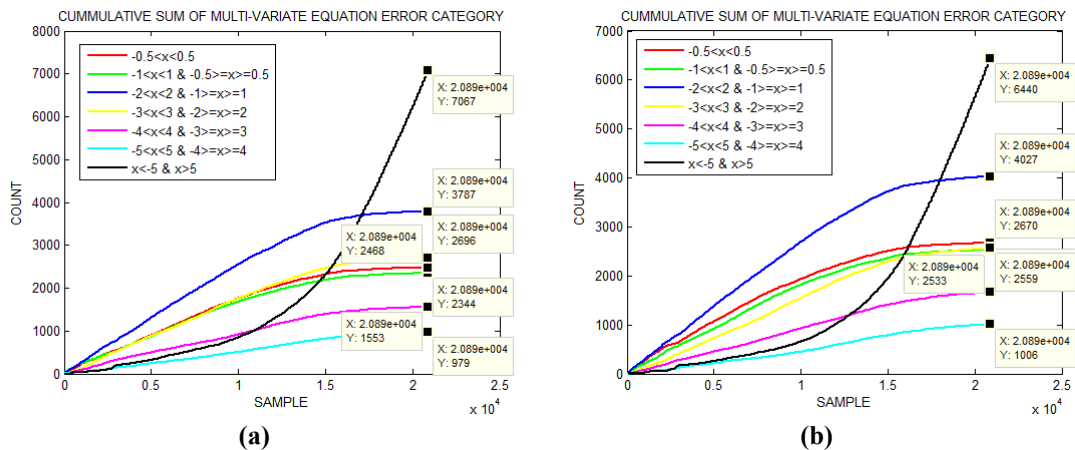
Figure 87: Multivariate Equation (a) Without Height and (b) With Height

A direct comparison between the greater than ±5 kg category and less than ±2 kg category is shown in Figure 88.
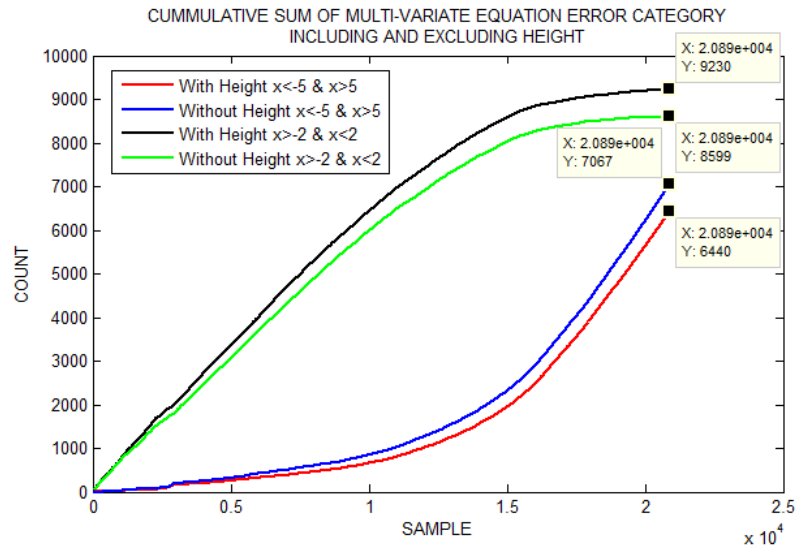
Figure 88: Cumulative Weight Estimate Error of the Multivariate Equation With and Without the Height Parameter

Overall, the multivariate equation with height parameter has improved estimation precision by 7.34% in the less than ±2 kg weight-estimation category compared to the multivariate equation without the height parameter included (Figure 88). Overall, in the greater than ±5 kg error-category the multivariate equation with height parameter has improved (reduced) the erroneous estimates by 8.87% compared to the multivariate equation without the height parameter. However, the benefit of using height as a variable in the weight-estimation equation is reduced when the integrity of the contour shape is taken into consideration. For example, the first 3500 output results as selected (filtered) by setting the shape filter to a deviation of 2.8 is shown in Table 26 below.

121

Method Error Category (kg)	With Height Passed Deviation		Without Height Passed Deviation	
	Count	%	Count	%
$w_{est} < 0.5$ kg	760	21.71	625	17.86
0.5 kg $\leq w_{est} < 1$kg	662	18.91	622	17.77
1 kg $\leq w_{est} < 2$ kg	945	27.00	900	25.71
2 kg $\leq w_{est} < 3$ kg	488	13.94	612	17.49
3 kg $\leq w_{est} < 4$ kg	315	9.00	361	10.31
4 kg $\leq w_{est} < 5$ kg	150	4.29	162	4.63
$w_{est} \geq 5$ kg	180	5.14	218	6.23
Total Samples	3500	100.00	3500	100.00
$w_{est} < 2$ kg	2367	67.63	2147	61.34

When the shape confirmation is present, a smaller increase of 6.29 % occurred in the category less than ±2 kg and a 1.09% decrease occurred in errors greater than ±5 kg (Table 26). These modest improvements and the logistical difficulties surrounding a method of obtaining the height measurement in parallel with other body measurements weaken any justification for including height as an input parameter for weight estimation. However, there is potential for height to improve estimation precision in the future. In addition, results may have been different had the height measurement been taken directly from the image at the same time the pose and body measurements were extracted from the animal rather than taking the height measurement manually a short time later.

3.6.2   The Shape Filter

Previously contours have been selected based on their fit to a template shape. Subsequently the body measurements extracted from these selected contours have been used to create both a weight-estimation equation and an average template shape for filtering purposes. This selection process has been shown to have a direct influence on the filter's performance and the selection of valid data for further processing. The filter's performance can be measured by its ability to discriminate between the shape of an extracted contour that will yield a good weight estimate ($W_{est} < \pm 2$ kg) or a poor one ($W_{est} > \pm 5$ kg). The benefit of filtering using an average shape contour is that this discrimination can occur early in the processing cycle before body measurements are extracted and therefore can save valuable processing time.

3.6.2.1   Testing the Template as a Shape Filter

To demonstrate how the shape filter works, observe Figure 89 below. This figure is a comparison between the filtered and unfiltered output of 20894 points of the AT_2 measurement. Filtered values are based on plotting the AT_2 values found from the top 3644 best fits between the samples and average template shape. This figure compares the result between a system with limited built-in intelligence to decipher whether the object observed is actually a pig and a system that can. It is clear to see that much of the randomness in the spread of data has been eliminated and the true representation between area and weight is clearly defined.
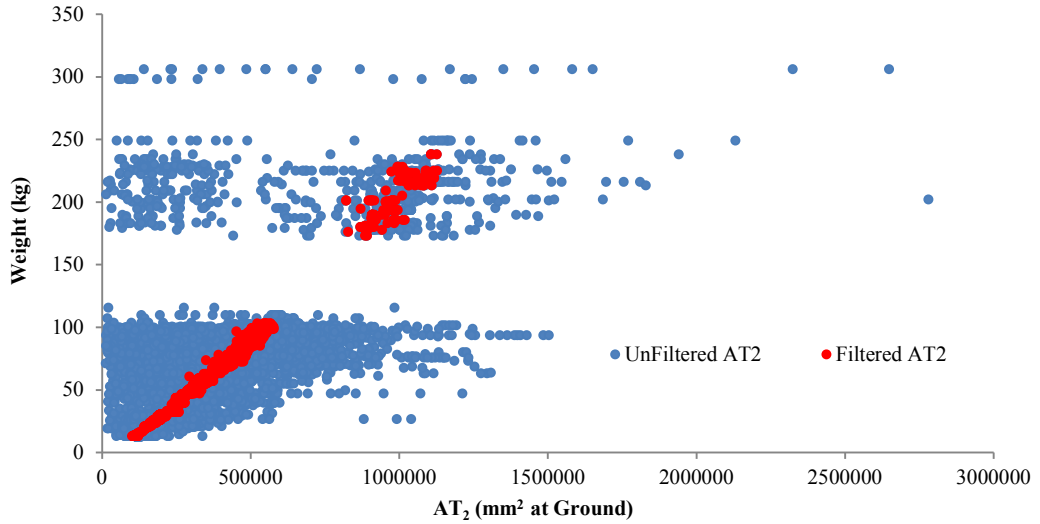
Figure 89: The Total Body Area Measurement (AT$_2$) With and Without Using a Shape Filter

This random error can also be observed in the original dataset that was collected by a system that is not part of this development (see Figure 90). The shape filter effectively and dramatically minimises the occurrence of this random error and also effectively automates the supervision process. Therefore, it was not necessary to manually go through the dataset to determine frames where the pig appeared to be in the correct posture as it could now be performed automatically based on shape recognition.
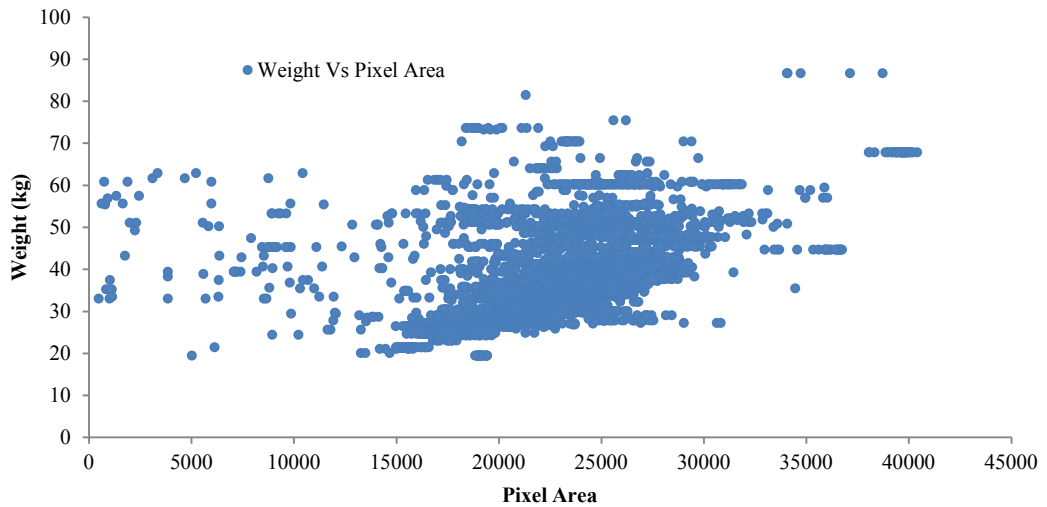
Figure 90: Randomness of the pixel area in respect to actual weight as acquired by the Original Vision System Developed in the CRC Project

3.6.3   Adjusting the Bounds of the Shape Filter

The filter deviation bounds can be adjusted to control (loosen or restrict) the amount of samples which have all their points pass. Figure 91 illustrates this (refer to the black line representing the cumulative sum of errors greater than ±5 kg).
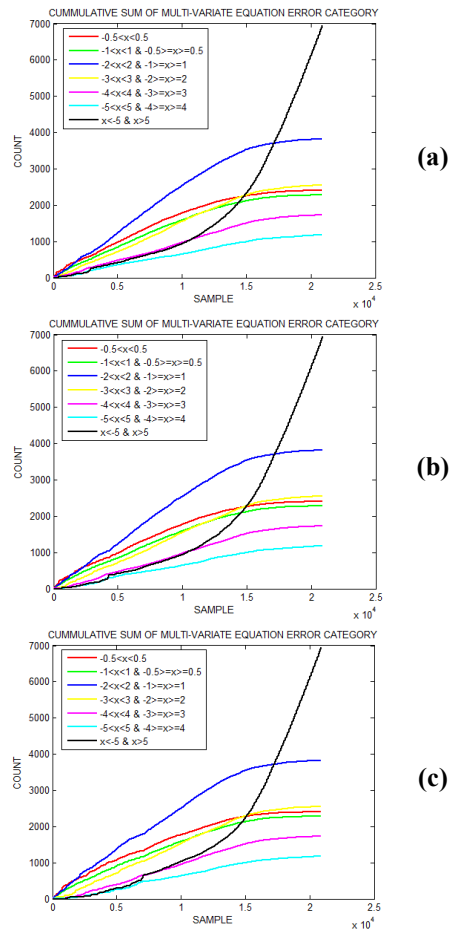
Figure 91: Selecting Different Filter Boundaries (a) 2.8, (b) 3.2 and (4) Times the Deviation from the Mean

During the equation and average template shape building process there are three different stages where an arbitrary deviation can be set. These are at Stage 5, 7 and 12 of Figure 77.

At Stage 5 the standard deviation over the entire dataset is determined and is multiplied by a factor to form a ± limiting boundary from which shapes must pass from the initial template shape if they are to be included in the subsequent model and shape building process. The deviation and the mean shape of the samples that pass are then calculated. Similar to Stage 5, Stage 7 involves multiplying the calculated deviation of the selected contours by a factor to form a ± limiting boundary from which the selected shapes must pass from the preliminary average template shape if they are to be included in the subsequent building process. Those of the selected contours which pass between these limits are used to construct the final average template shape and its standard deviation. The standard deviation of the average template shape is then multiplied by a factor in a similar manner as before such that it can be used during an online process to discriminate between a shape that will yield a good weight estimate and a poor weight estimate.

At these stages the multiplication factors used to construct the shape filtering are somewhat arbitrary. Therefore, testing was undertaken to determine what multiplication factors should be applied at these three stages to form adequate discrimination between a shape which would yield a good weight estimate and one

that would not. In total, 819 simulations were performed over the entire dataset of 20894 samples using different multiplication factors on the deviation of the selected contour shapes at the three stages. Multiplication factors ranged in 8 step sizes between 1.1 and 1.7 for Stage 5, between 2.3 and 3.1 for Stage 7 and between 2.2 and 4.6 for Stage 12. Table 27 shows a selection of these results which confirmed to the following criteria: (i) a mean-relative error less than 4%, (ii) less than 6% of weight estimates that passed were in the greater than ±5 kg error category and (iii) more than 64% of weight estimates that passed were less than ±2 kg.

Table 27: Filtered Weight Estimate Output Based on the Selection of Contours within Different Deviations from the Average Template Shape

Stage 5 Deviation Bounds	Stage 7 Deviation Bounds	Stage 12 Deviation Bounds	% Passed	Number Passed	Mean-relative error (%)	Weight Min (kg)	Weight Max (kg)	$w_{est} < 0.5kg$	$0.5kg \le w_{est} < 1kg$	$1kg \le w_{est} < 2kg$	$2kg \le w_{est} < 3kg$	$3kg \le w_{est} < 4kg$	$4kg \le w_{est} < 5kg$	$w_{est} > 5kg$	$w_{est} < 2kg$
1.2	2.9	3.4	18.64	3894	3.05	13	238	19.88	17.33	28.76	15.28	8.81	3.98	5.96	65.97
1.3	2.5	2.8	13.90	2904	2.88	13	238	20.76	17.70	25.55	16.43	9.26	4.34	5.96	64.02
1.3	2.6	3.2	20.93	4374	3.07	13	249	20.16	16.80	27.09	15.87	9.30	4.80	5.97	64.06
1.3	2.8	3.0	17.81	3721	2.96	13	238	19.54	17.71	26.90	16.58	9.33	4.46	5.48	64.15
1.3	2.8	3.2	21.12	4412	3.04	13	249	19.83	17.45	26.77	16.55	9.02	4.65	5.73	64.05
1.4	2.3	2.6	14.53	3035	2.86	13	249	18.91	16.90	28.47	16.90	8.63	4.65	5.54	64.28
1.4	2.3	2.8	18.46	3858	2.99	13	249	19.62	16.25	28.23	17.16	8.09	4.72	5.94	64.10
1.4	2.6	3.2	26.61	5559	3.16	13	249	19.52	17.04	27.49	15.34	10.09	4.79	5.74	64.04
1.5	2.4	2.8	24.69	5159	2.96	13	249	19.58	18.61	26.17	16.28	8.88	4.71	5.78	64.35
1.5	2.4	3.0	29.08	6075	3.07	13	249	20.02	18.70	26.06	15.90	8.66	4.74	5.93	64.77
1.5	2.6	3.0	29.42	6146	3.01	13	249	20.06	17.12	27.09	16.69	8.70	4.98	5.35	64.27
1.5	2.7	3.0	29.51	6165	3.01	13	249	19.58	18.39	26.72	16.45	8.16	5.01	5.69	64.69
1.5	2.7	3.2	33.42	6983	3.10	13	249	19.55	18.47	26.24	16.53	8.31	5.00	5.91	64.26
1.6	2.3	2.4	20.56	4295	2.72	13	249	19.79	17.28	27.31	17.07	8.22	4.87	5.47	64.38
1.6	2.3	2.6	25.83	5397	2.86	13	249	20.21	17.73	26.66	16.84	8.19	4.74	5.61	64.61
1.6	2.3	2.8	30.51	6375	3.02	13	249	19.78	17.91	26.54	17.02	8.11	4.69	5.95	64.24
1.6	2.4	2.6	25.98	5429	2.90	13	249	19.43	17.59	27.10	16.25	9.50	4.55	5.58	64.12
1.6	2.4	2.8	30.68	6410	3.05	13	249	19.39	17.64	27.05	16.29	9.19	4.49	5.94	64.09
1.6	2.5	2.6	26.14	5461	2.89	13	249	19.15	17.43	27.63	16.55	8.75	4.96	5.51	64.22
1.6	2.5	2.8	30.85	6445	3.01	13	249	19.29	17.80	27.21	16.34	8.75	4.92	5.69	64.30
1.6	2.7	2.4	21.03	4393	2.80	13	249	19.17	17.35	27.52	16.00	9.22	4.94	5.80	64.03
1.6	2.7	2.6	26.34	5503	2.88	13	249	19.90	17.30	27.40	16.05	8.69	4.91	5.76	64.60
1.6	2.7	2.8	31.07	6492	2.99	13	249	20.07	17.38	27.03	16.27	8.41	4.87	5.98	64.48
1.7	2.3	2.4	25.11	5246	2.83	13	249	19.54	17.59	27.47	15.84	9.66	4.37	5.53	64.60
1.7	2.3	2.6	30.24	6318	2.97	13	249	19.52	17.89	27.32	15.89	9.28	4.34	5.78	64.72
1.7	2.5	2.4	25.39	5304	2.82	13	249	19.17	17.23	27.83	16.16	9.62	4.45	5.54	64.23
1.7	2.5	2.6	30.57	6388	2.95	13	249	19.40	17.50	27.29	16.12	9.55	4.32	5.82	64.18

The selection of the deviation bounds in each of the three stages can be chosen based on the simulated performance in these three criteria. There is not one single outstanding result, however, those settings that have passed a large percentage of samples while maintaining accuracy and minimising error are of more interest. Figure 92 below shows the average template shape (black) with the deviation bounds (Rho) under the settings highlighted in Table 27. This average template shape has been chosen because the hypothetical objective in this scenario is to produce the least amount of weight estimation errors greater than ±5kg.
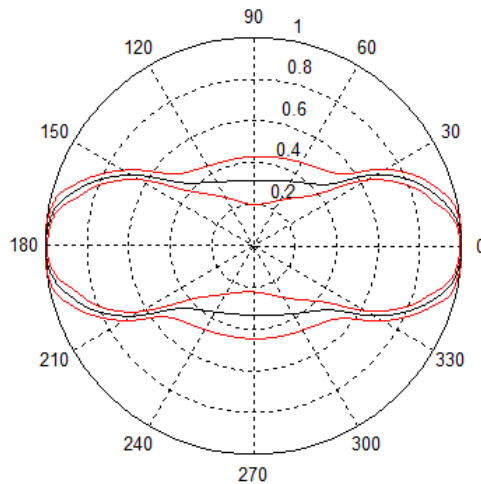
Figure 92: The Average Template Shape Constructed with Weight Ranges from 13 to 249kg

According to this particular simulation, when operating online, approximately 64% of the individual weight estimates which pass the filter shown in Figure 92, should reside between 0 and 2 kg error of the actual weight of the sample, and errors greater than ±5 kg should occur at a rate of less than 6%. Furthermore, the mean-relative error of the estimates which passed through the filter should be approximately 3.0% in the range of 13 to 249 kg. However, this figure depends on the weight range of the group observed. For example, a 3% mean-relative error on a 12 kg pig is just 0.36 kg as opposed to a 120 kg pig which is 3.6 kg. The average weight estimation error of the 6146 samples which passed through the shape filter was 1.94 kg using the settings highlighted in Table 27.

Most importantly the selection of a shape filter in this manner will provide a preliminary assessment of the integrity of the pose of the pig in relation to its weight estimate. Consequently, contours and their body measurements can be extracted efficiently and with confidence.

The body measurements were then validated further using the limiting filter. The body measurement limiting filter is assessed independently in the following section and then the two filters are combined in Section *3.6.5 Combining the Dimension Limiting Filter and Shape Filter*

3.6.4   The Dimension Limiting Filter

During normal operation, each contour sample that passed through the shape filter generated a weight estimate. However, in order for the weight estimate to be validated, the extracted body measurements were required to pass between previously defined limits (upper and lower) at the estimated weight range. The data used to define these upper and lower limits consisted of the 16 body measurements extracted from each of the contours that were used to build the average template shape. Confidence bounds (limits) were applied to each of the body measurements using the software.

The entire dataset of contours (total of 20894) was subject to the limiting process (without prior shape filtering) to assess the limiting filter's performance. During the performance testing, the limits of each body measurement were set to the same

126

confidence bounds. An example is given in Figure 93. If a given sample contour's body measurements was not within the upper or lower limit of the relationship defined by the limits software, the sample (estimate, frame and measurements) was disregarded preventing the estimate making its way through to output.
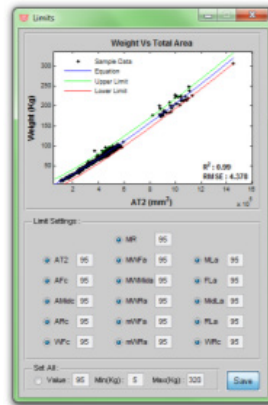
Figure 93: Setting the Confidence Bounds to 95% for the Total Body Area Measurement (AT$_2$) Over the Dataset

In order to test the filter, a weight estimate was required. The multiple regression equation was applied to the body measurements of the 20894 samples (see Section *3.6.1.1.3 Multivariate Linear Model*). These weight estimates were then used to compare the extracted body measurements with those of the weight and body measurements models. If all of the extracted body measurements passed within the limiting boundaries specified by the limiting software then the sample passed and its weight estimate was considered valid output.

Table 28: Weight Estimate Output after Setting the Dimension Limiting Filter to Different Confidence Bounds

Confidence bounds	% Passed	Number Passed	Mean Relative Error (%)	Min Weight (kg)	Max Weight (kg)	$w_{est} < 0.5kg$	$0.5kg \leq w_{est} < 1kg$	$1kg \leq w_{est} < 2$ kg	$2kg \leq w_{est} < 3$ kg	$3kg \leq w_{est} < 4$ kg	$4kg \leq w_{est} < 5$ kg	$w_{est} > 5kg$	$w_{est} < 2kg$
99%	69.74	14572	6.41	12.5	306	17.18	15.18	24.75	16.07	9.30	5.70	11.82	57.12
95%	65.49	13684	5.74	12.5	306	17.90	15.83	25.67	16.36	9.35	5.43	9.45	59.41
90%	62.63	13085	5.40	12.5	306	18.23	16.10	26.20	16.58	9.32	5.21	8.35	60.53
85%	60.08	12554	5.19	12.5	306	18.58	16.19	26.52	16.70	9.34	5.17	7.50	61.29
80%	57.47	12008	5.06	12.5	306	18.85	16.41	26.77	16.81	9.28	4.99	6.91	62.02
75%	55.15	11524	4.97	12.5	249	19.18	16.56	26.83	16.95	9.13	4.99	6.37	62.57
70%	52.91	11054	4.80	12.5	249	19.51	16.79	26.98	16.95	9.00	5.01	5.75	63.28
65%	50.49	10549	4.77	12.5	249	19.68	16.99	27.02	16.97	8.82	5.05	5.48	63.68
60%	47.88	10005	4.70	12.5	234	19.85	17.10	27.28	17.08	8.70	4.92	5.08	64.23
55%	44.87	9375	4.71	12.5	234	20.15	17.19	27.18	16.99	8.80	4.83	4.85	64.52
50%	41.62	8696	4.68	12.5	234	20.41	17.36	27.36	17.09	8.73	4.55	4.50	65.13
45%	38.28	7998	4.65	12.5	234	20.63	17.49	27.62	16.92	8.61	4.53	4.20	65.74
40%	34.71	7253	4.64	12.5	183.5	20.94	17.30	27.91	17.04	8.49	4.44	3.87	66.15
35%	30.98	6473	4.67	12.5	183.5	21.47	17.40	28.52	16.64	8.31	4.03	3.63	67.39
30%	26.87	5615	4.77	12.5	109.5	21.80	17.49	28.62	16.74	8.14	3.90	3.31	67.91
25%	22.56	4714	4.84	12.5	109.5	22.30	17.56	28.91	16.53	7.96	3.69	3.05	68.77
20%	17.68	3694	5.02	12.5	103	22.77	18.19	29.53	16.13	7.34	3.38	2.65	70.49
15%	12.88	2691	5.07	12.5	103	23.56	19.03	29.84	15.68	6.47	2.86	2.56	72.43
10%	8.10	1693	5.21	12.5	103	24.39	20.44	30.42	14.77	5.43	2.48	2.07	75.25
5%	3.11	650	4.84	12.5	98	27.69	24.00	30.15	13.08	3.54	1.38	0.15	81.85
4%	2.27	475	4.82	12.5	98	28.21	22.95	32.63	12.21	2.53	1.26	0.21	83.79
3%	1.38	289	4.56	13	95	32.18	21.11	34.26	10.03	2.42	0.00	0.00	87.54
2%	0.66	137	4.09	13	95	38.69	23.36	29.20	8.03	0.73	0.00	0.00	91.24
1%	0.11	22	2.53	15.5	29	68.18	18.18	13.64	0.00	0.00	0.00	0.00	100.00

The results after applying the limits at 24 different confidence bounds accounting for between 1 and 99% of the model relationships in each of the 16 weight and body measurement models are shown in Table 28. Table 28 shows that uniform narrowing of the limits of each body measurement, decreases the chance of errors greater than ±5 kg, while increasing the proportion of estimates within ±2 kg. This is desirable, however, the number of samples that pass through the filtering stage also drops considerably and the weight range narrows. Consequently, when configuring the limiting filter settings there is a trade-off between the inclusion of error and the volume and weight range of samples the system will collect. Potential confidence bounds settings are between 2 and 40% for grower-finisher pigs. A 1% or 2% confidence bound setting offers the highest accuracy but may be too selective in practice. A 40% confidence bound is less likely to be selective but is more likely to let through errors. Selection within this range will depend on various factors such as the variably in the environment caused by, non-pig objects, non-uniform lighting and dirty animals as these scenarios may reduce the quantity and quality of the available data. For this reason the software in Figure 93 was created so that the bounds could be modified easily during installation and setup.

Figure 94 shows the percentage relative error of each of the samples that passed through the filter when set to 10% confidence bounds; the black line indicates the percentage mean-relative error of the samples that passed. The mean-relative error of estimates for the weight ranges less than 40 kg is higher as a small error is a large proportion of a lighter animal.
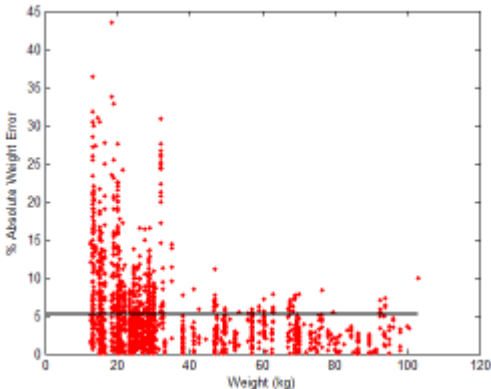
Figure 94: Percentage Weight Error of the Samples that Passed at 10 Percent Confidence Bounds The Black Line Indicates the Mean-relative error (%) of All the Samples that Passed

To generate the results in Table 28 all the limits of each body measurement have been changed in unison to the same percentage. However, it is also possible to change or remove any of the 16 limiting bounds independent of one another, which consequently could improve future filtering performance. To tune the limits filter, the feedback of the filters actions can be used. For example, Table 29 shows each of the body measurements and how they reacted in relation to the samples. The Column labelled *Correct Remove* corresponds to a sample which generated a result that was greater than ±5 kg and was filtered out, *Correct Leave* corresponds to a sample which generated a result that was less than ±5 kg and was left to output its weight estimate. *Incorrect Remove* is a false negative and *Incorrect Leave* is a false positive.

Table 29: The Dimension Limiting Filters Actions for Each of the 16 Body Measurements at 10% Confidence Bounds

Measurement	Correct Remove	Correct Leave	Incorrect Remove	Incorrect Leave
MWF_a	262	61	390	1
$MWMid_a$	50	5	160	0
MWR_a	476	92	373	1
AF_c	161	6	21	0
$AMid_c$	167	0	2	0
AR_c	298	1	22	0
AT_2	155	0	0	0
WF_c	247	15	169	0
WR_c	196	7	242	0
ML	108	8	64	2
FML_a	1086	854	2515	42
MidL	2224	2203	4143	94
RML_a	823	223	1076	13
mWF_a	60	33	430	1
mWR_a	154	87	935	3
ML_{Rho}	86	20	27	0
TOTAL	6553	3615	10569	157

As the MidL body measurement has contributed to the most false negatives, removing it from the limits filter has had a positive impact on the filtering results at 10% confidence bounds (see Table 30).

Table 30: Enhancing the Limits Filter by Excluding Certain Body Measurements

Confidence bounds	% Passed	Number Passed	Mean Relative Error (%)	Min Weight (kg)	Max Weight (kg)	$w_{est} < 0.5kg$	$0.5kg \leq w_{est} < 1kg$	$1kg \leq w_{est} < 2\,kg$	$2kg \leq w_{est} < 3\,kg$	$3kg \leq w_{est} < 4\,kg$	$4kg \leq w_{est} < 5\,kg$	$w_{est} > 5kg$	$w_{est} < 2kg$
10% With MidL	8.10	1693	5.21	12.5	103	24.39	20.44	30.42	14.77	5.43	2.48	2.07	75.25
10% Without MidL	9.96	2081	5.04	12.5	103	25.04	20.47	30.42	14.37	5.38	2.45	1.87	75.93

Note that this may not always be the case for other body measurements.

3.6.5 Combining the Dimension Limiting Filter and Shape Filter

Two different methods have been developed to restrict the output of incorrect weight estimates. These are based on the body measurements and shape extracted from the image, As the pig's shape is the first variable recovered from the image, it is important to determine the shape's prospect of providing an accurate weight-estimate before undertaking the extraction process. The shape filter has achieved this objective, as a shape and equation pair can effectively restrict erroneous results greater than ±5 kg to less than 6% at this early stage. If a sample passes through the shape filter they are then subject to the limits filter, which validates the weight estimate in respect to the body measurements extracted from the contour.

The dataset was filtered based on the average template shape at a deviation setting highlighted in Table 27 in Section *3.6.3 Adjusting the Bounds of the Shape Filter* and under a number of different limit settings between 1 and 99% confidence bounds. The results are presented in Table 31.

Table 31: Weight Estimate Output after Filtering the Contour Samples Based on Shape and Body Measurements

Limit Setting	Number Passed Shape Filter	Number Passed Limits Filter	Mean-relative error (%)	Weight Min (kg)	Weight Max (kg)	$w_{est} < 0.5\,kg$	$0.5kg \leq w_{est} < 1kg$	$1kg \leq w_{est} < 2\,kg$	$2kg \leq w_{est} < 3\,kg$	$3kg \leq w_{est} < 4\,kg$	$4kg \leq w_{est} < 5\,kg$	$w_{est} > 5kg$	$w_{est} < 2kg$
99%	6146	5873	2.98	13	228	20.43	17.57	27.79	16.94	8.36	4.92	3.98	65.79
95%	6146	5757	2.97	13	228	20.65	17.65	27.98	16.90	8.27	4.90	3.65	66.28
90%	6146	5657	2.96	13	228	20.79	17.69	28.21	16.90	8.20	4.70	3.50	66.70
85%	6146	5525	2.96	13	201	21.01	17.63	28.29	17.00	8.18	4.65	3.24	66.93
80%	6146	5326	2.95	13	201	21.22	17.86	28.56	16.92	8.00	4.43	3.02	67.63
75%	6146	5149	2.96	13	180	21.48	17.93	28.45	17.01	7.85	4.37	2.91	67.86
70%	6146	4984	2.97	13	180	21.63	18.16	28.33	16.91	7.70	4.47	2.79	68.12
65%	6146	4804	2.98	13	109.5	21.79	18.23	28.29	16.80	7.66	4.50	2.73	68.32
60%	6146	4602	2.99	13	109.5	21.90	18.27	28.44	16.84	7.58	4.32	2.63	68.62
55%	6146	4339	3.01	13	109.5	22.24	18.18	28.35	16.73	7.65	4.29	2.56	68.77
50%	6146	4052	3.04	13	103	22.24	18.34	28.46	16.78	7.63	4.10	2.47	69.03
45%	6146	3742	3.07	13	103	22.31	18.47	28.75	16.46	7.54	4.09	2.38	69.54
40%	6146	3396	3.12	13	103	22.56	18.23	28.86	16.52	7.54	4.03	2.27	69.64
35%	6146	3026	3.12	13	103	23.07	18.11	29.64	16.33	7.30	3.54	2.02	70.82
30%	6146	2622	3.16	13	103	22.85	18.50	30.17	16.55	6.79	3.36	1.79	71.51
25%	6146	2199	3.25	13	103	22.69	18.42	30.47	16.69	6.91	3.23	1.59	71.58
20%	6146	1688	3.41	13	103	23.52	19.49	30.04	16.35	6.64	2.43	1.54	73.05
15%	6146	1221	3.59	13	103	24.90	20.39	29.65	15.15	6.14	2.13	1.64	74.94
10%	6146	764	3.72	13	103	26.44	22.51	29.97	13.09	4.71	1.57	1.70	78.93
5%	6146	278	3.67	13	98	30.94	27.70	27.34	10.43	2.88	0.72	0.00	85.97
4%	6146	201	3.76	13	98	31.34	26.87	31.34	7.96	1.99	0.50	0.00	89.55
3%	6146	125	3.79	13	95	32.00	28.80	29.60	7.20	2.40	0.00	0.00	90.40
2%	6146	61	3.17	13	95	40.98	31.15	21.31	4.92	1.64	0.00	0.00	93.44
1%	6146	12	2.32	15.5	25.5	66.67	25.00	8.33	0.00	0.00	0.00	0.00	100.00

Table 31 indicates that higher limiting filter settings (greater than 40% confidence bounds) are acceptable when using the samples that have passed through the shape filter, compared to the results obtained when the filters are used independently. Thus, when using the filters in combination, limiting bounds between 2 and 75% are acceptable for pigs in the grower finisher range. However, as mentioned previously, the configuration of the both the shape and limit filter settings can be adjusted respect to the conditions that the system will be exposed too. For example, if the system was observing clean white pigs in a controlled black environment with structured lighting, then a satisfactory capture rate may occur at limit-filter settings of less than 20%. Selecting lower confidence bounds may also be more appropriate in practice, as on average the duration of the videos sampled to create the dataset only consisted of 41 frames (8.2 seconds of footage).The maximum duration of any one video was 33 seconds. Consequently, during these simulations the opportunity to collect a sample frame with the animal in the correct pose was limited in respect to what would occur around the feeder in normal production circumstances. Online testing in the installation environment needs to be undertaken to optimise filter settings in respect to the number of images acquired and the accuracy of the system. This can be achieved by adjusting the software settings in respect to Table 27, Table 28 and Table 31.

3.6.6 Determining the Appearance-Based Attributes of Pigs for Tracking

The pigs can be tracked in order to: (i) enhance segmentation, (ii) determine pig attendance at the feeder and (iii) determine bias in feeding behaviour.

Software was written to automatically extract and store data from video. This involved the in the automatic identification of the pig within the image using thresholding. Although thresholding was not effective at recovering the precise contour of a pig in the observed scene, it was useful for determining its approximate location . This localised region became the starting point for a search for the pig in subsequent frames and assisted with segmentation.

The first step in the identification process involved the application of an adaptive threshold (Niblack, 1985) over subregions of the image. This was followed by an erode operation on the binary image to separate any touching objects. An opening procedure was then applied, which removed any small to medium sized objects from the image that could not be a complete or larger proportion of a pig. A dilation procedure followed which joined large areas together that were in close proximity. If a shape that was consistent with a pig shape was identified in consecutive frames, a subtraction took place, such that all the information surrounding the region containing the pig was suppressed. An opening operation then limited the area of any remaining object to within a specified range of pixels. This range ensured pigs between 12.5 and 306 kg would not be excluded. Finally, the object was validated on several image-based attributes including:

- Standard deviation of the shapes pixel values (uniformity of appearance)
- Area (the original area found by applying a threshold algorithm (Niblack, 1985) over image regions across the entire image)
- Solidity (proportion of the area to the convex hull of the area)
- Mean Intensity (of the shape's pixels)
- Orientation
- Perimeter
- Eccentricity (ratio between the foci of an ellipse containing the shape and the length of its main axis)
- Area versus Perimeter Ratio
- Major Length versus Minor Length Ratio
- Minor Axis Length
- Major Axis Length
- Euler Number (number of objects in the region minus the number of holes in the objects)
- Area 2 (the area found after applying a threshold algorithm (Niblack, 1985) over the segmented image region that was likely to contain a pig)

These parameters were stored during the extraction process so that the parameters of the shapes used in the construction of the average template shape could be recovered. These recovered attributes, defined ranges for the image-based representation of a pig that would promote a good result. Table 32 shows the various statistics of twelve of these attributes as chosen by the system during the shape building process as highlighted in Table 27.

131

Table 32: Image-based Descriptors of a Pig for Early Identification

	Weight	Standard Deviation	Area	Solidity	Mean Intensity	Perimeter	Eccentricity	Area Perimeter Ratio	Major Length Minor Length Ratio	Minor Axis Length	Major Axis Length	Euler Number	Area 2
Max	238.0	0.114	523892	0.951	0.834	5639.7	0.975	142.2	4.457	460.5	1680.20	1.0	545071
Min	13.0	0.015	44927	0.643	0.350	996.2	0.883	38.0	2.132	140.6	413.57	-43.0	31707
Range	225.0	0.099	478965	0.308	0.484	4643.5	0.091	104.2	2.325	319.9	1266.63	44.0	513364
STD	39.3	0.015	73614	0.041	0.050	563.7	0.009	14.7	0.297	53.5	181.49	3.9	80751
AVE	74.5	0.057	194180	0.838	0.444	2654.3	0.954	71.3	3.383	276.4	931.62	-2.6	184444

These ranges can be used as references in future developments. For example, if all the observed pigs are white then the standard deviation of the pixel values on the animals back may indicate the cleanliness of the pig. The area may also be used to give a preliminary indication of the weight of the object being assessed. Hence, if the object area is too large or small in respect to the group average weight found on the previous day then the recovered object can be discounted. The minor and major axis length, eccentricity and perimeter can also be used in a similar manner. The grey-scale mean-intensity of the pixels making up the pig's back were collected so that the values could be applied as thresholding boundaries to suppress non-pig objects during image analysis. If the database was to be formed a second time, the mean intensity from the three separate colour channels would also be recovered to determine potential thresholding boundaries to suppress non-pig objects across the colour image. However, these thresholding boundaries will undoubtedly change with environmental conditions such as the luminance of the scene in respect to the time of day. As a result, further data collection may be required.

This attribute recovery facilities continuous-improvement code, thus in future it may be built-into the system to recover the image-based representation of pigs. This information would provide valuable feedback about the conditions that the system is operating under and consequently help with the optimisation of system settings.

3.6.6.1 *Tracking and Recording Pig Attendance at the Feeder*

Rather than searching and identifying the pig in every frame, it is much faster and easier to re-identify the pig in the subsequent image using its location in the current frame; using some form of temporal correspondence. A tracking routine can use temporal correspondence to link features recovered from a frame to an adjacent or subsequent frame.

The tracking method created during this study is linked to the shape filter. The shape filter was able to recognise the pig within a certain range of posture by the number of points which passed within a certain deviation of a constructed average template shape. If all the points passed this process then the shape passed through to have its body measurements extracted. However, if some of the shape's points did not pass the shape filter, then the information was not discarded entirely. Instead, the value of points which did pass the shape filter relative to the pass requirement (1500 points) was determined giving an indication of how likely the object was a pig and how close it was to the required pose. Even though the shape was not suitable for weight estimation it could be used to identify the pig with a high level of confidence. Hence the region within the image where a pig was in attendance could be determined and subsequently tracked to maximise the chance observing a pose appropriate to

undertake a weight estimate in subsequent images. Figure 95 below shows the bounding box surrounding the pig during a successful capture. The co-ordinates of this box region are relayed to the subsequent image to localise the image search space containing the pig and maximise the chance of relocation.
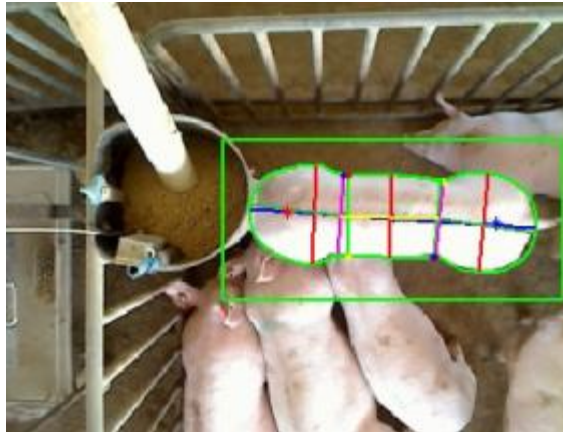
Figure 95: The Region from which the Pig was Re-identified

3.6.7   System Precision

Section *3.3.3.1 The Effect of Gut Fill* earlier made assumptions about what the practical precision of a device weighing pigs should be given the effect of gut fill. Table 33 shows the performance of the developed system at 65% limit settings over various weight ranges compared to the assumed practically obtainable precision of weighing pigs. This assumed acceptable error margin is 50% of the total range of gut-fill of the animal at a given weight.

Table 33: Comparing Simulated Precision with Acceptable Error

Simulated piGUI System Performance					Acceptable Error				
						50% GF		GF	
Weight Range	Number Samples Passed Filter	Mean Weight Error (kg)	Mean Weight (kg)	Mean Relative Error (%)	Weight	GF Error ΔW (kg)	GF /LBW (%)	GF Error (kg)	GF/ LBW (%)
15↔25	331	1.07	20.96	5.08	20	0.87	4.33	1.73	8.66
25↔35	498	1.49	28.34	5.26	30	1.11	3.70	2.22	7.40
35↔45	263	1.49	39.57	3.77	40	1.32	3.31	2.65	6.62
45↔55	477	1.24	49.61	2.50	50	1.52	3.04	3.04	6.07
55↔65	447	1.46	59.54	2.45	60	1.70	2.83	3.39	5.66
65↔75	695	1.74	70.81	2.46	70	1.86	2.66	3.73	5.33
75↔85	1169	1.73	79.38	2.17	80	2.02	2.53	4.05	5.06
85↔95	586	2.05	89.78	2.28	90	2.17	2.42	4.35	4.83
95↔105	295	2.28	97.99	2.33	100	2.32	2.32	4.64	4.64
105↔115	1	0.38	109.50	0.35	110	2.46	2.24	4.92	4.47

From Table 33 it can be seen that, on average, the piGUI system successfully calculates the weight of individual pigs greater than 45 kg to practical precision. On average, pigs weighing between 15 and 45 kg do not reside within this 50% gut fill range. However, they are well within the maximum and minimum ranges for gut fill at these weight ranges (within 67.5% of the maximum range). Lowering the camera to these smaller pigs could possibly enhance the results in the weight-range of 15 to 45 kg in future as body measurements can be obtained more precisely and subtle difference can be detected.

3.7 CONCLUSIONS

A method was created to segment the body contours of pigs from images and to exclude the head and tail from further analysis.

The reference points of sixteen body measurements along the contour shape were automatically identified and extracted using the developed techniques. Software was written to automatically carry out these functions on both streaming video and a database of collected videos.

Code facilitating the conversion from pixels to millimetres was written into the software. This conversion was automatically applied when a resolution and an installation height was entered by the user. This software feature ensured that the equation coefficients could remain the same irrespective of installation height and selected camera resolution.

Preliminary testing of the device highlighted areas of improvement. Subsequently, a filtering process was developed to validate the contour shape after segmentation. A filtering method in which each shape was evaluated on a point by point basis out performed an alternative method which attempted to describe the residual of the shape as a single value.

To estimate the weight of the pigs from the extracted body measurements, linear, non-linear and multivariate linear equations were formed. Results indicate that a multivariate linear equation built using a stepwise selection of the 16 extracted body measurements, 11 angles and their 351 paired interactions performed the best, with 3% less samples in the greater than ±5 kg category and 2% more samples in the less than ±2 kg error category than the closest non-linear equation.

During off-line analysis the chosen shape filtering process was shown to maintain weight estimate error between 0 and 2 kg of the actual weight at a rate of 64% and errors greater than ±5 kg a rate of less than 6%. This indicated that 94% of weight estimates that passed through the shape filter were within ±5 kg of the actual weight of the pig. This ensured that the integrity of extracted contour shapes could be discriminated against early in the processing loop, thus enhancing efficiency and reliability.

In addition, weight estimation precision was also enhanced by modelling the weight-estimation equation as function of shape. Compared to previous benchmarks a favourable 24% increase in the number of weight estimates between 0 and 2 kg occurred, while the number of weight estimates greater than ±5 kg reduced by 19%. A secondary filter was developed to validate the estimated weight against the body measurements extracted from the contour. During off-line analysis this limit filtering process was shown to maintain weight estimate error between 0 and 2 kg of the actual weight at a rate of 68% and errors greater than ±5 kg a rate of less than 3.5% over the grower finisher range. When these two filters were combined during off-line analysis the weight estimate error between 0 and 2 kg of the actual weight was maintained at a rate of greater than 68% and errors greater than ±5 kg a rate of less than 3% over the grower finisher range. Tables provided from these simulated results give grounds for the selection of the filtering parameters. This selection may be

134

based on the environment that the device will be exposed too and the weight range observed.

As pig height was manually determined during data collection, height was included in the weight-estimation equation to determine its effect on the performance of weight estimation. Over the entire dataset the multivariate equation including the height parameter improved estimation precision by 7.34% in the less than ±2 kg weight-estimation category and by 8.87% in the greater than ±5 kg category compared to the multivariate equation without the height parameter. However, heights positive effect was reduced when a subset of the dataset was considered based on the integrity of the contour samples. As after sorting, and selecting the first 3500 samples, the multivariate equation including height contributed to 6.29 % in the less than ±2 kg error category and only 1.09% in the greater than ±5 kg error category (compared to the multivariate equation without height as a parameter). Hence, due to the marginal benefit in precision and the practical issues related to finding a reliable reference point to obtain the height measure in practice, the height measurement was not pursued in this study. However, it may be considered for future work.

The image-based attributes of the pigs that were used in the shape and equation building process were recovered for use in future development, as they provide potential starting points for tracking and segmentation functions. A tracking procedure was integrated into the software to relocate the pig in subsequent frames and to enhance the likelihood of obtaining weight estimates. This tracking procedure was linked to the shape filtering stage, as a contour that did not pass the shape filters criteria could still be used to identify the presence of a pig.

Additional work can be carried out in several areas related to this methodology. First, the methodology itself is applicable to the weight estimation task of other livestock species. The code used to generate the database automatically from videos can be used to automatically extract the body measurements of other livestock species from video frames and store them in a format ready for analysis (some modification may be required). The code used to generate the equation and average template shape (shape filter) is directly linked to the database structure such that it can be used in a 'plug-in' manner. The shape building process may also be used to define a behavioural action. This can be done by first building a library of shapes describing the sequence of the action using the developed code. Then a sequence of average template shape can be used to validate a behavioural action when it is observed by cross-referencing between extracted contours obtained while tracking the animals. Other work surrounds the further development of the functional elements of the software.

During the shape filtering process the residual can potentially be used identify and repair sample contours that have not been segmented correctly. A second pass of the image frame could validate the re-constructed contour.

The technique described in Section *3.5.1.5 The Stitching Method to Enclose the Contour Shape* can potentially be used to identify multiple pigs. First, a blob analysis can be performed using the appearance information unique to pigs defined in Section *3.6.6 Determining the Appearance-Based Attributes of Pigs for Tracking*. The

centroid of each blob can be calculated and the sweeping algorithm can be applied to each object determining its gradient boundary. As the sweep progresses the extracted contour information could potentially be validated with the magnitude vector so that processing can terminate on blobs objects that are not likely to be pigs. However, removal of the tail and head may pose additional challenges using this technique.

On average, for individual pigs weighing in the range of 45 to 115 kg the system operated within an acceptable error margin of 50% of the gut fill. For pigs in the weight range of less than 45 kg, on average, the system operated within 67% of the weight attributed to gut fill. The percentage mean-relative error was between 5.1 % and 3.7% for pigs weighing between 15 and 45 kg and less than or equal to 2.5% for pigs between 45 and 115 kg. These results indicate that the system will, on average, operate to within the error margin attributed to gut fill. Therefore, this indicates that the system will be able to calculate the animal's body weight effectively and to practical precision. However, it will be unable to detect the small variation in body weight caused by the gut.

Chapter 4

Growth Recorded Automatically and Continuously by a Machine Vision System for Finisher Pigs

Tscharke, M. &Banhazi, T. M. (2011).Growth recorded automatically and continuously by a machine vision system for finisher pigs. In *The Bi-annual Conference of the Australian Society of Engineering in Agriculture (SEAg 2011)*, 454-464. (Eds C. Saunders and T. Banhazi). Gold Coast, Australia: Australian Society of Engineering in Agriculture.

ABSTRACT

Conventional livestock weighing methods require direct contact with the animals. Such contact is both physically demanding and hazardous for those undertaking weighing activities. Alternatively, a livestock animal's weight can be estimated from its body measurements using non-invasive methods. This chapter presents recent improvements in the ongoing development of a completely automatic, two dimensional machine vision system labelled the piGUI system, designed to obtain body measurements of pigs in order to estimate their live weight. Results comparing livestock weights obtained by a conventional method and the vision-based method are reported for pigs in their finisher stage of growth.

During off-line testing of a video dataset, the piGUI system demonstrated that it was capable of estimating the average group weight to within 2.5% error of the actual group average weight. In addition, the weight deviation of the groups was estimated within ±1 kg error of the actual group weight deviation. During on-farm testing the average group weight was accurate to 2.5% relative error and the estimated weight deviation was within ±2 kg of the actual weight deviation.

Recording the continuous live weight change of livestock (growth) is important as it can be used to measure animals' responses to various factors such as the surrounding climate, housing environment and nutrition. Assessing the animals' responses to these conditions is essential in improving the efficiency and welfare of livestock in both research and commercial settings.

4.1 INTRODUCTION

Recording the growth of livestock animals is important from an animal production perspective, as livestock produces rely on growth information to initiate and improve management procedures (Whittemore *et al.*, 2001; Whittemore, 2004). For example, periods of substandard growth may indicate poor health and may prompt further investigation and treatment (Maltz, 2010). The ability to detect such problems relies on the availability of growth data.

Conventionally, growth data has been determined by manually drafting the animals through an electronic livestock scale. This method is labour-intensive and hazardous. The data acquired is also often coarse, as it is only feasible to collect a few data points over the production cycle (Brandl and Jørgensen, 1996; Lundqvist and Gustafsson, 1992; Hartman *et al.*, 2004).

Alternatively, mechanised weighing methods can automatically record the growth of livestock animals on a daily basis (Weight Watcher™, Osborne Industries, Inc., Kansas, USA). However, despite their usefulness, the benefits of these automatic cage-type scales can easily be counteracted if (i) batches of animals are not successfully trained to (willingly) move through the scale, (ii) if the farmer fails to learn how to run and maintain the equipment accordingly or (iii) if the correct space allocation, gate placement and barn layout is not achieved during installation (Morrison, 2004). Notably, majority of the problems surrounding mechanised scales arise from (i) the physical interaction between the scale and the animals it services and (ii) the 'control' facilitated by the skilled workers drafting or training the animals.

Subsequently, machine vision systems are being developed which require no confinement or interference towards livestock during weight assessment (Banhazi *et al.*, 2011b). Machine vision systems determine livestock growth by first estimating each animals weight based on its image-derived body measurements, and then forming a group average weight estimate based on a representative sample of the individual estimates over the course of a day (Marchant *et al.*, 1999; Schofield *et al.*, 1999). In this manner, machine vision systems can determine both group and individual growth information automatically and continuously. Thus, information can be readily obtained daily, without depleting labour resources. Consequently this method overcomes much of the safety risk and costs associated with conventional and mechanised methods (Tscharke and Banhazi, 2011).

Previously a machine vision system was developed to estimate the weight of pigs during the grower-finisher growth period (Banhazi *et al.*, 2011b). The main aims of the work reported in this chapter were to determine whether (i) the group average weight and (ii) the group weight deviation of groups of finisher pigs could be estimated within practical accuracy using the system, thus, further extending the concept of the developed vision-based weighing system.

4.2 MATERIALS AND METHODS

A machine vision system was developed to acquire and process images obtained from a camera (Quickcam Pro 9000, Logitech, Quarry Bay, Hong Kong). Several

processing routines were programmed in Matlab (MathWorks, Inc., Natick, MA) to search the image, identify a pig shape, extract a pig's body measurements, estimate a pig's weight and finally validate the weight with reference to the body measurements. These routines ensured that no operator involvement was required to obtain weight estimates, as all required intelligence was built into the program. The process is illustrated in Figure 96. The systems processing tasks were undertaken by a nettop PC (fit2PC, CompuLab Ltd, Technion, Haifa, Israel). This computer was chosen to overcome several problems experienced using desktop computers in the piggery environment. The compactness of the PC ($115 \times 101 \times 27$ mm) reduced the chance of rodent or insect infestation. The small size also enabled the system to be easily mounted and transported and its fan-less operation prevented moisture and dust from being drawn into the PC.

Two filters were constructed in order to recognise a pig within an image when it was in a particular pose. The first shape filter was created from an average of different sample contours of a set weight reference pose. The second filter contained the various body measurements of pigs at different weights. These filters were then used to validate a segmented body contour as a 'pig shape' and to cross-validate between body measurements and weight estimates.
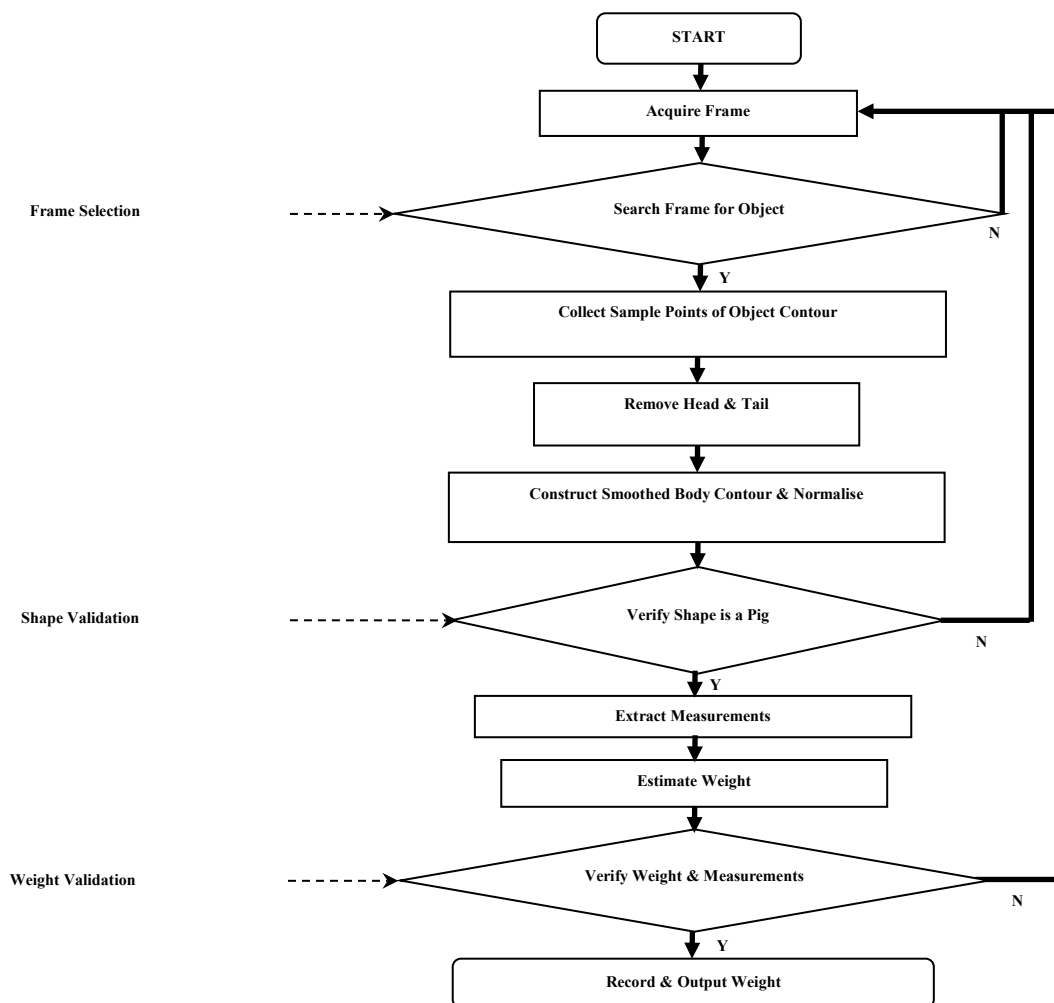
Figure 96: The Main Steps Used During the Image Analysis and the Weight Estimation Process

4.2.1 Experimental Setup and Location of the PiGUI System

To determine the relative precision of the system, an off-line validation and on-farm validation was conducted using the data collected from a commercial research piggery (PPPI, University of Adelaide, Roseworthy campus).

4.2.1.1 Off-line Validation

For the off-line validation, 412 videos of finishing pigs (55 to 125 kg) were acquired directly before they entered an electronic weigh scale (Pig Weigh Crate, Ruddweigh, Guyra, Australia, ±1%). The weights of the animals were recorded to the nearest ±0.5 kg. The videos were taken at a resolution of 1200x1600 and at a height of 2 m lens to ground. The 412 videos were separated into three groups; Group 1 containing all 412 male and female pigs, Group 2 containing 242 male pigs and Group 3 containing 170 female pigs. The pigs in the three groups were also evaluated on an individual basis by the system.

The filtering processes ensured that the estimations made would be as accurate as possible by removing redundant data, such as when the pig's body pose was not suitable for weight assessment. The underlying philosophy of both the off-line and on-line trial was to measure a single pig once daily to get a good estimate (similar to an electronic scale) rather than obtaining many erroneous measurements and attempting to average them out. In addition, it was noted that if each individual weight measurement was precise enough, the deviation of the animals' weight as a group may be estimated. In practice, this measure may prove to be a valuable gauge to assist farmers in maintaining their pigs in groups of similar weight ranges.

4.2.1.2 On-farm Validation

The farm trial involved setting up the piGUI system above a small pen at the piggery. Located inside the pen were 15 male pigs and a single feeder and drinker. The camera was placed above the feeder to give the system adequate opportunity to assess each pig's weight of over the course of the day. Thus at this location, sufficient data would be available to estimate the average weight of the group. To guarantee that the system could successfully operate under natural lighting conditions in commercially realistic environments, artificial lighting was not used within the pen. The automatic exposure feature of the camera compensated for much of the light variation encountered.

Figure 97 (a) provides a top view of the experimental setup and location and Figure 97 (b) shows the equipment interface. Radio frequency identification was integrated but not active during this trial.
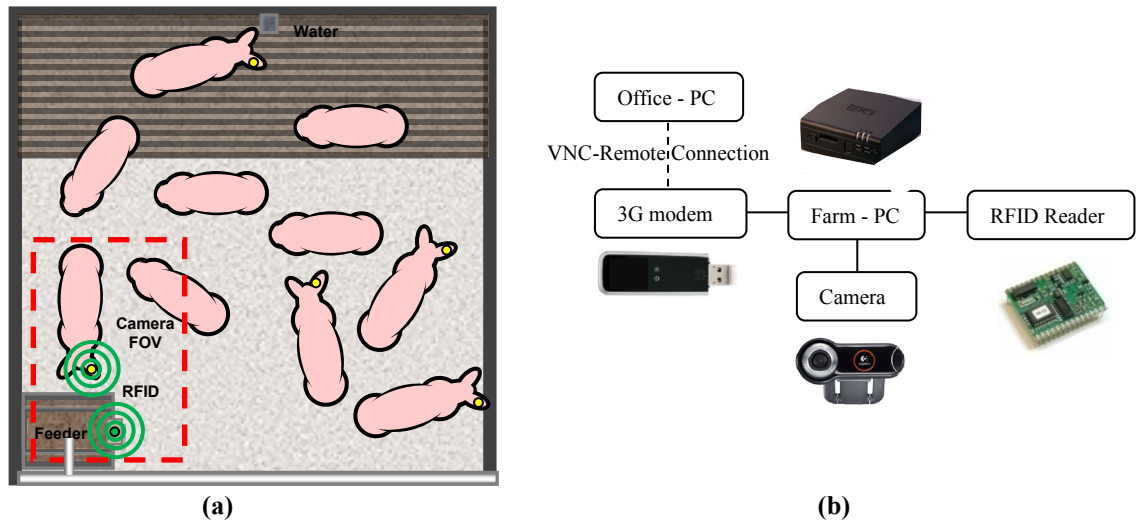
Figure 97: (a) The Experimental Setup at the Facility; (b) The Equipment Interface

After the piGUI system was setup and initialised, the following key information was recorded when successful weight assessment had taken place: (i) an image of the pig with an overlay of contour shape detected (Figure 98 (a)), (ii) the shape information of the contour, (iii) the body measurements used to estimate the weight (Figure 98 (b)), (iv) an weight estimate using several equations and (v) a time-date stamp of when the image was taken.

Figure 98: (a) An Image Recorded by the System; (b) An Image with the Extracted Body Measurements Overlayed

In total, 15 body measurements were extracted from the body of the pigs observed in the images (Figure 99). The body measurements WF_c and WR_c refer to the widths derived from the points directly behind the shoulders and in front of the hams respectively. These measurements are often different from the minimum widths recorded (mWF_a, mWR_a) due to the pose of the pig.
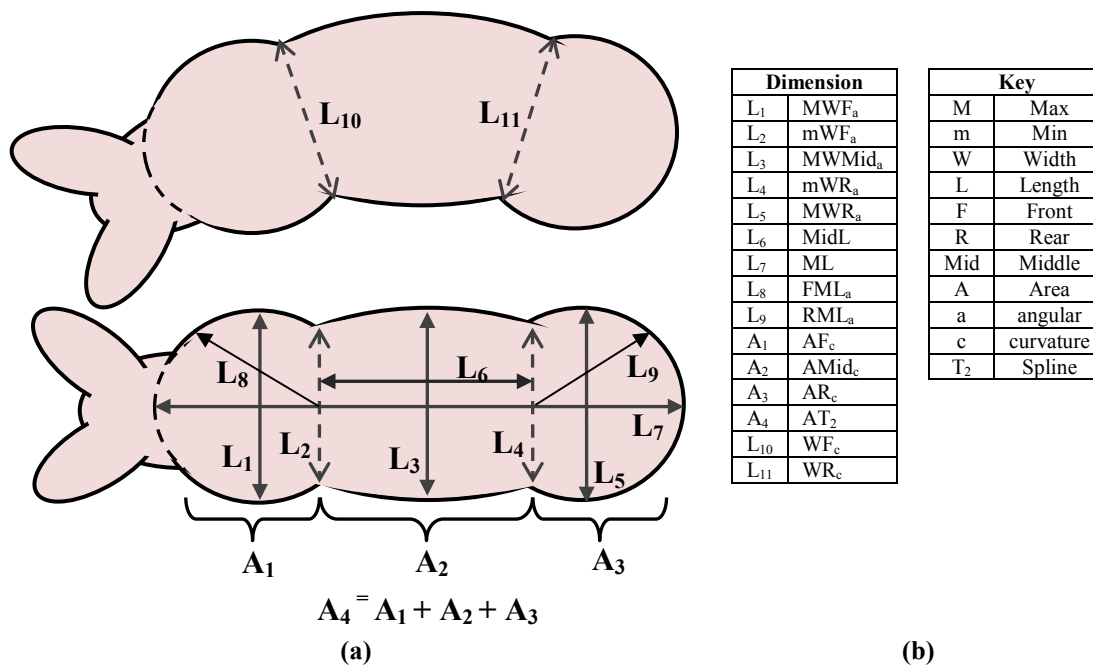
Figure 99: (a) The Locations of the Various Body Measurements which were Extracted from the Images of Pigs; (b) A Key Giving Further Detail on the Name of Each Dimension

To validate the vision systems group average and individual weight estimates, the entire group of animals were weighed manually seven times over a 22 day period using the pig weigh crate specified previously. The weigh crate had a relative error of ±1% according to manufacturing specifications and was located a short distance from the experimental pen. To enable easy identification by visual observation on future weigh days, the pigs' backs were marked with livestock paint in a unique pattern during weighing.

The pigs chosen for the experiment were in their finishing stage, weighed between 60 and 120 kg and were a cross between a Large White, Landrace and terminal sire. This is a common Australian breed-combination for pigs produced for their meat. Twelve pigs were observed in total during the field trial, however, one of the pigs was only in the pen for a short period of two and a half days.

Weights were estimated using 22 different equations. A lookup table was created and used to determine the ability of each of the 15 body measurements in estimating the animals' group average weight. The first column of the lookup table consisted of 0.5 kg increments of weight from 10 to 120 kg and the remaining adjacent 15 columns contained the corresponding body measurements at the weight located in the first column. These body measurements were based on the extracted measurements from a separate data sample. The table was used in reverse such that the closest match of each of the 15 body measurements obtained from the image was found before recovering the corresponding weight estimate from the first column. The average of the each of the 15 individual weight assessments became a further mean-body measurement weight-estimation equation. The remaining six equations were a mixture of linear equations constructed from regression and multiple regression analysis and power based equations. A list of the equations and their respective variable input and type can be found in Table 34.

Table 34: List of Equations and Respective Variable Input Dimension(s)

Equation	Type	Variable(s)
EQ_1	Lookup Table	MWF_a
EQ_2	Lookup Table	$MWMid_a$
EQ_3	Lookup Table	MWR_a
EQ_4	Lookup Table	AF_c
EQ_5	Lookup Table	$AMid_c$
EQ_6	Lookup Table	AR_c
EQ_7	Lookup Table	AT_2
EQ_8	Lookup Table	WF_c
EQ_9	Lookup Table	WR_c
EQ_{10}	Lookup Table	ML
EQ_{11}	Lookup Table	FML_a
EQ_{12}	Lookup Table	$MidL$
EQ_{13}	Lookup Table	RML_a
EQ_{14}	Lookup Table	mWF_a
EQ_{15}	Lookup Table	mWR_a
EQ_{16}	Average LUT	$(EQ_1+EQ_2+EQ_3\ldots+EQ_{15})\,/15$
EQ_{17}	Linear Regression	AT_2
EQ_{18}	Power	AT_2
EQ_{19}	Multiple Regression	MWF_a, MWR_a, AT_2, mWF_a, mWR_a
EQ_{20}	Multiple Regression	All 15 Variables $MWF_a \rightarrow mWR_a$
EQ_{21}	Multiple Regression	MWF_a $MWMid_a$ MWR_a WF_c WR_c ML mWF_a mWR_a
EQ_{22}	Multiple Regression	14 Variables $MWF_a \rightarrow mWR_a$ excluding AT_2

4.3 RESULTS AND DISCUSSION

4.3.1 Off-line Trial Results

During the off-line trial, the frames of the 412 videos were subject to an automatic extraction procedure, whereby the body contour and measurements of the finisher pigs were recovered. The extracted information was used to make a weight estimate only when the shape and limits filter deemed it appropriate. Each frame that passed the filtering processes was used to assess the system's ability to determine the weight of individual pigs. As radio frequency identification is unavailable during normal system operation, the daily group average weight estimate must be formed by averaging all individual weight estimates, regardless of whether estimates have been collected of each pig uniformly. Hence, this method has potential to yield a different result than obtaining the group average weight by dividing the combined weight of the pigs by the number of pigs. Results presented in this section show the error between these approaches and determine the group average estimates both before and after the filters' actions. During these tests the shape filter was set to 1.5, 2.6 and 3 deviations and the limits filter was set to 80% bounds.

4.3.1.1 *Individual and Group Average Weights*

Group 1 contained all 412 video samples of a mixture of 412 male and female pigs. Table 35 shows the vision system's ability to calculate the group average weight with and without the filters. Two actual weights are also presented. The first, 'Actual Weight Frames' is the actual average weight and deviation based on weights obtained from the electronic livestock scale for the frames that were extracted from the videos (see Before Filtering on row 1). The second, 'Actual Weight Videos' is the actual average group weight and weight deviation based on weights obtained from the electronic livestock scale for the each of the pigs in the 412 videos (see

Before Filtering on row 1). Hence, the result given on the row one containing the unfiltered Actual Weight Videos is the average (80.3 kg) and deviation (12.3 kg) of the group as determined by conventional means. All other results are based on the data that were available to the system after the extraction (row 1) and various filtering operations (rows 2 to 4).

Table 35: Performance of the piGUI System Estimating the Weight of Group 1

Filter Method	Estimated Weight Frames (kg)		Actual Weight Frames (kg)		Actual Weight Videos (kg)	
	AVE	STD	AVE	STD	AVE	STD
Before Filtering	79.6	40.6	79.3	12.2	80.3	12.3
Limit Filter	77.6	12.0	77.8	11.6	79.3	12.2
Shape Filter	78.9	11.9	79.0	11.7	79.3	12.0
Combined Filters	78.8	11.7	78.9	11.5	78.7	12.1

Table 36 shows the error in individual weight estimates of the sample frames which passed through the filtering processes. Each sample has been assigned to an error category based on the difference between the weight estimate and the actual weight.

Table 36: Performance of the piGUI System Estimating the Individual Weights of the Pigs in Group 1

Method	Before Filtering		Passed Shape		Passed Limits		Combined	
Error Category (kg)	Count	%	Count	%	Count	%	Count	%
$w_{est} < 0.5$ kg	1473	11.0	760	18.4	1065	16.8	630	19.1
0.5 kg $\leq w_{est} < 1$kg	1362	10.1	643	15.6	942	14.9	516	15.6
1 kg $\leq w_{est} < 2$ kg	2364	17.6	1118	27.0	1660	26.2	921	27.9
2 kg $\leq w_{est} < 3$ kg	1779	13.2	774	18.7	1218	19.2	621	18.8
3 kg $\leq w_{est} < 4$ kg	1146	8.5	410	9.9	679	10.7	301	9.1
4 kg $\leq w_{est} < 5$ kg	729	5.4	240	5.8	386	6.1	194	5.9
$w_{est} \geq 5$ kg	4586	34.1	190	4.6	391	6.2	120	3.6
Total Samples	13439	100.0	4135	100.0	6341	100.0	3303	100.0
$w_{est} < 2$ kg	5199	38.7	2521	61.0	3667	57.8	2067	62.6

Group 2 contained all 242 video samples of male pigs. The result for the weight estimates of Group 2 can be seen in Table 37, with individual weights for the group presented in Table 38.

Table 37: Performance of the piGUI System Estimating the Weight of Group 2

Filter Method	Estimated Weight Frames (kg)		Actual Weight Frames (kg)		Actual Weight Videos (kg)	
	AVE	STD	AVE	STD	AVE	STD
Before Filtering	80.2	46.3	81.1	14.1	82.4	13.8
Limit Filter	78.7	14.4	79.2	14.1	81.0	14.0
Shape Filter	80.2	14.8	80.5	14.7	80.9	14.1
Combined Filters	80.5	14.4	80.8	14.3	80.4	14.1

Table 38: Performance of the piGUI System Estimating the Individual Weights of the Pigs in Group 2

Method Error Category (kg)	Before Filtering Count	%	Passed Shape Count	%	Passed Limits Count	%	Combined Count	%
$w_{est} < 0.5$ kg	724	9.7	372	19.0	514	16.5	301	19.3
0.5 kg $\leq w_{est} < 1$kg	634	8.5	275	14.1	430	13.8	226	14.5
1 kg $\leq w_{est} < 2$ kg	1114	14.9	487	24.9	767	24.6	410	26.3
2 kg $\leq w_{est} < 3$ kg	903	12.1	373	19.1	602	19.3	294	18.8
3 kg $\leq w_{est} < 4$ kg	584	7.8	214	10.9	337	10.8	156	10.0
4 kg $\leq w_{est} < 5$ kg	418	5.6	127	6.5	218	7.0	104	6.7
$w_{est} \geq 5$ kg	3114	41.6	109	5.6	246	7.9	71	4.6
Total Samples	7491	100.0	1957	100.0	3114	100.0	1562	100.0
$w_{est} < 2$ kg	2472	33.0	1134	58.0	1711	55.0	937	60.0

Group 3 contained all 170 video samples of female pigs. The result for the weight estimates of Group 3 can be seen in Table 39, with individual weights for the group presented in
Table 40.

Table 39: Performance of the piGUI System Estimating the Weight of Group 3

Filter Method	Estimated Weight Frames (kg)		Actual Weight Frames (kg)		Actual Weight Videos (kg)	
	AVE	STD	AVE	STD	AVE	STD
Before Filtering	78.9	32.0	77.0	8.7	77.5	9.2
Limit Filter	76.5	8.9	76.4	8.2	77.1	8.9
Shape Filter	77.7	8.2	77.6	7.9	77.5	9.1
Combined Filters	77.4	8.3	77.3	8.0	77.0	9.1

Table 40: Performance of the piGUI System Estimating the Individual Weights of the Pigs in Group 3

Method Error Category (kg)	Before Filtering Count	%	Passed Shape Count	%	Passed Limits Count	%	Combined Count	%
$w_{est} < 0.5$ kg	749	12.6	388	17.8	551	17.1	329	18.9
0.5 kg $\leq w_{est} < 1$kg	728	12.2	368	16.9	512	15.9	290	16.7
1 kg $\leq w_{est} < 2$ kg	1250	21.0	631	29.0	893	27.7	511	29.4
2 kg $\leq w_{est} < 3$ kg	876	14.7	401	18.4	616	19.1	327	18.8
3 kg $\leq w_{est} < 4$ kg	562	9.5	196	9.0	342	10.6	145	8.3
4 kg $\leq w_{est} < 5$ kg	311	5.2	113	5.2	168	5.2	90	5.2
$w_{est} \geq 5$ kg	1472	24.8	81	3.7	145	4.5	49	2.8
Total Samples	5948	100.0	2178	100.0	3227	100.0	1741	100.0
$w_{est} < 2$ kg	2727	45.9	1387	63.7	1956	60.6	1130	64.9

4.3.1.2 Discussion of Off-line Results

Coincidently, the unfiltered data obtained from Group 1 yielded the closest average group estimate of 79.6 kg to the actual group average weight of 80.3 kg (see Table 35 Before Filtering). However, the integrity of this estimate should be scrutinised as the weight deviation of the samples used to form this estimate was 41 kg when it should have been closer to 12 kg. This indicated that there was a large range and variability in the estimates used to form this average and therefore these errors should ideally be removed. Subsequently the filtering operations did successfully remove these erroneous samples. This can be seen in the drop in the weight deviation to a level that resembles the actual group weight deviation of around 12 kg (refer to the last three rows of STD in the 'Estimated Weight Frames' column of Table 35). This demonstrates how it is possible to obtain the correct group average weight from datasets where large weight estimation errors are present, it appeared that the

commercial system tested in *Chapter 8* worked on this merit (refer to the variability in weight estimates in Figure 142 between the piGUI system and the commercial system 'System-A').

The results in Table 35 also indicate that the frames containing information of the heavier pigs were rejected during the extraction process, which has impacted the ability to estimate the actual group average. This can be seen in the average of the 'Actual Weight Frames' column of Table 35 where the frames successfully extracted from the videos have formed an average weight of 79.3 kg; a difference of 1 kg from the actual group weight determined from each pig (80.3 kg). This difference was not surprising, as on average each video contained just 43 frames over a ~9 second period and during this time the pig was required to conform to a rough range of a particular pose in order for its shape and body measurements to be extracted. Only the information that made it through these loose constraints during extraction could be used to form the 'Actual Weight Frames' and the systems weight estimates. In this case the videos of the heavier pigs contained a large amount of redundant frames and data which was excluded at the extraction stage. Subsequently the filters could only refine the data that were available to them; data which were inclined to a group average of 79.3 kg and a weight deviation of 12.2 kg in Group 1 after the extraction process was complete.

This system behaviour is not too concerning as in practice far more time than nine seconds will be available for the system to extract good quality data from each animal to form group averages. However, it does highlight a limitation of the method if only a limited amount of quality data are available of certain animals.

The Group 2 results indicate that the heavier pigs which were missed during the extraction procedure were male. The actual group average of the males was 82.4 kg, while the average based on the frames differed by 1.3 kg at 81.1 kg.

The performance of the filters can be seen in the first column ('Estimated Weight Frames') of Table 35, Table 37 and Table 39 rows 2 to 4. The combined shape and limit filtering method has performed very well over all three groups, as the actual average weight of the frame samples which made it through the extraction stage ('Actual Weight Frames') and passed through this filtering method resulted in estimates with errors no greater than 0.6 kg from the actual group average weights determined by conventional means.

Group 3 containing the female pigs represented a case where 'good quality' information was available for the system to extract and assess. Here actual group average weight was 77.5 kg while the frame based average was similar at 77.0 kg. Subsequently, the filter successfully passed pigs in all weight ranges representative of those in the group and after the combined filtering processes the group. Consequently, after the combined filtering processes, the average group weight estimate differed by only 0.1 kg from the actual group average weight.

The weight deviation of Groups 1, 2 and 3 was calculated within ±1 kg for the combined filtering process indicating that the system also has strong potential be used to determine the group weight deviation. Although, in practice the duration and frequency in which each pig is captured may vary and impact weight estimates so

on-farm validation is required. The individual weight assessment of Groups 1, 2 and 3 indicate that when using the combined shape and limit filter the piGUI system can obtain 60% or more of the weight estimates of finisher pigs within ±2 kg while estimation errors greater than ±5 kg are reduced to less than 5%.

4.3.2   On-Farm Trial Results

More extensive testing was undertaken at the piggery to assess the precision of the programs weight estimates for both individual pigs and groups of pigs.

4.3.2.1   Group Growth

Results for the group average weights are presented in this section over the period between the 24/1/11 and the 15/2/11. During this period the animals were weighed seven times using the electronic livestock scale. Figure 100 shows the actual group average weight in conjunction with the piGUI systems daily group average estimate, which was formed by averaging the weight estimates which passed through the combined filter on each day. To show a direct comparison between scale-based and vision-based estimates the average weight of the group determined by the vision system on the days other than these seven days have been removed. The standard growth curve derived from Carr (1998) has been projected from the first actual weight recorded over the period (see Appendix E).
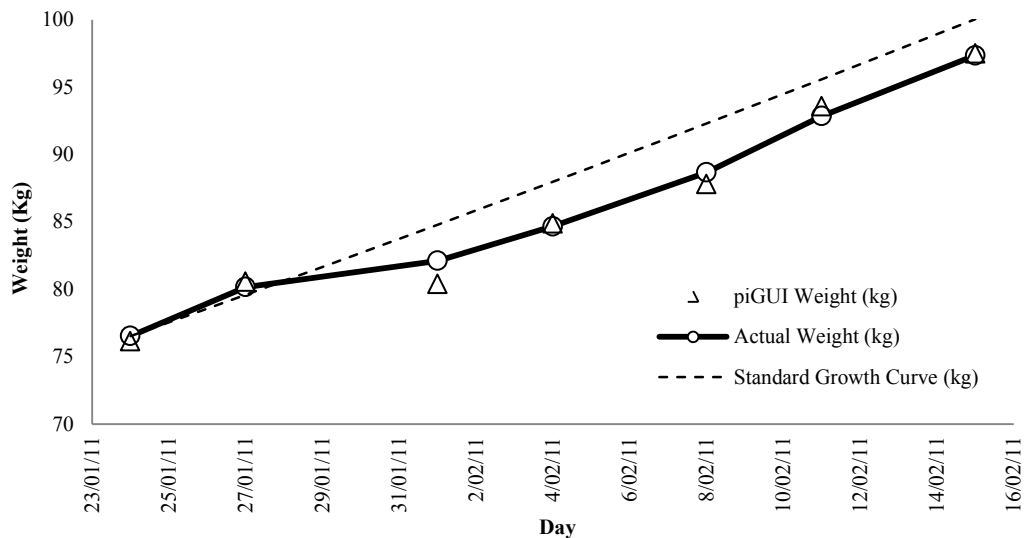
Figure 100: Comparison between the Estimated Group Average Weight determined by the piGUI System and the Actual Weights Obtained from the Electronic Scale

The errors between the estimates and actual weights are shown in Table 41 for Figure 100.

149

Table 41: Estimated and Scale Weight Data Obtained from the Trial; Values Coincide with Figure 100

Date	Weight (kg)			Deviation (kg)		
	Vision Estimate	Scale	Error	Vision Estimate	Scale	Error
24/1/11	76.2	76.6	-0.4	4.14	4.80	0.66
27/1/11	80.6	80.2	0.4	3.47	5.04	1.57
1/2/11	80.4	82.1	-1.7	4.53	4.74	0.21
4/2/11	84.9	84.7	0.2	7.17	5.25	-1.92
8/2/11	87.8	88.7	-0.9	5.10	5.10	0.00
11/2/11	93.6	92.9	0.7	6.30	6.19	-0.11
15/2/11	97.5	97.4	0.6	N/A	5.51	N/A

During the on-farm trial, the precision of the piGUI system was within ±1 kg error of the actual group average weight on six of the seven days when an actual group weight was obtained (see Table 41). The worst error recorded on 1/2/11 was also possibly due to three pigs in the group jumping over a pen gate into an adjacent pen, sometime between the 1/2/11 and 4/2/11. The temporary removal of these three animals may have contributed to the 1.7 kg error in group weight.

The ability of the vision system to determine the weight deviation of the group was also calculated using the data obtained from the vision system each day. The system determined the deviation of the group within ±2 kg on all days when the actual weight deviation was recorded.

4.3.2.2 *Individual Growth*

As the pigs were marked with livestock paint, their individual growth could be recovered by matching the sample images taken of them with their weight and body measurement information. This was carried out for all days when an actual weight observation was made, except for 15/2/11, as on this day the unique markings were unrecognisable due to wet conditions. Figure 101 of 'Pig 7' shows that the growth of the individual pigs was not as smooth as one might expect, although it does bend its way according to the standard growth curve derived from Carr (1998) which has been projected from the first actual weight recorded over the period.
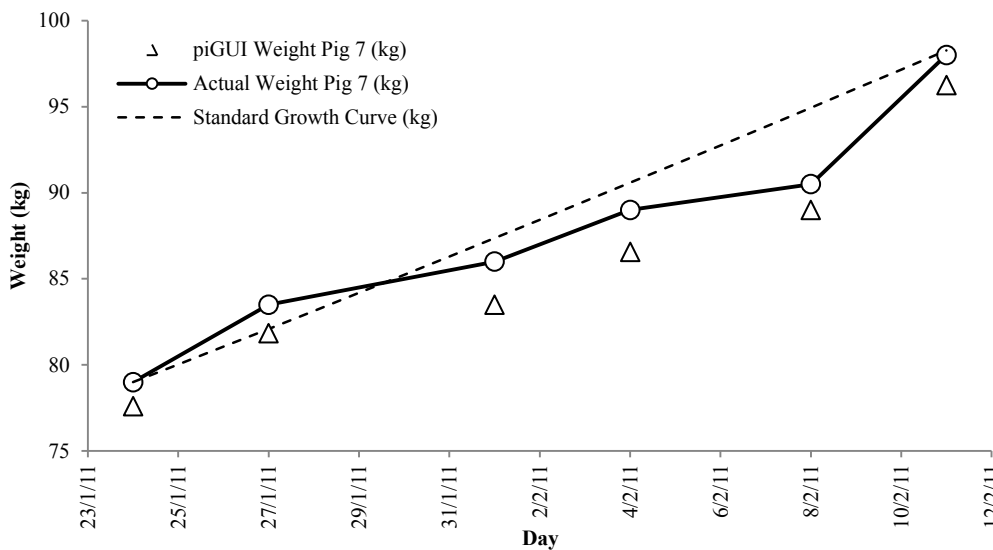
Figure 101: Actual Growth of Pig 7 and its Estimated Weight According to the PiGUI System

The piGUI system recorded the growth of Pig 7 reasonably well as it follows its actual growth (see Figure 101). However, on average the systems estimates are 1.9 kg less than the actual growth recorded. This indicates that the system needs to be refined further to improve the growth estimation of individual pigs to practical levels.

4.4 CONCLUSIONS

The system performed well during both the off-line and on-farm trial in comparison to the conventional method. During off-line testing, weight estimates were obtained within 2.5% relative error of the actual group average weight. During the farm trial, the precision of the piGUI system was within ±1 kg error of the actual group average weight on six of the seven trial days where comparative information was available. This indicated that piGUI system was recording growth to sufficient practical accuracy. Relative weight estimation errors were within 2.5% of the actual weight on all seven of the days during the on-farm trial reinforcing the results obtained during the off-line trial.

The weight deviation of the group was also estimated well, as during off-line testing the weight deviation of all three groups was estimated within ±1 kg using the combined filtering process. During the farm trial the vision system estimated the weight deviation to within ±2 kg.

Discrepancies in the weight deviation recorded by the system indicate that there is potentially bias occurring. This is a result of either favouritism toward certain animals from the systems filtering operations or the availability of data of each pig from their attendance in the sampling area of the pen. Therefore, further studies involving the individual identification of animals within the sampling region of the pen may be necessary to determine whether these types of bias in estimates can occur. Refining the filter settings to obtain optimum acceptance rate of weight samples may overcome the former of these two potential causes of precision loss.

Sixty percent or more of individual weight estimates generated by the vision system were within ±2 kg of the finisher pigs' actual weight, while estimation errors greater than ±5 kg were reduced to less than 5% using the combined shape and limit filtering method. The growth recorded by the system of the individual pigs was similar to their actual growth. However, it is apparent that adjustments are required to improve the accuracy of the system in this area. To counteract this type of error, different equations might be adapted to suit to the shape or body measurements of particular animals. A commercially feasible method to determine individual identities of the pigs is also required (such as RFID) so that individual growth data can be determined efficiently from within the group.

Chapter 5

Determining the Growth of Grower Pigs in Commercial Facilities Using Machine Vision: Off-line and On-line Results

Banhazi, T. M., **Tscharke, M.**, Ferdous, W. M., Saunders, C. &Lee, S.-H. (2009).Using image analysis and statistical modelling to achieve improved pig weight predictions. In *The Bi-annual Conference of the Australian Society of Engineering in Agriculture (SEAg 2009)*, p. CD publication. (Eds T. M. Banhazi and C. Saunders). Brisbane, Australia: Australian Society of Engineering in Agriculture.

Banhazi, T. M., **Tscharke, M.**, Lewis, B. &Broek, D. (2009). Practical and continuous measurement of feed intake and pig weight. Final report for the PORK CRC. (108 pages). Adelaide, Australia.

Banhazi, T. M., Lewis, B. &**Tscharke, M.** (2011). The development and commercialisation aspects of a practical feed intake measurement instrumentation to be used in livestock buildings. *Australian Journal of Multi-disciplinary Engineering* 8(2): 131-138.

ABSTRACT

A vision system was developed to determine the live weight of pigs from their body measurements non-invasively. This chapter presents off-line and on-farm results obtained from the piGUI system while estimating the weight of grower pigs. Off-line results indicated that the group average weights of the grower pigs could be estimated within ±1.3 kg error and group weight deviations within ±1.2 kg error. More than 65% of all the estimates of individual pigs were within ±2 kg of their actual weight, while estimates greater than ±5 kg in error were restricted to less than 5% of all estimates. During the on-farm trial the system recorded the growth of four successive batches of grower pigs at a commercial piggery. Subsequently, the systems practical potential in helping to diagnose undesirable conditions was founded, as according to the system extreme summer temperatures decrease the activity of the animals and have an adverse effect on growth.

5.1 INTRODUCTION

Monitoring and managing livestock growth is desirable as growth information can be used to increase the efficiency and productivity of farms. Specifically, growth information can be used to (i) optimise market sale date (Korthals, 2001), (ii) determine future feed, space and transport requirements (Petherick, 1983; Pastorelli *et al.*, 2006), (iii) identify disadvantaged animals which display periods of poor weight gain (Maltz, 2010), (iv) minimise the competitive behaviour between animals by sorting them based on weight (Morrison, 2004), and (v) optimise and standardise the production process via monitoring and analysing the animals' response to different feed and environmental scenarios (Green and Whittemore, 2005; Frost *et al.*, 1997; Doeschl-Wilson *et al.*, 2005; Whittemore and Schofield, 2000). Addressing these issues can increase the profitability of livestock production and improve the welfare of the animals concerned (Niemi *et al.*, 2010; Black *et al.*, 2004; Morrison, 2004)

Conventional methods used to determine the growth of livestock are time consuming and pose a safety risk to both the animals and farm workers involved (Criddle, 2001; Erkal *et al.*, 2008; Brandl and Jørgensen, 1996). Consequently, automated techniques that do not require physical contact between the weigh scale and animal, and the worker and animal, are preferable. Machine vision systems present an effective non-invasive solution to these problems while maintaining the ability to estimate the live body weight of livestock to practical precision (Schofield, 1990; Green *et al.*, 2003; Tscharke and Banhazi, 2011).

A machine vision system was developed to determine the daily average weight of groups of pigs so that their growth could be monitored (Banhazi *et al.*, 2011b). This chapter reports further findings as determined from the data collected in Banhazi *et al.* (2011b) and additional data collected from an commercial Australian piggery in relation to growth, temperature and animal activity.

5.2 MATERIALS AND METHODS

A camera (Logitech Quickcam Pro 9000, Logitech, Quarry Bay, Hong Kong) a computer and Matlab software (MathWorks, Inc., Natick, Massachusetts, USA) were interfaced to form a machine vision system to estimate the live weight of grower pigs. Routines within the software automatically searched the image, determined pig shapes and extracted various body measurements. Other routines were then used to estimate and validate the pigs' weights based on their shape and body measurements.

5.2.1 Experimental Setup and Location of the PiGUI System

5.2.1.1 On-Farm Validation

The on-farm validation involved installing and testing the vision system at a commercial facility where it was left to operate continuously. During this time the system observed a section of a pen which housed between 100 and 165 pigs. The installation location of the system within the pen is shown in Figure 102. When a successful weight assessment took place, key information was recorded including: (i) an image of the animal with an overlay of contour shape detected, (ii) the body

measurements used to estimate the weight, (iii) the weight estimate and (iv) the time and date. Feed information was also collected during the trial period and can be found in Banhazi *et al.* (2011a). The location of the feed-meter can be observed in the yellow dashed rectangle in Figure 102. The computer was accessed periodically using a remote desktop connection and the information recorded was downloaded. Using this remote connection link, the status of the computer and software was monitored, and revised versions of the software were uploaded and tested.

Groups of pigs are currently weighed (at most) a few times during the production cycle, so determining daily weight estimates of groups of pigs would be a marked improvement. The system did not focus on obtaining a weight estimate of every pig within the pen. Instead a representative sample was collected and used to estimate the average weight of the group of pigs. Hence, the systems main focus was on the quality of the weight assessments rather than quantity of assessments made.
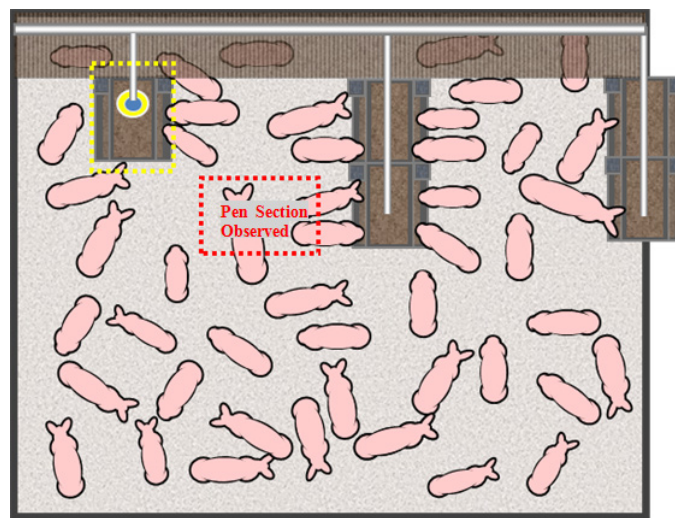
Figure 102: The Experimental Setup at the Commercial Facility

5.2.1.2   Off-line Validation

The off-line validation involved an analysis of video data collected of grower pigs between 25 and 65 kg from a commercial research piggery. The videos were taken at 1200x1600 resolution and at a height of 2 m from the lens of the camera to the ground. Directly after each video was captured, pigs were weighed to the nearest half kilogram in a pig weigh crate (Ruddweigh, Pig Weigh crate ±1%). These video files were then subjected to off-line testing to determine the relative precision of the system for both individual and groups of grower pigs.

5.3   RESULTS AND DISCUSSION

5.3.1   On-Farm Trial Results

In a six month period between July 2009 and January 2010, approximately 16,000 images and weight samples were collected using the piGUI system at the facility. During this time four batches of grower pigs were recorded as they grew in the range of 30 to 60 kg. Staff kindly provided the actual weights of the +100 pigs within the pen on five occasions. As staff resources were limited, the actual group weight

information was used as a reference in conjunction with a standard growth curve to estimate the performance of the system within the batches. The standard growth curve equation (found in Appendix E) was first re-arranged to determine the age of the group of pigs at their actual weight. It was then used to project the weight from this age over the days of the trial period.

5.3.1.1 System Performance

The ability of the system to work automatically under commercially realistic conditions was assessed. During the trial period the system successfully determined, when a pig was inside the field of view of the camera, its contour, its body measurements and its weight estimate. Figure 103 demonstrates the system's ability to recognise and assess pigs of different sizes and also highlights the size variation within the pen.
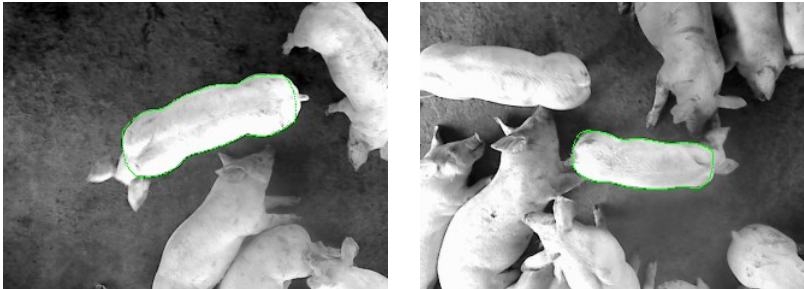
Figure 103: Difference in Size of Pigs Captured in Consecutive Days within the Same Pen

Many of the images collected illustrate the variation caused by natural lighting conditions and difficulties caused by dirt on the pigs' backs and non-uniform skin colour. Figure 104(a) highlights the difficulty in obtaining the contour of a spotted pig that has similar skin colour to the background. Figure 104(b) illustrates the system correctly identifying the contour in non-uniform lighting conditions.
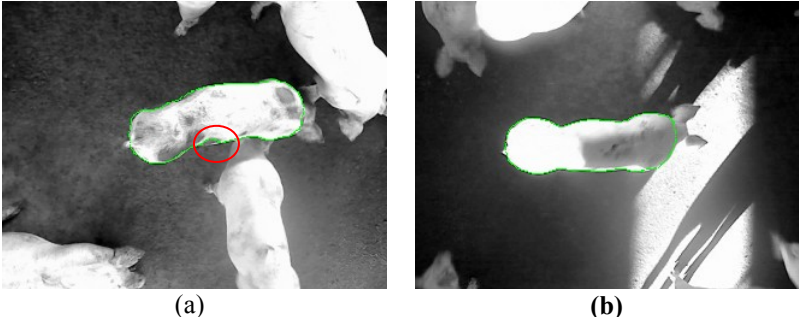
(a)   (b)
Figure 104: Images Recorded by the System; (a) A Spotted Pig with Partial Error Circled; (b) Correct Capture in Largely Variable Lighting

Occlusion was also a problem in this environment. Figure 105 shows the successful capture of the pig's body contour which has avoided any occlusion with surrounding animals.
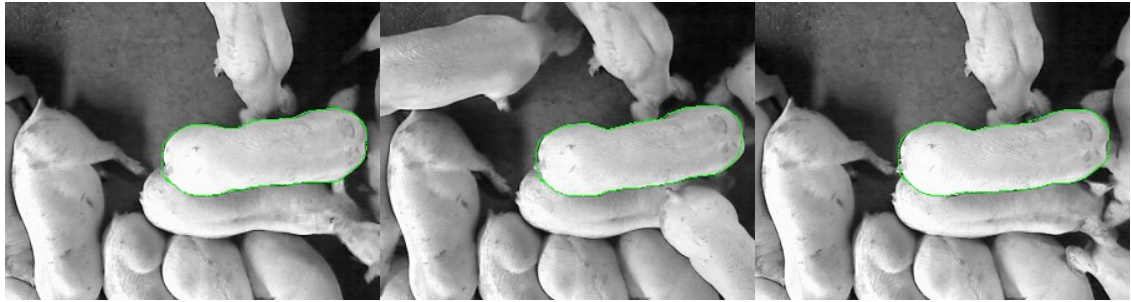
Figure 105. Sequence of Successful Captures Avoiding Occlusion of Surrounding Pigs

On occasion the system returned false positives where the animals' contour had not been recognised correctly. This was largely a consequence of the animal's posture and environmental factors. Despite these issues the piGUI system managed to automatically identify and extract measurements of the pigs' bodies out of the images and recorded growth over the four trials.

5.3.1.2 Growth Records of Batches of Grower Pigs

During testing the system was in a continuous state of development. Consequently, alterations were made to the software based on the data output obtained during the four grower growth cycles. The data for the last three batches of pigs presented in the following sections can be found in Banhazi *et al.* (2011b). However, the data found here has been fitted to a standard growth curve obtained from literature (Carr, 1998) (see Appendix E). Thus, the growth recorded by the system for these batches is revisited in relation to standard growth.

5.3.1.2.1 Batch 1

The growth of the first group of grower pigs is shown in Figure 106. Piggery staff recorded the average weight of the group of pigs as 42.6 kg on 12/8/09. This average was determined by weighing half of the ~100 pigs using an electronic scale. The standard growth curve was then fitted to the data point corresponding to the actual weight in order to make comparisons with the system.
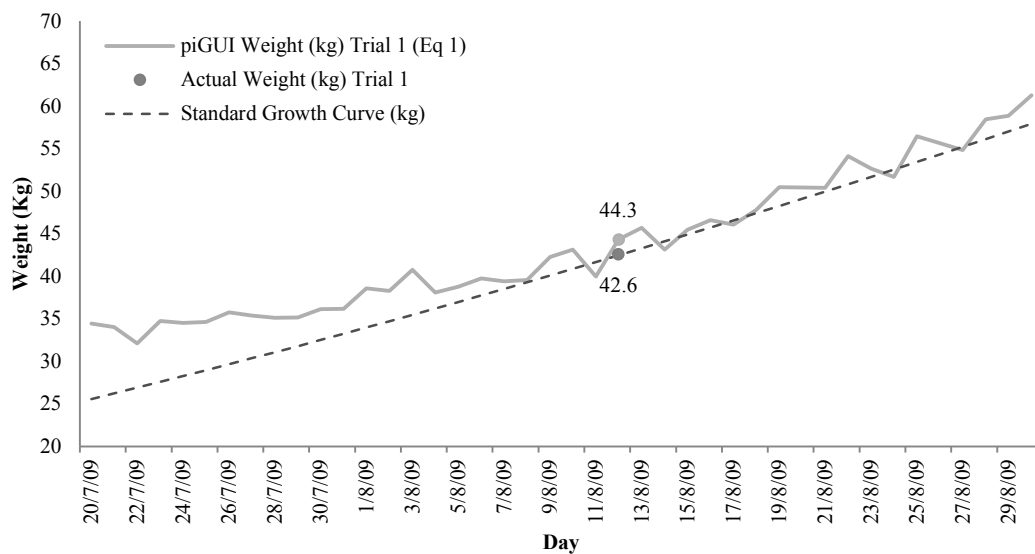
Figure 106: Comparison between Standard Growth and the Growth Recorded by the PiGUI System for the First Batch of Grower Pigs

157

As Figure 106 illustrates, the daily average weight estimate for the group recorded by the piGUI system compared reasonably well with the standard growth curve from 4/8/09 onward. This was encouraging considering that, on average, only 26 samples were being recorded of the group daily due to a software-related problem. This small quantity of samples was believed to be responsible for the noisy (jagged) appearance of the data. The growth before 4/8/09 was also of interest as it tended to be higher than the standard growth curve.

5.3.1.2.2 Batch 2

While the software was being debugged and modified, four actual group average weights were obtained by staff for a second batch of 165 pigs. The software was updated and restarted remotely on 5/10/09 after the software problem was resolved.
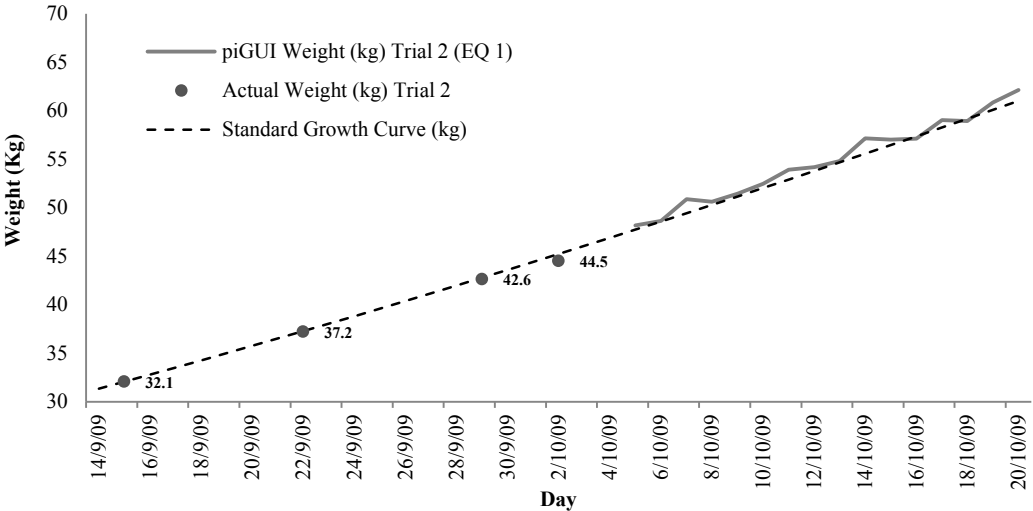
Figure 107: Comparison between Standard Growth and the Growth Recorded by the PiGUI System for the Second Batch of Grower Pigs (Banhazi *et al.*, 2011b)

The standard error curve in Figure 107 was fitted to the first actual group weight obtained. The three subsequent actual group weights were within 0.8 kg of the standard curve indicating that the standard curve was effective at describing the growth data relative to days of age. As in the previous trial, the system managed to record the weights of the second batch closely in respect to the standard growth curve (Figure 107). The modifications to the software had successfully increased the average samples collected daily to 188 samples and the growth data recorded appeared smoother. The software was then left operating to record the growth curve of subsequent batches of pigs.

5.3.1.2.3 Batch 3

The third batch also followed the standard curve reasonably well (Figure 108). However, up to the 1/11/09 and after the 16/11/09 there was a noticeable deviation away from the standard curve. Consequently, the software settings were revised to identify whether a problem was present.

158
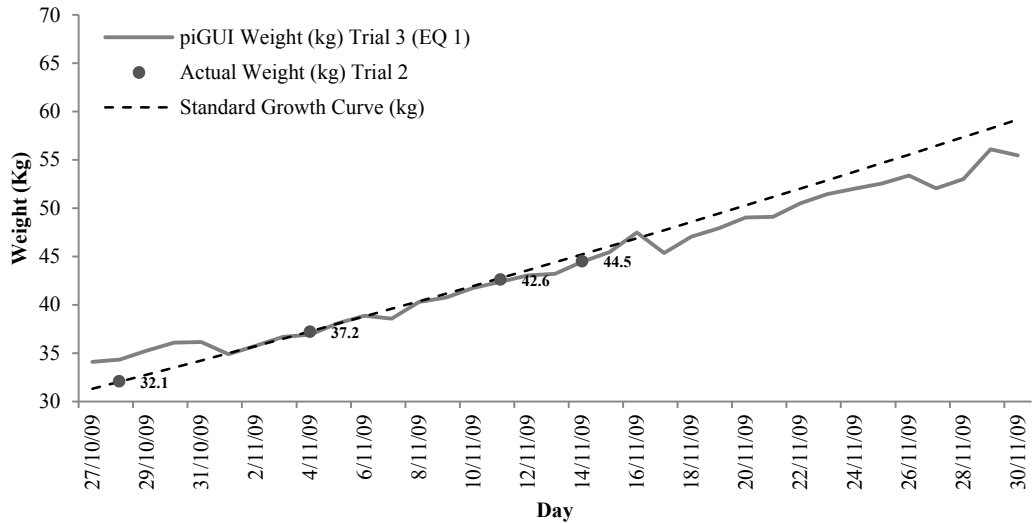
Figure 108: Comparison between Standard Growth and the Growth Recorded by the PiGUI System for the Third Batch of Grower Pigs (Banhazi *et al.*, 2011b)

At the start of the third batch, the system was set to record pigs weighing between 30 and 100 kg. To determine whether the convergence and divergence was caused by the software excluding weights above or below these limits, the distribution of weight data collected over these periods was evaluated. Figure 109 shows the distribution of weight samples acquired over the first days of the trial period to the 4/11/09.
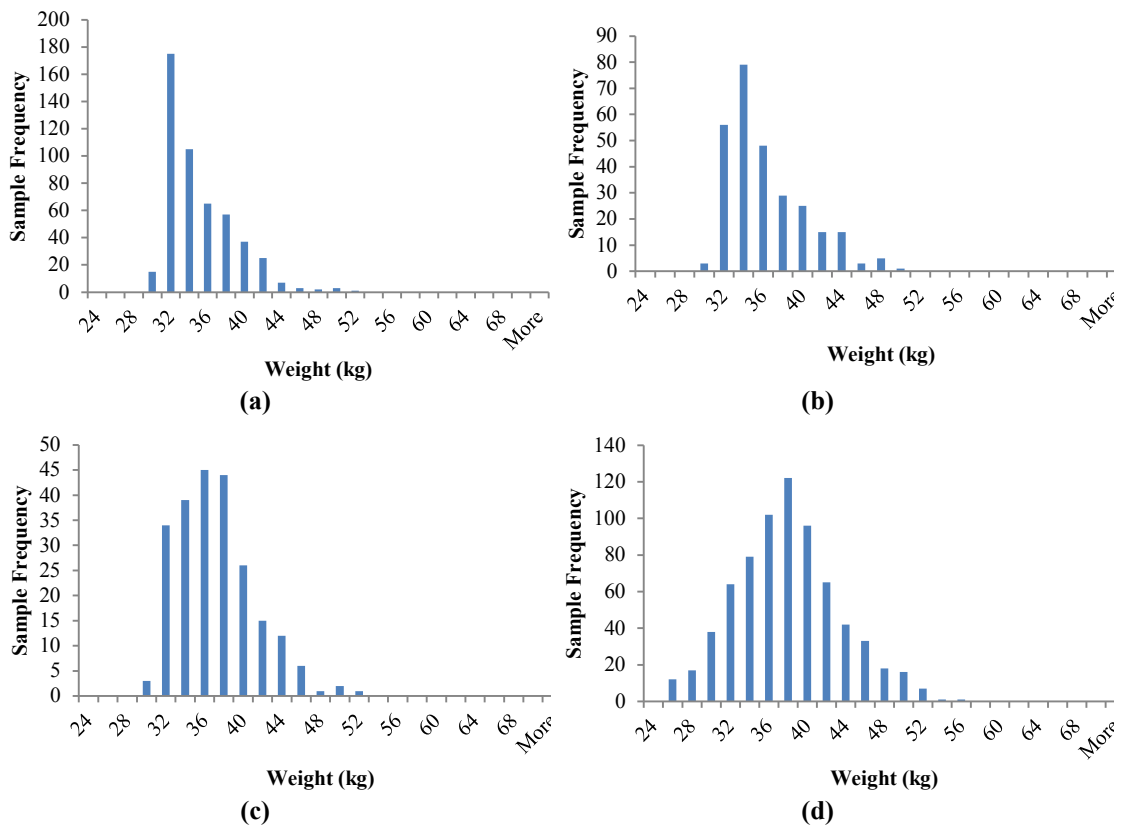
Figure 109: Weight Distribution According to the Weight Samples Acquired on: (a) the 27/10/09 (b) the 29/10/09 (c) the 31/10/09 and (d) the 4/11/09.

159

Figure 109 (a) through to (c) show a clear bias in the weight distribution of the group of pigs as a direct result of the software excluding pigs weighing less than 30 kg from analysis. As a result, on the 1/11/09, the setting was changed to include pigs weighing more than 25 kg. The result was a normal distribution of weight estimates (shown in Figure 109 (d)) which had a mean value coinciding closely with the standard growth curve (Figure 108).

The weight distributions recorded on the days after the 16/11/09 were also observed to identify whether a similar cause of bias was responsible for the deflection away from the standard curve later in the trial. There were no obvious issues with the distribution of the acquired data (Figure 110).
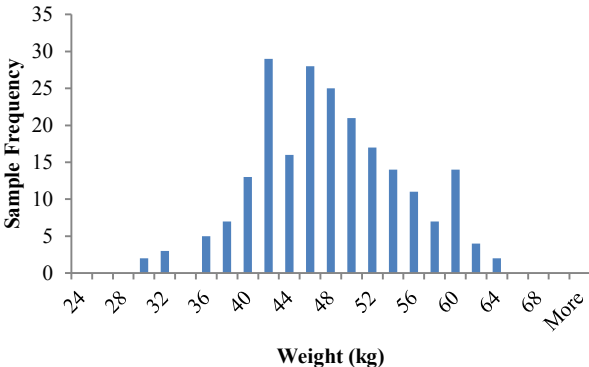
Figure 110: Weight Distribution According to Acquired Weight Samples on (a) the 18/11/09.

Therefore, the cause of the growth deflection from the 16/11/09 onward was unknown.

5.3.1.2.4 Batch 4

During the fourth batch the system estimated the group's weight within 1.3 kg of the standard curve up to the 1/1/12 indicating that the bias experienced in the first and third batches was no longer having a dramatic effect. An unknown problem caused the computer to shut down on the 1/1/12 which was rectified on the 15/1/12. The system then operated without fault until the 27/1/12 when the pigs were removed.
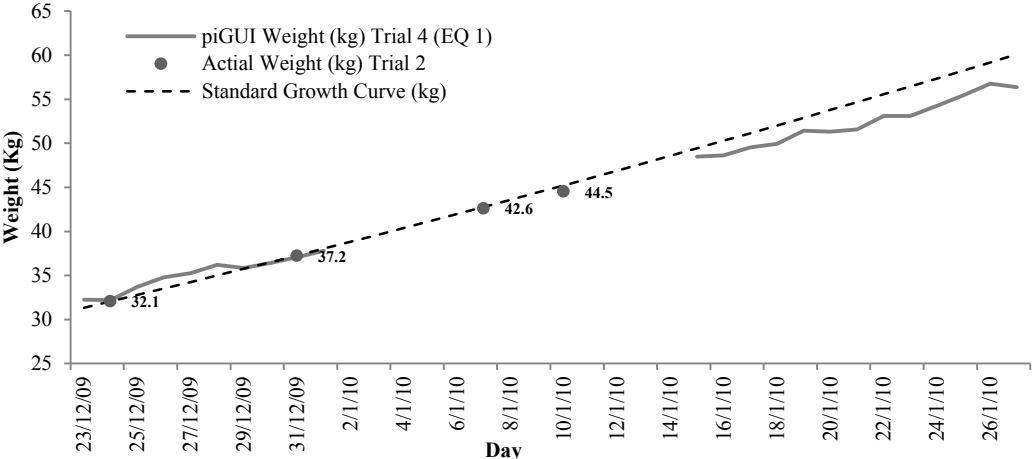
Figure 111: Comparison between Standard Growth and the Growth Recorded by the PiGUI System for the Fourth Batch of Grower Pigs (Banhazi *et al.*, 2011b)

160

A clear deviation could be seen away from the standard curve in similar manner to that experienced in the third batch of growers. The temperature was investigated as the growth recorded of the third and fourth batches of pigs was obtained during the summer months.

5.3.1.3   *Possible Temperature Effects on Batches of Grower Pigs*

In this study, the temperature information was obtained from a weather station located a distance of 8 km from the piggery (Bureau of Meteorology, 2010). The maximum temperature information was compared to the growth data acquired during the third and fourth batches. This is graphically shown in Figure 112.
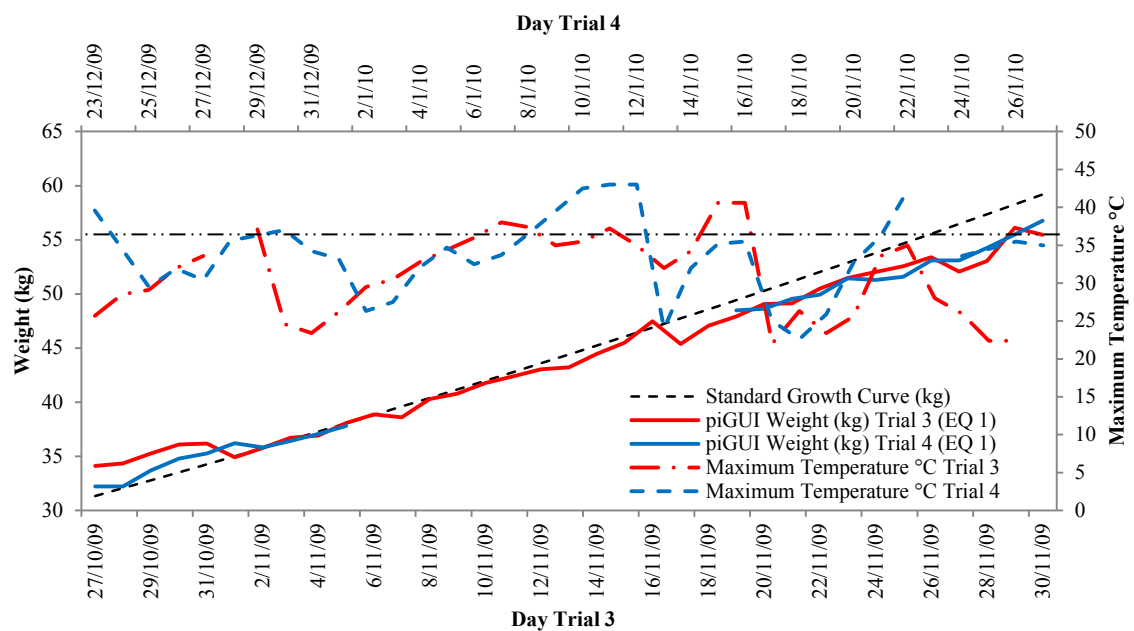
Figure 112: Maximum Temperature and Growth during the 3rd and 4th Batches of Pigs

Coincidently, the maximum temperature profiles between the third and fourth batch were remarkably similar when the pigs of both batches were at the same stage of growth (Figure 112). The piGUI system also recorded a similar deflection away from the standard curve during both of these batches. However, the growth recorded by the system for the second batch of grower pigs followed the standard growth curve well. The following figures (Figure 113 and Figure 114) compare the growth and temperature results of the second and third batches and the second and fourth batches respectively.

161
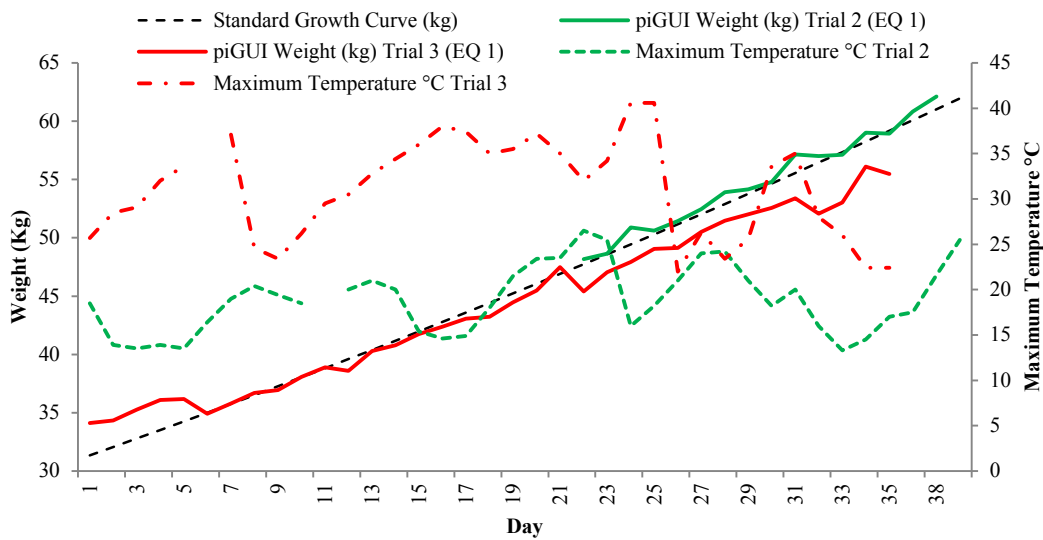
Figure 113: Maximum Temperature and Growth during the 2nd and 3rd Batches of Pigs
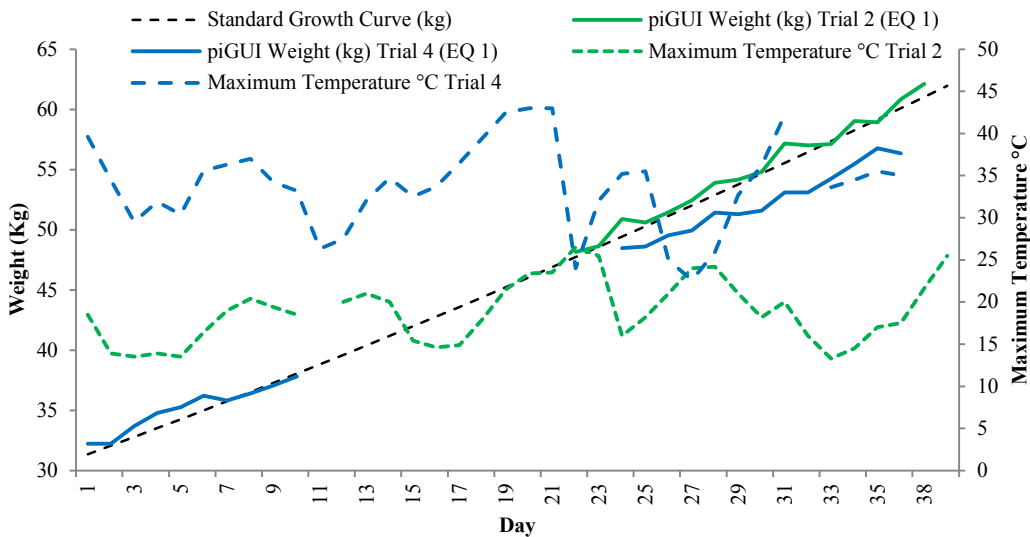
Figure 114: Maximum Temperature and Growth during the 2nd and 4th Batches of Pigs

Figure 113 and Figure 114 demonstrate that the pigs in the second batch were exposed to far cooler temperatures (average maximum daily temperature of 18.9°C) than the third and fourth batches. The growth encountered during the second batch followed the standard growth curve closely, however, the third and fourth batches of pigs experienced average temperatures of 31°C and 33.8°C respectively and a negative deflection in growth occurred (see Figure 113 and Figure 114). This appears to indicate that the hotter summer temperatures played a role in the poor growth performance recorded in the third and fourth batches. Supporting evidence lies in the fact that the temperature was above 35°C for consecutive days immediately prior to the growth deflection. With the third and fourth batches of pigs experiencing seven and five consecutive days of temperatures greater than 35°C, respectively, with three of the five days in the fourth batch also greater than 42°C. Therefore, the deflection in growth data acquired by the system is most probably the result of prolonged heat stress. Alternatively other factors related to hotter conditions may have indirectly affected the health and growth of the animals.

162

Heitman and Hughes (1949) studied the effects of temperature and humidity on pig growth. In their study the respiration and pulse rate of grower-finisher pigs were monitored in relation to different temperature and humidity scenarios. Temperatures greater than 38°C caused noticeable distress to the animals when housed in a room with a dry floor. Wetting the floor of the room had a cooling effect and subsequently the animal's distress only became noticeable at higher temperatures (46°C). It was determined that pigs in the grower range (between 32 and 65 kg) grew at the optimal rate (minimum feed consumption and maximum weight gain) at temperatures around 24°C. The feed utilisation and weight gain of the pigs decreased either side of this average temperature.

More recent studies indicate that voluntary feed intake begins to reduce at temperatures greater than 25.4°C (Huynh *et al.*, 2005). These figures are consistent with the poor growth of the pigs recorded by the system in this study where consecutive days of temperatures greater than 35°C were experienced. Notably, prolonged exposure to high temperatures also raises concerns about the welfare of the animals as, during Heitman and Hughes (1949) study, a 103 kg pig lost 8 kg and died after being exposed to temperatures of 38°C for 5 consecutive days in a room with a dry floor.

5.3.1.4 *The Activity of Grower Pigs in Relation to Temperature*

As the piGUI system required the pig to be standing or moving around the vicinity of the feeders to make a sample estimate, the system was evaluated to see whether the number of samples it recorded daily could be used to determine the level of animal activity. The total numbers of samples collected daily were then compared to the maximum daily temperature to see whether temperature and activity were related. The activity versus temperature relationship is shown in a scatter plot in Figure 115 for the third and fourth batches of grower pigs.
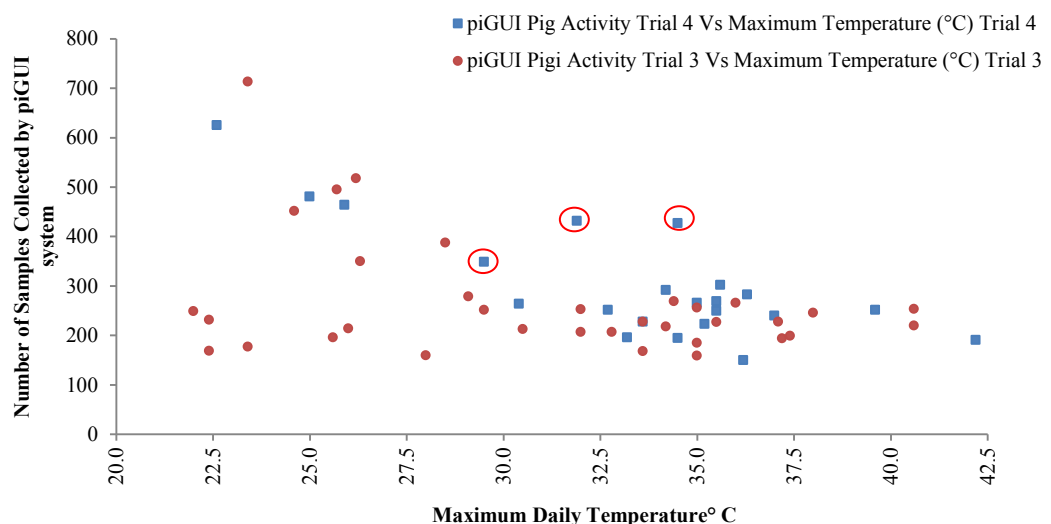
Figure 115: Comparing the Total Number of Samples Recorded by the PiGUI System Daily (Activity) to the Maximum Daily Temperature of the 3rd and 4th Batches of Grower Pigs

A spike in the number of samples collected by the piGUI system occurred on the days during the third and fourth batch when the temperature was approximately 23

degrees Celsius. A similar optimum room temperature was specified for the grower weight range by Heitman and Hughes (1949). The activity shown in Figure 115 also tends to decrease with increasing temperature from 23 degrees onwards. This is consistent with other studies which report that lying behaviour increases with temperature increases (Aarnink *et al.*, 2006). Heitman and Hughes (1949) state that at temperatures greater than 26°C pigs are more likely to lie on the cooler concrete flooring and conserve energy rather than move around. Blackshaw and Blackshaw (1994) found that in temperatures greater than 35°C, 93.9% of grower pigs lay in the shade. Spikes in activity recorded during the batches also coincide with gaps between periods of hotter weather as Figure 116 below illustrates. However, outlying peaks in activity on the 24th, 25th and 26th of December were experienced (refer to circled data points in Figure 115 and Figure 116). This is possibly due to the animals exploring their surroundings or fighting after their introduction to the pen on the 23rd of December (Stukenborg *et al.*, 2010).
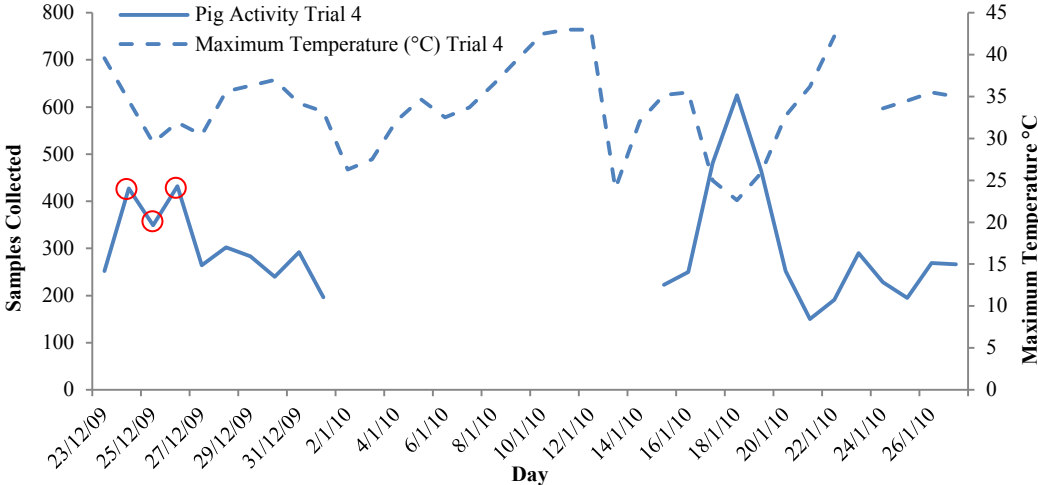
Figure 116: Comparing the Total Number of Samples Recorded by the PiGUI System Daily (Activity) to the Maximum Daily Temperature of the 4th Batch of Grower Pigs

As the pigs' activity was monitored in close proximity to the location of the feeder, an investigation into the relationship between the activity levels and feed consumption was performed. Results published in Banhazi *et al.* (2011a) show that temperature and level of activity do appear to relate to each other, and to feeding behaviour and consumption during the fourth trial (see Figure 117 below).

164
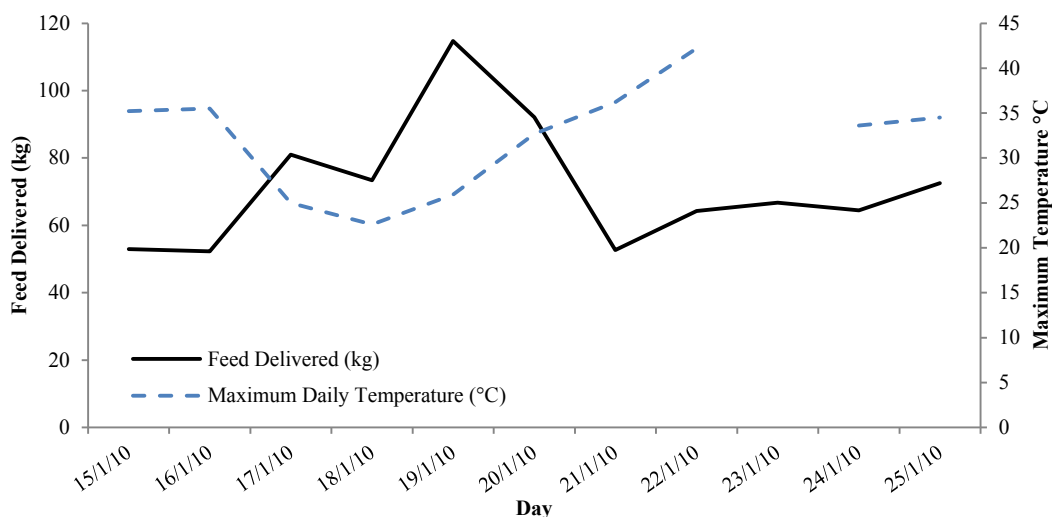
**Figure 117: The Amount of Feed Delivered vs. Thermal Conditions at a Commercial Piggery
(Banhazi *et al.*, 2011a)**

Consequently, the deviation away from the standard growth curve is probably the result of the animals consuming less feed in a hotter environment. Further large scale validation of the instrument would help confirm and quantify these effects.

5.3.2   Off-line Trial Results

Modifications to the software were carried out after testing to further fine-tune the instrument to enhance the group weight estimates. Videos of pigs in different weight ranges were then acquired so that the system's performance could be simulated off-line. A total of 180 videos of male and female grower pigs were obtained. A total of 6304 contour shapes were automatically extracted from these videos. After each contour was extracted it was subjected to two filtering processes to determine whether it was satisfactory to form a weight estimate, or should be discarded. Consequently, the data that passed through the filters gave an indication of the performance of the filtering methods and, more importantly, the expected performance of the system when tested on-farm. Thus, the system's ability in determining both the weight of individual grower pigs and groups of grower pigs was evaluated using this filtered data.

The videos were broken into three groups:

Group 1: Female and male pigs (all 180 videos)
Group 2: Male pigs (103 videos)
Group 3: Female pigs (77 videos)

The weight deviation was also calculated for the groups as it may be useful for gauging when it is appropriate to sort the animals into weight classes. The grower pigs analysed weighed between 25 and 65 kg. The shape filter settings were set to 1.5, 2.6 and 3 deviations and the limits filter setting was set to 80%.

165

5.3.2.1   Individual and Group Average Weights

Group 1 contained all 180 video samples of female and male pigs. The vision systems ability to estimate the group average weight using different filtering methods is shown in Table 42.

Two different 'actual' group average weights were calculated using the weight information obtained from the electronic scale and videos. The first group's average weight (AVE) can be found on row one and contains the unfiltered data 'before filtering' (see Table 42 under the column 'Actual Weight Videos'). This group-average weight has been determined by conventional means: dividing the group's total weight by the number of pigs in the group (180). However, during operation, the vision system uses a different method to form the group average weight as the system relies on the frames sampled from the group to make an estimate. Consequently, a second group average has been formed to demonstrate the information that was available to the system after the extraction process. This involved summing the actual weight of the pig in each extracted frame sample and then dividing this value by the total number of frames extracted (refer to column Actual Weight Frames). Notably, this average may yield a different result compared to the actual group average depending on how many frames of each pig were sampled and what their weight was. The different filtering operations then selected sample frames that would yield a good result from the total pool of extracted frames (rows 2 to 4).

Table 42: Performance of the PiGUI System Estimating the Weight of Group 1

Filter Method	Estimated Weight Frames (kg)		Actual Weight Frames (kg)		Actual Weight Videos (kg)	
	AVE	STD	AVE	STD	AVE	STD
Before Filtering	48.5	29.2	45.5	12.7	45.3	12.4
Limit Filter	44.2	12.4	44.4	12.7	45.5	12.4
Shape Filter	45.8	12.4	45.9	12.6	46.3	12.3
Combined Filters	45.3	12.4	45.4	12.6	46.4	12.4

The errors attributed to the samples which passed through the filtering processes are categorised in Table 43. These errors are based on the difference between the weight estimate for a frame-sample and the actual weight of the pig as recorded from the electronic scale.

Table 43: Performance of the piGUI System Estimating the Individual Weights of the Pigs in Group 1

Method	Before Filtering		Passed Shape		Passed Limits		Combined	
Error Category (kg)	Count	%	Count	%	Count	%	Count	%
$w_{est} < 0.5$ kg	989	15.7	484	24.4	869	20.4	455	24.6
0.5 kg $\leq w_{est} < 1$kg	883	14.0	410	20.7	778	18.3	391	21.2
1 kg $\leq w_{est} < 2$ kg	1368	21.7	592	29.9	1217	28.6	566	30.6
2 kg $\leq w_{est} < 3$ kg	784	12.4	268	13.5	660	15.5	249	13.5
3 kg $\leq w_{est} < 4$ kg	463	7.3	129	6.5	344	8.1	110	6.0
4 kg $\leq w_{est} < 5$ kg	247	3.9	56	2.8	146	3.4	46	2.5
$w_{est} \geq 5$ kg	1570	24.9	42	2.1	237	5.6	30	1.6
Total Samples	6304	100.0	1981	100.0	4251	100.0	1847	100.0
$w_{est} < 2$ kg	3240	51.4	1486	75.0	2864	67.4	1412	76.4

Group 2 contained all 103 video samples of male pigs. The result for the weight estimates of Group 2 can be seen in Table 44, with individual weights for the group presented in Table 45.

Table 44: Performance of the piGUI System Estimating the Weight of Group 2

Filter Method	Estimated Weight Frames (kg)		Actual Weight Frames (kg)		Actual Weight Videos (kg)	
	AVE	STD	AVE	STD	AVE	STD
Before Filtering	47.2	25.9	45.0	13.6	44.9	13.7
Limit Filter	43.6	13.1	43.8	13.3	45.2	13.7
Shape Filter	45.2	13.4	45.3	13.6	45.6	13.8
Combined Filters	44.6	13.3	44.7	13.4	45.6	13.8

Table 45: Performance of the piGUI System Estimating the Individual Weights of the Pigs in Group 2

Method	Before Filtering		Passed Shape		Passed Limits		Combined	
Error Category (kg)	Count	%	Count	%	Count	%	Count	%
$w_{est} < 0.5$ kg	748	17.9	373	26.6	656	22.2	350	26.5
0.5 kg $\leq w_{est} < 1$kg	638	15.2	321	22.9	568	19.2	306	23.2
1 kg $\leq w_{est} < 2$ kg	985	23.5	428	30.5	879	29.7	412	31.2
2 kg $\leq w_{est} < 3$ kg	530	12.7	173	12.3	447	15.1	162	12.3
3 kg $\leq w_{est} < 4$ kg	287	6.9	79	5.6	219	7.4	70	5.3
4 kg $\leq w_{est} < 5$ kg	143	3.4	20	1.4	84	2.8	17	1.3
$w_{est} \geq 5$ kg	855	20.4	10	0.7	108	3.6	4	0.3
Total Samples	4186	100.0	1404	100.0	2961	100.0	1321	100.0
$w_{est} < 2$ kg	2371	56.6	1122	79.9	2103	71.0	1068	80.8

Group 3 contained all 77 video samples of female pigs. The result for the weight estimates of Group 3 can be seen in Table 46, with individual weights for the group presented in Table 47.

Table 46: Performance of the piGUI System Estimating the Weight of Group 3

Filter Method	Estimated Weight Frames (kg)		Actual Weight Frames (kg)		Actual Weight Videos (kg)	
	AVE	STD	AVE	STD	AVE	STD
Before Filtering	50.9	34.7	46.4	10.8	46.0	10.5
Limit Filter	45.6	10.6	45.7	11.2	45.9	10.3
Shape Filter	47.4	9.2	47.3	9.9	47.4	9.8
Combined Filters	47.3	9.3	47.2	10.1	47.5	9.8

Table 47: Performance of the piGUI System Estimating the Individual Weights of the Pigs in Group 3

Method	Before Filtering		Passed Shape		Passed Limits		Combined	
Error Category (kg)	Count	%	Count	%	Count	%	Count	%
$w_{est} < 0.5$ kg	241	11.4	111	19.2	213	16.5	105	20.0
0.5 kg $\leq w_{est} < 1$kg	245	11.6	89	15.4	210	16.3	85	16.2
1 kg $\leq w_{est} < 2$ kg	383	18.1	164	28.4	338	26.2	154	29.3
2 kg $\leq w_{est} < 3$ kg	254	12.0	95	16.5	213	16.5	87	16.5
3 kg $\leq w_{est} < 4$ kg	176	8.3	50	8.7	125	9.7	40	7.6
4 kg $\leq w_{est} < 5$ kg	104	4.9	36	6.2	62	4.8	29	5.5
$w_{est} \geq 5$ kg	715	33.8	32	5.5	129	10.0	26	4.9
Total Samples	2118	100.0	577	100.0	1290	100.0	526	100.0
$w_{est} < 2$ kg	869	41.0	364	63.1	761	59.0	344	65.4

5.3.2.2 Discussion of Off-line Results

The combined filter has worked exceptionally well calculating the weight deviation and the average weight of Group 1 (refer to the actual average group weight and deviation in row 'Before Filtering', column 'Actual Weight Videos' in Table 42 and estimated group average weight and deviation in row 'Combined Filters' and column 'Estimated Weight Frames'). This has occurred because there was sufficient good quality data available during analysis that represented the actual weight of the group well (row 'Before Filtering', column 'Actual Weight Frames'). Subsequently, the data which passed through the filters estimated the average weight and weight variability correctly.

A similar effect occurred in Group 2, Table 44, where the group average has been estimated to 0.3 kg. However, the estimates of the females in Group 3 were less accurate, with a 1.3 kg error in the estimate of the group's average weight and a 1.2 kg error in the estimate of the group's weight deviation. In this case the filters have excluded some of the data from the videos which has directly affected the estimates. However, this is not too concerning considering that on average only ~9 seconds of video footage was captured (of each animal) to form these estimates. In practice, far more time than this will be available for the system to extract quality data while it is operating continuously in the pen. Overall, the data that passed through the filters maintained the correct group averages and weight deviation, indicating that they were not causing any bias in the samples which were considered valid. However, the data of the females in Table 46 does highlight a potential cause of system bias if good quality samples of certain animals are not available.

Individual weight estimation results for Groups 1, 2 and 3 (found in Table 43, Table 45 and Table 47) show that combining the shape and limiting filter restricts the output of weight estimates that are greater than ±5 kg in error to less than 5% while increasing the number of weight estimates within ±2 kg error to above 65%. In addition, when using these filters in combination, 20% or more of the frame samples (that passed) were found to be within ±0.5 kg of the actual weight.

5.4 CONCLUSIONS

The piGUI system's performance while operating in a commercial facility, was evaluated and its diagnostic power explored. The system automatically identified and extracted measurements of grower pigs from streaming video and used the information to record growth over four batches of grower pigs. Issues related to occlusion, and other environmental variables such as natural lighting and pig appearance were highlighted. Hardware problems caused by the harsh environment were also encountered.

A standard growth curve obtained from literature was effective at describing weight relative to days of age. The output of piGUI system also followed this standard growth profile during the second batch and during periods of the other three batches of grower pigs. A software setting caused a bias to be recorded, which was identified and rectified during the third batch. A deflection away from the standard growth curve was experienced in the third and fourth batches when the pigs reached weights greater than ~45 kg. It is believed that these growth deflections may have been

168

caused by stress (related directly or indirectly) to temperature. The level of animal activity recorded by the system, the temperatures leading up to the growth deflections and figures reported in literature support this theory (Heitman and Hughes, 1949; Aarnink *et al.*, 2006; Huynh *et al.*, 2005).

Given these preliminary findings, further large scale testing of the system at commercial facilities is warranted. These should specifically target quantifying and monitoring the effect of temperature on growth, the system's ability to determine animal activity and its relationship to growth, feed consumption and temperature.

After testing and further code modification, a simulation was run off-line to determine the system's ability to evaluate the individual weight and group average weight of grower pigs. Results indicated that the group average weights of grower pigs could be estimated within 1.3 kg error and group weight deviations within 1.2 kg error. When using the two filters in combination, the weight of individual pigs were estimated within ±2 kg of their actual weight more than 65% of the time, while estimates greater than ±5 kg in error were restricted to less than 5%. These filters did not cause bias during the selection of valid samples, as the average weight and weight deviation of the group remained relatively steady for all filtering methods. However, the occurrence of any bias related to sampling in the actual installation environment should also be investigated.

Chapter 6

Weight Estimation of Sows during Pregnancy

ABSTRACT

The body condition of sows, before and during pregnancy, has been shown to affect the quality and survivability of their offspring. Therefore, it is desirable to monitor and manage the body condition of sows to ensure that their nutritional and environmental requirements are met. A sow's condition can be determined from its body shape, back-fat measurement and weight relative to its age and parity. However, often these factors are not monitored frequently due to the high level of labour required. As weight is a strong indicator of condition, a machine vision system was developed to continuously estimate, without operator involvement, the weights of pigs from their size. This chapter presents the weight estimation results achieved by the system for sows between days 71 and 82 of pregnancy, and a brief insight into the morphological changes in two sows' body measurements determined by the system which occurred in the days before and after giving birth. The system determined the average weight of the group of pregnant sows to within 1.5% mean-relative error of the actual group average weight. Eighty-two percent of the individual weight assessments of these sows were within ±5 kg of their actual weight using the system's combined limit and shape filtering method. The system identified clear changes in body measurements for two sows before and after giving birth. The effect that pregnancy has on the shape and body measurements of sows should be investigated further as it is likely to be a contributing factor to poorer weight estimates. Body measurements may also be used to model and classify condition or the onset of pregnancy.

6.1 INTRODUCTION

It is important to manage the body condition of sows closely as their body condition has proven to enhance the survival prospects of their progenies (O'Dowd *et al.*, 1997). Sows with poor body condition are more likely to have (i) small litter sizes, (ii) fewer piglets born alive and (iii) piglets with low birth weights. Further implications are also experienced, as generally piglets with low birth weights will have poor growth performance throughout their lives (Gondret *et al.*, 2005; Rehfeldt *et al.*, 2008). To classify the condition of sows, back-fat thickness and body weight are generally used along with other visual cues (Maes *et al.*, 2004; Charette *et al.*, 1996).

The conventional method used to acquire condition-related information, involves moving and confining each sow to a weigh scale, before determining its weight and back-fat depth using an ultrasonic device. Alternatively, a sow's weight can also be estimated from its body measurements. In this method, the heart girth and length of the sow are determined using a tailor's rule and then used in an equation which estimates the weight of the sow to within 3% (Pope and Moore, 2002; Yeo and Smith, 1977). Condition scoring can also be performed visually by skilled workers or using the physical body measurements of the sows (Charette *et al.*, 1996). The body measurements of sows have also been shown to increase during pregnancy and subsequently have been used to determine space requirements (McGlone *et al.*, 2004a). However, weighing and assessing large numbers of heavy animals by these means is laborious and also increases the risk of injury to the animals and workers involved (Brandl and Jørgensen, 1996). Consequently, automated methods have been developed which minimise the involvement of workers in these processes.

The two previously described methods have evolved into new methods that automatically obtain condition-related information. These methods are electronic sow feeding systems (ESF) and machine vision systems.

In an ESF system, an automated feed and weigh-station are integrated within the sows' pen. For an ESF system to work automatically, each sow must be trained to progress through a series of raceways and gates which lead up to these stations. The primary functions of an ESF system are (i) to automatically manage each sow's condition by controlling feed intake and body weight and (ii) to avoid competition for feed by separating each sow from its pen mates while it is feeding. However, despite the effectiveness of ESF systems, comparative studies between ESF systems and alternative housing methods indicate that most injuries occur in group-housing systems where ESF systems are utilised (McGlone *et al.*, 2004b). These injuries are believed to be caused, indirectly, by the mechanical components of an ESF system (Jensen *et al.*, 1995). Aggressive (possibly territorial) actions have also been noted towards the sow using the feeder in an ESF system (Edwards *et al.*, 1988; Rhodes *et al.*, 2005). Some studies indicate that aggressive behaviour and injuries may be reduced by giving sows access to multiple feeding locations (Rhodes *et al.*, 2005). However, to be cost effective generally an ESF system only consists of a single feed and weighing station for a large group of sows. Hence, ideally, both the contact between the worker and pigs and the pig and condition-assessment-apparatus should be minimised. Furthermore, to reduce the risk of injury to sows in group housing

systems, it would be beneficial to determine the condition of sows located at separate feeding locations.

A machine vision system is the most attractive method to determine the condition of sows, as condition assessment can be performed in a loose housing environment without making contact with the animal. A machine vision system can also simultaneously asses multiple animals. To make a condition assessment, a machine vision system infers a relationship between an image-based representation of an animal's body measurements and its weight and fat content (Doeschl-Wilson *et al.*, 2005). The live weight of pigs have been estimated to within 5% using the machine vision method (Schofield, 1990). In future, to parallel the task of an EFS system, a machine vision system could be linked to feed delivery devices in order to deliver the correct feed ration to individual sows.

To enhance their productivity and maintain their welfare, it is desirable that the condition of sows be monitored and managed during and after pregnancy. Condition assessment may be achieved using machine vision systems that do not require direct contact with animals and allow them to feed simultaneously, thus reducing the risk of injury (Rhodes *et al.*, 2005). This chapter presents the preliminary results of an off-line machine vision system in estimating the weight of sows in their early stages of pregnancy. The ability of the machine vision system to monitor morphological changes recorded during and after pregnancy is also briefly explored.

6.2   MATERIALS AND METHODS

A camera (Logitech Quickcam Pro 9000, Logitech, Quarry Bay, Hong Kong) a computer (fit2PC, CompuLab Ltd, Technion, Haifa, Israel) and Matlab software (MathWorks, Inc., Natick, MA) were interfaced to form a machine vision system to estimate the live weight of sows. The computer was chosen to overcome issues surrounding rodent infestation, dust, moisture, and corrosion that are commonly associated with the piggery environment. Routines within the software searched the image to determine pig shapes and extracted body measurements when they were found. Other routines were then used to estimate and validate each pig's weight. Collectively these routines automated the weight estimation task (Banhazi *et al.*, 2011b).

6.2.1   Experimental Setup and Location

Thirteen sows were weighed to the nearest half kilogram by an electronic scale at a commercial piggery (PPPI, University of Adelaide, Roseworthy campus). Directly after each sow exited the scale a number of short videos were recorded by a camera located 2 meters above the weighing area (layout shown in Figure 118). A total of twenty-seven videos were collected of the thirteen Large White × Landrace and Large White sows. During the recording period the sows were at different stages of their pregnancy. Eleven of the sows were recorded between day 71 and 82 of pregnancy. These eleven sows were considered to be a group which may be housed together. Subsequently, they were evaluated for their weight by the vision system on an individual and group basis. In addition, the system recovered the shapes and body measurements of two Large White × Landrace sows before and after giving birth to

determine whether the system could detect any morphological alteration in the sows' body shape.
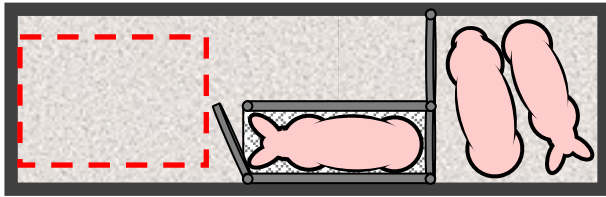
Figure 118: The Experimental Setup at the Facility
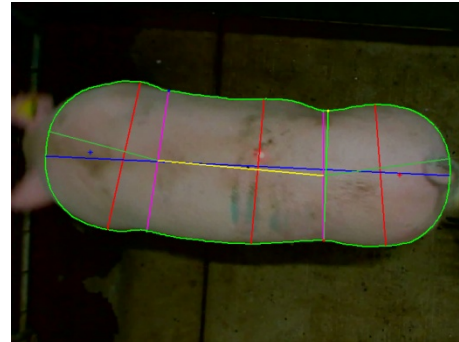
Figure 119: An Analysed Video Frame with the Body Measurements Extracted Overlayed

The following information was recorded by the machine vision system when a successful weight assessment took place: (i) the image frame of the sow with an overlay of contour shape recovered (Figure 119), (ii) the shape information of the sow's body contour, (iii) the sow's body measurements and (iv) the weight estimate.

6.3 RESULTS

6.3.1 Weight Estimation of Sows as a Group

In total, 694 frames were processed off-line by the machine vision system. Of these frames, 444 successfully passed through to the body measurement extraction stage. The 444 frames that passed were then subjected to a shape and body measurement filtering procedure to determine whether the sows' body poses were adequate to make a weight estimate. These frames were then used to estimate the weight of the sows between days 71 and 82 of pregnancy on both an individual and a group basis.

Table 48 shows the actual average group weight of the sows and the systems weight estimates after analysing the video frames. The average weight of the group of sows was determined to be 201.3 kg by the electronic scale (see Table 48 row 'Before Filtering' column 'Actual Weight Videos'). The average formed by averaging the actual weights from all the extracted frames was similar at 201.4 kg (see Table 48 row 'Before Filtering' column 'Actual Weight Frames'). These frames were then subjected to various filtering operations (rows 2 to 4) and those body measurements that passed were used to estimate the group average weight (column 'Estimated Weight Frames').

Table 48: Performance of the PiGUI System Estimating the Weight of the Sows

Filter Method	Estimated Weight Frames (kg)		Actual Weight Frames (kg)		Actual Weight Videos (kg)	
	AVE	STD	AVE	STD	AVE	STD
Before Filtering	185.0	95.0	201.4	15.7	201.3	16.0
Limit Filter	201.2	17.7	199.6	17.1	203.1	17.0
Shape Filter	203.2	18.3	200.2	16.9	201.1	17.3
Combined Filters	198.4	18.5	196.6	17.9	203.9	17.7

Table 49 shows the error between the actual group weight and the weight estimates after applying the filters to the 444 frames to remove redundant data.

Table 49: Error in Weight Estimation of the Group of Sows Using the PiGUI Filters

| | Estimation Error (kg) | |
	AVE	STD
Before Filtering	16.3	-79
Limit Filter	0.1	-1.7
Shape Filter	-1.9	-2.3
Combined Filters	2.9	-2.5

The weight of the sows as a group was estimated using four different filtering methods.

The unfiltered estimate on row one was made using the body measurements directly extracted from the videos. Other than some very basic filtering that occurred in the extraction stage, no attempt was made to remove redundant data for this estimate. As the redundant information was still included, a large amount of error was introduced to the group weight estimate which can be seen in the large standard deviation (STD = 95 kg).

The second limit filter only included the frame samples which had all extracted body measurements of the sow within a range determined by its projected weight estimate. Thus, this filter cross validated between the estimated weight and extracted body measurements to give an indication whether they were recovered correctly. Of all the filtering methods, the limit filter was most accurate, estimating the group weight to 0.1 kg of the actual group weight and the weight deviation of the group to 1.7 kg of the actual weight deviation.

The shape filter removed redundant data based purely on the extracted shape of the sow. As the weight-estimation equation is built around a particular pose (the shape filter), ensuring that the sow conform to this pose during weight assessment would enable more robust estimates. However, the fact that the shape filter has not performed as well as the limit filter is not necessarily a reflection of the method, but is actually more likely to be the result of limited shape data being available that conformed to the pose required to make a weight estimate. On average 32 frames per video (6.4 seconds of footage) was acquired. The combined filter was also less precise at calculating the group average weight for this reason. Thus, collecting additional shape information for sows during pregnancy would be desirable in future. This would allow modelling and analysis of shape and weight differences between individual sows.

Despite the limited amount of data available, the group weight estimates calculated using the shape and combined shape and limit filtering methods were still both within 1.5% of the actual group average weight.

6.3.2 Weight Estimation of Individual Sows

The manual method which uses a tailor's rule to determine the weight of sows is accurate to within 3%. Therefore, individual image-based weight estimates within ±5 to ±6 kg error can be considered practical as the average weight of the group of

eleven sows was 201.3 kg. Individual weights for the group of eleven sows are presented in Table 50.

Table 50: Performance of the piGUI System Estimating the Individual Weights of the Sows

Method	Before Filtering		Passed Shape		Passed Limits		Combined	
Error Category (kg)	Count	%	Count	%	Count	%	Count	%
$w_{est} < 0.5$ kg	22	5.0	14	8.6	9	12.7	5	10.0
0.5 kg $\leq w_{est} < 1$kg	18	4.1	14	8.6	9	12.7	8	16.0
1 kg $\leq w_{est} < 2$ kg	36	8.1	25	15.4	13	18.3	10	20.0
2 kg $\leq w_{est} < 3$ kg	27	6.1	21	13.0	8	11.3	6	12.0
3 kg $\leq w_{est} < 4$ kg	34	7.7	18	11.1	9	12.7	4	8.0
4 kg $\leq w_{est} < 5$ kg	29	6.5	15	9.3	10	14.1	8	16.0
$w_{est} \geq 5$ kg	278	62.6	55	34.0	13	18.3	9	18.0
Total Samples	444	100.0	162	100.0	71	100.0	50	100.0
$w_{est} < 2$ kg	76	17.1	53	32.7	31	43.7	23	46.0

Table 50 shows eighty-two percent of the samples which passed the combined limit and shape filter were within a ±5 kg range of the actual weight of the sow. This indicates that the system can achieve practical precision when estimating the individual weights of sows. However, Table 50 also indicates that to enhance precision, additional data collection is warranted, as the shape filter is less accurate than was found in *Chapter 4* and *Chapter 5* for finisher and grower pigs. This is likely to be a consequence of limited shape data being available to build the shape filters in this trial and greater variability in the appearance of the sows than grower-finisher pigs.

6.3.3 Sow Shape Before and After Giving Birth

The morphological change in the body of two sows before and after they gave birth was assessed. Large differences in the body shape of the sow were identifiable in the days immediately prior and after birth as Figure 120 illustrates.
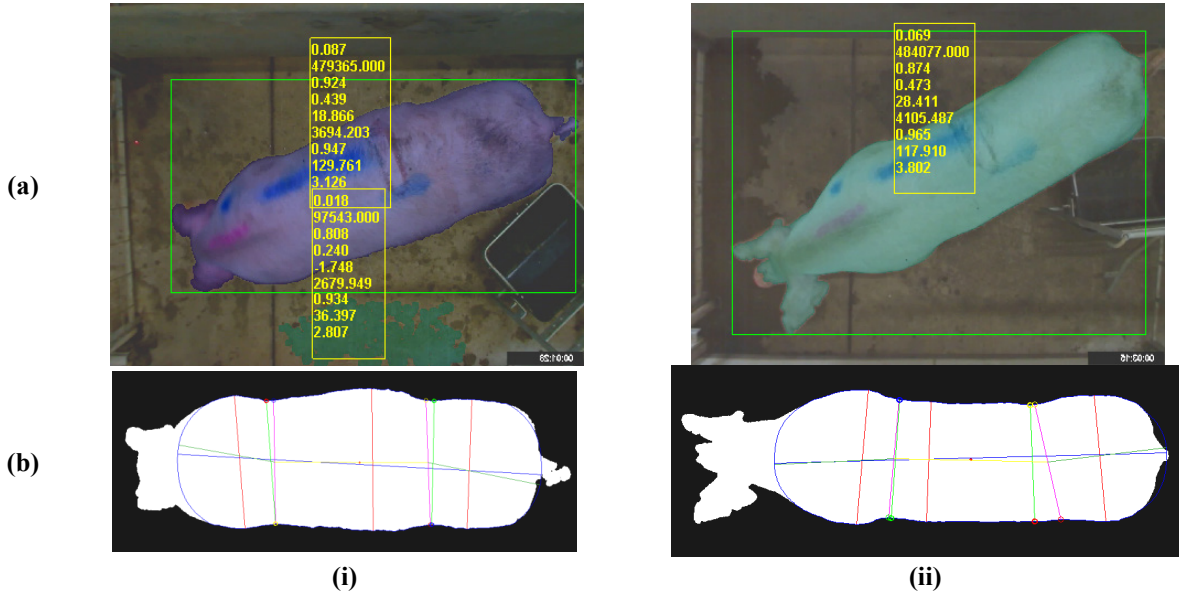
Figure 120: Change in Sow Body Shape Before (i) and After Giving Birth (ii); (a) Superimposed Transparency on the Original Image and Region Information; (b) The sow segmented from the image

Table 51: Changes in the Body Measurements of Two Sows Before and After Giving Birth as Determined by the Machine Vision System

		MWF$_a$ (mm)	MWMid$_a$ (mm)	MWR$_a$ (mm)	AF$_c$ (mm^2)	AMid$_c$ (mm^2)	AR$_c$ (mm^2)	AT$_2$ (mm^2)	ML (mm)	FML$_a$ (mm)	MidL (mm)	RML$_a$ (mm)	mWF$_a$ (mm)	mWR$_a$ (mm)
Sow 1 Before Birth n = 15	AVE	378.5	398.3	367.6	99419.3	162223.0	106541.4	368183.8	1057.3	305.2	428.2	325.9	360.6	352.0
	STD	4.6	8.2	1.5	7549.5	8250.5	3974.4	4884.0	26.1	23.9	21.8	12.3	10.2	7.0
	MIN	367.1	381.3	365.2	90391.7	150108.1	101300.6	363112.8	1026.1	277.0	386.8	310.6	348.0	340.9
	MAX	383.9	407.3	369.1	108638.7	172070.3	115033.8	377640.3	1103.2	331.7	453.1	352.3	377.6	362.7
	RANGE	16.8	25.9	3.9	18247.0	21962.2	13733.1	14527.5	77.1	54.7	66.3	41.7	29.6	21.7
Sow 1 After Birth n = 29	AVE	367.1	329.1	350.9	102676.3	134957.9	103534.0	341168.2	1082.5	332.4	419.9	333.2	321.8	316.6
	STD	4.7	1.7	2.0	3890.2	4953.3	2827.6	3310.7	9.0	11.2	14.3	10.3	2.9	1.7
	MIN	356.7	325.9	347.1	95800.9	126427.3	98245.2	335823.7	1068.6	313.3	396.0	313.3	315.4	313.7
	MAX	374.4	331.6	356.0	112722.0	144802.7	109132.0	350062.8	1110.6	365.0	445.8	351.9	327.1	321.4
	RANGE	17.7	5.7	8.9	16921.1	18375.4	10886.9	14239.1	42.0	51.7	49.8	38.6	11.7	7.8
Sow 2 Before Birth n = 7	AVE	398.0	402.8	379.5	103600.6	153429.7	109477.2	366507.5	1025.4	305.9	399.1	326.6	372.7	359.4
	STD	4.9	6.9	5.1	3108.0	4546.6	4500.6	1071.3	14.7	8.8	10.0	16.7	8.5	10.1
	MIN	391.1	393.3	373.4	98641.6	148205.3	104708.8	364794.8	1008.4	294.7	389.2	309.3	363.2	346.8
	MAX	403.0	410.8	387.1	106769.2	160533.7	116750.4	367755.6	1045.5	318.7	412.8	350.4	382.6	370.7
	RANGE	11.8	17.5	13.7	8127.6	12328.3	12041.6	2960.9	37.2	24.0	23.6	41.1	19.4	23.9
Sow 2 After Birth n = 20	AVE	367.8	321.3	346.2	116683.9	136967.9	97795.2	351447.0	1138.2	377.6	433.9	329.0	316.9	302.9
	STD	2.9	4.3	1.1	3127.0	1893.5	1804.1	2782.4	12.5	10.5	4.8	6.7	5.1	3.3
	MIN	360.4	311.4	344.6	112113.1	134595.4	92457.0	344062.3	1109.3	363.7	424.8	309.0	311.4	298.3
	MAX	371.6	328.8	348.4	124641.6	141668.9	100227.8	357571.2	1167.6	407.7	443.8	338.0	326.8	311.7
	RANGE	11.2	17.4	3.8	12528.4	7073.5	7770.8	13508.9	58.3	44.1	19.0	29.1	15.5	13.4

		MWF$_a$ (mm)	MWMid$_a$ (mm)	MWR$_a$ (mm)	AF$_c$ (mm^2)	AMid$_c$ (mm^2)	AR$_c$ (mm^2)	AT$_2$ (mm^2)	ML (mm)	FML$_a$ (mm)	MidL (mm)	RML$_a$ (mm)	mWF$_a$ (mm)	mWR$_a$ (mm)	Weight (kg)
Sow 1	AVE Before	378.5	398.3	367.6	99419.3	162223.0	106541.4	368183.8	1057.3	305.2	428.2	325.9	360.6	352.0	234
	AVE After	367.1	329.1	350.9	102676.3	134957.9	103534.0	341168.2	1082.5	332.4	419.9	333.2	321.8	316.6	224
	% Difference	-3.0	-17.4	-4.5	3.3	-16.8	-2.8	-7.3	2.4	8.9	-1.9	2.2	-10.8	-10.1	-4.3
Sow 2	AVE Before	398.0	402.8	379.5	103600.6	153429.7	109477.2	366507.5	1025.4	305.9	399.1	326.6	372.7	359.4	222
	AVE After	367.8	321.3	346.2	116683.9	136967.9	97795.2	351447.0	1138.2	377.6	433.9	329.0	316.9	302.9	205
	% Difference	-7.6	-20.2	-8.8	12.6	-10.7	-10.7	-4.1	11.0	23.4	8.7	0.7	-15.0	-15.7	-7.7

The body measurements recovered from the n frames of the two sows in the days before and after giving birth are shown in Table 51. These body measurements have been converted from pixels to real world body measurements using the known characteristics of the camera lens, the installation height of the camera and the sows' heights which were determined manually using a sliding right angled ruler.

The large variability of the sows' body measurements obtained using the machine vision system are small with, the width and length measurements having standard deviations less than or equal to 2.6cm. This indicates high repeatability in width and length measurements. Consequently, the differences between many of the measurements obtained before and after giving birth are clearly distinguishable.

The percentage difference between the weight and the extracted body measurements, before and after giving birth, are presented in the last section of Table 51. The majority of these differences are negative indicating that the size of the sow decreased after birth. The sows' weights decreased, with sow 1 and sow 2 loosing 10 kg and 17 kg respectively. Not surprisingly, over this period the sows experienced the largest decrease in the width at their middle, with a reduction of greater than 17% in the $MWMid_a$ measurement. The minimum width measurements of the sows, taken from behind the shoulder (mWF_a) and in front of the ham (mWR_a) have also decreased by 10% after giving birth. The area of the middle section has also reduced by greater than 10% for both sows. Many of these body changes are visually obvious in Figure 120.

In contrast, some of the measurements have also increased. These measurements include the total length (ML) and the area of the front body section (AF_c). These increases are most likely to be related to the head-trimming method which removes the pig's head as a function of the pig's width. Consequently, some modification of the software is necessary to facilitate the assessment of sows in the later stages of pregnancy as the changes in width may be impacting the front area and maximum length measurements.

6.4   DISCUSSION AND CONCLUSIONS

The sows between days 71 and 82 of pregnancy had their weight estimated accurately on both an individual and a group basis. The limit filtering method yielded the most accurate group weight estimate, within 0.1 kg of the actual group weight and to 1.7 kg of the actual weight deviation of the group. On an individual basis, eighty-two percent of the samples which passed the combined limit and shape filter were within a practical ±5 kg range of the actual weight of the sow. It is believed that these results could be enhanced further with additional data collection and modelling surrounding the shape and body measurements of sows throughout pregnancy.

The metric body measurements of the two Large White × Landrace gestating sows recovered by the vision system in Table 51 are consistent with those manually measured by McGlone *et al.* (2004a) of 222 gestating sows of the same genotype. The shoulder width (MWR_a) and ham width (MWR_a) of the sows assessed during this study are within the 95% limit bounds of the same measurements reported in McGlone *et al.* (2004a). Furthermore, the sows were consistently wider at the shoulder than at the ham, and averages of sow shoulder width (40.4cm) and ham

width (38.1cm) reported in McGlone *et al.* (2004a) are similar to the measurements found here (which were in the range of 36.9 to 39.8cm and 34.6 to 38.0cm, respectively). In addition, McGlone *et al.* (2004a) reported that the body length of the sows (excluding the head), had a mean of approximately 115.6cm. The lengths of the two sows (head excluded) measured by the piGUI system were in this vicinity, ranging from 102.5 to 113.8cm.

The information recorded by a device that can monitor the condition and morphological changes of sows may assist in solving and managing a wide variety of problems. Primarily the information can be used as a basis for (i) nutritional programs to ensure that each sow maintains an adequate level of condition and (ii) the design of housing systems during pregnancy and farrowing to ensure that adequate space requirements of individual sows are met. Furthermore, as the machine vision system is capable of pose recognition, the shape information can be used to identify important behaviours which may impact the survivability of a sow's piglets. It is not uncommon for certain sows to savage (Chen *et al.*, 2008) their piglets. Sows may also accidently crush piglets when they lie down during farrowing (Weary *et al.*, 1996). Therefore, automatically identifying basic behaviours, such has the transition between a sow standing and sitting, could be useful in farrowing systems to instigate measures to prevent the occurrence of crushing (Banhazi and Tscharke, 2011). Although more complex, determining behaviours and environmental scenarios that promote fighting between sows or savaging of piglets may also be identified so that management protocols can intervene before fights and injuries occur (Banhazi and Tscharke, 2011). It is also possible that the morphological changes recorded may be used to recognise when a sow becomes pregnant and provide an alternative means to manual pregnancy checking. The shape and growth may also serve as an indication of a sow's likely litter size. Also the variability in the appearance of sows may be sufficient enough to provide grounds for a machine vision system to individually identify sows.

In order to extract the correct body measurements automatically, the morphology caused by movement and the morphology caused by growth must be separated. Thus, the ability to recognise body posture is very important, as it provides a base reference to determine the growth. The effect that the morphology caused by movement has on body measurements is suppressed by the shape filter used in this study, however, its effectiveness could be improved extensively by modelling the shape change throughout pregnancy and lactation.

Chapter 7

Integrating RFID into the PiGUI System to Detect for Bias and
Feeding Behaviour

ABSTRACT

A machine vision system was developed to determine the live weight and growth rate of groups of pigs. During development, it was important to determine whether the sampling method had potential to cause bias and subsequent error in the daily weight estimates calculated by the system. Sampling bias can occur toward certain pigs because of their appearance or the frequency and duration in which they reside in the pen-region beneath the camera. To determine whether these forms of bias could occur, Radio Frequency Identification was integrated into the system to monitor the attendance of individual pigs in the pen-region observed by the camera. Test results indicated that both forms of bias had occurred as a result of the system's filter settings and its installation position.

As the system observed a single feeder space, the opportunity arose to analyse the data further and determine whether the feeding behaviour of individual animals could be recovered from their attendance at the feeder. Preliminary findings indicate that the attendance recorded by the RFID system at the feeder is related to weight gain and that attendance might be useful in detecting feeder demand and out of feed events. In addition, it is believed that the RFID-recorded interactions between pigs at the feeder may provide a novel way of automatically recording competitive behaviour between individual animals in a group.

Continuously identifying individual pigs at the feeder helps to fine tune the vision systems parameters to overcome bias related issues concerning layout and sampling. Additional information can be gained by the RFID system which prompts further investigation.

7.1 INTRODUCTION

A vision-based weight estimation system was developed to determine the average weight of groups of grower and finisher pigs (Banhazi *et al.*, 2011b; Banhazi *et al.*, 2009c). During normal operation, the system observes a pen region and makes weight estimates when a pig is observed standing in a particular posture. Over the course of a day these samples are collected and averaged to form a daily group weight estimate. To ensure that each pig is assessed for its weight daily, the system was installed above a feeding space. However, at this location the feeding duration and frequency of each pig has the potential to cause bias in the group's daily average weight estimate. Therefore, to determine and manage the presence of any bias, an analysis of the attendance of the animals (observed by the system) is required.

Consequently, Radio Frequency Identification (RFID) was integrated into the system as it could be used to determine the feeding duration and frequency of each animal with respect to the frequency of weight estimates gathered by the vision system of each animal. This information could also be used to indicate whether bias toward certain animals was occurring due to the systems filtering operations. The systems filtering operations could then be loosened or tightened accordingly.

Radio frequency identification is a standardised method for identifying individual animals (ISO 11784/11785). This form of identification is used to enhance the traceability of meat products as well as helping producers to determine, (i) individual growth rates, (ii) the location of pigs on-farm, (iii) pigs appropriate for breeding programs, (iv) feeding behaviour and (v) welfare issues. RFID devices can be either injected into an animal or attached to an external appendage such as an ear (Marchi *et al.*, 2007; Stärk *et al.*, 1998).

As the RFID system monitored each pig's attendance at the feeder, the data were subsequently analysed to determine both individual and group feeding behaviour. Feed behaviour has been monitored in this manner in previous studies (Brown-Brandl and Eigenberg, 2011; Weixing *et al.*, 2010; Eigenberg *et al.*, 2008; Naas *et al.*, 2001; Georgsson and Svendsen, 2002).

This chapter is broken into two main messages: (i) to identify whether bias is present and thus whether the feeder is the appropriate installation position for the vision system and to (ii) determine whether the RFID system could pick up on the behaviour of the animals around the feeder.

7.2 MATERIALS AND METHODS

7.2.1 Experimental Setup and Location of the PiGUI System

The piGUI vision system (Banhazi *et al.*, 2011b) and a RFID system was installed inside a pen at a commercial research piggery (PPPI, University of Adelaide, Roseworthy campus). A Texas RFID reader (model RI-K3A-001A-00) was used to collect identification information via an ear tag transponder (Figure 122). The reader and antenna can be seen in Figure 121 (a). The reader was secured to the top-inside of a single space feeder located in the corner of the pen (reader location circled in Figure 121 (b)).

(a)   **(b)**

Figure 121: (a) The RFID Reader and Antenna; (b) An Image Recorded by the System and the RFID Reader (Circled)

Figure 122: Allflex Ear-tag Transponder Used

The antenna of the RFID system was fixed to the inside the feeder in close proximity to the trough. At this location the maximum read-range between an ear-tag transponder and the antenna was approximately 20 cm. The position of the antenna ensured that each pigs RFID ear tag could be read while its head was inside the feeder. The antenna was also installed at a height that avoided the chance of read errors occurring from pigs that were not feeding; such as when they were lying down in close proximity to the antenna. This ensured the best chance of logging individual feeding behaviour as well as preventing curiosity and damage from the pigs.

Sixteen slow growing pigs weighing between 38.5 kg and 63.5 kg were selected to be observed in the trial. This particular type of pig was chosen to challenge the systems operation, as they would be most likely to have a different shape than normal due to their growth history and body condition. In addition, if the pigs were disadvantaged, their contour shape could be recovered and potentially used for future condition recognition purposes. The pigs were tagged with Allflex FDX-B electronic ear tags for identification purposes (diameter 2.6 cm, weight 5.12 g see Figure 122). As the trial progressed some pigs were removed from the pen to fulfil space requirements.

The RFID logging feature of the piGUI software was activated. Consequently when a pig's ear-tag transponder was within the read-range its unique identification number (Figure 122) was logged to two separate files. The first file logged the identification number under the condition that the pig was present; every time a successful read took place. The second log file recorded the identification number under the condition that the piGUI system had performed a weight estimate, so that each pig's identity could be paired with the body measurements and weights determined by the vision system. These log files gave an indication of the minimum duration that the

each animal spent at the feeder and how often they were captured by the piGUI system, respectively. The second log file could also be used to determine individual growth and individual body characteristics. Logging preference was always given to the closest ID tag to the antenna.

Every time a successful weight assessment took place the piGUI system recorded an image of the animal with an overlay of contour shape detected (Figure 121 (b)), the RFID tag number (Figure 122), the shape information of the contour, the body measurements used to estimate the weight, the weight estimate and a time-date stamp of when each image or RFID read was taken. Software was written using Matlab (MathWorks, Inc., Natick, MA) to automatically structure the acquired data so that each pig's feeding time, duration and frequency could be compared against others in the group.

During the trial the pigs' backs were marked with livestock paint in a unique pattern to enable easy identification on future weigh days; as a RFID reader was not available in the location of the electronic scale. The pigs were manually weighed using an electronic weigh scale (Pig Weigh Crate, Ruddweigh, Guyra, Australia, ±1%) on seven occasions during the period between the 18/3/11 and the 24/4/11. During this time, attendance and weight information was recorded around the feeder by the RFID system and piGUI vision system.

7.3   RESULTS AND DISCUSSION

7.3.1   PiGUI System Performance and the Data Collected

The piGUI system began logging individual information via RFID on the 29/3/11 (12:05). A RFID read timeout caused the piGUI system to crash on the night of the 1/4/11 (21:00) and 16/4/11 (13:00). These issues were rectified on the 7/4/11 (9:15) and the 20/4/11 (12:15) respectively. The system continued to record identities and weight information until the 24/4/11 when the trial ended. In total 803,877 records were obtained using the RFID system over the period. Of these 72 were read errors and were discarded. The number of ID records of each pig can be seen in Table 52. As multiple reads occurred per second, Table 52 shows both the number of reads acquired for each animal and the unique data records which eliminate any repetition of ID-reads that occurred within a second. The total number of unique ID-reads collected was 282,758 (35% of the total ID-reads).

Table 52: RFID Data Collected of Each Pig: Number of Successful Reads and Unique Read-seconds

Pig #	4906205	4906481	4906764	4906514	4906217	4906733	4906356	4906223	4906816	4906710	4906826	4906777	4906776	4906538	4906610	4906678
Total ID Reads	147908	83678	72853	26825	39404	10664	16164	87648	22182	71253	47723	44138	1753	41591	19883	69165
Unique ID Reads (per second)	49573	27721	26936	12799	14806	3489	6959	30927	8409	21737	18194	15998	734	12464	9401	22611

7.3.2 Bias Detection

7.3.2.1 Detecting Layout Bias

The number of seconds each pig attended the feeder was calculated over each of the trial days using the unique RFID data to determine whether the time spent at the feeder by each pig could cause bias to occur in weight estimates of the group. The total number of images captured for each animal by the piGUI system was also calculated in the same manner. The results of the RFID and piGUI log file are shown in Table 53 and Figure 123.

Table 53: Aggregated Data of the RFID and PiGUI Vision System

Tag #	Total Samples[*]	Total Minutes[^]
4906205	229	826
4906481	50	462
4906764	42	449
4906514	72	213
4906217	44	247
4906733	3	58
4906356	7	116
4906223	46	515
4906816	22	140
4906710	9	362
4906826	34	303
4906777	6	267
4906776	7	12
4906538	12	208
4906610	40	157
4906678	100	377

[*] Samples recorded by vision system, [^] Minutes recorded by RFID

The varying duration that the pigs spent at the feeder indicates that bias has occurred. This is most obvious for Pig 4906205 (row 1 of Table 53) which spent considerably more time at the feeder than its pen-mates, and as a consequence, contributed considerably more weight estimate samples to the vision system's calculation of the group average weight (see top right corner of Figure 123).
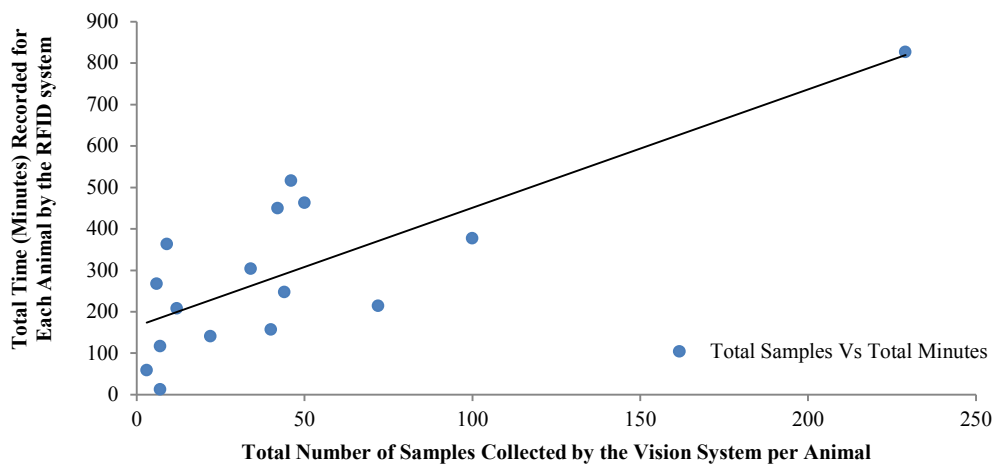
Figure 123: Total Weight Estimate Samples (Vision System) Versus Total Time (Minutes) Spent at the Feeder (RFID Reader)

The graph in Figure 123 abides by the logic that one would expect, which is that the number of weight estimates of individual pigs performed by the piGUI system increases with time spent at the feeder (the test location of the sampling device).

7.3.2.2 *Detecting Appearance-Based Bias*

It was important to determine whether the system's filtering processes were correctly validating the geometry of pigs and that no bias was occurring as a result of the system discriminating between certain pig appearances. This was achieved by comparing the number of minutes each pig attended the feeder to the number of samples taken by the piGUI vision system; indicating how many minutes were required to obtain a sample for each pig. The results are show in Table 54.

Table 54: Duration Required to Obtain a Weight Estimate Using the PiGUI System

Tag #	4906205	4906481	4906764	4906514	4906217	4906733	4906356	4906223	4906816	4906710	4906826	4906777	4906776	4906538	4906610	4906678
Minutes / Sample	3.6	9.2	10.7	3	5.6	19.4	16.6	11.2	6.4	40.3	8.9	44.4	1.7	17.3	3.9	3.8

The minutes required to take a sample depend on the parameters set in the piGUI vision system's filtering settings, as they can be adjusted to record more or less estimates at the cost of accuracy. Under the particular settings used during the trial, the filtering procedure appears to show the most positive bias toward pig 4906776 and then pigs 4906514, 4906205, 4906678, and 4906610 which all required four minutes or less of activity around the feeder to obtain a sample (Table 54). In contrast the vision system was less inclined to sample pigs 4906777 and 4906710 as the system required 40 to 45 minutes of activity around the feeder to obtain a sample weight estimate. These pigs are of particular interest as their body type, shape and appearance (possibly a consequence of health) may be hindering the system's ability to sample them. However, it is also quite possible that this bias may have been caused by the pigs' behaviour around the feeder as, throughout the trial, pigs were observed attempting to access the feeder trough from the side where the RFID antenna was mounted, while another pig was feeding.

Two images in Figure 125 (a) and (b) of pig 4906777 illustrate how it was trying to gain access to the feeder at the time its ID was read. Thus, it is possible that these two pigs may have not been captured as frequently by the system due to the style in which they fed or from changes in their body posture due to other pigs pushing them out the way. Figure 125 also illustrates the competition around the feeder. Regardless of the cause of the bias the sampling was not normally distributed at the feeder location using the piGUI system for the slow growing pigs; the histogram of the minutes per sample in Figure 124 clearly illustrates this.
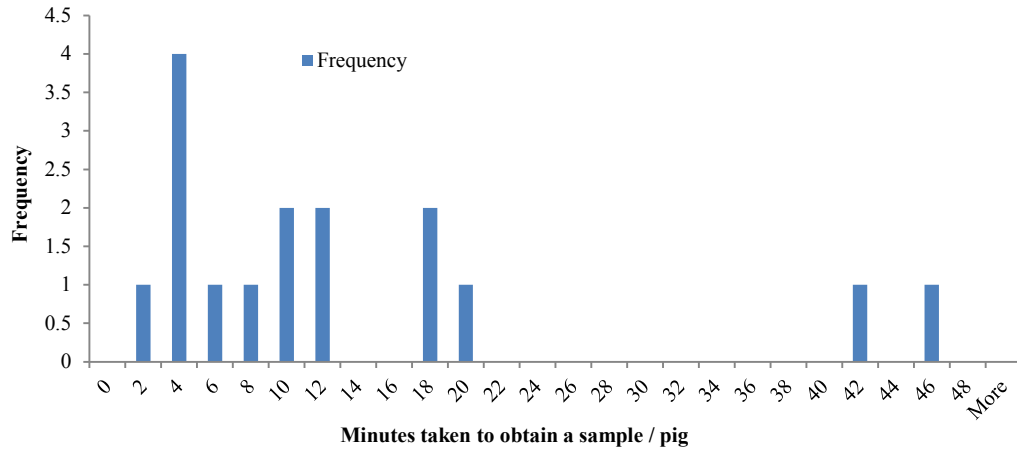
Figure 124: Histogram of the Minutes Taken for the PiGUI System to Obtain a Weight Estimate Samples of Each of the 16 Pigs

Apart from pigs 4906777 and 4906710 located on the far right of Figure 124 another subgroup of three pigs were in the range of 16 to 20 minutes per sample which the system may have been discriminating against. Regardless of filter settings, the remainder of the pigs, requiring less than 12 minutes to sample, can be considered to be 'normal' and reflect the operation in respect to the filter settings used in this trial. From an appearance perspective, the system successfully identified pig 4906678 which had a slight Duroc appearance once every 3.8 minutes it was in attendance at the feeder (Figure 125 (c)), indicating that the system was effective at capturing pigs with different skin colour under natural lighting conditions.
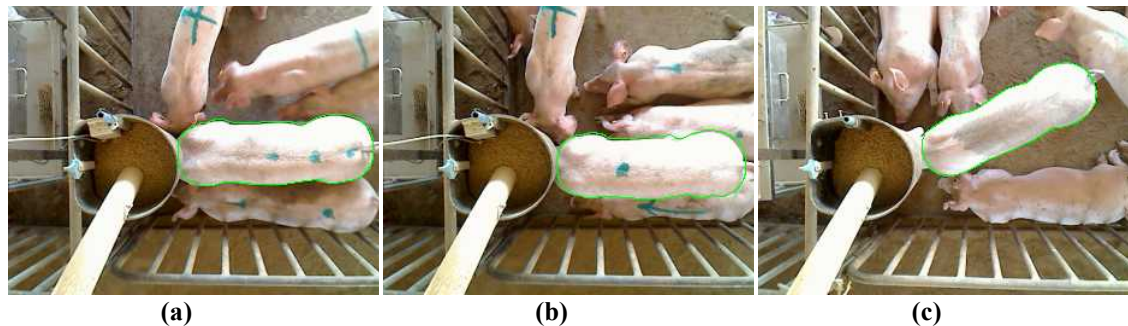
(a)   **(b)**   **(c)**
Figure 125: (a, b) Pig 4906777 ('+' Marking) Trying to Gain Access to the Feeder; (c) Pig 4906678 with Duroc Appearance Being Captured by the System

These findings indicate that there is a potential cause of bias related to the attendance of individual animals at the feeder or a combination of their shape, posture and behaviour at this location. Consequently the filter settings should be loosened in subsequent trials. Also the shape information of the animals with low and high sample pass rates should be cross-referenced to determine whether any large differences exist. In this manner, new shape types can be incorporated into the systems recognition procedure in future.

7.3.3 Feeding Behaviour

7.3.3.1 Attendance at the Feeder and Weight Gain

The fifteen pigs that were housed in the pen during the nine day period between the 29/3/11 and the 7/4/11 were assessed for their weight gain and their attendance at the feeder. Two pigs lost weight over this period, with pig 4906733 loosing 6 kg and pig 4906777 loosing 1 kg. The pig which lost 6 kg was medicated and removed from the pen altogether. Unfortunately some data for this pig was lost due to a read timeout error between the first and seventh of April. As a result, no feeding pattern could be recovered documenting its sickness for future diagnostic purposes. Only modest weight gain was experienced by majority of the remaining pigs which was to be expected as they were slow growers. The weights of the pigs used to calculate the weight gain over this nine day period are shown in Table 55 along with the other weight records collected.

Table 55: Weights (kg) of the 16 Pigs Throughout the Trial

ID-Tag #	18/3/11 (kg)	23/3/11 (kg)	25/3/11 (kg)	29/3/11 (kg)	7/4/11 (kg)	14/4/11 (kg)	21/4/11 (kg)
4906205	55.5	59.5	63	69	77	84.5	97.5
4906481	51.5	57.5	58	59.5	69	75.5	88
4906764	63.5	67.5	68	71.5	79	86.5	99
4906514	43	43.5	46.5	50	55	62.5	73.5
4906217	50.5	57.5	55	58	62	68.5	80.5
4906733	42	42	43.5	45.5	39.5		
4906356	38.5	41.5	42.5	47	48.5	48.5	57.5
4906223	46.5	51	51.5	55.5	58	66.5	81.5
4906816	61.5	67	69.5	73.5	79	85.5	97.5
4906710	55	58.5	62	67	72.5		
4906826	47.5	53	50	54	55.5	63	72
4906777	44.5	45.5	46	46.5	45.5	48.5	56.5
4906776	57.5	60	63.5	69	72.5		
4906538	49	53	56	61			
4906610	48	52	52.5	57.5	60	65	75.5
4906678	55	57.5	61	65.5	72.5		

Figure 126 shows the weight gain and minutes spent at the feeder during the nine day period after the RFID logging commenced versus the weight of the 15 pigs on the 29/3/11. Two logical effects can be observed. Firstly, with reference to the blue diamonds in Figure 126, over the same growth period the smaller pigs have experienced less gain in respect to the larger pigs. This indicates that a pig will have different weight gain potential depending on its size. Secondly, the amount of weight a pig gains correlates with the amount of time it spent at the feeder. This can be seen by comparing both series represented by the circles and diamonds in Figure 126.
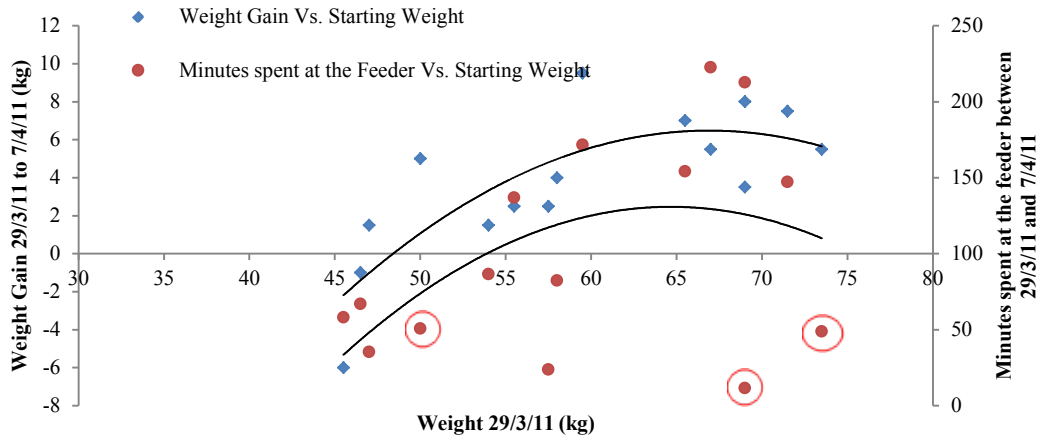
Figure 126: Weight Gain and Minutes Spent at the Feeder Vs. Starting Weight (29/3/11 to 7/4/11)

The data points in Figure 126 shows that the five pigs that spent the most time at the feeder gained the most weight. However, pigs 4906776, 4906514, and 4906610 spent only a small amount of time at the feeder yet had modest weight gain of 3.5 kg or greater (circled in Figure 126). These three pigs are of interest as they are likely to either have the best conversion efficiency, or do not dominate the feed space and therefore give more opportunity for other pigs to feed. It is possible that the low number of reads (minutes) of pig 4906776 was caused by the presence of cauliflower ear, although it did have the least gain of those pigs with a weight greater than 60 kg on the 29/3/11.

The eleven pigs that remained in the pen for the duration of the trial between the 29/3/11 and the 24/4/11 were also assessed. Figure 127 shows the relationship between weight gain of these pigs and time they spent at the feeder.
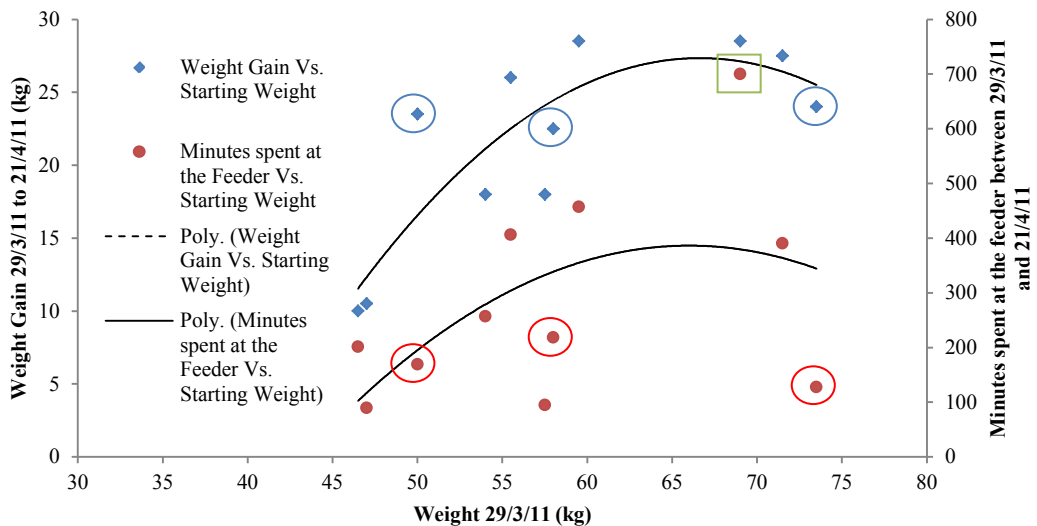
Figure 127: Weight Gain and Minutes Spent at the Feeder versus Starting Weight (29/3/11 to 21/4/11)

Similar to Figure 126, the data in Figure 127 shows that the four pigs that spent the most time at the feeder gained the most weight. Also, the pattern between the minutes recorded at the feeder for those pigs that remained in the pen over the 23 day

189

period, is similar to that recorded by the RFID system over the shorter nine day period. Likewise a few pigs spent considerably less time at the feeder than the others and still maintained modest weight gain (circled in Figure 127). Pig 4906205 shown in the square in Figure 127 is of interest as it appears to dominate the feeder space and is also potentially overfeeding as it spent 1.8 times longer at the feeder than its nearest pen-mate (pig 4906481), while there was no difference in weight gain between these two animals (refer to Table 53 and Table 55). The poor gain experienced by the two pigs with the lightest starting weights (left of Figure 127) indicated that these two pigs were potentially sick. In fact these two pigs (4906356 and 4906777) were medicated on the 7/4/11 and grew substantially after the treatment, indicating that the treatment had worked (see Table 55).

7.3.3.2 *Individual and Group Feeding Behaviour*

Each pig's attendance at the feeder was broken into an hour by hour, minute by minute and second by second account. The matrices in Figure 128 contain the attendance at the feeder during the day in the columns and the ID of the pig that attended the feeder in the rows, as structured by the software. A green rectangle at a given hour (0-23) indicates that the pig was recorded present at the feeder for a second during that hour. All 16 pigs were recorded at the feeder. The left hand column of Figure 128 shows the first four days of logged data by the RFID system. The right hand column contains data collected from all the days when the RFID system was running.
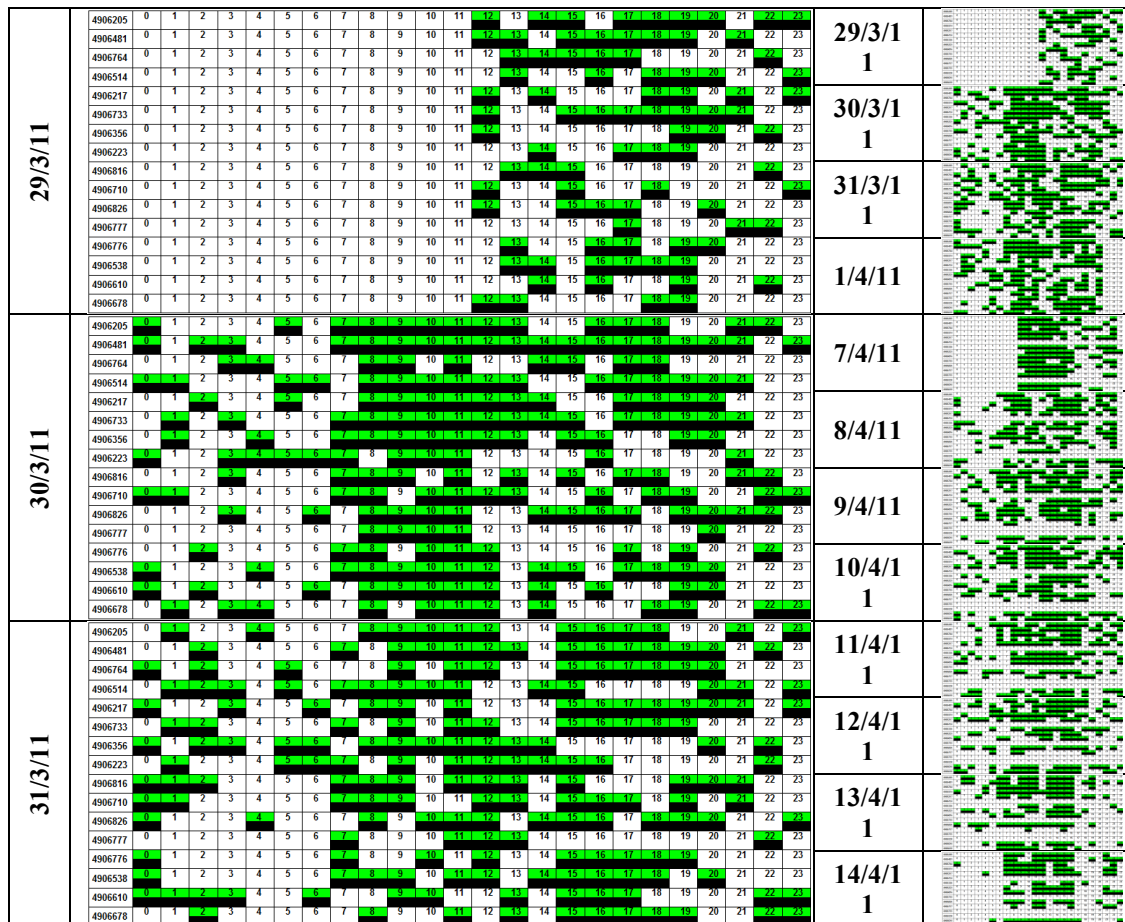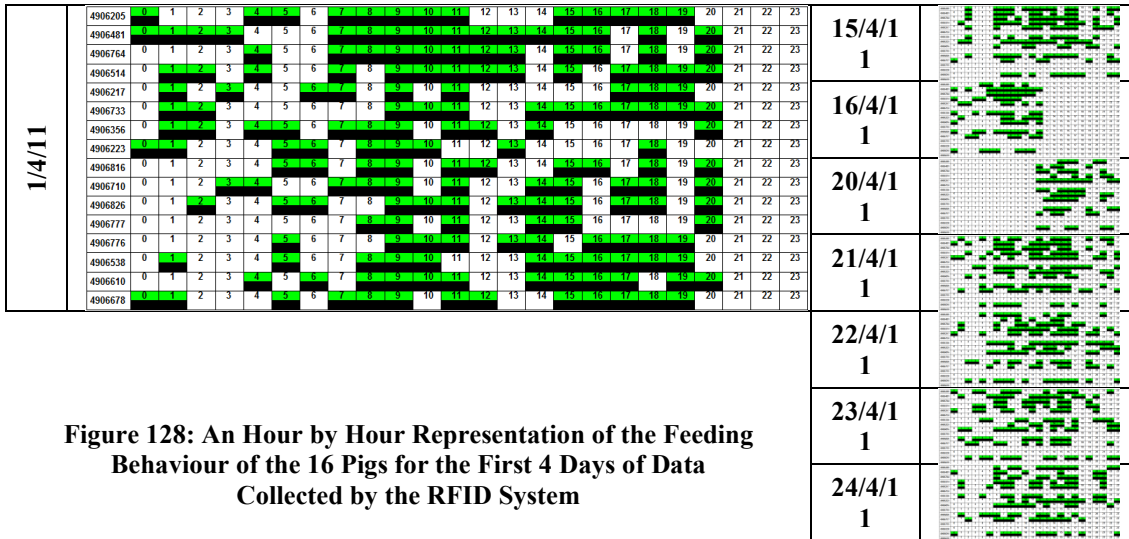
Figure 128: An Hour by Hour Representation of the Feeding Behaviour of the 16 Pigs for the First 4 Days of Data Collected by the RFID System

The demand for the feeder can be observed across the days by looking down the columns at each hour of Figure 128. During some hours all 16 pigs visited the feeder, while during other hours only two or three animals fed.

To determine demand for the feeder, all of the complete days of data when the system was operational were assessed (30/3/11 to the 31/3/11, the 8/4/11 through to the 15/4/11 and the 21/4/11 through to the 24/4/11). The average hourly demand for the feeder was calculated by summating the number of seconds pigs were in attendance at the feeder within each hour from these days. A profile of the demand for the feeder over the course of a day based on the seconds of attendance within each hour can be seen in Figure 129.
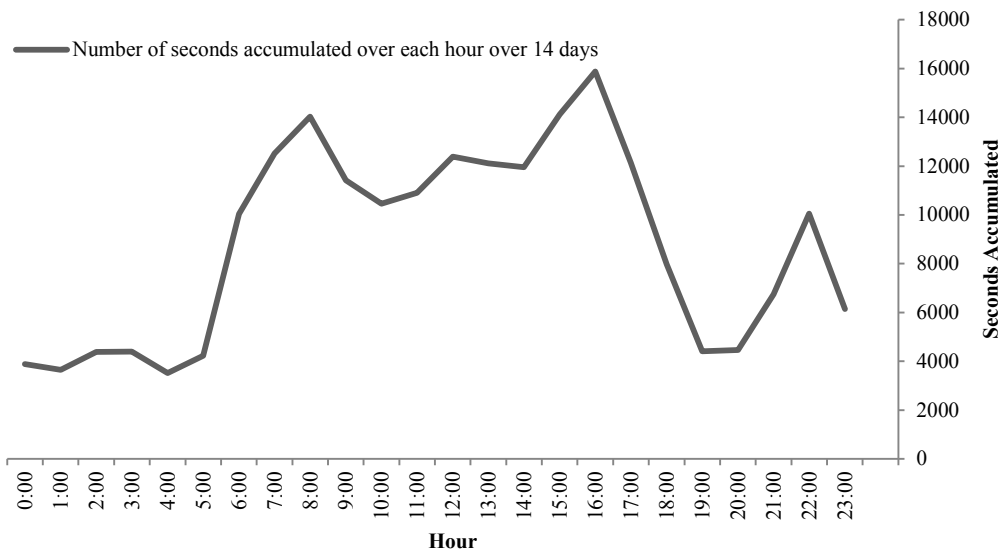
Figure 129: Demand Profile at the Feeder over the Course of a Day; Seconds Accumulated During Each Hour over 14 days

Peak demand for the feeder in this pen occurs in the afternoon between 15:00 and 16:00 and in the morning at 08:00. A considerable drop in presence at the feeder is experienced between 18:00 and 19:00 and a large increase is experienced between 05:00 and 06:00.

191

Figure 130 shows the accumulated attendance at the feeder across each hour of the day for the 14 complete days of data. There are three key effects which can be observed from this Figure. First, the data logged on March 30th and 31st had the most attendance at the feeder. This is probably because, as the trial progressed, pigs were removed from the pen and demand decreased accordingly. This demand decrease can be seen between the 31/3/11 and the 8/4/11 as during this time two pigs were removed. Dates when pigs were removed are circled in the legend of Figure 130.
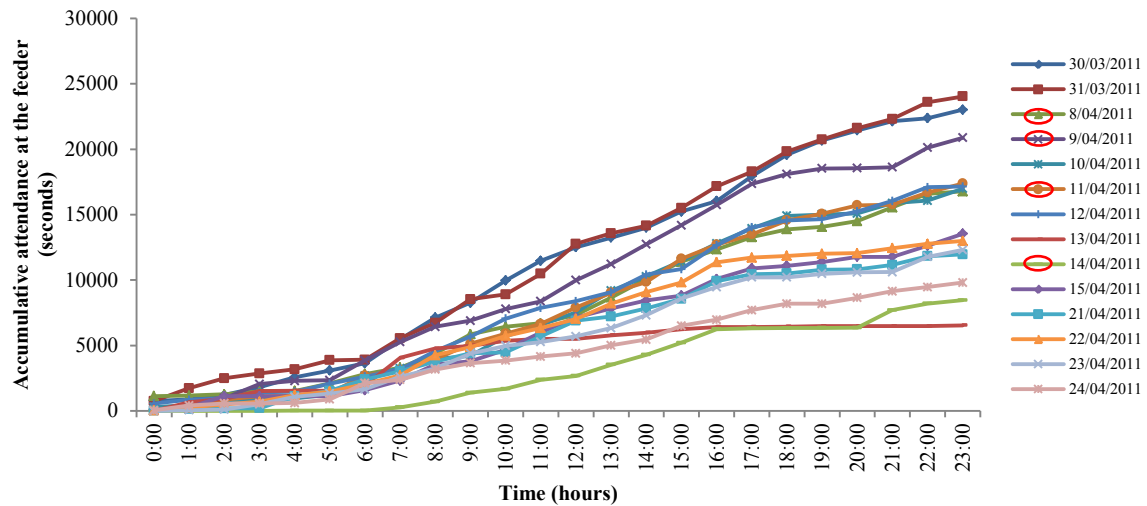
Figure 130: Accumulative Attendance at the Feeder on 14 Trail Days

The second effect can be seen on the 9/4/11 where there is considerably more activity around the feeder, even though another pig was removed on this day. This was potentially caused by the weather, as the 8/4/11 was the hottest day (31.0°C) since the 7/3/11. Thus, this may suggests that the pigs feed more frequently in the comfortable and relatively constant conditions occurring on the 9/4/11 (min 16.5°C, max 19.4°C). The third effect occurred on the 13/4/11 and 14/4/11 of April. The days surrounding this data are plotted again in Figure 131 for clarity. A plateau can be observed between 08:00 on the 13/4/11 and 07:00 on the 14/4/11 after a relatively normal attendance profile on the 12/4/11. This plateau meant that the pigs were not attending the feeder during this time.
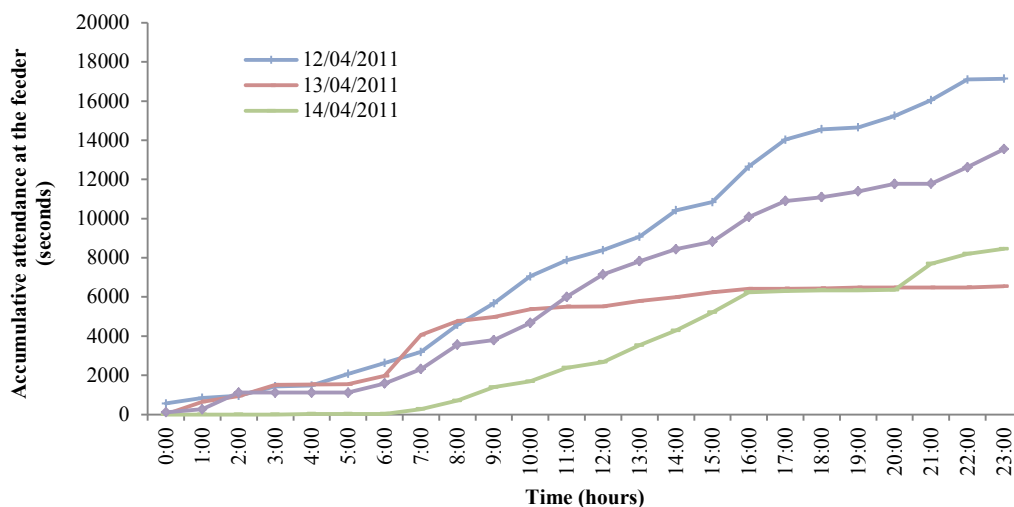
Figure 131: Accumulative Attendance at the Feeder on Four Trail Days Surrounding an Out of Feed Event

192

The likely cause of this lack of attendance was an out of feed event which was caused by coagulation of feed in the base of the feeder-hopper, which subsequently blocked the delivery of the feed through to the trough. A worker at the piggery discovered and fixed this problem on the 14/4/11, however, the plateau in attendance first began on the 13/4/11 which may indicate that the checks performed the previous day failed to detect the problem and the pigs were without feed for over a 24hr period. Such a delay in fault-identification would be understandable, as the underlying problem was well hidden by the fresh feed on the surface of the feeder hopper and was only visually identifiable by observing that the trough had been licked clean. All the feed had to be removed to get to the blockage and was spread around the pen which would have had an effect on the attendance at the feeder on the 14/4/11.

7.3.3.3 *Competitive Behaviours between the Pigs*

Previously, Figure 128 presented the attendance of each pig at the feeder for each hour of the day. However, the content of the black region under each of the green rectangles in Figure 128 is hard to observe without first zooming-in. Figure 132 (a) and (b) show that the minutes that each pig was present are within these rectangles.
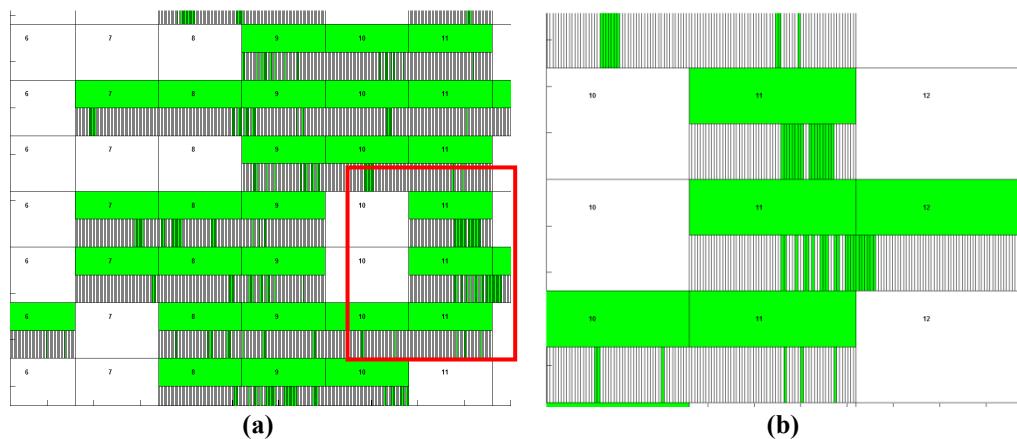
Figure 132: (a) Observing the Minute by Minute Attendance at the Feeder between Pigs; (b) Close-up of the Rectangular Section Shown in (a)

Overlapping minutes between two different pigs may indicate that a competitive interaction occurred to gain access to the feeder (Figure 132 (b)). Subsequently an investigation was undertaken to determine whether the system had logged any conclusive interactions between pigs at the feeder.

To achieve this, a data search was undertaken to find seconds where the identity of two different animals had been recorded. Identification numbers recorded with identical timestamps indicated that both animals must have had their head inside or within close proximity to the single space feeder. Consequently, it is highly likely that one of the pigs involved was attempting to gain access to the feeder and an interaction between two pigs had taken place (examples have been shown previously in Figure 125 (a) and (b)). Over the complete days of data, there were 918 occasions when two or more ID reads were recorded in this manner.

Table 56 shows the interaction between pigs ranked in order of most interactions to least interactions. Note that some of the pigs were removed over the trial period and

therefore will have fewer counts; these were pigs 4906733, 4906710, 4906776, 4906538 and 4906678.

Table 56: Interaction Matrix Between the 16 Pigs

	4906764	4906481	4906826	4906710	4906223	4906514	4906777	4906205	4906678	4906217	4906356	4906816	4906610	4906733	4906776	4906538	Counts	Weight 29/3/11	Weight 21/4/11
4906764	0	27	33	4	20	33	21	30	18	8	13	4	6	10	0	12	239	71.5	99
4906481		0	24	18	20	12	11	7	9	8	9	10	5	6	4	2	172	59.5	88
4906826			0	10	22	13	14	4	2	16	8	9	4	0	9	1	169	54	72
4906710				0	15	14	20	10	17	12	12	7	3	9	9	2	162	67	
4906223					0	6	6	12	6	12	13	8	6	3	4	0	153	55.5	81.5
4906514						0	14	12	9	13	2	4	1	2	0		137	50	73.5
4906777							0	6	2	4	7	1	11	4	3	0	124	46.5	56.5
4906205								0	7	5	5	7	4	0	4	1	114	69	97.5
4906678									0	8	9	5	11	1	1	1	106	65.5	
4906217										0	1	5	2	1	2	1	98	58	80.5
4906356											0	3	1	1	1	2	87	47	57.5
4906816												0	1	13	0	0	75	73.5	97.5
4906610													0	0	2	1	61	57.5	75.5
4906733														0	1	9	59	45.5	
4906776															0	3	45	69	
4906538																0	35	61	

The pig which experienced the most interactions (239) with its pen-mates was pig 4906764. This pig was also the largest in the group when the group was formed; starting at 63.5 kg on the 18/3/11 and finishing at a 99 kg on the 21/4/11 (see Table 55).

To determine which pigs initiated the interaction and subsequent competitive behaviour the identity of the pig ID logged prior to the interaction was determined. This indicated which animal was at the feed space first; the one defending the feed space. The following table (Table 57) shows the previous matrix broken up into aggressive and defensive interactions based on this assumption.

Table 57: Defensive and Aggressive Actions Between the 16 Pigs

	4906764	4906481	4906826	4906710	4906223	4906514	4906777	4906205	4906678	4906217	4906356	4906816	4906610	4906733	4906776	4906538	Counts	Weight 29/3/11	Weight 21/4/11
4906764	125	14	11	3	7	14	10	16	12	3	8	1	5	3	0	7	239	71.5	99
4906481	13	82	13	7	9	8	6	3	5	6	5	6	2	4	3	0	172	59.5	88
4906826	22	11	74	5	12	6	11	1	1	9	2	5	3	0	6	1	169	54	72
4906710	1	11	5	82	6	6	9	7	9	7	3	4	0	5	5	2	162	67	
4906223	13	11	10	9	74	3	2	5	4	7	8	4	0	2	1	0	153	55.5	81.5
4906514	19	4	7	8	3	66	8	5	5	5	2	1	3	1	0	0	137	50	73.5
4906777	11	5	3	11	4	6	65	2	0	3	6	1	5	1	1	0	124	46.5	56.5
4906205	14	4	3	3	7	7	4	54	4	2	3	5	2	0	2	0	114	69	97.5
4906678	6	4	1	8	2	4	2	3	56	4	4	4	5	1	1	1	106	65.5	
4906217	5	2	7	5	5	8	1	3	4	53	1	1	0	1	1	1	98	58	80.5
4906356	5	4	6	9	5	0	1	2	5	1	47	2	0	0	0	1	88	47	57.5
4906816	3	4	4	3	4	1	0	2	1	3	1	41	0	7	0	0	74	73.5	97.5
4906610	1	3	1	3	6	1	2	6	2	1	1	1	25	0	2	1	61	57.5	75.5
4906733	7	2	0	4	1	0	3	0	0	0	1	6	0	30	0	5	59	45.5	
4906776	0	1	3	4	3	2	2	2	0	1	1	0	0	1	23	2	45	69	
4906538	5	2	0	0	0	0	0	1	0	0	1	0	0	4	1	21	35	61	

The total number of potentially defensive actions that each pig was involved in are highlighted along the main diagonal of Table 57. The remaining cells in the columns show which individuals initiated the competitive interaction at the feeding space for the pig identity in the top row. The remaining cells along the rows show the potentially aggressive actions caused by each pig towards the others to gain access to the feeder. For example, pig 4906764 had 125 defensive actions out of 239 total

194

interactions. Of these interactions, pig 4906764 was most likely to be defending the feeder space against pig 4906826 which made 22 attempts to gain access to the feeder while it was feeding. Pig 4906764 was potentially most competitive and aggressive toward pig 4906205 as it made 16 attempts to gain access to the feeder while pig 4906205 was feeding. Interestingly pig 4906481 that had the second highest attendance rate and weight gain also had the second highest number of interactions, however in contrast, pig 4906205 which had the highest attendance at the feeder and greatest weight gain was in the middle of the list of interactions at 8th position. Perhaps this indicates that other pigs were intimidated by pig 4906205 and avoided the feeding area while pig 4906205 was feeding.

The percentage of aggressive and defensive actions for each pig was determined relative to the total interactions. These were also ordered in relation to their weight when the RFID system commenced operation on the 29/3/11 to indicate what role weight might play in these interactions.

Table 58: Potentially Passive and Aggressive Actions from Each Pig within the Pen

Pig	Total	Aggressive	Passive	Aggressive %	Passive %	Weight 18/3/11	Weight 29/3/11
4906733	59	29	30	49	51	42	45.5
4906777	124	59	65	48	52	44.5	46.5
4906356	88	41	47	47	53	38.5	47
4906514	137	71	66	52	48	43	50
4906826	169	95	74	56	44	47.5	54
4906223	153	79	74	52	48	46.5	55.5
4906610	61	36	25	59	41	48	57.5
4906217	98	45	53	46	54	50.5	58
4906481	172	90	82	52	48	51.5	59.5
4906538	35	14	21	40	60	49	61
4906678	106	50	56	47	53	55	65.5
4906710	162	80	82	49	51	55	67
4906205	114	60	54	53	47	55.5	69
4906776	45	22	23	49	51	57.5	69
4906764	239	114	125	48	52	63.5	71.5
4906816	74	33	41	45	55	61.5	73.5

The data presented in Table 58 indicates that the lighter pigs were more likely to be pushed out of the feeder, while the most aggressive interactions were caused by pigs in the lower half of the middle of the group. The data indicates that the heavier pigs were also more inclined to be passive, although, of the heavier pigs 4906205 stood out as the most aggressive. The results from Table 58 are plotted in Figure 133 for the eleven pigs that remained in the pen for the duration of the trial. It is believed that this may illustrate the group dynamic on some level in respect to weight.
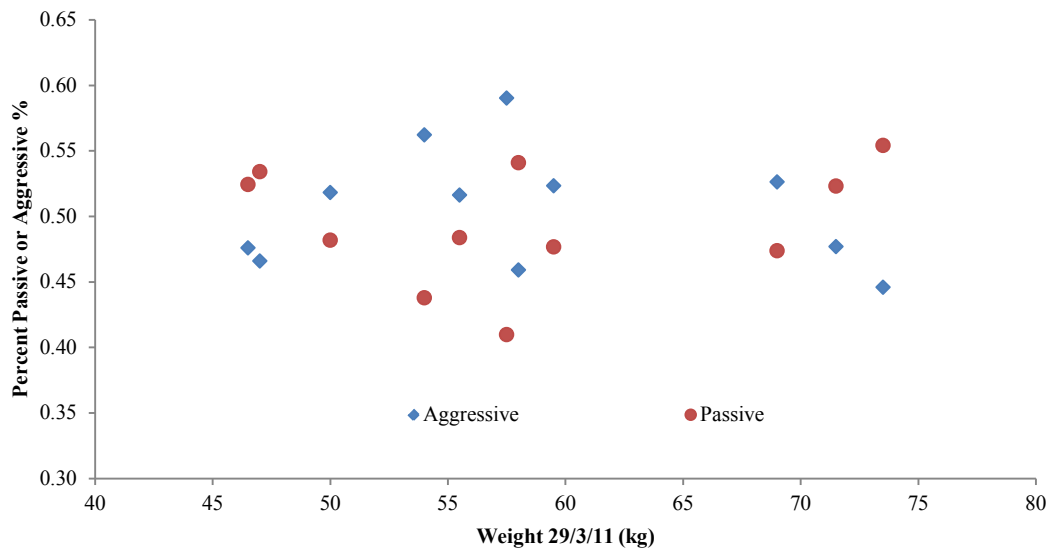
Figure 133: Plot of Potential Passive and Aggressive Actions of the Group

7.3.4 Discussion on Feeding and Social Behaviour

Previously, feeding systems that include individual identification have been used to determine the feeding behaviour of small groups of grower-finisher pigs. Georgsson and Svendsen (2002) found that pigs in the middle-weight group gained the most weight and "neither the large nor the small pigs showed any tendency to have different eating rates in the two treatments". These comments are consistent with the weight gain trends shown in Figure 126 and Figure 127.The high rate of feeding by the middle-weight pigs in a pen with a single feeder is also consistent with their findings (shown in the trend of minutes spent at the feeder in Figure 126 and Figure 127). Furthermore, this study arrived at similar theories why this was so. Large pigs "were expected to have high positions in the hierarchy and thereby had the privilege of eating in their preferred manner", while medium pigs were "put under a higher social pressure" and were effectively trying to catch the larger ones (Georgsson and Svendsen, 2002, p 380-382). The smaller pigs struggled to keep up with the group (such as Pig 4906777 Figure 125 (a) and (b)).

Gathering information in this manner may be useful in determining the social hierarchy within groups of pigs in production scenarios, as highly competitive animals may be identified and managed to benefit both animal production and animal welfare (Hoy *et al.*, 2009). Some studies show that the order in which sows enter electronic sow feeding stations can be used to indicate the social hierarchy of the group on some level, with higher ranking sows entering the feed station earlier in the day (Jensen *et al.*, 2000; Hoy *et al.*, 2009). Alternatively, multiple RFID monitoring stations strategically placed in the pen environment can be used to record and model the behaviour of livestock species (Naas *et al.*, 2001). RFID might also be used to identify and select placid, fast-growing pigs within breeding programs to improve the production performance of herds.

7.4 CONCLUSIONS

The piGUI system was integrated with RFID to facilitate the recording of individual animals. Subsequently, the piGUI system was tested under challenging commercial

196

conditions in a pen housing slow growing pigs. Feeding behaviour and bias in the vision system was determined at the installation location. Modifications were made to the software to overcome RFID communication issues. During the trial the piGUI system had difficulty identifying certain pigs. The three primary causes of this bias were, (i) certain pigs did not feed as frequently leaving less opportunity to gather a weight estimate for that individual (a layout bias), (ii) the shape filter was excluding the assessment of certain pigs as it was set to strictly or required further modification and (ii) the behaviour of the pigs around the feeder made it more difficult for estimates to take place, which is most probably related to feeder demand. The RFID system also produced potential causes of bias that the reader should be wary of including, (i) the body positioning (style) in which the pig feeds in relation to the antenna, (ii) the positioning of the ear tag on the pig's ear, (iii) the condition of the pig's ear (cauliflower ear), (iv) the position of the antenna in the feed space and (v) environmental interference such as a build-up of dirt on the ear tag.

The minimum amount of time a pig spent in close proximity to the feeder was used to give an indication of its feeding behaviour (attendance). Weight gain appears to share a similar trend with the amount of time spent at the feeder, with the pigs that spent the most time around the feeder gaining the most weight. Certain pigs appear to dominate the feed space, potentially overfeeding while others are potentially underfeeding. Further trials and modelling in this area are warranted to determine the relationship's strength and use in practice. Future trials in this area should also ensure that an ID read will occur every time a pig's head is inside the feeder. This may require shielding and a secondary antenna.

Peak demand for the feeder was found to be in the afternoon between 15:00pm and 16:00pm and in the morning at 8:00am for the 14 days of data recorded. During these times the feed supply should be monitored and adjusted accordingly to ensure that the demand is fulfilled. The accumulative attendance data obtained in this trail indicated that the attendance at the feeder decreases when there is no feed available. If this is the case, a system with the ability to determine the presence of animal at the feeder (such as an RFID system or the piGUI system) has great potential to identify out of feed events so that they can be better managed. The accumulative attendance also has potential to be used to standardise or regulate the stocking density of a pen in relation to the number of feeders, as attendance appears to be related to weight gain. High levels of attendance may indicate under-supply and increased competition, while low levels may indicate space wastage. The accumulative attendance may also be used to identify when animals have been removed from the pen (traceability), to identify when workers undertake jobs within the pen and to quantify feeding behaviour in respect to temperature fluctuations.

The number and type of interactions around the feeder was determined between pigs under the assumption that a pig was passive if it resided at the feeder, while a pig was aggressive if it was trying to gain access to the feeder. The pig with the heaviest starting weight and ending weight had the most number of interactions. The lighter pigs were more likely to be pushed out of the feeder, while the most aggressive interactions were caused by pigs in the lower half of the middle of the group. The data indicated that overall the heaviest pigs were also more inclined to be passive. These findings were consistent with similar studies. Interestingly, the most aggressive of the heavier pigs spent 1.8 times longer at the feeder and gained more

weight than any other pig. In future studies, the duration between the interactions at the feeder can be assessed over an extended interval of several seconds or more rather than just a single second, as this could be used to determine whether any regular swapping between animals occurred and whether certain pigs had a tendency to feed at particular times.

Integrating both weight information from the piGUI system and the identification information from the RFID component can also be used to determine the growth and weight gain of individual pigs and provide more robust estimates of group averages. Although, related studies have demonstrated that the average weight of groups of pigs can be determined with acceptable practical accuracy without the aid of RFID tags. Potential also exists to identify pigs that are more likely to have good or poor feed conversion, and pigs that are likely to require medical treatment. The pigs that dominate or are competitive around the feeder can also be identified so that control measures can be implemented. The software written to analyse the RFID data presented here could be up-scaled to cater for much larger groups of animals and additional RFID stations at extra feeding points.

Chapter 8

Comparison between PiGUI and a Commercial System

ABSTRACT

Machine vision can be used to recognise and determine the live weight and growth of pigs. This chapter presents a comparative study between two vision systems performing this task. These two systems are (i) a commercially available system labelled 'System-A' and (ii) the system developed as part of this thesis named piGUI. Both of these methods are non-invasive and operate under very similar principles. They both extract the pig's body measurements from video frames and use them to estimate the pig's weight and subsequent growth. Despite following calibration and installation procedures correctly, System-A failed to yield accurate weight estimates during testing. During the second trial, the piGUI system estimated the group average weight to within 2.1% on each the seven days when the actual weight of the pigs were determined using the electronic scale. Over the same period, System-A reported group average weight estimates in excess of 16 kg error of the actual group average weight of the pigs on each of these seven days. Consequently, the data outputted by System-A would need to be scaled by a factor to obtain weight estimates close to actual group weights. Overall the piGUI system was more accurate, simpler to install, and was better suited to the environment.

8.1   INTRODUCTION

Phillips and Dawson (1936) presented a manual method to estimate the weight of pigs from body measurements recovered from images. However, they experienced practical limitations related to identification and manual recovery of a pig's body measurements within the images. Since the invention of computers, these limitations have been overcome. As intelligent software methods can now effectively automate the body measurement and extraction process. This allows for a continuous stream of weight estimates and growth information to be recorded with no operator involvement (Schofield *et al.*, 1999).

Only a few machine vision systems are currently commercially available that are able to provide, daily, non-invasive estimates of pigs' growth rate. These systems such as eYeScan (Fancom, Panningen, The Netherlands) and Qscan (Innovent Technology Limited, Turriff Aberdeenshire, UK) are based on a system developed at the Silsoe Research Institute, and originally sold by Osborne Industries Incorporated as a product called Vista™ (Wang *et al.*, 2006). Promotional material of these products, found on the respective company's websites and in some articles (Stickney, 2009), are synonymous with the features of the Vista™ system. Another separate development is the OPTisort system (Hoelscher & Leuschner, Emsbüren, Germany). This system operates as a vision-based classifier to sort the pigs into respective pens depending on their weight range. While this system operates under similar principles, it has invasive hardware components, such as sorting gates, which are physically present within the pen area and has environmental control in the form of artificial lighting. As this product's characteristics do not align with the non-contact and flexible aims of the piGUI system it was not assessed.

The literature states that machine vision systems have been shown to estimate the weight of pigs to within 5% of the pig's actual weight in literature (Schofield, 1990). However, commercial systems claim that they can perform within a maximum deviation of 3% in precision.

The commercial system tested and evaluated against the piGUI system in this chapter has been labelled 'System-A'. System-A was chosen as it most similar in its function to the piGUI system.

8.2   MATERIALS AND METHODS

The software and hardware components (camera and frame grabber) of System-A were purchased and supplied from the company and installed. The software and piccolo frame grabber was installed on a Hewitt Packard DC7100 computer 2GB RAM, Pentium 4 (3 GHz) PC (frame grabber is pictured on the right of Figure 134 and Figure 135). The dimensions of the PC were 100.3 × 337.8 × 378.5 mm. The piGUI system software developed as a part of this study was installed onto a Fit2pc (fit2PC, CompuLab Ltd, Technion, Haifa, Israel) (Figure 134 and Figure 135 left). This computer was chosen to overcome several problems experienced using desktop computers in the piggery environment. The compactness of the Fit2pc (115 × 101 × 27 mm) effectively minimise the chances of rodent or insect infestation.

Figure 134: Comparison between equiptment size, PC for piGUI system (Left), System-A's frame grabber board (right)

The Fit2pc is 40 times smaller than PC used for the System-A (see Figure 135) and uses a passive cooling system which avoids moisture and dust being drawn into the PC by fans. The small size of the PC used in the piGUI system enabled the system to be easily mounted and transported.
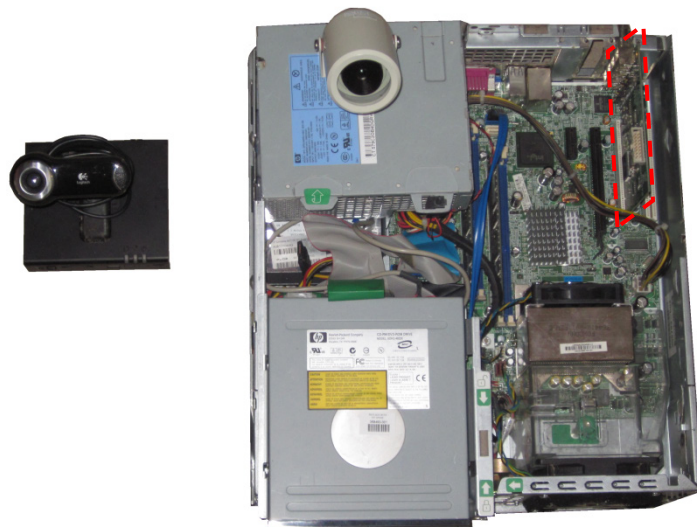
Figure 135: Comparison between equiptment size; piGUI system (left top); System-A (right, frame grabber location dashed); System-A's camera (top centre)

8.2.1   Experimental Setup and Location

For comparative purposes, both systems were setup to observe an identical location within a pen of finisher pigs at a commercial facility (PPPI, University of Adelaide, Roseworthy campus). In this manner the growth of the same group of pigs could be recorded by each systems simultaneously. The pigs' weights were obtained periodically during the trial using an electronic weigh scale (Pig Weigh Crate, Ruddweigh, Guyra, Australia, ±1%). The cameras were positioned above a single feeder located in a corner of the pen which could house up to 17 finisher pigs (see Figure 136 for layout).
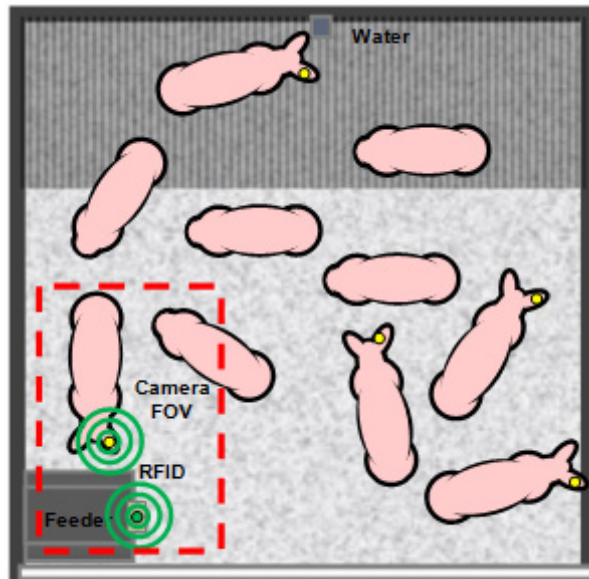
Figure 136: The Experimental Setup at the Facility

8.2.1.1 System-A Installation

System-A was calibrated according to instructions provided by the software distributer. This involved the creation of a bone-shaped template that the system was required to observe at initialisation of the system (Figure 137).

(a)   (b)
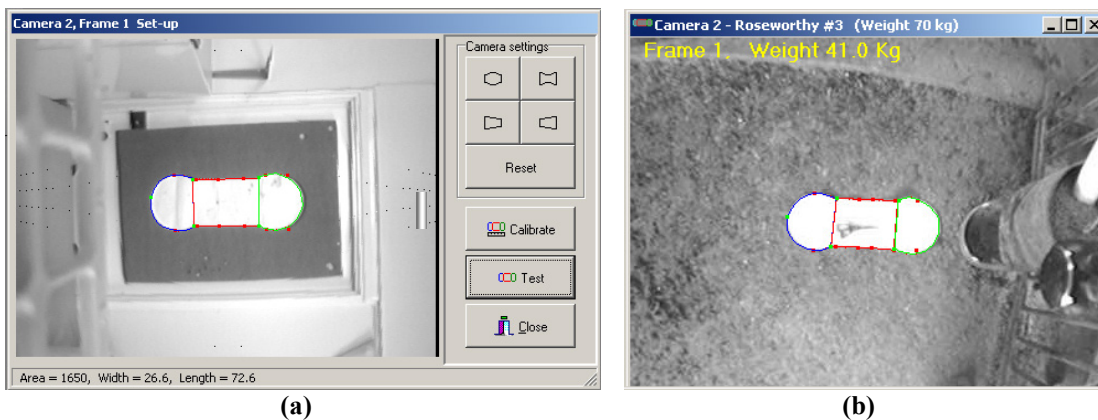
Figure 137: (a) Example of System-A's Calibration Setup and Bone-Shaped Template (a and b)

According to System-A's instructions, when calibrated correctly the weight estimate of the bone-shaped template should yield a result of 41 kg (Figure 137 (b)). During calibration, any image-distortion caused by the wide angle lens could also be corrected Figure 137 (a).

System-A was installed at a height of 2100 mm and this value was entered into the software settings. The actual average group weight of the pigs was also entered into System-A's settings as a guide to a base future estimates on (Figure 138). However, the installation height and calibration procedure for the System-A varied as attempts were made to calibrate the software to output accurate weight estimates. These calibration attempts failed to yield accurate weight estimates.
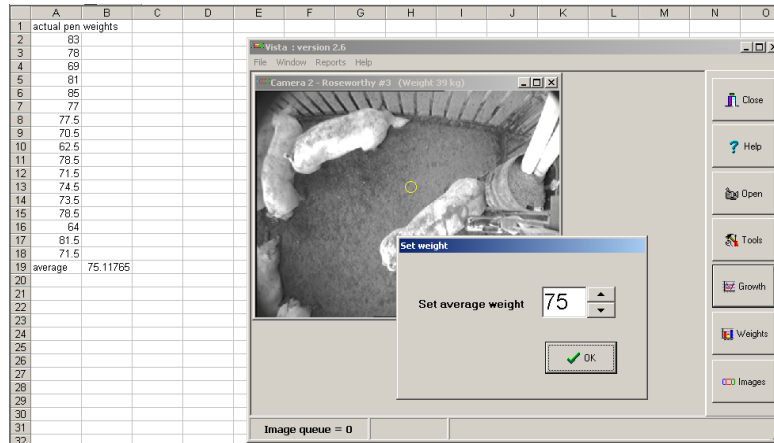
Figure 138: Setting the Average Weight of the Group of Pigs for System-A

8.2.1.2 PiGUI Installation

The piGUI systems camera (Quickcam Pro 9000, Logitech, Quarry Bay, Hong Kong) was installed at a height of 1680 mm. The only calibration and user input required for the piGUI system to operate correctly was the installation height of the camera (lens to ground) (see Figure 144). The piGUI systems camera firmware automatically took care of the image distortion and large light variances.
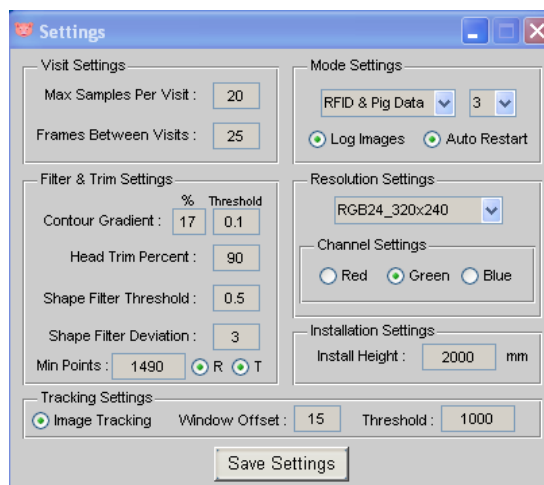
Figure 139: Setting the Installation Height among Other Parameters in the PiGUI System

8.3   RESULTS AND DISCUSSION

8.3.1   Trial 1

System-A and the piGUI system were set up to observe a group of finisher pigs between the 9/1/10 and the 11/1/10. A similar pattern of growth was recorded by both systems, however, System-A was reporting weights outside the finisher pig weight range (see Figure 140).
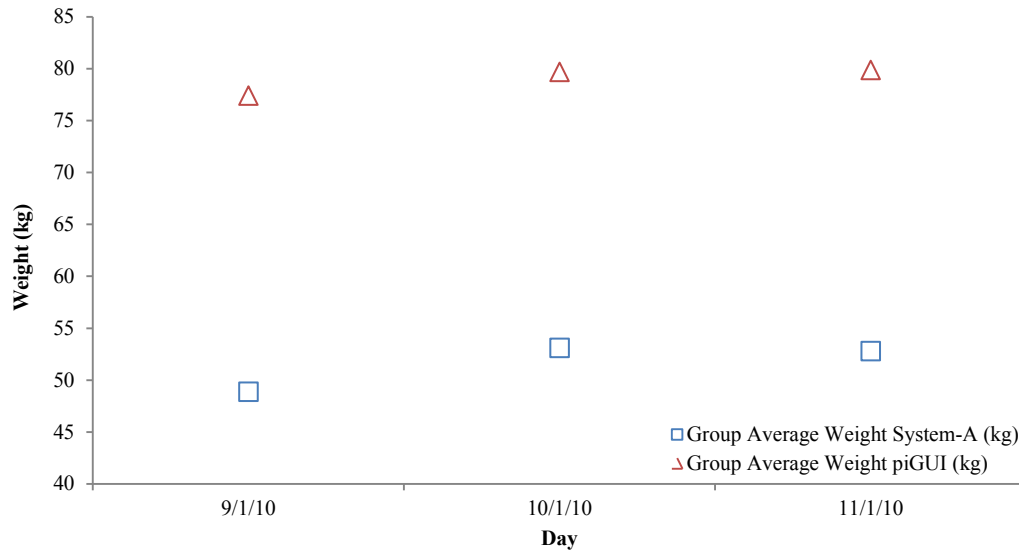
Figure 140: Weight Estimates Reported by the PiGUI System and System-A for Finisher Pigs

A summary of the data collected can be found in Table 59.

Table 59: Summary of Data Collected by System-A and the piGUI System from 9/1/10 to 11/1/10

	piGUI 9/1/10	System-A 9/1/10	piGUI 10/1/10	System-A 10/1/10	piGUI 11/1/10*	System-A 11/1/10*
Samples	315	60	454	140	164	35
Images	1923	108	3476	296	1185	61
Average	77.39	48.86	79.66	53.09	79.87	52.78
Deviation	9.79	11.64	12.17	13.91	14.23	15.34
Min	21.72^	23.79	21.15^	28.45	19.89^	27.30
Max	99.84	65.42	103.10	76.61	101.63	75.68
Range	78.12	41.63	81.95	48.15	81.74	48.39

*Results are shown up to 10:45am, ^Result of false of identification

The cameras were mounted on the same stand above the same feeder. However, System-A captured considerably less data than the piGUI system under the same conditions, as the histograms of the acquired data in Figure 141 (a) and (b) illustrate. An identical Y-axis scale has been used to highlight the difference between the numbers of samples collected by the two systems.

(a)

(b)
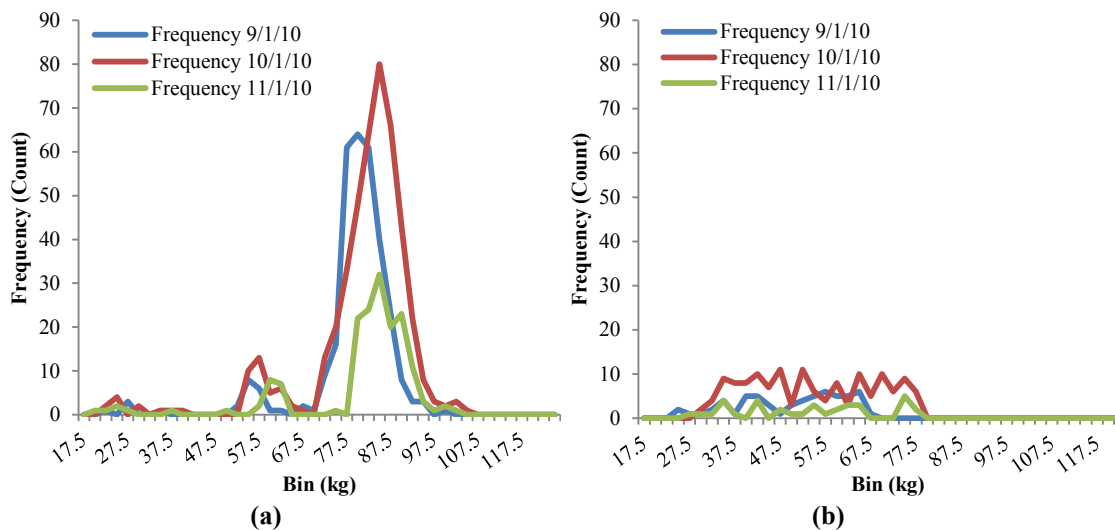
Figure 141: Comparing Histograms of the PiGUI System (a) and System-A (b)

206

A scatter plot of the raw data collected by the data piGUI system and System-A are shown in Figure 142 (a) and (b) respectively. The data collected by System-A is spaced out over a 40 kg range whereas the piGUI data are more heavily clustered around a mean value.
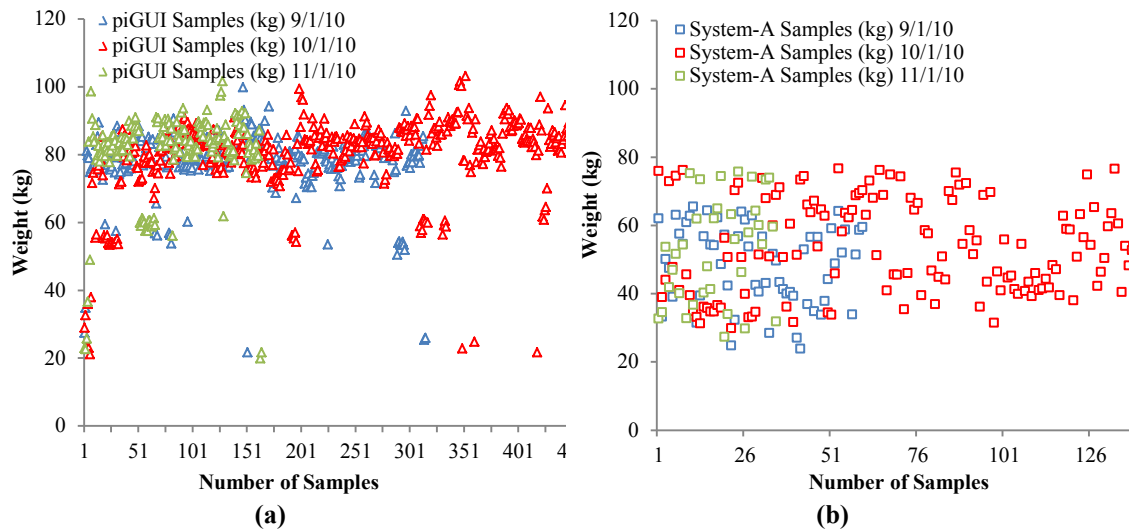
Figure 142: Scatter Plot Weight Estimate Samples Obtained by piGUI (a) and System-A (b)

Interestingly, it also appears that System-A did not pick up on the smaller pig (~60 kg) within the pen shown in Figure 143.
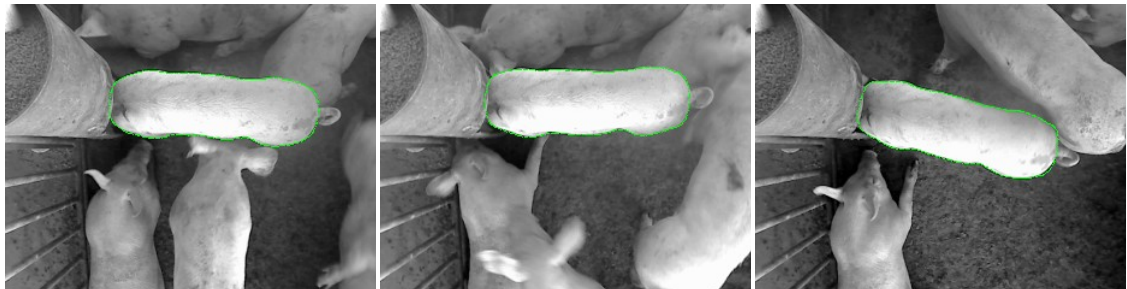
Figure 143: A Considerably Smaller Pig Identified by the piGUI System Within the Pen

Further work on the piGUI system was required to eliminate the small number of errors (~1% of the total estimates) shown below 40 kg in Figure 142 (a). These errors generally occurred at dusk and dawn from false identification.

8.3.2 Trial 2

Twelve finishing pigs were housed in a pen between the 24/1/11 and the 15/2/11. The System-A and the piGUI system were installed and in a protected region of a pen adjacent to the trial pen. The cameras were orientated such that they observed the region surrounding the feeder (Figure 144 (a) and (b)). Both systems were checked routinely between the 24/1/11 and 27/1/11. During this time the average weight of the group of pigs was determined using an electronic scale so that the results of the two vision-based methods could be validated against the conventional weighing method. In addition, a shape filter was incorporated into the piGUI software to reduce the occurrence of the false positives experienced in the first trial.

<center>(a)   (b)</center>
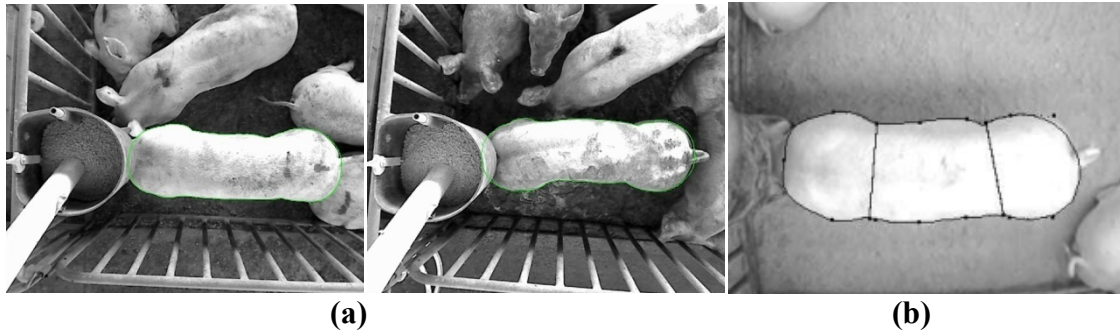
Figure 144: Examples of Pigs Captured by the (a) PiGUI System and (b) System-A

The pigs were temporarily removed from the pen by farm staff on the 1/2/11 for routine cleaning of the pens. A pig which had sustained an injury was set aside and the remaining eleven pigs were returned. On the 4/2/11 System-A reported an error and the backup camera settings were applied to correct the problem. It was discovered that backup settings applied to System-A on the 4/2/11 were incorrectly configured. Subsequently, the camera installation height and the zoom level and were modified. At this time the pigs were weighed. The average weight for System-A was set at 89 kg (88.7 kg) and System-A was calibrated to one of the animals.

A comparison between the actual group average weight and the averages determined by the piGUI and commercial system is shown in Table 60.

Table 60: Weight Estimates Calculated by System-A and the PiGUI System between the 24/1/11 and 15/2/11

		Average	Error				Average	Error
24/1/211	Scale (Actual)	76.6	-		**8/2/11**	Scale (Actual)	88.7	-
	piGUI	76.2	-0.4			piGUI	87.8	-0.9
	System-A	114.3	37.7			System-A *	50.4	-38.3
27/1/11	Scale (Actual)	80.2	-		**11/2/11**	Scale (Actual)	92.9	-
	piGUI	80.6	0.4			piGUI	93.6	0.7
	System-A	114.9	34.7			System-A	40	-52.9
1/2/11	Scale (Actual)	82.1	-		**15/2/11**	Scale (Actual)	97.4	-
	piGUI	80.4	-1.7			piGUI	97.5	0.1
	System-A	115.8	33.7			System-A	43.3	-54.1
4/2/11	Scale (Actual)	84.7	-					
	piGUI	84.9	0.2					
	System-A	101.1	16.4					

<center>* After 16:50pm System-A's zoom was changed after applying backup settings</center>

System-A's software consistently reported large errors in weight estimates (see Table 60). Changing the zoom level increased this error. The fact that changing the zoom level of the camera changed the weight estimation output indicated that a fundamental hardware and software conversion procedure was absent in System-A. Despite System-A's error margin, the data it recorded did indicate that it was recording growth on some level, but the recordings were considerably out of scale in relation to the installation instructions and zoom level settings. The raw weight data obtained from the piGUI and System-A system is shown in Figure 145. The effect that the change in zoom level had on System-A can be seen after the 8/2/11. The piGUI system estimated the group average weight to within 2.1% on each the seven

<center>208</center>

days when the actual weight of the pigs were determined using the electronic scale. Over the same period, System-A reported group average weight estimates in excess of 16 kg error of the actual group average weight.
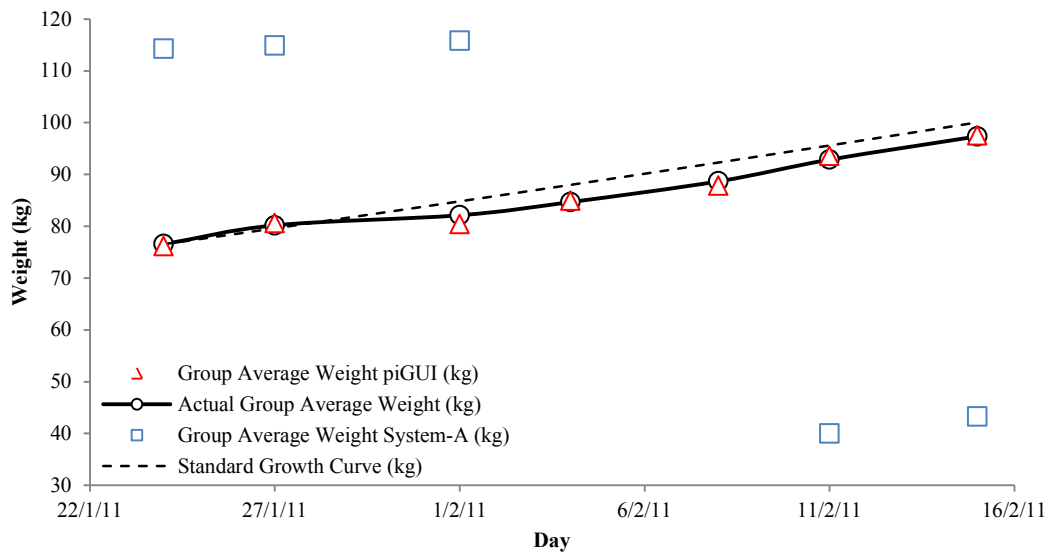
Figure 145: Comparative Data Recorded by the PiGUI system and System-A between the 24/1/11 and the 15/2/11

8.3.3 Trial 3

Both systems monitored a group of eleven pigs between the 22/2/11 and the 18/3/11. So that the weight estimates of both systems could be validated, the average weight of the pigs was determined using the electronic scale on three days during this period. The raw weight data obtained from the piGUI and System-A system is shown in Figure 146.
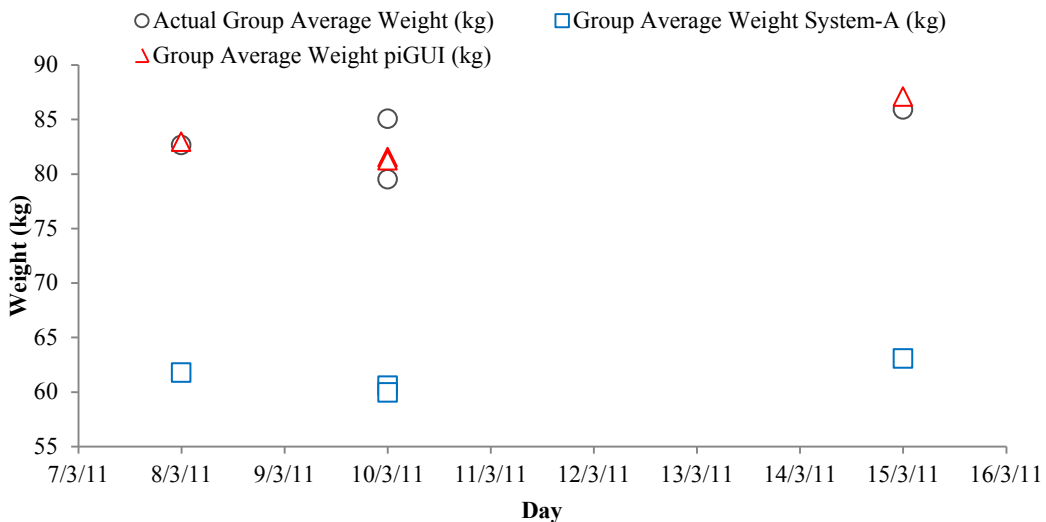
Figure 146: Comparative Data Recorded by the PiGUI system and System-A between the 22/2/11 and the 18/3/11

On the 10/3/11 six pigs that were greater than 85 kg were removed from the pen to be taken to market. This separation occurred at 13:30. Hence, two data points are

given on the 10/3/11 in Figure 146 indicating the group average weight before and after the six pigs were removed. Both systems did not pick up on this step down in group average after the pigs were removed at 13:30. This is indicates that the larger pigs had not been captured up to this point of the day.

Table 61: Comparative Data Obtained of the piGUI System and System-A between the 22/2/11 and the 18/3/11

		Average	Error
8/3/11	**Actual**	82.6	
	piGUI	83	0.4
	System-A	61.8	-20.8
10/3/11 (a)	**Actual**	85	
	piGUI	81.5	-3.5
	System-A	60.6	-24.4
10/3/11 (b)	**Actual**	79.5	
	piGUI	81.2	1.7
	System-A	60	-19.5
15/3/11	**Actual**	85.9	
	piGUI	87.1	1.2
	System-A	63.1	-22.8

(a) Actual Group Weight recorded before 13:30; (b) Actual Group Weight recorded after 13:30

8.4 DISCUSSION AND CONCLUSIONS

System-A failed to estimate the group weight of the finisher pigs correctly during the trials. There were three potential causes for this error: (i) the error was indirectly caused during installation and calibration, (ii) the camera and installation settings did not match the hardware provided and consequently the weight-estimation equations coefficients distorted estimates, or (iii) the error was caused during weight assessment by the system. It was most likely that the second cause was responsible for the erroneous growth output as it was apparent that zoom level distorted weight estimates. Thus, it is clear that necessary conversions were not taking place within the software to normalise the extracted body measurements to suit weight-estimation equation coefficients. This would explain why the weight data recorded by System-A appeared to require a scaling factor to adjust the data to compensate for the large errors in weight estimates.

However, a scaling factor is not required in practice as the piGUI system demonstrates. The piGUI system only requires one input for calibration which is the installation height from lens to ground. Conversions are then performed by the software based on the resolution and installation-height set by the user and the known angles of the FOV of the camera.

System-A had two additional software calibration procedures that could be removed to un-complicate the installation and initialisation process. One of these was calibrating the bone shaped template. Every attempt to calibrate the system using the template required the pigs to be removed from the pen. Unfortunately during testing not once did the system report the correct weights of the pigs when they were reintroduced into the pen, although the template returned the correct weight during calibration. This was despite moving the pigs in an out of the pen dozens of times and making additional attempts to modify the installation instructions to get the system to work correctly. The template did not remain clean for long in its surrounds either making it unpleasant or impossible to handle. Although the distortion

correction achieved by this calibration procedure is critical when using a wide angle lens, many cameras overcome the need for such procedures with inbuilt firmware that automatically corrects for lens distortion. This calibration feature is built into the camera used by the piGUI system. The other user input used by the System-A for calibration was the actual group weight of the batch of animals. Some confusion surrounded its function within the commercial systems software for two main reasons. First, this information should not even be required as the piGUI system demonstrates. Second, although it is undesirable, the actual group average weight could be used by System-A to determine an offset value to correct for the apparent systematic error that was encountered in this study. However, entering the group average weight into the software had no effect on System-A reporting the correct weight information. In fact any one of the three calibration procedures active in System-A's software could have been used by the software to output the correct weight output but seemingly not one of them worked independently or in unison to achieve this.

Both systems suffered from similar problems related to image processing. During the tests both systems experienced contour related problems where the body outlines of certain pigs were not identified correctly. The frequency of this occurrence was dependent upon the filtering settings specified during setup of each system. System-A offered a post processing tool for removal of these errors and to correct the weights obtained by the system (Figure 147).
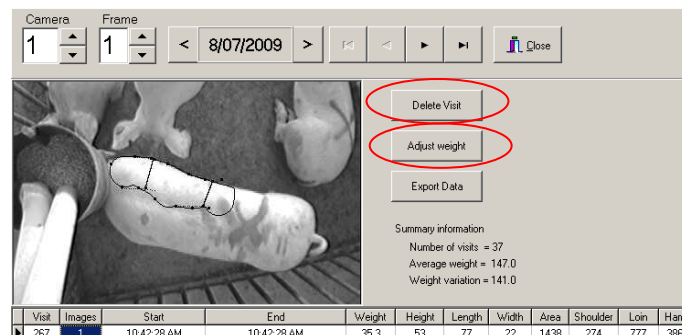
Figure 147: Incorrect Contour Recognition by System-A and Options to Adjust the Weight or Delete the Sample

Although it only occurred several times, the false detection of pigs was also an issue for both systems, as false positives had potential to distort the systems estimates of the weight deviation and the weight range of the group.

Both systems suffered from hardware and software related errors and limitations in relation to the piggery environment. A signal issue between the camera and the frame grabber board caused an error to occur in the System-A. The piGUI system restarted in safe mode during the trial, however, the cause of this event was unknown as no information was present in the log file.

From an installation and transport point-of-view the piGUI system was by far easier to use as it is smaller than the commercial system. System-A requires a larger computer case to facilitate the PCI slot of the frame grabber.

211

The size of the System-A's computer and its reliance on fans to maintain a safe working temperature led to insect and rodent infestation and excessive amounts of dust within the casing. Consequently, an additional protective casing was required to minimise these effects.

The cameras of both systems required cleaning due to the build-up of dust and insect waste. The corrosive environment and insect waste also caused rust to occur on some of the cable connections.

It is possible that new versions of System-A and the piGUI system may have overcome the shortcomings presented here.

Despite many calibration attempts, the data outputted by System-A needs to be scaled by a factor to obtain weight estimates close to actual group weights. It was apparent that this was due to the absence of necessary conversions within System-A's software to normalise the extracted body measurements to suit weight-estimation equation coefficients. The comparative data obtained indicated that both systems were capable of estimating growth, however, only the piGUI system was capable of determining growth without scalar adjustment of output. The distribution of data recorded by the piGUI system was far more concentrated around mean values. The small size and fan-less operation of the piGUI system's computer also overcame many of the issues posed by rodents, insects, dust and transportation within the piggery environment. Overall the piGUI system was better suited to the environment, obtained more accurate data and was simpler to calibrate.

Chapter 9

Discussion and Conclusions

Chapter 1 reviewed four methods which could continuously and automatically monitor the weight of livestock species. Of these methods the vision-based method had the greatest potential to overcome the challenges of the farm environment while performing to practical precision. Specifically, the vision-based method was the preferred choice as it: (i) is non-invasive and does not make any contact with the animals, (ii) it can determine multiple animals' weights in parallel, (iii) it has no moving parts and is therefore the safest of alternatives, (iv) it is the easiest to transport, (v) it is the easiest to maintain, (vi) it provides the greatest opportunity for additional functionality and is able to (vii) generate weight estimates accurate enough to be useful in practice.

The *Chapter 1* review found that the live weight of several different livestock species had been estimated using the vision-based method. The majority of the systems developed, estimated the weight of livestock to a practical level of accuracy. In some cases the vision-based method proved to be more accurate than conventional methods. Commercially available systems were also identified and a system was later subject to testing in *Chapter 8* . Despite the many benefits of the vision-based approach, four key limitations of the method were identified. The following areas were identified for improvement: *system automation, repeatability in measurements, environmental control* and *bias and fine tuning.*

The large majority of reported developments were not completely automated and therefore could not operate continuously without the incurring the cost of skilled operators. Consequently, the machine vision system, developed in this project, was required to be capable of continuous and automatic operation.

Many authors indicated that the pose of the animal was likely to have led to fluctuations in the extracted body measurements which, in retrospect, may have introduced error into weight estimates. Thus, determining the body measurements precisely in respect to a given pose of the animal would potentially reduce error in weight estimates. The body measurements themselves were also used by researchers to record and classify genetic and body composition characteristics. Therefore, it was of added importance to construct a methodology that could extract certain reference body measurements from the images with high repeatability. Some studies indicated that removing the head and tail of the pig from the analysis would assist with this goal.

Environmental control was considered. Integrating any form of hardware components into the animals' environment was disregarded, as such a device would require frequent cleaning and, in some cases, would require additional labour resources and cost to move or train the animals to interact with it correctly. Furthermore, this would nullify many of the non-invasive benefits of a using machine vision system in the farm environment. The colour and cleanliness of the livestock created problems when distinguishing the boundaries between an animal's body and the background. Extraction and filtering methods were required to overcome these issues.

The conditions where bias may affect weight estimation precision were identified to understand the causes of the error in weight estimates. Bias may result as a consequence of: (i) the time of day when the livestock are assessed, (ii) certain

animals re-visiting the scale area more than others and remaining in the scale for longer durations, (iii) missed weight recordings due to multiple animals in the scale area causing redundant data, (iv) missed weight recordings due to certain animals not visiting the scale area, (v) large daily weight fluctuations from excessive fouling, health or nutrition problems and (vi) from manual removal of sick or market ready animals from the pen. Radio Frequency Identification (RFID) could be used to determine the presence of many of these forms of bias so actions can be undertaken to reduce or eliminate it.

The findings of these reviews indicated that a large amount of work in this research area was still required, as the full potential of weight estimation using vision-based techniques had not been achieved.

To appreciate the issues related to pose identification, *Chapter 2* reviewed vision systems that could determine animal behaviour. It was found that behaviour recognition systems that can identify pose and complex behaviours in and between animals were not commercially available. Of the systems that were available commercially, the majority tracked a single animal inside a laboratory environment under controlled lightning conditions. However, in the piggery environment the developed device was required to assess individual animals within a group of animals, in dirty and challenging conditions, where the ability to provide and maintain structured lighting may be limited. Consequently, it was necessary to develop a machine vision system to recover the body pose of livestock for weight estimation. Furthermore, it was beneficial to generalize the body-pose identification method so that animal poses could be used as controlled building blocks during modelling of the weight-estimation equation, whereby the weight-estimation equation could become a function of the animal's body pose. This approach would not only be suitable for weight estimation tasks, but may also be useful in creating welfare related applications to recognise animal behaviour based on body pose in future.

Chapter 3 commenced with a breakdown of the functional elements of livestock weighing methods to provide an understanding of the types of software routines that may be necessary to facilitate the overall control and intelligence of the system. Hardware selection was discussed and devices suitable for use within the piggery environment were selected. Software was written to segment the body contour of pigs from images, excluding the head and tail.

After the segmentation process was complete, the software automatically identified and extracted 16 body measurements from specific reference points along the pig's body contour. Both the segmentation and extraction functions were adapted to assess streaming video and a database of collected videos.

Software was written to automatically convert pixels to millimetres at ground level when either resolution or installation height was entered by the user. This ensured that equation coefficients could remain the same irrespective of installation height and selected camera resolution.

Areas of improvement were identified during preliminary testing of the prototype device. Subsequently, a shape filtering process was developed to validate the contour

shape of the pig's body after segmentation against an average template shape. The average template shape was built using a user specified template shape and an automatic selection of closely matching sample body contours which were identified within a database of over 20,000 pig body contours. The database contained both male and female pigs between 12.5 kg and 306 kg in weight.

Linear, non-linear and multivariate linear equations were formed to estimate the weight of pigs from their extracted body measurements. Superior estimation results were obtained using a multivariate linear equation built using a stepwise selection of the 16 extracted body measurements, 11 angles and their 351 paired interactions. The multivariate linear equation estimated 2% more sample weights within ±2 kg error and 3% less sample weights greater than ±5 kg error than the closest non-linear equation.

During an off-line analysis the shape filtering process controlled weight estimate error such that 64% of the shapes that passed resulted in a weight estimate between 0 and ±2 kg of the actual weight and only 6% of the shapes that passed were greater than ±5 kg in error over the grower-finisher weight range. Thus, 94% of weight estimates that passed through the shape filter were within ±5 kg of the actual weight of the pig. The shape filtering process also ensured that the integrity of each segmented contour shape could be discriminated against early in the processing loop, and therefore, the overall efficiency and reliability of the system was enhanced. In addition weight estimation precision was also improved by modelling the weight-estimation equation as function of shape. Results using the shape filtering method (compared to previous methods) indicate a favourable 24% increase in the number of weight estimates within ±2 kg of the actual weight of the pigs and a 19% reduction in the number of weight estimates greater than ±5 kg.

A secondary filter was also developed to validate each estimated weight against the body measurements extracted from the pig's body contour. During an off-line analysis this limit filtering process controlled weight estimate error over the grower-finisher weight range such that 68% of body measurement vectors that passed resulted in a weight estimate within ±2 kg of the actual weight of the pigs, and only 3.5% of the body measurement vectors that passed were greater than ±5 kg in error.

The shape and limit filters were then combined in series and analysed off-line. The resulting filtering process controlled the weight estimate error over the grower-finisher weight range such that: (i) 68% of the samples that passed resulted in a weight estimate between 0 and ±2 kg of the actual weight, and (ii) less than 3% of the samples which passed were greater than ±5 kg in error. Simulated results found in Table 27, Table 28 and Table 31 provide grounds for the selection of various filtering parameters. Selection of these parameters may be based on the environment in which the piGUI system is subject and the weight range of the pigs observed.

Pig height was measured manually and was included in the weight-estimation equation to determine its effect on weight estimation performance. Overall the multivariate equation, including the height parameter, improved estimation precision by 7.34% in the less than ±2 kg weight estimation category, and by 8.87% in the greater than ±5 kg category (compared to the multivariate equation without the height parameter). However, the positive effect of including the pig height as a

217

parameter in the estimation equation was reduced when a subset of the dataset was considered based on the integrity of each sample's shape. After sorting and selecting the 3500 closest matching samples to the average shape template, the multivariate equation (including height) contributed a 6.29% improvement in the number of estimates within ±2 kg error and only a 1.09% improvement in the greater than ±5 kg error, category (compared to the multivariate equation without height as a parameter). Hence, due to the marginal benefit and the practical problems related to finding a reliable reference point to obtain the height measure in practice, the height measurement was not pursued in this study.

A tracking procedure was integrated into the software to relocate the pig in subsequent frames and to enhance the likelihood of obtaining weight estimates. This tracking procedure was linked directly to the shape filtering stage as a body contour that did not pass the shape filters criteria could still be used to identify the presence of a pig.

The piGUI system was found to operate within an acceptable error margin of 50 % of the gut fill, as on average, pigs in the weight-range of 45 to 115 kg had their live body weight estimated to within 3.16 % and 2.20 % of their respective actual live body weight, respectively. For pigs less than 45 kg in weight, the piGUI system operated on average, to within 67% of the weight attributed to gut fill or 1.07 kg error. During off-line simulations, the percentage mean-relative error obtained by the piGUI system was between 5.1 and 3.7% for pigs weighing between 15 and 45 kg and less than or equal to 2.5% for pigs between 45 and 115 kg. Therefore, on average, the system will operate to within the error margin attributed to gut fill and the system will be able to estimate a pig's body mass effectively and to practical precision.

In *Chapter 4* the ability of the piGUI system to estimate the weight of finisher pigs was tested. Compared to the conventional method, the piGUI system performed well during the both the off-line and on-farm trial.

The off-line analysis (see Section *4.3.1*) determined how well the extraction and filtering processes performed on the data available for finisher pigs. The actual group average weight of the finisher pigs was calculated based on the average weight of all the pigs in the videos. The data available to the piGUI system was determined by the frames which passed a loosely bound body measurement extraction stage. The average actual weight of the pigs in all frames which passed this stage was also calculated. The weight averages of these two groups gave an indication of how the actual average group weight would be collected in practice using the sampled frames of individual pigs in respect to the actual weight and total data available. Considering on average each video contained just 43 frames over a ~9 second period, the results obtained from the sample frames were close to the actual average weight of the group based on both the videos and individual sample frames (within ±1.5 kg). These frames were then subject to four filtering and estimation methods; before filtering, limit filter, shape filter, and combined shape and limit filter. The information was divided into three groups consisting of males and females (Group 1), males (Group 2), and females (Group3).

Coincidently, the unfiltered data obtained from Group 1 yielded the closest average group estimate to actual group average weight. This demonstrated how it was possible to obtain the correct group average weight from datasets where large weight estimation errors are present. It appeared that the commercial system tested in *Chapter 8* worked on this merit. The filtering operations successfully removed erroneous samples indicated by the ability to calculate the weight deviation of Groups 1, 2 and 3 within 1 kg using the combined filtering process. The estimated group average weight of Groups 1, 2 and 3 were all within 2.5% of error of the actual group average weight using the combined filtering process. An individual weight assessment of the finisher pigs in the three groups was also undertaken. When using the combined filtering process, more than 60% of the samples that passed were within ±2 kg of the actual weight, while errors greater than ±5 kg between the actual weight and weight estimates were reduced to less than 5%.

During the farm trial the precision of the piGUI system was recorded within ±1 kg error (~1%) of the actual group average weight on 6 of the 7 trial days where comparative information was available. This confirmed off-line results and indicated that the piGUI system could record growth to sufficient practical accuracy in practice. Relative weight estimation errors were within 2.5% of the actual weight on all seven of the days during the on-farm trial. The vision system calculated the weight deviation of the group to within ±2 kg of the actual weight deviation during the farm trial. The increased error in the estimate of the group's weight deviation indicated that there was potentially some form of bias occurring during the farm trial. The growth of the individual pigs recorded by the system was similar to the actual growth they experienced.

Chapter 5 explored the diagnostic power of the piGUI system and contained an evaluation of its performance in estimating the weight of grower pigs both off-line and on-farm. During testing on-farm, various hardware and software problems related to the piggery environment were encountered. The majority of these issues were overcome by the software, including those related to occlusion, natural lighting, pig appearance and posture. Once these issues were resolved, four batches of grower pigs were monitored by the piGUI system.

To provide an adequate growth reference, an equation for standard pig growth found in literature was validated against growth data obtained from the farm. The equation was found to be effective at describing the pigs' group average weight relative to days of age. The piGUI system's growth output agreed with the equation for standard growth during the second batch of pigs, and for periods of the other three batches. A deflection away from the standard growth curve was experienced during the third and fourth batches when the pigs reached weights greater than ~45 kg. These growth deflections were believed to be caused by stress directly or indirectly related to temperature, as Summer temperatures reached over 38°C during these batches. This theory is supported by the level of animal activity recorded by the system, the temperatures leading up to the negative deflection in growth and figures found in literature.

After testing and modification of the software code, a simulation was run off-line to determine whether the piGUI system's ability to evaluate the group average weight,

the group weight deviation and the individual weight of grower pigs (see Section *5.3.2*).

The group average weights of three groups of grower pigs were estimated within 1.3 kg error from their actual average group weight. The three groups had their weight deviation estimated to within 1.2 kg from their actual group weight deviation.

The individual pigs within these three groups were also assessed. Using the system's combined filtering process, more than 65% of the individual weight estimates output were within ±2 kg of the pig's actual weight and less than 5% of the individual weight estimates were greater than ±5 kg in error. As the average weight and weight deviation of the group remained relatively steady for all filtering methods it was clear that the filters did not cause a dramatic level of bias during the selection of valid samples. However, this was based on a short video of each animal. In practice the duration and frequency in which each pig is present beneath the camera may differ and therefore cause bias in group weight estimates in the pen environment. As a result, in *Chapter 7* the system was tested to determine whether this form of bias could occur.

Chapter 6 determined whether the piGUI system could estimate the weight of sows in their early stages of pregnancy and whether the system could detect changes in the body measurements of individual sows before and after giving birth.

The group of sows, which were between days 71 and 82 of pregnancy, had their individual and group weight estimated accurately. The most accurate group weight estimate was within 0.1 kg of the actual group weight performed by the limit filtering method. The same method also estimated the weight deviation of the group to 1.7 kg of the actual weight deviation of the group.

Eighty-two percent of the samples which passed the combined filtering process were within a practical ±5 kg range of the actual weight of the sow. It is believed that these results could be enhanced further, with additional data collection and modelling surrounding the shape and body measurements of sows throughout pregnancy.

The metric body measurements of two Large White × Landrace sows were recovered by the vision system before and after giving birth. The shoulder and ham widths and the sows' body lengths were consistent with those found in literature.

In *Chapter 7* RFID was integrated into the piGUI system to record the identity of individual animals when they were present beneath the system's camera to detect for bias. The system was tested under commercial conditions in a pen housing slow growing pigs. Bias was discovered as a result of the systems installation location above the feeder. At this installation location, certain pigs were found to feed more frequently and for longer durations than others. Bias was also occurring as a result of the piGUI system having difficulty identifying certain pigs. Consequently, it was recommended to build additional shape filters and estimation equations to cater for slow growing pigs. However, the behaviour of the pigs around the feeder may have also contributed to the difficulties experienced while sampling certain pigs.

The minimum amount of time a pig spent in close proximity to the feeder was used to give an indication of its feeding behaviour (attendance). A similar trend was found between the amount of time the pigs spent at the feeder and the amount of weight they gained. The pigs that spent the most time around the feeder gained the most weight. Certain pigs appeared to dominate the feed space, potentially overfeeding, while others were potentially underfeeding.

According to the RFID data, the peak demand for the feeder was found to be between 15:00pm and 16:00pm and at 8:00am. It would be recommended that during these times the feed supply should be monitored and adjusted to ensure that the demand is fulfilled.

Interactions between pigs were determined around the feeder under the assumption that a pig was passive if it resided at the feeder, while a pig was aggressive if it was trying to gain access to the feeder. The type and number of these interactions were determined from the RFID data. The pig with the heaviest starting weight and ending weight had the most number of interactions. The lighter pigs were more inclined to be pushed out of the feeder, while the most aggressive interactions were caused by pigs in the lower half of the middle of the group. The data indicated that overall the heaviest pigs were also more inclined to be passive. These findings were consistent with similar studies. Interestingly, the most aggressive of the heavier pigs spent 1.8 times longer at the feeder and gained more weight than any other pig.

A comparative study was undertaken between a commercial system 'System-A' and the piGUI system in *Chapter 8* . System-A failed to estimate the group average weight of the finisher pigs correctly in the trials. The three potential causes of this error were: (i) the error was indirectly caused during installation and calibration, (ii) the camera and installation settings did not match the hardware provided and consequently the weight-estimation equations coefficients distorted estimates, or (iii) the error was caused during weight assessment by the system. It was most likely that the errors in System-A's growth output was caused by the second reason, as the zoom level distorted weight estimates. Thus, necessary conversions were not taking place to normalise the extracted body measurements to suit weight-estimation equation coefficients within the software (as was done automatically in the piGUI software see Section *3.5.3*). This would explain why System-A's growth data would require a multiplication by a scalar factor to adjust the growth data to valid weight ranges. The piGUI system estimated the group average weight to within 2.1% on each of the 7 days when the actual weight of the pigs were determined using the electronic scale. On the same days, System-A reported group average weight estimates in excess of 16 kg error of the actual group average weight.

To simplify System-A's installation and initialisation process, its two additional software calibration procedures (other than installation height) could be removed. Entering the actual group average weight into System-A's software seemingly had no effect on the system reporting the correct weight information. The bone shaped template used to correct image distorting was unpleasant to handle in the dirty environment. Using a camera with inbuilt distortion correction would be desirable to avoid this calibration procedure. Not one of System-A's calibration procedures worked independently or in unison to achieve correct weight output.

Both systems suffered from similar problems related to image processing. The body outlines of some pigs were not identified correctly and on several occasions false positives occurred where the background was incorrectly identified as a pig. The number of body outlines incorrectly identified by system-A pigs made it very hard for system-A to estimate the weight deviation and the weight range of the group correctly. The distribution of weight data recorded daily by the piGUI system was far more concentrated around a mean value than System-A.

Both systems suffered from hardware and software related errors and limitations in relation to the piggery environment. The cameras of both systems required cleaning due to the build-up of dust and insect waste. The corrosive environment and insect waste also caused rust to develop on some of the cable connections. From an installation and transport point-of-view the piGUI system was by far easier to use as it was comparatively smaller than the commercial system. The piGUI system, therefore, overcame much of the issues posed by rodents, insects, dust and transportation within the piggery environment.

The comparative data obtained indicated that both systems were capable of estimating growth, however, only the piGUI system was capable of determining growth without scalar adjustment of output.

9.1 FUTURE WORK

To enhance environmental control an optical filter, could be designed in future to suppress background artefacts and assist in segmentation. In addition, other imaging sensors may be adopted such as NIR or thermal IR to enhance results.

Determining a method to find the pig height may also be considered as either a height estimate, or height measurement is required to determine the actual metric body measurements of the pigs.

The image-based characteristics of the pigs that were recorded during the data extraction process, can be used to enhance the tracking and segmentation functions.

There is potential to improve the accuracy of the system in estimating the weight of individual pigs. Potentially, weight estimation errors may be reduced by adapting different equations to suit to the shape or body measurements of particular pigs using the equation-shape building methodology. With modification, the same methodology could also possibly be used for data acquired from alternate camera configurations (such as 3D) by using the animal's surface rather than its contour.

Future work related to sows include creating software to identify important behavioural actions such the transition between a sow standing and sitting, or fighting, or savaging actions. Shape and or optical flow information could be used in this instance. The morphological changes recorded may also be used as an alternative means to manually check pregnancy or to recognise problems in a pregnancy. It is also possible that a sow's likely litter size may also be determined from body morphology. The variability in the appearance of sows may also be sufficient enough to provide grounds for individual identification. It is believed that weight estimation results of sows could be enhanced further, with additional data collection and

modelling surrounding the shape and body measurements of sows throughout pregnancy.

Further trials to model and determine the strength of the relationship between a pig's attendance at a feeder and its weight gain are recommended. Future trials in this area should also ensure that an ID read will occur every time a pig's head is inside the feeder. This may require shielding and a secondary antenna. Although it was not investigated in this study, the vision system's tracking component is capable of logging when a pig is in attendance at the feeder or any location around the pen when it is standing (in a similar manner to the RFID system). Investigating the similarities between the attendance recorded using the RFID system against the vision system's would be an interesting exercise. Creating software code to attempt to automatically identify individual pigs from their appearance and geometry is also a task worthwhile pursuing using the large database of information already gathered.

The accumulative attendance data obtained in the trial in Chapter 7 indicated that the attendance at the feeder decreases when there is no feed available. If this is the case, a system with the ability to determine the presence of animals at the feeder (such as an RFID system or the piGUI system) has great potential to identify out of feed events so that they can be better managed. As attendance appears to be related to weight gain, the cumulative attendance has potential to be used to standardise or regulate the stocking density within a pen in relation to the number of feeders. High levels of attendance may indicate under supply and increased competition, while low levels may indicate space wastage. Attendance may also be used to identify when animals have been removed from the pen (traceability), to identify when workers undertake jobs within the pen and to quantify feeding behaviour in respect to temperature fluctuations.

In future studies, the duration between the interactions at the feeder can be assessed over an extended interval of several seconds rather than those that occurred within a single second, to determine whether any regular swapping between animals occurred and whether certain pigs had a tendency to feed at particular times.

Integrating both weight information from the piGUI system and the identification information from the RFID component can be used to determine the growth and weight gain of individual pigs, and provide more robust estimates of group averages. Potential also exists to identify pigs that are more likely to have good or poor feed conversion, and pigs that are likely to require medical treatment. The pigs that dominate or are competitive around the feeder may also be identified so that corrective measures can be implemented. The software written to analyse the RFID data could also be up-scaled in future to cater for much larger groups of animals and additional RFID stations at extra feeding points.

9.2   CONCLUDING REMARK

In order to extract the correct body measurements automatically, the morphology caused by movement and the morphology caused by growth must be separated. As it provides a base reference to determine the growth automatically, the ability to recognise body posture is very important. The effect that the morphology caused by

movement has on body measurements is suppressed by the filtering processes documented in this study, weight estimation is enhanced as a result.

REFERENCES

Aarnink, A. J. A., Schrama, J. W., Heetkamp, M. J. W., Stefanowska, J. &Huynh, T. T. T. (2006). Temperature and body weight affect fouling of pig pens. *Journal of Animal Science* 84(2224-2231).

Actimetrics (2010). *Actimetrics, Available on www.actimetrics.com, Accessed on 8th July 2010.*

Agricultural Research Council (ARC) (1981). *The Nutrient requirements of pigs : technical review.* London: On behalf of the Agricultural Research Council by the Commonwealth Agricultural Bureaux.

Allen, J. A. (1877). The influence of physical conditions in the genesis of species. *Radical Review* 1: 108-140.

Andersen, H., Jørgensen, E., Dybkjær, L. &Jørgensen, B. (2008). The ear skin temperature as an indicator of the thermal comfort of pigs. *Applied Animal Behaviour Science* 113(1-3): 43-56.

Arias, N., Molina, M. &Gualdron, O. (2004).Estimate of the weight in bovine livestock using digital image processing and neural network. In *Proceedings of the SPIE, 5th Iberoamerican Meeting on Optics and 8th Latin American Meeting on Optics, Lasers, and Their Applications*, Vol. 5622, 224-228 (Eds A. Marcano O. and J. L. Paz).

Aydin, A., Cangar, O., Ozcan, S. E., Bahr, C. &Berckmans, D. (2010). Application of a fully automatic analysis tool to assess the activity of broiler chickens with different gait scores. *Computers and Electronics in Agriculture* 73(2): 194-199.

Bahlmann, C. &Burkhardt, H. (2004). The writer independent online handwriting recognition system frog on hand and cluster generative statistical dynamic time warping. *Pattern Analysis and Machine Intelligence, IEEE Transactions on* 26(3): 299-310.

Banhazi, T., Kitchen, J. &Tivey, D. (2009a). Potential of using infrared thermography for determination of skin wetness and thus perceived thermal comfort of pigs. *Australian Journal of Multi-disciplinary Engineering* 7(1): 47-54.

Banhazi, T. M. &Black, J. L. (2009). Precision livestock farming: a suite of electronic systems to ensure the application of best practice management on livestock farms. *Australian Journal of Multi-disciplinary Engineering* 7(1): 1-14.

Banhazi, T. M., Lewis, B. &Tscharke, M. (2011a). The development and commercialisation aspects of a practical feed intake measurement instrumentation to be used in livestock buildings. *Australian Journal of Multi-disciplinary Engineering* 8(2): 131-138.

Banhazi, T. M. &Tscharke, M. (2011). Review of Image Analysis (IA) technologies for the Australian pig industry. Final report for APL. (54 Pages). Canberra, Australia

Banhazi, T. M., Tscharke, M., Ferdous, W. M., Saunders, C. &Lee, S.-H. (2009b).Using image analysis and statistical modelling to achieve improved pig weight predictions. In *SEAg 2009*, Vol. 1, CD publication (Eds T. Banhazi and C. Saunders). Brisbane, Australia: SEAg

Banhazi, T. M., Tscharke, M., Ferdous, W. M., Saunders, C. &Lee, S.-H. (2011b). Improved image analysis based system to reliably predict the live weight of

pigs on farm: Preliminary results. *Australian Journal of Multi-disciplinary Engineering* 8 (2): 107-119.

Banhazi, T. M., Tscharke, M., Lewis, B. &Broek, D. (2009c). Practical and continuous measurement of feed intake and pig weight. Final report for the PORK CRC. (108 pages). Adelaide, Australia.

Barron, J. L., Fleet, D. J. &Beauchemin, S. S. (1994). Performance of optical flow techniques. *International Journal of Computer Vision* 12(1): 43-77.

Baumberg, A. M. &Hogg, D. C. (1994).An efficient method for contour tracking using active shape models. In *Proceedings of the IEEE Workshop on Motion of Non-Rigid and Articulated Objects*, 194-199 Austin , Texas.

Baxter, S. (1984). *Intensive pig production: environmental management and design.* Granada Technical Books.

Beddow, T. A. &Ross, L. G. (1996). Predicting biomass of Atlantic salmon from morphometric lateral measurements. *Journal of Fish Biology* 49(3): 469-482.

Bengsen, A., Leung, L. K. P., Lapidge, S. J. &Gordon, I. J. (2008). The development of target-specific vertebrate pest management tools for complex faunal communities. *Ecological Management & Restoration* 9(3): 209-216.

Bergmann, C. (1847). *Über die Verhältnisse der Wärmeökonomie der Thiere zu ihrer Grösse.*

Bewley, J., Peacock, A., Lewis, O., Boyce, R., Roberts, D., Coffey, M., Kenyon, S. &Schutz, M. (2008). Potential for Estimation of Body Condition Scores in Dairy Cattle from Digital Images. *Journal of dairy science* 91(9): 3439.

Bharatkumar, A. G., Daigle, K. E., Pandy, M. G., Cai, Q. &Aggarwal, J. K. (1994).Lower Limb Kinematics of Human Walking with the Medial Axis Transformation. In *In Workshop on Motion of Non-Rigid and Articulated Objects*, 70-76.

Bhattacharyya, A. (1943). On a measure of divergence between two statistical populations defined by their probability distributions. *Bull. Calcutta Math. Soc* 35(99-109): 4.

Biobserve (2010). *Biobserve, Available on www.biobserve.com, Accessed on 9th July 2010.*

Black, J., Vaschina, B. &Little, B. (2004).The economical benefits of precision livestock farming: AUSPIG Analyses for Business Case for the Pig Industry. Report to Australian Pork Limited.

Black, J. L., Giles, L. R., Wynn, P. C., Knowles, A. G., Kerr, C. A., Jone, M. R., Gallagher, N. L. &Eamens, G. J. (2001). A Review - Factors Limiting the Performance of Growing Pigs in Commercial Environments. In *Manipulating Pig Production VIII*, Vol. 8, 9-36 (Ed P. D. Cranwell). Adelaide, Australia: Australasian Pig Science Association, Victorian Institute of Animal Science, Werribee, Victoria, Australia.

Blackshaw, J. K. &Blackshaw, A. W. (1994). Shade-seeking and lying behaviour in pigs of mixed sex and age, with access to outside pens. *Applied Animal Behaviour Science* 39(34): 249-257.

Boisen, S., McNamara, J. P., France, J. &Beever, D. E. (2000). A simple nutrient-based production model for the growing pig. *Modelling nutrient utilization in farm animals*: 183-196.

Brandl, N. &Jørgensen, E. (1996). Determination of live weight of pigs from dimensions measured using image analysis. *Computers and Electronics in Agriculture* 15(1): 57-72.

Branson, K. &Belongie, S. (2005).Tracking multiple mouse contours (without too many samples). In *Computer Vision and Pattern Recognition, 2005. CVPR 2005. IEEE Computer Society Conference on*, Vol. 1, 1039-1046 vol. 1031.

Bregler, C. (1997).Learning and recognizing human dynamics in video sequences. 568-574.

Brosnan, T. &Sun, D.-W. (2002). Inspection and grading of agricultural and food products by computer vision systems--a review. *Computers and Electronics in Agriculture* 36(2-3): 193-213.

Brosnan, T. &Sun, D.-W. (2004). Improving quality inspection of food products by computer vision--a review. *Journal of Food Engineering* 61(1): 3-16.

Brown-Brandl, T. M. &Eigenberg, R. A. (2011). Development of a Livestock Feeding Behavior Monitoring System *American Society of Agricultural and Biological Engineers (ASABE)* 54(5): 1913-1920.

Bull, C. (1993). A review of sensing techniques which could be used to generate images of agricultural and food materials. *Computers and Electronics in Agriculture* 8(1): 1-29.

Bureau of Meteorology (2010).Commonwealth of Australia, Bureau of Meteorology (BOM). Available on http://www.bom.gov.au/climate. Accessed on February 10, 2010.

Burges, C. J. C. (1998). A tutorial on support vector machines for pattern recognition. *Data mining and knowledge discovery* 2(2): 121-167.

Burghardt, T. &Calic, J. (2006). Analysing animal behaviour in wildlife videos using face detection and tracking. *Vision, Image and Signal Processing, IEE Proceedings -* 153(3): 305-312.

Burghardt, T., Calic, J. &Thomas, B. (2004).Tracking animals in wildlife videos using face detection. Citeseer.

Burke, J., Nuthall, P. &McKinnon, A. (2004). An Analysis of the Feasibility Of Using Image Processing To Estimate the Live Weight of Sheep. Farm and Horticultural Management Group Applied Management and Computing Division, Lincoln University.

Cangar, Ö., Leroy, T., Guarino, M., Vranken, E., Fallon, R., Lenehan, J., Mee, J. &Berckmans, D. (2008). Automatic real-time monitoring of locomotion and posture behaviour of pregnant cows prior to calving using online image analysis. *Computers and Electronics in Agriculture* 64(1): 53-60.

Carr, J. (1998). *Garth pig stockmanship standards*. 5M Enterprises Limited.

Carr, J., Done, S. H., Taylor, D. J., Tucker, D. A. W. &Miller, H. (2008). Feed cannot be wasted on pig farms. *Pig Veterinary Society Proceedings Supplement*: 41-49.

Chan, D., Hockaday, S., Tillett, R. D. &Ross, L. G. (1999).A trainable n-tuple pattern classifier and its application for monitoring fish underwater. In *Seventh International Conference on Image Processing and Its Applications*, Vol. 1, 255-259: IET.

Chao, K., Chen, Y.-R., Hruschka, W. R. &Gwozdz, F. B. (2002). On-line inspection of poultry carcasses by a dual-camera system. *Journal of Food Engineering* 51(3): 185-192.

Chao, K., Park, B., Chen, Y. R., Hruschka, W. R. &Wheaton, F. W. (2000). Design of a dual-camera system for poultry carcasses inspection. *Applied Engineering in Agriculture* 16(5): 581-587.

Charette, R., Bigras-Poulin, M. &Martineau, G.-P. (1996). Body condition evaluation in sows. *Livestock Production Science* 46(2): 107-115.

Chedad, A., Aerts, J.-M., Vranken, E. &Berckmans, D. (2000).Behaviour of chickens towards an automatic weighing system. In *Biorobotics II*, 202-207 Japan.

Chen, C., Gilbert, C. L., Yang, G., Guo, Y., Segonds-Pichon, A., Ma, J., Evans, G., Brenig, B., Sargent, C., Affara, N. &Huang, L. (2008). Maternal infanticide in sows: Incidence and behavioural comparisons between savaging and non-savaging sows at parturition. *Applied Animal Behaviour Science* 109(2-4): 238-248.

Chen, Z. &Lee, H. J. (1992). Knowledge-guided visual perception of 3-D human gait from a single image sequence. *IEEE Transactions on systems, man and cybernetics* 22(2): 336-342.

Chiao-Fe, S., Hampapur, A., Lu, M., Brown, L., Connell, J., Senior, A. &Yingli, T. (2005).IBM smart surveillance system (S3): a open and extensible framework for event based surveillance. In *IEEE Conference on Advanced Video and Signal Based Surveillance, 2005. AVSS 2005.*, 318-323.

Cootes, T. F., Cooper, D. H., Taylor, C. J. &Graham, J. (1992). Trainable method of parametric shape description. *Image and Vision Computing* 10(5): 289-294.

Cootes, T. F., Edwards, G. J. &Taylor, C. J. (1998). Active appearance models. In *5th European Conference on Computer Vision* Vol. 2, 484-498 Springer, Berlin.

Cootes, T. F. &Taylor, C. J. (1992). Active shape models. In *3rd British Machine Vision Conference*, 266-275 (Eds D. Hogg and R. Boyle). Springer-Verlag.

Cootes, T. F. &Taylor, C. J. (1995). Combining point distribution models with shape models based on finite element analysis. *Image and Vision Computing* 13(5): 403-409.

Cootes, T. F., Taylor, C. J., Cooper, D. H. &Graham, J. (1995). Active shape models-their training and application. *Computer Vision and Image Understanding* 61(1): 38-59.

Cornou, C. (2006). Automated oestrus detection methods in group housed sows: Review of the current methods and perspectives for development. *Livestock Science* 105(1-3): 1-11.

Costa, C., Scardi, M., Vitalini, V. &Cataudella, S. (2009). A dual camera system for counting and sizing Northern Bluefin Tuna (Thunnus thynnus; Linnaeus, 1758) stock, during transfer to aquaculture cages, with a semi automatic Artificial Neural Network tool. *Aquaculture* 291(3-4): 161-167.

Criddle, L. M. (2001). Livestock trauma in central Texas: Cowboys, ranchers, and dudes. *Journal of Emergency Nursing* 27(2): 132-140.

Cucchiara, R., Grana, C., Piccardi, M., Prati, A. &Sirotti, S. (2001). Improving shadow suppression in moving object detection with HSV color information. In *Proceedings of IEEE Intelligent Transportation Systems*, 334-339.

Cveticanin, D. (2003). New Approach to the Dynamic Weighing of Livestock. *Biosystems Engineering* 86(2): 247-252.

De Lange, C. F. M., Morel, P. C. H. &Birkett, S. H. (2003). Modeling chemical and physical body composition of the growing pig. *Journal of Animal Science* 81(Number 14 Electronic Supplement 2): E159.

De Wet, L., Vranken, E., Chedad, A., Aerts, J., Ceunen, J. &Berckmans, D. (2003). Computer-assisted image analysis to quantify daily growth rates of broiler chickens. *British Poultry Science* 44(4): 524-532.

del Pilar, E. R., Valdez, C. A., Flor, J. A. C. G. &del Barrio, A. N. (2002). Determination of Body Weight in Philippine Carabao-Murrah Crossbred

Buffaloes Using External Body Measurements. *Philippine Journal of Veterinary and Animal Sciences* 28(1).

Demuth, H. &Beale, M. Neural network toolbox. *User's Guide Version* 4.

Deumens, R., Jaken, R. J. P., Marcus, M. A. E. &Joosten, E. A. J. (2007). The CatWalk gait analysis in assessment of both dynamic and static gait changes after adult rat sciatic nerve resection. *Journal of Neuroscience Methods* 164(1): 120-130.

Doeschl-Wilson, A. B., Green, D. M., Fisher, A. V., Carroll, S. M., Schofield, C. P. &Whittemore, C. T. (2005). The relationship between body dimensions of living pigs and their carcass composition. *Meat Science* 70(2): 229-240.

Donkersgoed, R. v. (2004).Automatic Sorters. In *4th London Swine Conference*, 153 (Eds J. M. Murphy, T. M. Kane and C. F. M. d. Lange). London, Ontario.

Duarte, S., Reig, L. &Oca, J. (2009). Measurement of sole activity by digital image analysis. *Aquacultural Engineering* 41(1): 22-27.

Dunn, M., Billingsley, J. &Finch, N. (2003).Machine vision classification of animals. In *10th IEEE International Conference on Mechatronics and Machine Vision in Practice* Perth, Australia.

Dusenbery, D. B. (1985). Using a microcomputer and video camera to simultaneously track 25 animals. *Computers in Biology and Medicine* 15(4): 169-175.

Edwards, S. A., Armsby, A. W. &Large, J. W. (1988). Effects of feed station design on the behaviour of group-housed sows using an electronic individual feeding system. *Livestock Production Science* 19(3-4): 511-522.

Eigenberg, R. A., Brown-Brandl, T. M. &Nienaber, J. A. (2008). Sensors for dynamic physiological measurements. *Computers and Electronics in Agriculture* 62(1): 41-47.

Ekkel, E. D., Spoolder, H. A. M., Hulsegge, I. &Hopster, H. (2003). Lying characteristics as determinants for space requirements in pigs. *Applied Animal Behaviour Science* 80(1): 19-30.

Elgammal, A., Duraiswami, R., Harwood, D. &Davis, L. S. (2002). Background and foreground modeling using nonparametric kernel density estimation for visual surveillance. *Proceedings of the IEEE* 90(7): 1151-1163.

Enevoldsen, C. &Kristensen, T. (1997). Estimation of Body Weight from Body Size Measurements and Body Condition Scores in Dairy Cows. *Journal of dairy science* 80(9): 1988-1995.

Erkal, S., Gerberich, S. G., Ryan, A. D., Renier, C. M. &Alexander, B. H. (2008). Animal-related injuries: A population-based study of a five-state region in the upper midwest: Regional rural injury study II. *Journal of Safety Research* 39(4): 351-363.

Ermias, E. &Rege, J. E. O. (2003). Characteristics of live animal allometric measurements associated with body fat in fat-tailed sheep. *Livestock Production Science* 81(2-3): 271-281.

Fancom eYeScan Permanent stress-free weighing of fatteners: Fancom B.V. Available on http://www.fancom.com/uk/projects/81/eyescan-growth-monitor/. Accessed on February 24, 2011. .

Favreau, L., Reveret, L., Depraz, C. &Cani, M.-P. (2006). Animal gaits from video: Comparative studies. *Graphical Models* 68(2): 212-234.

Fear, A. C. &Herz, W. S. (2008).Methods and systems of calculating the height of an object observed by a camera. Google Patents.

Filby, D. E., Turner, M. J. B. &Street, M. J. (1979). A walk-through weigher for dairy cows. *Journal of Agricultural Engineering Research* 24(1): 67-78.

Fisher, A., Green, D., Whittemore, C., Wood, J. &Schofield, C. (2003). Growth of carcass components and its relation with conformation in pigs of three types. *Meat Science* 65(1): 639-650.

FLIR (2010). *FLIR Systems, Available on www.flir.com/thermography/, Accessed on 4th Aug 2010*.

Fraser, A. (1983). The behaviour of maintenance and the intensive husbandry of cattle, sheep and pigs. *Agriculture, Ecosystems and Environment* 9(1): 1-23.

Freson, L., Godrie, S., Bos, N., Jourquin, J. &Geers, R. (1998). Validation of an infra-red sensor for oestrus detection of individually housed sows. *Computers and Electronics in Agriculture* 20(1): 21-29.

Freund, Y. &Schapire, R. (1995).A desicion-theoretic generalization of on-line learning and an application to boosting. 23-37: Springer.

Frost, A. R., Schofield, C. P., Beaulah, S. A., Mottram, T. T., Lines, J. A. &Wathes, C. M. (1997). A review of livestock monitoring and the need for integrated systems. *Computers and Electronics in Agriculture* 17(2): 139-159.

Gariepy, C., Amiot, J. &Nadai, S. (1989). Ante-mortem detection of PSE and DFD by infrared thermography of pigs before stunning. *Meat Science* 25(1): 37-41.

Georgsson, L. &Svendsen, J. (2002). Degree of competition at feeding differentially affects behavior and performance of group-housed growing-finishing pigs of different relative weights. *Journal of Animal Science* 80(2): 376-383.

Gillespie, J. R. &Flanders, F. B. (2009). *Modern livestock and poultry production.* Cengage Learning.

Gondret, F., Lefaucheur, L., Louveau, I., Lebret, B., Pichodo, X. &Le Cozler, Y. (2005). Influence of piglet birth weight on postnatal growth performance, tissue lipogenic capacity and muscle histological traits at market weight. *Livestock Production Science* 93(2): 137-146.

Gonyou, H. W., Zhou, J. H. &Stricklin, W. R. (1997).Applying Animat Technology to the Design and Evaluation of Pens for Growing/Finishing Pigs. In *5th International Symposium - Livestock Environment V*, Vol. II, 836-842 (Eds R. W. Bottcher and S. J. Hoff). Bloomington, Minnesota: American Society of Agricultural Engineers.

Green, D., Brotherstone, S., Schofield, C. &Whittemore, C. (2003). Food intake and live growth performance of pigs measured automatically and continuously from 25 to 115 kg live weight. *Journal of the Science of Food and Agriculture* 83(11).

Green, D. M. &Whittemore, C. T. (2005). Calibration and sensitivity analysis of a model of the growing pig for weight gain and composition. *Agricultural Systems* 84(3): 279-295.

Guo, Y., Xu, G. &Tsuji, S. (1994).Understanding human motion patterns. In *Pattern Recognition, 1994. Vol. 2 - Conference B: Computer Vision & Image Processing., Proceedings of the 12th IAPR International. Conference on*, Vol. 2, 325-329 vol.322.

Haritaoglu, I., Harwood, D. &Davis, L. S. (2000). W4: real-time surveillance of people and their activities. *Pattern Analysis and Machine Intelligence, IEEE Transactions on* 22(8): 809-830.

Harmsen, S. R. &Koenderink, N. J. J. P. (2009). Multi-target tracking for flower counting using adaptive motion models. *Computers and Electronics in Agriculture* 65(1): 7-18.

Hartman, E., Frankena, K., Oude Vrielink, H. H. E., Nielen, M., Metz, J. H. M. &Huirne, R. B. M. (2004). Risk factors associated with sick leave due to work-related injuries in Dutch farmers: an exploratory case-control study. *Safety Science* 42(9): 807-823.

Heap, T. &Hogg, D. (1996).Towards 3D hand tracking using a deformable model. In *Proceedings of the Second International Conference on Automatic Face and Gesture Recognition*, 140-145.

Heinrichs, A. J., Rogers, G. W. &Cooper, J. B. (1992). Predicting Body Weight and Wither Height in Holstein Heifers Using Body Measurements. *Journal of dairy science* 75(12): 3576-3581.

Heitman, H. J. &Hughes, E. H. (1949). The effects of air temperature and relative humidity on the physiological well being of swine. *Journal of Animal Science* 8: 171-181.

HERMES (2009).HERMES - Human Expressive graphic Representation of Motion and their Evaluation in Sequences, EU Sixth Framework Programme, Final Project Report. (24 Pages).

Herring, S. W., Sola, O. M., Huang, X., Zhang, G. &Hayashida, N. (1993). Compartmentalization in the pig latissimus dorsi muscle. *Cells Tissues Organs* 147(1): 56-63.

Hile, M. E., Hintz, H. F. &Erb, H. N. (1997). Predicting body weight from body measurements in Asian elephants (Elephas maximus). *Journal of Zoo and Wildlife Medicine* 28(4): 424-427.

Hoelscher&Leuschner optiSORT - optimum sorting for feeding and commercial exploitation for pigs: Hoelscher&Leuschner. Available on http://www.hl-agrar.de/startseite.php?id=129&parent=127. Accessed on February 24, 2011.

Horn, B. K. P. &Schunck, B. G. (1981). Determining optical flow. *Artificial intelligence* 17(1-3): 185-203.

How-Lung, E., Junxian, W., Wah, A. H. K. S. &Wei-Yun, Y. (2006). Robust human detection within a highly dynamic aquatic environment in real time. *IEEE Transactions on Image Processing* 15(6): 1583-1600.

Hoy, S., Bauer, J., Borberg, C., Chonsch, L. &Weirich, C. (2009). Impact of rank position on fertility of sows. *Livestock Science* 126(1-3): 69-72.

Huynh, T. T. T., Aarnink, A. J. A., Gerrits, W. J. J., Heetkamp, M. J. H., Canh, T. T., Spoolder, H. A. M., Kemp, B. &Verstegen, M. W. A. (2005). Thermal behaviour of growing pigs in response to high temperature and humidity. *Applied Animal Behaviour Science* 91(1-2): 1-16.

InnoventTechnology Real-Time Herd Monitoring: Innovent Technology Ltd, Available on http://www.qscan.co.uk/. Accessed on May 11, 2010.

Jain, A. K. &Dubes, R. C. (1988). *Algorithms for clustering data.*

Jain, A. K., Murty, M. N. &Flynn, P. J. (1999). Data clustering: a review. *ACM Computing Surveys (CSUR)* 31(3): 264-323.

Jensen, K. H., Pedersen, B. K., Pedersen, L. J. &JÃ¸rgensen, E. (1995). Well-being in pregnant sows: confinement versus group housing with electronic sow feeding. *Acta Agriculturae Scandinavica, Section A - Animal Sciences* 45(4): 266-275.

Jensen, K. H., Sorensen, L., Bertelsen, D., Pedersen, A. R., Jorgensen, E., Nielsen, N. &Vestergaard, K. (2000). Management factors affecting activity and aggression in dynamic group housing systems with electronic sow feeding: a field trial. *Animal Science* 71(3): 535-546.

Johansson, G. (1975). Visual motion perception. *Scientific American* 232(6): 76-88.

Kaihilahti, J., Suokannas, A. &Raussi, S. (2007). Observation of Cow Behaviour in an Automatic Milking System using Web-based Video Recording Technology. *Biosystems Engineering* 96(1): 91-97.

Kakadiaris, I. A. &Metaxas, D. (1996).Model-based estimation of 3D human motion with occlusion based on active multi-viewpoint selection. 81: Published by the IEEE Computer Society.

Kakadiaris, I. A. &Metaxas, D. (1998). Three-dimensional human body model acquisition from multiple views. *International Journal of Computer Vision* 30(3): 191-218.

Kalafatic, Z., Ribaric, S. &Stanisavljevic, V. (2001).A system for tracking laboratory animals based on optical flow and active contours. In *11th International Conference on Image Analysis and Processing.*, 334-339.

Kalman, R. E. (1960). A new approach to linear filtering and prediction problems. *Journal of basic Engineering* 82(1): 35-45.

Kato, S., Tamada, K., Shimada, Y. &Chujo, T. (1996). A quantification of goldfish behavior by an image processing system. *Behavioural Brain Research* 80(1-2): 51-55.

Kharat, G. U. &Dudul, S. V. (2008).Neural Network Classifier for Human Emotion Recognition from Facial Expressions Using Discrete Cosine Transform. In *Emerging Trends in Engineering and Technology, 2008. ICETET '08. First International Conference on*, 653-658.

Kmet, J., Sakowski, T., Huba, J., Peskovicova, D., Chrenek, J. &Polak, P. (2000). Application of video Image analysis in the slaughter value estimation of live Simmental bulls. *Arch. Tierz., Dummerstorf* 43: 411-416.

Kollis, K., Phang, C. S., Banhazi, T. M. &Searle, S. J. (2007). Weight Estimation Using Image Analysis and Statistical Modelling: A Preliminary Study. *Applied Engineering in Agriculture* 23(1): 91-96.

Korthals, R. L. (2001).Monitoring Growth and Statistical Variation of Grow-Finish Swine. In *Livestock Environment VI. Proceedings of the Sixth International Symposium*, 64-71 (Eds R. R. Stowell, R. Bucklin and R. W. Bottcher). Louisville, Kentucky: The Society for engineering in agricultural, food, and biological systems.

Kristensen, R. A. (2003).Information from on-line live weight assessment for optimal selection of slaughter pigs for market. In *4th EFITA*, Vol. 2, 754-759 (Eds Z. Harnos, M. Herdon and T. B. Wiwczaroski). Hungary: University of Debrecen.

Kvame, T. &Vangen, O. (2006). In-vivo composition of carcass regions in lambs of two genetic lines, and selection of CT positions for estimation of each region. *Small Ruminant Research* 66(1-3): 201-208.

Lambe, N. R., Navajas, E. A., Fisher, A. V., Simm, G., Roehe, R. &Bünger, L. (2009). Prediction of lamb meat eating quality in two divergent breeds using various live animal and carcass measurements. *Meat Science* 83(3): 366-375.

Lambe, N. R., Navajas, E. A., Schofield, C. P., Fisher, A. V., Simm, G., Roehe, R. &Bünger, L. (2008a). The use of various live animal measurements to predict carcass and meat quality in two divergent lamb breeds. *Meat Science* 80(4): 1138-1149.

Lambe, N. R., Schofield, C. P., Navajas, E. A., Roehe, R. &Bünger, L. (2008b).Video image analysis of live lambs to predict live weight, carcass composition and meat quality. In *Proceedings of the British society of animal science 2008*, 48.

Liang, Z. &Thorpe, C. (1999).Stereo- and neural network-based pedestrian detection. In *Intelligent Transportation Systems, 1999. Proceedings. 1999 IEEE/IEEJ/JSAI International Conference on*, 298-303.

Lichtenauer, J. F., Hendriks, E. A. &Reinders, M. J. (2008). Sign Language Recognition by Combining Statistical DTW and Independent Classification. *Pattern Analysis and Machine Intelligence, IEEE Transactions on* 30(11): 2040-2046.

Lind, N. M., Vinther, M., Hemmingsen, R. P. &Hansen, A. K. (2005). Validation of a digital video tracking system for recording pig locomotor behaviour. *Journal of Neuroscience Methods* 143(2): 123-132.

Lines, J. A., Tillett, R. D., Ross, L. G., Chan, D., Hockaday, S. &McFarlane, N. J. B. (2001). An automatic image-based system for estimating the mass of free-swimming fish. *Computers and Electronics in Agriculture* 31(2): 151-168.

Little, J. &Boyd, J. (1998). Recognizing people by their gait: the shape of motion. *Videre: Journal of Computer Vision Research* 1(2): 1-32.

Liu, Z. J., Kayalioglu, M., Shcherbatyy, V. &Seifi, A. (2007). Tongue deformation, jaw movement and muscle activity during mastication in pigs. *Archives of oral biology* 52(4): 309-312.

Lomas, C., Piggins, D. &Phillips, C. (1998). Visual awareness. *Applied Animal Behaviour Science* 57(3): 247-257.

Lorschy, M. L., Patience, J. F. &Gillis, D. A. (1997).Protein Deposition in Pigs. Prairie Swine Centre, Inc. Saskatoon, SK, Canada.: Monograph no. 97-03.

Lott, B., Reece, F. &Mc Naughton, J. (1982). An automated weighing system for use in poultry research. *Poultry Science* 61: 236-238.

Lundqvist, P. &Gustafsson, B. (1992). Accidents and accident prevention in agriculture a review of selected studies. *International Journal of Industrial Ergonomics* 10(4): 311-319.

Maes, D. G. D., Janssens, G. P. J., Delputte, P., Lammertyn, A. &de Kruif, A. (2004). Back fat measurements in sows from three commercial pig herds: relationship with reproductive efficiency and correlation with visual body condition scores. *Livestock Production Science* 91(1-2): 57-67.

Maes, P., Darrell, T., Blumberg, B. &Pentland, A. (1997). The ALIVE system: Wireless, full-body interaction with autonomous agents. *Multimedia Systems* 5(2): 105-112.

Maltz, E. (2010).Novel Technologies: Sensors, Data and Precision Dairy Farming. In *The First North American Conference on Precision Dairy Management*.

Manik, R. S., Jadhav, K. E. &Nath, I. (1981). Predicting weight from body measurements in Murrah buffaloes. *Indian J. of Dairy Science* 34: 448-450.

Marchant, J. (1993).Adding grey level information to point distribution models using finite elements. In *Proceedings of The British Machine Vision Conference 1993*, 309-318.

Marchant, J. A. &Schofield, C. P. (1993). Extending the snake image processing algorithm for outlining pigs in scenes. *Computers and Electronics in Agriculture* 8(4): 261-275.

Marchant, J. A., Schofield, C. P. &White, R. P. (1999). Pig growth and conformation monitoring using image analysis. *Animal Science* 68(1): 141-150.

Marchi, E., Ferri, N. &Comellini, F. (2007). Pig identification: comparison of results from injected transponders and electronic ear tags. *Veterinaria Italiana* 43(1): 97-102.

Martin, S. C., Barnes, K. K. &Bashford, L. (1967). A step toward automatic weighing of range cattle. *Journal of Range Management*: 91-94.

Martinez, A. M. &Kak, A. C. (2001). PCA versus LDA. *Pattern Analysis and Machine Intelligence, IEEE Transactions on* 23(2): 228-233.

McFarlane, N. &Schofield, C. (1995). Segmentation and tracking of piglets in images. *Machine Vision and Applications* 8(3): 187-193.

McFarlane, N., Wu, J., Tillett, R., Schofield, C., Siebert, J. &Ju, X. (2007). Shape measurements of live pigs using 3-D image capture. *Animal Science* 81(03): 383-391.

McGlone, J. J., Vines, B., Rudine, A. C. &DuBois, P. (2004a). The physical size of gestating sows. *J. Anim Sci.* 82(8): 2421-2427.

McGlone, J. J., Von Borell, E. H., Deen, J., Johnson, A. K., Levis, D. G., Meunier-Salaün, M., Morrow, J., Reeves, D., Salak-Johnson, J. L. &Sundberg, P. L. (2004b). Review: Compilation of the scientific literature comparing housing systems for gestating sows and gilts using measures of physiology, behavior, performance, and health. *The Professional Animal Scientist* 20(2): 105-117.

McLaren, D., McKeith, F. &Novakofski, J. (1989). Prediction of carcass characteristics at market weight from serial real-time ultrasound measures of backfat and loin eye area in the growing pig. *Journal of Animal Science* 67(7): 1657.

Med Associates Inc (2010). *Med Associates, Inc , Available on www.med-associates.com, Accessed on 9th July 2010*.

Minagawa, H. (1994). Surface area, volume, and projected area of Japanese-shorthorn cattle measured by stereo photogrammetry using non-metric cameras. *Journal of Agricultural Meteorology* 50: 17-22.

Minagawa, H. (1997).Estimating Pig Weight with a Video Camera. In *Livestock Environment V - 5th International Symposium*, Vol. I, 543-460 (Eds R. W. Bottcher and S. J. Hoff). Bloomington, Minnesota: American Society of Agricultural Engineers.

Minagawa, H. &Ichikawa, T. (1994). Determining the Weight of Pigs with Image Analysis. *Transactions of the American Society of Agricultural Engineers (ASAE)* 37(3): 1011-1015.

Minagawa, H., Taira, O. &Nissato, H. (2003).A color technique to simplify image processing in measurement of pig weight by a hands-off method. In *Proceedings of the 2003 Swine Housings II Conference* 166-173 (Ed L. D. Jacobson). North Carolina, USA.

Minagawa, H., Tanaka, H. &Akagawa, M. (1997).Developing an estimation method of pig weight with a video camera by image analysis. 362-363.

Mitchell, A. D., Scholz, A. &Pursel, V. (2002). Prediction of the in vivo body composition of pigs based on cross-sectional region analysis of dual energy x-ray absorptiometry (DXA) scans. *ARCHIV FUR TIERZUCHT* 45(6): 535-546.

Moeslund, T. B. &Granum, E. (2001). A Survey of Computer Vision-Based Human Motion Capture. *Computer Vision and Image Understanding* 81(3): 231-268.

Moeslund, T. B., Hilton, A. &Krüger, V. (2006). A survey of advances in vision-based human motion capture and analysis. *Computer Vision and Image Understanding* 104(2-3): 90-126.

Mollah, M. B. R., Hasan, M. A., Salam, M. A. &Ali, M. A. (2010). Digital image analysis to estimate the live weight of broiler. *Computers and Electronics in Agriculture* 72(1): 48-52.

Morrison, R. (2004).Observations on automatic sorting. In *4th London Swine Conference*, 45.

Myers, C., Rabiner, L. &Rosenberg, A. (1980). Performance tradeoffs in dynamic time warping algorithms for isolated word recognition. *Acoustics, Speech and Signal Processing, IEEE Transactions on* 28(6): 623-635.

Naas, I. A., Curto, F. P. F., Pereira, D. F., Amedola, M. A. &Behrens, F. H. (2001).Using Transponders For Determining Breeder Behavior Versus Environmental Temperature. In *Livestock Environment VI. Proceedings of the Sixth International Symposium*, 626-631 (Eds R. R. Stowell, R. Bucklin and R. W. Bottcher). Louisville, Kentucky: The Society for engineering in agricultural, food, and biological systems.

National Research Council (1998). *Nutrient requirements of swine.* National Academies Press.

Negretti, P. &Bianconi, G. (2004).Morphological survey through computerised image analysis. In *Proceedings of the 7th World Conference of the Brown Swiss cattle breeders.*, 3-7 Verona, Italy.

Negretti, P., Bianconi, G., Bartocci, S. &Terramoccia, S. (2007a). Lateral Trunk Surface as a new parameter to estimate live body weight by Visual Image Analysis. *Italian Journal of Animal Science* 6(2s): 1223-1225.

Negretti, P., Bianconi, G. &Finzi, A. (2007b). Visual image analysis to estimate morphological and weight measurements in rabbits. *World Rabbit Science* 15(1): 37-41.

Negretti, P., Bianconi, G., Bartocci, S., Terramoccia, S. &Verna, M. (2008). Determination of live weight and body condition score in lactating Mediterranean buffalo by Visual Image Analysis. *Livestock Science* 113(1): 1-7.

Neitz, J. &Jacobs, G. H. (1989). Spectral sensitivity of cones in an ungulate. *Visual Neuroscience* 2(02): 97-100.

Ng, E. &Acharya, R. (2009). Remote-sensing infrared thermography. *Engineering in Medicine and Biology Magazine, IEEE* 28(1): 76-83.

Niblack, W. (1985). *An introduction to digital image processing.* Strandberg Publishing Company Birkeroed, Denmark, Denmark.

Niemi, J. K., Sevón-Aimonen, M.-L., Pietola, K. &Stalder, K. J. (2010). The value of precision feeding technologies for grow-finish swine. *Livestock Science* 129(1-3): 13-23.

Noldus (2010). *Software and labs for behavioural research and video tracking | Noldus Information Technology, Available on www.noldus.com, Accessed on 9th July 2010.*

Noldus, L., Spink, A. J. &Tegelenbosch, R. A. J. (2001). EthoVision: a versatile video tracking system for automation of behavioral experiments. *Behavior Research Methods, Instruments, & Computers* 33(3): 398.

Noldus, L. P. J. J., Spink, A. J. &Tegelenbosch, R. A. J. (2002). Computerised video tracking, movement analysis and behaviour recognition in insects. *Computers and Electronics in Agriculture* 35(2-3): 201-227.

O'Dowd, S., Hoste, S., Mercer, J. T., Fowler, V. R. &Edwards, S. A. (1997). Nutritional modification of body composition and the consequences for reproductive performance and longevity in genetically lean sows. *Livestock Production Science* 52(2): 155-165.

Onyango, C. M., Marchant, J. A. &Ruff, B. P. (1995). Model based location of pigs in scenes. *Computers and Electronics in Agriculture* 12(4): 261-273.

Ostersen, T., Cornou, C. &Kristensen, A. R. (2010). Detecting oestrus by monitoring sows' visits to a boar. *Computers and Electronics in Agriculture* 74(1): 51-58.

Otsu, N. (1979). A Threshold Selection Method from Gray-Level Histograms. *Systems, Man and Cybernetics, IEEE Transactions on* 9(1): 62-66.

Parsons, D. J., Green, D. M., Schofield, C. P. &Whittemore, C. T. (2007). Real-time Control of Pig Growth through an Integrated Management System. *Biosystems Engineering* 96(2): 257-266.

Pastorelli, G., Musella, M., Zaninelli, M., Tangorra, F. &Corino, C. (2006). Static spatial requirements of growing-finishing and heavy pigs. *Livestock Science* 105(1-3): 260-264.

Pearson, K. (1901). Llll. On lines and planes of closest fit to systems of points in space. *Philosophical Magazine Series 6* 2(11): 559-572.

Pedersen, B. K. &Madsen, T. N. (2001).Monitoring Water Intake in Pigs: Prediction of Disease and Stressors. In *Livestock Environment VI*, 173-179 Louisville, Kentucky: The Society for engineering in agricultural, food, and biological systems.

Pedersen, B. K., Petersen, L. B., Hjelholt, K., Andersen, H. M. L., Ruby, V. &Kai, P. (1998).Growing-Finishing Pigs: Cooling Reduces Aggressive Behaviour and Pen Fouling. In *15th International Pig Veterinary Society Congress*, 5 Birmingham, England.

Pellis, S. M. (1988). Agonistic versus amicable targets of attack and defense: Consequences for the origin, function, and descriptive classification of play-fighting. *Aggressive Behavior* 14(2): 85-104.

Pellis, S. M. &Pellis, V. C. (1987). Play-fighting differs from serious fighting in both target of attack and tactics of fighting in the laboratory rat Rattus norvegicus. *Aggressive Behavior* 13(4): 227-242.

Perner, P. (2001). Motion tracking of animals for behavior analysis. *Visual Form 2001*: 779-786.

Petherick, J. C. (1983).A Biological Basis for the Design of Space in Livestock Housing. In *Farm Animal Housing and Welfare*, 103-120 (Eds S. H. Baxter, M. R. Baxter and J. A. C. MacCormack). Dordrecht: Martinus Nijhoff.

Phillips, R. W. &Dawson, W. M. (1936). A study of methods for obtaining measurements of swine. *Am. Soc. Anim. Prod.* 1936b(1): 93-99.

Pope, G. &Moore, M. (2002).Estimating sow liveweights without scales. Department of Primary Industries and Resources, Government of South Australia, From the web site of the Department of Agriculture, Fisheries and Forestry, Queensland, Australia.

Pressley, A. N. (2010).How much does a curve curve? In *Elementary differential geometry*, Vol. 2, 29-54 London Springer-Verlag.

Qubit Systems Inc (2010). *Qubit Systems, Inc , Available on www.qubitsystems.com, Accessed on 9th July 2010*.

Rabiner, L. R. (1989). A tutorial on hidden Markov models and selected applications in speech recognition. *Proceedings of the IEEE* 77(2): 257-286.

Rainwater-Lovett, K., Pacheco, J. M., Packer, C. &Rodriguez, L. L. (2009). Detection of foot-and-mouth disease virus infected cattle using infrared thermography. *The Veterinary Journal* 180 (3): 317-324.

Ramaekers, P., Huiskes, J., Verstegen, M., Hertog, L., Vesseur, P., Swinkels, J. &Peet-Schwering, C. (1995a). Modern techniques for automatic

determination of individual body weight of growing-finishing pigs housed in groups. *Uebersichten zur Tierernaehrung (Germany)*.

Ramaekers, P. J. L., Huiskes, J. H., Verstegen, M. W. A., den Hartog, L. A., Vesseur, P. C. &Swinkels, J. W. G. M. (1995b). Estimating individual body weights of group-housed growing-finishing pigs using a forelegs weighing system. *Computers and Electronics in Agriculture* 13(1): 1-12.

Rehfeldt, C., Tuchscherer, A., Hartung, M. &Kuhn, G. (2008). A second look at the influence of birth weight on carcass and meat quality in pigs. *Meat Science* 78(3): 170-175.

Rhodes, R. T., Appleby, M. C., Chinn, K., Douglas, L., Firkins, L. D., Houpt, K. A., Irwin, C., McGlone, J. J., Sundberg, P. &Tokach, L. (2005). A comprehensive review of housing for pregnant sows. *Journal of the American Veterinary Medical Association* 227(10): 1580-1590.

Rohr, K. &Systeme, A. K. (1997). Human movement analysis based on explicit motion models, chapter 8. *In Motion-Based Recognition*.

Rosenblum, M., Yacoob, Y. &Davis, L. (1994).Human emotion recognition from motion using a radial basis function network architecture. In *Motion of Non-Rigid and Articulated Objects, 1994., Proceedings of the 1994 IEEE Workshop on*, 43-49.

Roweis, S. (1998). EM algorithms for PCA and SPCA. *Advances in neural information processing systems*: 626-632.

Roweis, S. &Ghahramani, Z. (1999). A unifying review of linear Gaussian models. *Neural Computation* 11(2): 305-345.

Schaefer, A. L., Cook, N. J., Church, J. S., Basarab, J., Perry, B., Miller, C. &Tong, A. K. W. (2007). The use of infrared thermography as an early indicator of bovine respiratory disease complex in calves. *Research in Veterinary Science* 83(3): 376-384.

Schaefer, A. L. &Tong, A. K. W. (2000).Process for determining a tissue composition characteristic of an animal. Google Patents.

Schofield, C., Tillett, R., McFarlane, N., Mottram, T., Frost, A. &Cox, S. (2005). Emerging technology for assessing the composition of livestock. In *Proceedings of the second European conference on precision livestock farming,*Uppsala, Sweden.

Schofield, C. P. (1990). Evaluation of image analysis as a means of estimating the weight of pigs. *Journal of Agricultural Engineering Research* 47: 287-296.

Schofield, C. P., Marchant, J. A., White, R. P., Brandl, N. &Wilson, M. (1999). Monitoring Pig Growth using a Prototype Imaging System. *Journal of Agricultural Engineering Research* 72(3): 205-210.

Schofield, C. P., Wathes, C. M. &Frost, A. R. (2002).Integrated Management Systems for Pigs - Increasing Production Efficiency and Welfare. In *Animal Production in Australia*, Vol. 24, 197-200 (Eds D. K. Revell and D. Taplin). Adelaide, South Australia.

Schreer, O., Feldmann, I., Golz, U. &Kauff, P. (2002).Fast and robust shadow detection in videoconference applications. In *4th EURASIP - IEEE Region 8 International Symposium on Video/Image Processing and Multimedia Communications* 371-375.

Sergeant, D., Boyle, R. &Forbes, M. (1998). Computer visual tracking of poultry. *Computers and Electronics in Agriculture* 21(1): 1-18.

Shao, B. &Xin, H. (2008). A real-time computer vision assessment and control of thermal comfort for group-housed pigs. *Computers and Electronics in Agriculture* 62(1): 15-21.

Shao, J., Xin, H. &Harmon, J. D. (1998). Comparison of image feature extraction for classification of swine thermal comfort behavior. *Computers and Electronics in Agriculture* 19(3): 223-232.

Smulders, D., Verbeke, G., Mormède, P. &Geers, R. (2006). Validation of a behavioral observation tool to assess pig welfare. *Physiology & Behavior* 89(3): 438-447.

Stacey, K. F., Parsons, D. J., Frost, A. R., Fisher, C., Filmer, D. &Fothergill, A. (2004). An Automatic Growth and Nutrition Control System for Broiler Production. *Biosystems Engineering* 89(3): 363-371.

Stajnko, D., Brus, M. &Hocevar, M. (2008). Estimation of bull live weight through thermographically measured body dimensions. *Computers and Electronics in Agriculture* 61(2): 233-240.

Stajnko, D., Lakota, M. &Hocevar, M. (2004). Estimation of number and diameter of apple fruits in an orchard during the growing season by thermal imaging. *Computers and Electronics in Agriculture* 42(1): 31-42.

Stärk, K. D. C., Morris, R. S. &Pfeiffer, D. U. (1998). Comparison of electronic and visual identification systems in pigs. *Livestock Production Science* 53(2): 143-152.

Starner, T. &Pentland, A. (1997). Real-time american sign language recognition from video using hidden markov models. *Computational Imaging and Vision* 9: 227-244.

Statham, P., Green, L., Bichard, M. &Mendl, M. (2009). Predicting tail-biting from behaviour of pigs prior to outbreaks. *Applied Animal Behaviour Science* 121(3-4): 157-164.

Stauffer, C. &Grimson, W. E. L. (1999).Adaptive background mixture models for real-time tracking. In *IEEE Computer Society Conference on Computer Vision and Pattern Recognition*, Vol. 2.

Stewart, M., Webster, J. R., Verkerk, G. A., Schaefer, A. L., Colyn, J. J. &Stafford, K. J. (2007). Non-invasive measurement of stress in dairy cows using infrared thermography. *Physiology & Behavior* 92(3): 520-525.

Stickney, K. (2009). Reducing Grower-Finisher Feed Costs. In *9th London Swine Conference,* (Ed J. M. Murphy).

Stranks, M., Cooke, B., Fairburn, C., Fowler, N., Kirby, P., McCracken, K., Morgan, C., Palmer, F. &Peers, D. (1988). Nutrient allowances for growing pigs. *Research and Development in Agriculture* 5(2): 71-88.

Stricklin, W., De Bourcier, P., Zhou, J. &Gonyou, H. (1998). Artificial pigs in space: using artificial intelligence and artificial life techniques to design animal housing. *J Anim Sci.* 76(10): 2609-2613.

Stukenborg, A., Traulsen, I., Puppe, B., Presuhn, U. &Krieter, J. (2010). Agonistic behaviour after mixing in pigs under commercial farm conditions. *Applied Animal Behaviour Science* 129(1): 28-35.

Sumpter, N., Boyle, R. &Tillett, R. (1997).Modelling collective animal behaviour using extended point-distribution models. University of Leeds, School of Computer Studies.

Šustr, P., Špinka, M., Cloutier, S. &Newberry, R. C. (2001). Computer-aided method for calculating animal configurations during social interactions from two-

dimensional coordinates of color-marked body parts. *Behavior Research Methods, Instruments, & Computers* 33(3): 364.

Tasdemir, S., Urkmez, A. &Inal, S. (2011). Determination of body measurements on the Holstein cows using digital image analysis and estimation of live weight with regression analysis. *Computers and Electronics in Agriculture* 76(2): 189-197.

Tillett, R., McFarlane, N. &Lines, J. (2000). Estimating Dimensions of Free-Swimming Fish Using 3D Point Distribution Models. *Computer Vision and Image Understanding* 79(1): 123-141.

Tillett, R., McFarlane, N., Wu, J., Schofield, C., Ju, X. &Siebert, J. (2004).Extracting morphological data from 3D images of pigs. In *Proceedings of the international conference on agricultural engineering* Vol. 1, 492-493 Leuven, Belgium,.

Tillett, R. D. (1991). Model-based image processing to locate pigs within images. *Computers and Electronics in Agriculture* 6(1): 51-61.

Tillett, R. D., Onyango, C. M. &Marchant, J. A. (1997). Using model-based image processing to track animal movements. *Computers and Electronics in Agriculture* 17(2): 249-261.

Tscharke, M. &Banhazi, T. M. (2011).Review of methods to determine weight, size and composition of livestock from images. In *The Bi-annual Conference of the Australian Society of Engineering in Agriculture (SEAg 2011)*, 465-483. (Eds C. Saunders and T. Banhazi). Gold Coast, Australia: Australian Society of Engineering in Agriculture.

TSE-Systems (2010). *phenotyping, behaviour, metabolism, inhalation research -TSE Systems, Available on www.tse-systems.com, Accessed on 8th July 2010*.

Turner, M., Gurney, P., Crowther, J. &Sharp, J. (1984a). An automatic weighing system for poultry. *Journal of Agricultural Engineering Research (UK)*.

Turner, M. J. B., Gurney, P., Crowther, J. S. W. &Sharp, J. R. (1984b). An Automatic Weighing System for Poultry. *Journal of Agricultural Engineering Research* 29: 17-24.

Tweed, D. &Calway, A. (2002).Tracking multiple animals in wildlife footage. In *16th International Conference on Pattern Recognition.*, Vol. 2, 24-27 vol.22.

Vajda, T. (2010).Behavior recognition using Pictorial Structures and DTW. In *IEEE International Conference on Automation Quality and Testing Robotics (AQTR)*, Vol. 3, 1-4.

Vangen, O. &Jopson, N. B. (1996).Research application of noninvasive techniques for body composition. 25–29.

Vaughan, R., Sumpter, N., Henderson, J., Frost, A. &Cameron, S. (2000). Experiments in automatic flock control. *Robotics and Autonomous Systems* 31(1-2): 109-117.

Vicon (2010).

Vidal, R., Yi, M. &Sastry, S. (2003).Generalized principal component analysis (GPCA). In *Computer Vision and Pattern Recognition, 2003. Proceedings. 2003 IEEE Computer Society Conference on*, Vol. 1, I-621-I-628 vol.621.

Vivek, E. P. &Sudha, N. (2006). Gray Hausdorff distance measure for comparing face images. *Information Forensics and Security, IEEE Transactions on* 1(3): 342-349.

von Wachenfelt, H., Nilsson, C. &Pinzke, S. (2010). Gait and force analysis of provoked pig gait on clean and fouled rubber mat surfaces. *Biosystems Engineering* 106(1): 86-96.

Wang, Y., Yang, W., Winter, P. &Walker, L. (2008). Walk-through weighing of pigs using machine vision and an artificial neural network. *Biosystems Engineering* 100(1): 117-125.

Wang, Y., Yang, W., Winter, P. &Walker, L. T. (2006). Non-contact sensing of hog weights by machine vision. *Applied Engineering in Agriculture* 22(4): 577-582.

Wathes, C. M., Abeyesinghe, S. M. &Frost, A. R. (2001).Environmental Design and Management for Livestock in the 21st Century: Resolving Conflicts by Integrated Solutions. In *Livestock Environment VI. Proceedings of the Sixth International Symposium*, 5-14 Louisville, Kentucky: The Society for Engineering in Agricultural, Food and Biological Systems.

Weary, D. M., Pajor, E. A., Fraser, D. &Honkanen, A.-M. (1996). Sow body movements that crush piglets: a comparison between two types of farrowing accommodation. *Applied Animal Behaviour Science* 49(2): 149-158.

Weaver, M. E. &Ingram, D. L. (1969). Morphological Changes in Swine Associated with Environmental Temperature. *Ecology* 50(4): 710-713.

Weixing, Z., Fangkui, Z. &Xiangping, L. (2010).Automated Monitoring System of Pig Behavior Based on RFID and ARM-LINUX. In *Third International Symposium on Intelligent Information Technology and Security Informatics (IITSI)*, 431-434.

White, R., Parsons, D., Schofield, C., Green, D. &Whittemore, C. (2003).Use of visual image analysis for the management of pig growth in size and shape. In *Proceedings of the British Society of Animal Science*, 101.

White, R., Schofield, C., Green, D., Parsons, D. &Whittemore, C. (2004). The effectiveness of a visual image analysis (VIA) system for monitoring the performance of growing/finishing pigs. *British Society of Animal Science* 78: 409-418.

Whittemore, C. (2004). Production control systems for pigs. In *4th London Swine Conference*, 111-118.

Whittemore, C., Green, D. &Schofield, C. (2001). Nutrition management of growing pigs. *Integrated management systems for livestock, BSAS Occasional Publication* 28: 89-96.

Whittemore, C. T. &Schofield, C. P. (2000). A case for size and shape scaling for understanding nutrient use in breeding sows and growing pigs. *Livestock Production Science* 65(3): 203-208.

Whittemore, C. T., Tullis, J. B. &Emmans, G. C. (1988). Protein growth in pigs. *Animal production* 46(03): 437-445.

Willeke, H. &Dursch, T. (2002). Prediction of the body weight of Simmental heifers using heart girth measurements. *Archiv Tierzucht* 45(1): 23-28.

Williams, S. R. O., Moore, G. A. &Currie, E. (1996). Automatic Weighing Of Pigs Fed Ad Libitum. *Journal of Agricultural Engineering Research* 64(1): 1-10.

Wilson, L. L., Egan, C. L. &Terosky, T. L. (1997). Body Measurements and Body Weights of Special-Fed Holstein Veal Calves. *Journal of dairy science* 80(11): 3077-3082.

Wouters, P., Geers, R., Parduyuns, G., Goossens, K., Truyen, B., Goedseels, V. &Van der Stuyft, E. (1990). Image-analysis parameters as inputs for automatic environmental temperature control in piglet houses. *Computers and Electronics in Agriculture* 4: 233-246.

Wren, C. R., Azarbayejani, A., Darrell, T. &Pentland, A. P. (1997a). Pfinder: Real-time tracking of the human body. *IEEE Transactions on Pattern Analysis and Machine Intelligence* 19(7): 781.

Wren, C. R., Sparacino, F., Azarbayejani, A. J., Darrell, T. J., Starner, T. E., Kotani, A., Chao, C. M., Hlavac, M., Russell, K. B. &Pentland, A. P. (1997b). Perceptive spaces for performance and entertainment untethered interaction using computer vision and audition. *Applied Artificial Intelligence: An International Journal* 11(4): 267 - 284.

Wu, J., Tillett, R., McFarlane, N., Ju, X., Siebert, J. P. &Schofield, P. (2004). Extracting the three-dimensional shape of live pigs using stereo photogrammetry. *Computers and Electronics in Agriculture* 44(3): 203-222.

Wu, S. &Amin, A. (2003). Automatic thresholding of gray-level using multi-stage approach. *Document Analysis and Recognition* 1: 493.

Xin, H. (1999). Assessing swine thermal comfort by image analysis of postural behaviors. *Journal of Animal Science* 77(E-Suppl 2): 1.

Xin, H. &Shao, B. (2002).Real-time Assessment of Swine Thermal Comfort by Computer Vision. In *Proceedings of the World Congress of Computers in Agriculture and Natural Resources*, 362-369 (Eds F. S. Zazueta and J. Xin). 13-15, March 2002, Iguacu Falls, Brazil: ASAE.

Xue, X. &Henderson, T. (2006). Video based animal behavior analysis. *University of Utah, TechReport UUCS-06-006*.

Yamato, J., Ohya, J. &Ishii, K. (1992).Recognizing human action in time-sequential images using hidden Markov model. 379–385.

Yang, Y. &Teng, G. (2008).Estimating Pig Weight From 2D Images. In *IFIP International Federation for Information Processing, Volume 259, Computer and Computing Technologies in Agriculture*, Vol. 2, 1471–1474 (Ed D. Li). Boston: Springer.

Yeo, M. &Smith, P. (1977). A note on relationships between girth measurements and sow liveweight gain. *Experimental Husbandry* 33: 81-84.

Zaragoza, L. E. O. (2009).Evaluation of the accuracy of simple body measurements for live weight prediction in growing-finishing pigs. University of Illinois.

Zhong, J. &Sclaroff, S. (2003).Segmenting foreground objects from a dynamic textured background via a robust kalman filter. In *Proceedings of the Ninth IEEE International Conference on Computer Vision (ICCV)*, 44: IEEE Computer Society.

Zivkovic, Z. (2004).Improved adaptive Gaussian mixture model for background subtraction. In *Proceedings of the 17th International Conference on Pattern Recognition (ICPR 2004),* , Vol. 2, 28-31.

APPENDIX A

Modelling Time Dependant Behaviour

The identification of behaviours is a *random* or *stochastic process*; we often observe behaviour in our day to day activities that we would not expect. In this case we are instinctively determining the probability of an event occurring and have a preconceived perspective of what we are about to witness. However, this perspective is not guaranteed to be correct, it may not result with the same outcome if the event is repeated - like in a *deterministic process* where the outcome(s) is the same given the same input(s). Thus the path to an outcome in a *stochastic process* is defined through probability distributions; what is the most likely outcome given the past and current state of the system. There are three ways in which we can determine the occurrence of a future event; using the current value(s), past value(s) or a combination of both. Here we only concentrate on the most relevant process where the conditional probability is based only on the current state (feature values) of the system which is commonly called a Markov process. In addition to these processes, a model can be either based on inputs from a predetermined range of information (discrete) or continuous and constantly changing information. The application of behaviour modelling largely involves the design of systems which continually stream data from as sensory source, therefore specific attention is centred on models which have the ability to deal with continuous inputs and adaptation. Static data methods result in a model that will have fixed (continuous) hidden states once it is defined. Observations for static data are assumed to have been collected instantaneously and they neglect any temporal conditions. In contrast dynamic data are considered temporal and therefore models that utilise dynamic data have hidden states which may vary. Models for dynamic data are progressive meaning that they are bounded by their state which typically changes in respect to a continuous linear variable such a time. Static models can be thought of as a generic representation of a dynamic data model.

A few temporal methods can be used to translate and transcribe a behaviour over time such as 'dynamic time warping' (DTW), 'hidden Markov models' (HMM), Kalman filters and artificial neural networks (ANN). These methods all function in a similar manner. Also note that some of the techniques presented here in the behavioural recognition process can also be used interchangeably in the spatial and temporal feature identification process.

Dynamic Time Warping

Dynamic time warping (DWT) refers to the development of algorithms which compress or expand data which is dependent on a variable time scale. This type of algorithm normalises the data based on the following constraints; path endpoint, global path, continuity of localised path sections, orientation, and distance measures (Myers *et al.*, 1980). DWT techniques have successfully been applied to sign language recognition and body pose recognition (Vajda, 2010) with the help of artificial neural network classification. Statistical DWT (SWDT) (an extension of the DWT) has proved to perform better in some cases than Hidden Markov models such as in handwriting recognition (Bahlmann and Burkhardt, 2004) and sign language recognition (Lichtenauer *et al.*, 2008).

Hidden Markov Models

A Markov process simply put is a process where the present interpretation of the system is used to estimate the future interpretation of the system; but it does not depend on the past interpretation of the system. Assuming the possibly dependant variables in vector $\boldsymbol{p} = (p_1, p_2, \ldots p_n)$ which has a new variable periodically appended to it based on a parameter (such as time t) in a Markov process the prediction of p_{t+1} (future value) is based only on p_t (current value). Hidden Markov models have a random input state which in this case is defined by the image features at time t and they generate an output state (estimated pose or behaviour) based on probability constraints on the input. The probability constraints are held in a transition matrix which describes the relationship between the current state and all other predefined states. The model values within transition matrix are generally determined in a supervised training process prior to on-line execution; in this case using a dataset of *a priori* features, cues or poses extracted from video sequences of transitions between the given behaviour(s). During training the behaviour is normalised such that checkpoint states are defined which provide a generic representation the variance of the behaviour over time (describes the behaviour most efficiently). Each individual behaviour defined within the HMM can be visualised as a predefined path 'through' a behaviour which compensates for a varying degree of behavioural resolution (time/space scale). During execution a HMM will follow a behavioural path using conditional probability between the current state and the projected output or future state (a function of the current or the current state) to the checkpoints defined in its HMM model. A correct or incorrect match is then confirmed based on this probabilistic association. Hidden Markov models have been applied in vision applications such as sign language recognition (Starner and Pentland, 1997) and body movement actions (Yamato *et al.*, 1992). More details on HMM can be found in (Rabiner, 1989).

Kalman Filter

The hidden Markov model (HMM) and a Kalman filter model have many similarities. A Kalman filter model also known as a linear dynamic model is a recursive mathematical process used to determine a best estimation of a systems state. The estimation of the current systems state based is on temporal measurements of a systems variable(s) which may contain random variation or error. The collected information is used to minimise the error between the current measurement and the underlying true measurement of the variable. The filter works by first predicting a value that is assumed to be close to the *true* measurement. The probability that the predicted value is the true value is also calculated as the uncertainty. Finally a weighted average between the predicted value and the measured value are determined from the covariance between variable(s) in the system. The value with the highest weighting has the least uncertainty. The weighted averages are incorporated into the system parameters after a time step which points the system in the most likely direction in the following time step. The filter system alternates between updating and predicting and can perform these steps in any combination depending on the availability of the incident data into the process or the integrity of the current predictive precision. For example due to a delay in the response from a sensor the process may predict future values for three time steps ahead for every one update from the sensor or alternatively two sensor updates could be applied for every

prediction if the system began to diverge. The new state of the system is calculated based on the previous 'best' estimate of the system. Technical details of the filter can be found in (Kalman, 1960).

Artificial Neural Networks

Artificial neural networks (ANN) have a layered structure and function as a linear auto encoder. An ANN architecture is displayed in Figure 7. This particular network is constructed with one hidden layer containing 20 neurons and 1 output layer that provides the estimate(s) as output. The figure is based on abbreviated notation found in (Demuth and Beale). In this example a tan-sigmoid transfer function was used in the hidden layer and a linear transfer function was used in the output layer. Input measurement vectors are generally normalised before training so that they have zero mean and a standard deviation of one in order to scale the network inputs appropriately.

$$a_2 = f^2\big(LW_{2,1}f^1\big(IW_{1,1}p + b^1\big) + b^2\big) = y$$
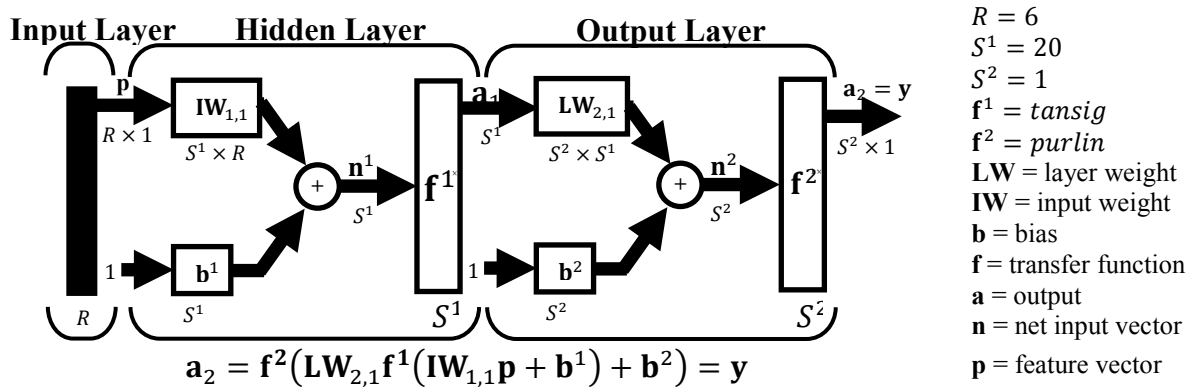
Figure 148: An Example of an Artificial Neural Network Structure

Here the input is either the output of another artificial neuron or a vector of the original data. The input(s) are passed through a transfer function that contributes a given weight value 'w_i' to the input(s). These weights are then combined in a way to represent the input in terms of the output (they collectively determine the underling systems model). A learning function aims to provide reasoning between the input and the output and establish sound link between the two. The ANN obtains this reasoning by analysing and 'taking notes' (weights) on an incident data flow. A cost function is used to control the learning it does this by recording and assessing the systems projected output based on an input and an actual known observation.

Neural networks can be trained in one of two ways mentioned previously; through supervised learning where the output targets are known or unsupervised learning where the output targets are not known to begin with. Although different methods, both unsupervised and supervised training methods have the same end goal to generalise incident input data into its correct output class or classes via a learning rule. In addition to these learning methods there are two general ways to structure the flow data into the training process, concurrently and sequentially. Networks that adopt a concurrent method push all inputs into the network simultaneously. A sequentially orientated network pushes the inputs into the system in a predetermined sequence. Furthermore networks can be either static with no delays or dynamic that the delay weight updates through a time step. Networks are trained either incrementally or in batches and adopt variations of the different types of information

flow mentioned previously. Neural networks have been used to determine human emotion recognition (Rosenblum *et al.*, 1994; Kharat and Dudul, 2008) and pose detection (Liang and Thorpe, 1999; Guo *et al.*, 1994).

Static Data

Methods to generalise a model using static data include factor analysis, principal component analysis, linear discriminate analysis (LDA) and support vector machine (SVM) (Burges, 1998). A number of variations of PCA also exist such as sensible principal component analysis (SPCA) (Roweis, 1998) and generalised principal component analysis (GPCA) (Vidal *et al.*, 2003). A comparison between PCA and LDA can be found in (Martinez and Kak, 2001).

Principal Component Analysis

Principle component analysis (PCA) is an effective way of simplifying the feature data when the data is considered static. Features that are poorly or uncorrelated (dissimilar) to one another are found during the analysis. By performing a PCA the features can be observed which best represent the variance in the data and provide grounds for separation, as the resulting principle components are the features which best represent the data. The principal components are generally found using an Eigen value decomposition of a covariance matrix based on the feature data (Pearson, 1901).

APPENDIX B

Clustering and Classification Methods

A Conceptual Description of Model Training Through Clustering and Classification

Classification and clustering methods are data dependant structures which make a decision based on filtering observation data through a predefined system of conditions. A ball maze can be used to exemplify the clustering and classification process, where it is the objective of a ball to move from the top layer of the maze through to a lower layer by dropping through different size holes located on each level in the maze. The level in which the ball stops (the decision) will depend on the size of the ball (input) and the size of the holes (conditions or system constraints). Here the condition would be if the ball is less than or equal to the size of the hole then it can progress to the next level. The decision at each level can be based on logic if the ball goes through the hole or not (True or False). Or alternatively the probability, where one could assume that the ball is small in comparison to several holes varying in size and the ball has the highest chance of going through the hole which is greatest in size.

Figure 149 illustrates this concept with the layers of the maze from input level 1 to output level 6. In a trial the red ball would eventually get stuck on level 5 the blue on level 6 and the green would make it beyond level 6.
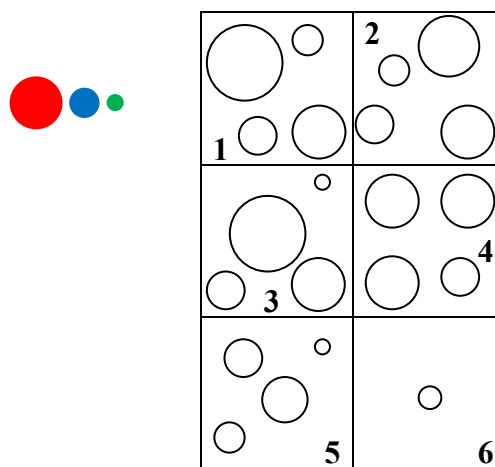
Figure 149: Layers of the Ball Maze Concept

Now consider the same system only this time the size of the holes in each level and the number of levels are hidden. A question one may ask is how are the conditions defined? How do we know what level a particular size ball will stop? The answer is that training is required. By putting many different sized balls into the system and measuring how long it takes to get the ball through the maze we can start to understand the conditions behind the system (its model). Intuitively we can use different states of the ball to help with understanding the underlying system model. For example the ball can be described as rolling, landing or silent based on the noise coming from the system; here silence would be an indication that the ball is stationary from being partially stuck in a hole. By starting with the smallest ball during training and gradually increasing them in size we would quickly find the threshold for the range of ball sizes that make it through level 6. This repetitious

training results in the definition of clusters where patterns or behaviours of similar sized balls are grouped together. This follows with a classification stage where the conditional probability between the resulting output state (noise from the input) is compared with the information in the predefined clusters. In this example the size of the ball does not need to be known in the classification stage and can be estimated based on what cluster the state suggests it belongs to. This basic conceptual model is synonymous with model building techniques such as artificial neural networks (ANN) where the underlying conditions are learned in an iterative learning process using known inputs and sometimes but not always known outputs.

Clustering and Classification

This section presents machine learning techniques which enable one to derive a computer readable model off-line or alternatively adapt or begin the execution of their models on-line. Machine learning algorithms automatically cluster and classify pattern occurrences. There are two types of learning mechanisms used in machine learning these are supervised learning and unsupervised learning. Supervised learning refers to learning where the underlying pattern structure is found off-line using training data. The model derived from training data is then used for comparison or validation purposes when the system becomes on-line. Unsupervised learning refers to a system that determines the groupings or arrangement of incident data (learns) on-line after the system has been activated. That is in order for an unsupervised vision system to adapt or operate model free it must self-record features with time and then self-classify them based on previously identified clusters of patterns which were defined by the system while on-line.

Clustering is a data driven unsupervised learning process which attempts to determine relationships between data based on (i) goodness-of-fit to a proposed model, or (ii) natural groupings (Jain *et al.*, 1999). Clustering techniques are used to investigative a hypothesis or help confirm a decision.

Unlike clustering, classification (also known as discriminant analysis) is a supervised learning process which categorises groups based on quantitative information of the observed feature data. A classification process involves training a set of previously labelled data to describe a pattern(s) before using the pattern(s) to sort (classify) incident feature data into their respective groups (Jain *et al.*, 1999).

Clustering

Jain and Dubes (1988) define a system of processes for a clustering task involving pattern representation, definition of a pattern, clustering or grouping, data abstraction and assessment of output or validation.
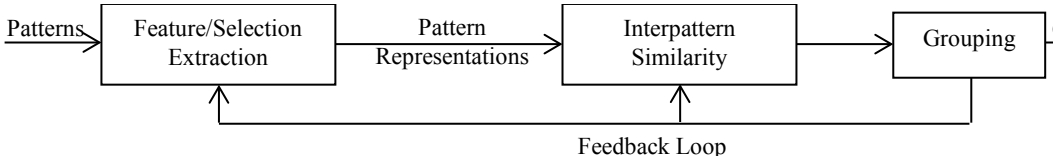
Figure 150: The Sequence of Pattern Representation, Pattern Definition and Clustering (Grouping) (Jain and Dubes, 1988)

The pattern representation stage identifies the number of available patterns and classes (groups) as well as the type and scale of the systems parameters. The feature selection process involves an analysis of the features to determine which ones best describe a pattern; identification of the most explanatory features of a set of inputs. The feature extraction process involves the combination of features to develop hybrid patterns which have good correlation. The clustering or grouping process involves the division of the feature derived data points up into their relative classes. Jain *et al.* (1999) defines a class as "a source of patterns whose distribution in feature space is governed by a probability density specific to the class" (Jain *et al.*, 1999, p 270). There are many different ways which one can cluster data, however, one common underlying trait of a clustering algorithm is that they use a proximity or distance measure to associate the different points or patterns in the solution space. The association between data points and their classes can be either 'hard' where the decision of cluster algorithm forces the analysed point into a group or 'fuzzy' where a point can take on a number(s) which shows its partial membership to surrounding classes. Once a cluster is found it is often beneficial to represent it as a simplified representation of its population. Simplifying a cluster into a more basic form generally increases the computational efficiency of the system through the compression of the data as the time taken to identify the correct group(s) for the values incident into the system is reduced. An example is using a centroid to represent a cluster of associated points (Jain *et al.*, 1999). There are many different types of clustering algorithms used to group data into efficient and meaningful groups. The clustering technique forms the constraints on of the data layout of the system. A classification technique is then the process of labelling which cluster input feature data belongs to. Once the data are separated into efficient and isolated groups a classification method is required to deal with new input data and assign it to its appropriate group. Some examples of clustering techniques are presented in the following paragraphs.

Hierarchical algorithms cluster the data one of two ways. Top down (divisive) where the data are partitioned into clusters starting from the whole dataset or 'bottom up' (agglomerative) where there is a progressive merger of clusters to form groups of larger clusters. The hierarchical process is usually represented by a dendrogram which outlines the sequence in which the clusters were grouped. These are time based in that they require a certain number of iterations before they converge to a solution. Clustering techniques that determine the clusters simultaneously are known as *partitional clustering algorithms*. An example of a *Graph Theoretic algorithm* is the minimal spanning tree or MST which divides data based on links between data points the edges created between them. If edges between points can be more intuitively described other than by distance, various weightings can be applied to edge(s) to provide appropriate bias. The minimal spanning tree can be identified as the shortest path between all points. The edges which contribute the largest percentage of the shortest path can then be removed to form the desired number of clusters.

Shown below in Figure 151 is the trivial example of a MST process based on Euclidian metric. Removing the two longest lines (dashed) of the MST isolates the three clusters (**ABC**)(**DEF**)(**GH**).
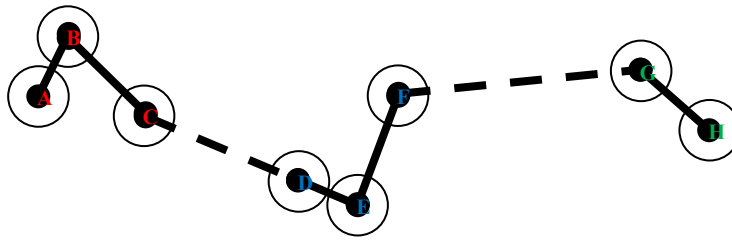
Figure 151: Example of Minimal Spanning Tree (MST) Clustering

An example of a basic hierarchical agglomerative process illustrating how distances are used to group the data can be seen below in Figure 152.

0 →(A)(B)(C)(D)(E)(F)(G)(H) |1 → (AB)(C)(DE)(F)(G)(H) | 2 →(ABC)(DE)(F)(GH) |3 → (ABC)(DEF)(GH)
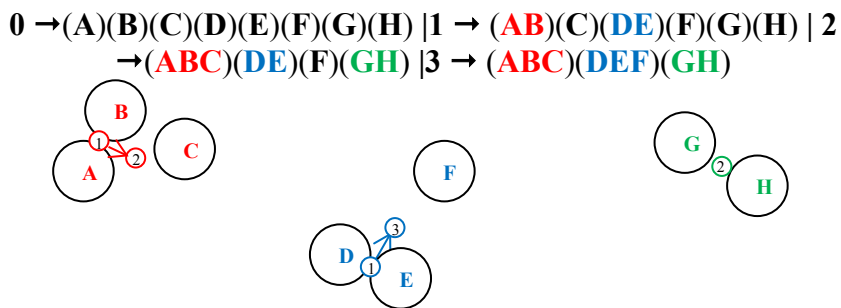
Figure 152: Hierarchical Clustering using the Distance from the Clusters Centroids

The circled numbers (①) in Figure 152 represent the change of centre (centroid) of the cluster. These points are adaptively learnt; as a cluster increases in size its new centroid is calculated which then acts as the ground point for calculating distance between a cluster and a potentially associated point.

Fuzzy logic can also be used to allocate a fractal weighting to each point which indicates the points association to each cluster. The fractal weighting of each point can be visually represented as a pie chart in which each slice segment of the pie represents a cluster and the size of the slice is the probability of the point belonging to a cluster as shown in Figure 153 below.
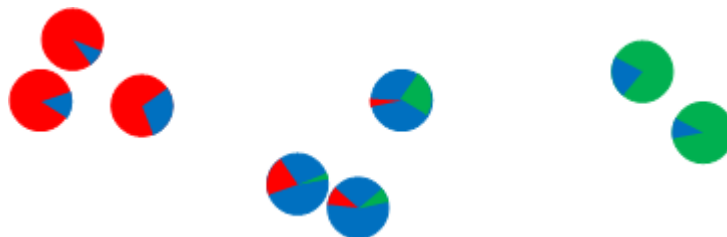
Figure 153: Fractal Weighting (Membership) between Surrounding Clusters

Density Estimators

Density estimators attempt to describe an unknown probability density function using observed sample data to represent the larger population (extrapolate). Many different density estimation methods can be used, a commonly used one is described below.

Kernel Density

Kernel density estimators (also known as Parzen window method) operate by placing a density function at each data point within the dataset before calculating the sum of the density function across the range of the data.

This is a similar process to the convolution kernels mentioned previously in a section on image enhancement. The sample of the variable $(x_1, x_2, x_3 \dots x_n)$ must be (or assumed to be) independently and identically distributed (iid).

$$\hat{f}_h(x) = \frac{1}{nh} \sum_{i=1}^{n} K\left(\frac{x - x_i}{h}\right)$$

$$K = kernal$$
$$h = bandwidth \ (smoothing \ parameter)$$

An example of a kernels density estimator is the *Gaussian kernel* with mean zero and variance one.

$$K\left(\frac{x - x_i}{h}\right) = \frac{1}{\sqrt{2\pi}} e^{-\frac{(x - x_i)^2}{2h^2}}$$

Distance measures

As mentioned previously a distance measure is generally used to group data points into clusters which are in close proximity or alternatively separate points which are dissimilar. Here you will find details on some of these distances.

Minkowski Distance

The Minkowski Distance generalises to either Euclidian metric, Manhattan metric or the Chebysev metric depending on the input value of P where $\boldsymbol{p} = (p_1, p_2, \dots p_n), \boldsymbol{q} = (q_1, q_2, \dots q_n) \in \mathbb{R}$
Manhattan distance when $(P = 1)$ or Euclidian distance when $(P = 2)$ in the following equation

$$\left(\sum_{i=1}^{n} |p_i - q_i|^P\right)^{1/P}$$

Or the Chebysev Distance when $(P = \infty)$ in the following equation

$$\lim_{P \to \infty} \left(\sum_{i=1}^{P} |p_i - q_i|^P\right)^{1/P} = \max_{i}^{n} |p_i - q_i|$$

These three types of metric distances are shown below in Table 62 along with their contrasting values for *a* and *b* given three identically positioned points in space.
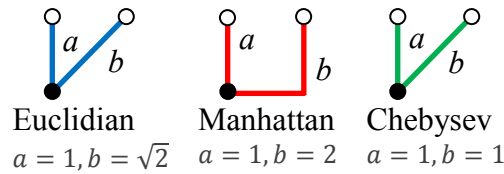
Table 62: Metric Distances and their Values for Three Identically Positioned Points in Space

Non metric, string or tree structures can also be used to separate data in what is known as syntactic clustering. An example of this type of string is the hamming distance.

Hamming Distance

Refers to the minimum number of changes required converting one representation into another or the number of errors that occurred during the conversion, some binary examples are;

1110110101 and 1111111111 → hamming distance is 3
000 and 111 → hamming distance is 3
These binary strings can be represented by a Hypercube as illustrated in Figure 154.
An alternate way of describing the hamming distance is A XOR B where A and B must be equal in length.
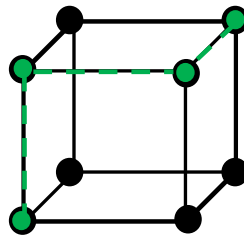
Figure 154: Hyper cube

Other distance measures include the *bhattacharyya distance* which can be used to measure the correspondence between two different population distributions (Bhattacharyya, 1943). The *Hausdorff distance* which is used to determine the minimum distance between two sets of points. The Hausdorff distance has been used in image processing to match templates of objects to objects in images such as the human face (Vivek and Sudha, 2006). The *Mahalanobis distance* which can be used to classify an unscaled covariance matrix of a feature vector (Roweis and Ghahramani, 1999).

Learning methods

Cost function

To learn a system there has to first be a set of original observations (data sample) and an input observation. A cost function is used to determine the difference between the current perception of the systems output based on the input observation and the actual optimum system output based on a known value from our original set of

observations. When a system is learning it has the aim to find the function which has the minimal cost; the function that has the results which are closest to the optimum solution. An example of a cost function is the square error cost function.

Expectation Maximisation

Expectation Maximisation (EM) is an extension of the maximum likelihood algorithm (Jain *et al.*, 1999). This learning method acts like a Chinese finger trap where the learned model is only allowed to progress in one direction towards maximum likelihood using two steps. First an expectation step (E-step) determines covariance matrix of the state vector with the parameters of the feature set then a maximisation step (M-step) uses the covariance matrix of the state vector to determine the parameters. The algorithm alternates between the E and M step in a manner that it is guaranteed not to decrease the likelihood (Roweis and Ghahramani, 1999).

Boosting

Boosting is a supervised learning process which combines several poorly correlated feature values into a single value that has enhanced correlation to the target output. During the boosting process relationships between the poorly correlated feature values are iteratively learnt and manipulated to convert the many poor classifiers into a more powerful one (Freund and Schapire, 1995).

Data collection methods

An animal like a human is a non-rigid deformable object, however, they do not have an infinite range of movement; there are limitations to the kinematics and shape of their model. The *a priori* data used to derive describe a behaviour feature can be collected using commercially available marker-based motion capture systems. A marker is a feature based object(s) (usually a high intensity colour) placed on the subject. The marker-based vision system is programmed to identify and track the marker object(s) and records the kinematic motion and position of the body to which the marker is attached.

Šustr (2001) uses a similar approach to determine the identity and behaviour of pigs. The two other methods used to determine the feature reference data are *active* and *passive* learning. Active learning uses physical sensors such as accelerometers attached to the body to determine the kinematics of the model and no vision system is required. Positional sensors can be used to detect the dimensions and distance between sensor nodes throughout the range of movement. However, having to place a marker or sensor on the subject is not always practical so as an alternative passive systems must be used. Passive learning systems build their own feature references such as the body's kinematic constraints and dimensions using a vision system without physically interfering with the subject; a look and learn approach (Kakadiaris and Metaxas, 1998; Kakadiaris and Metaxas, 1996).

APPENDIX C

Contour Extraction Procedure from Images Sample Records

So that further off-line shape analysis could be undertaken a greyscale sample image was recorded when a pig was in an adequate posture for a weight estimate to take place. The body contour recovered during the process was imbedded into the sample image as a green line (See Figure 155 (a)). As the grey values have identical values across all three colour channels of the image samples an image processing routine was created to recover the body contour by first identifying the pixels which were not the same across all the three colour channels. As the jpeg images were compressed some manipulation was necessary to extract the single pixel width boundary contour from the images as shown in Figure 155 (b→f).

(a) Original Image	(b) Subtracting
(c) Shrinking	(d) Thinning
(e) Removing Spurs	(f) Removing Isolated Pixels (cleaning)
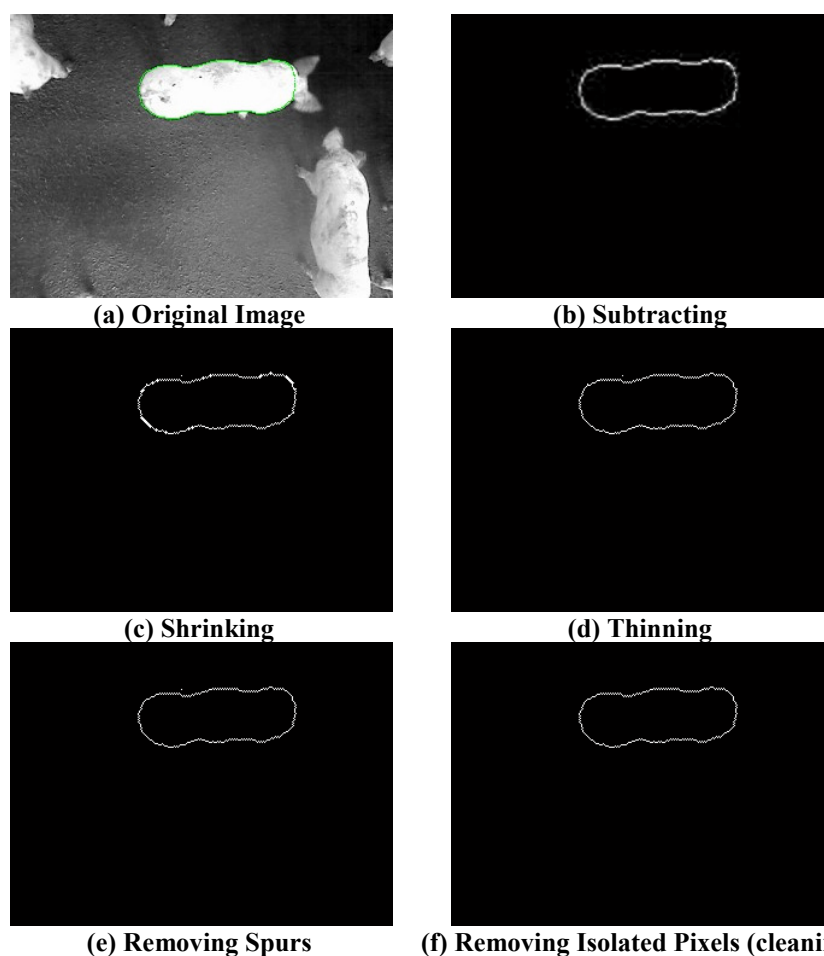
Figure 155: Process to Extract the Body Contour Out of the Recorded Sample Images
(a) Example of an Image Sample with the Recovered Body Contour Shape in Green; (b) After Subtracting the Blue and Red Channel from the Green Channel and Adding the Result; (ImageG-ImageB) + (ImageG-ImageR). (c) Shrinking the Image in b; (d) Thinning the Image in c; (e) Removing Spurs from the Image in (e) and then (f) Removing any Single Pixel Values using a Cleaning Operation on (e).

After this contour extraction process the X and Y coordinates of the contour was recovered. The mean X and Y coordinates were taken as the contour shapes geometric centre. The resulting contour and geometric centre or centroid can be seen in Figure 156 below.

Figure 156: The Recovered Body Contour and Geometric Centre of the Pig in Red

From the centroid of the contour the X and Y points which made up the contour were then converted into polar coordinates representing angle (vector THETAs) and magnitude (vector RHOs).

Table 63: Weight-Estimation Equations Built from a Stepwise Selection of Parameters

Model 1			Model 2			Model 3			Model 4			Model 5		
Term	Self Selected	Self Selected Ave	Term	Stepwise	Stepwise Ave	Term	Stepwise Angles Ave	Stepwise Angles	Term	Stepwise (120)	Stepwise (120) Ave	Term	Stepwise (378) Angles	Stepwise (378) Angles Ave
c	13.02300784	19.54728506	c	17.02231831	21.89984025	c	-3.681234002	2.51085847	c	-124.7189315	-4.13305975	c	-114.3830095	5.527334731
'AT2'	0.000314618	0.000359672	'MWFa'	-0.011664187	0	'MWFa'	0	0	'MWFa'	0.195851247	0	'MWFa'	0.110429482	0
'MR'	-0.470447623	-1.161151277	'MWMida'	-0.049677938	0	'MWMida'	-0.014212979	-0.04552995	'MWMida'	0.473291094	0	'MWMida'	0.216748878	0
'ML'	0.171989464	0.498728982	'MWRa'	0	0	'MWRa'	-0.02671342	0	'MWRa'	0.065516021	0	'MWRa'	0.227245095	0
'ARc'	-0.000115385	-0.000178912	'AFc'	0.000317881	0	'AFc'	0.000388051	0	'AFc'	0.00123338	0	'AFc'	-0.000203596	0
'WRc'	-0.025439999	-0.039668816	'AMidc'	0.00035283	0	'AMidc'	8.78E-05	0	'AMidc'	-0.002263435	0	'AMidc'	-0.001991822	0
'RL'	0.069684159	0.097546169	'ARc'	0.000162723	0	'ARc'	9.50E-05	-0.000267164	'ARc'	0.00012338	0	'ARc'	0.001188772	0
			'AT2'	0	0.000314962	'AT2'	0	0.00027436	'AT2'	0	0	'AT2'	0	0
			'WFc'	0.008609517	-0.054224123	'WFc'	0	-0.054253502	'WFc'	-0.411769343	0	'WFc'	0	0
			'WRc'	0	0	'WRc'	-0.028288635	0	'WRc'	0	0	'WRc'	0	0
			'ML'	0.16957172	-0.05241333	'ML'	0.116944075	0.511090752	'ML'	0	0	'ML'	0	0
			'FL'	0	0	'FL'	0	0	'FL'	0.127335058	0	'FL'	0.091173515	0
			'MidL'	0	0	'MidL'	0	0	'MidL'	0.529623662	0	'MidL'	0.512202926	0
			'RL'	0.10711414	0	'RL'	0.055273659	0.158669239	'RL'	0	0	'RL'	0	0
			'mWFa'	0.012874492	0	'mWFa'	0.010957196	0.067379717	'mWFa'	0.130060025	0	'mWFa'	0	0
			'mWRa'	0	0	'mWRa'	0	0	'mWRa'	0.137923658	0	'mWRa'	0	0
			'MR'	-0.486680048	0	'AMWFa'	-0.231675364	-1.11705016	'MR'	0	0	'AMWFa'	0	0
						'AMWMida'	0	0	'MWFa_MWMida'	0	0.00017574	'AMWMida'	0.031944098	0
						'AMWRa'	6.09E-05	0	'MWFa_MWRa'	0	0	'AMWRa'	0	0
						'AWRc'	0	0	'MWFa_AFc'	7.99E-07	0	'AWRc'	0	0
						'A_ML'	0	0	'MWFa_AMidc'	1.60E-06	0.00E+00	'A_ML'	0	0
						'AFL'	0	0	'MWFa_ARc'	0	0.00E+00	'AFL'	0	0
						'AMidL'	0	0	'MWFa_AT2'	-2.21E-07	0	'AMidL'	0	0
						'ARL'	0.000119322	0	'MWFa_WFc'	-0.000538829	0.00E+00	'ARL'	0	0
						'AmWFa'	0	0	'MWFa_WRc'	0	0	'AmWFa'	0	0
						'AmWRa'	-0.000235076	0	'MWFa_ML'	0	-0.000103753	'MR'	0	-0.052023202
						'MR'	-5.86E-05	-0.000126492	'MWFa_FL'	-0.000174998	0	'MWFa_MWMida'	0	0
									'MWFa_MidL'	-0.000496233	0	'MWFa_MWRa'	0	0
									'MWFa_mWFa'	0	0.000234574	'MWFa_AFc'	0	0
									'MWFa_mWRa'	0	0	'MWFa_AMidc'	1.02E-06	0
									'MWFa_AMWFa'	0	0	'MWFa_ARc'	0	0
									'MWMida_MWRa'	-0.001132435	0	'MWFa_AT2'	0	0
									'MWMida_AFc'	0	0	'MWFa_WFc'	-0.00035295	0
									'MWMida_AMidc'	0	0	'MWFa_WRc'	0	0
									'MWMida_ARc'	-5.65E-06	0	'MWFa_ML'	0	0
									'MWMida_AT2'	2.57E-06	0.00E+00	'MWFa_FL'	0	0
									'MWMida_WRc'	0	0.00E+00	'MWFa_MidL'	-0.000368456	0
									'MWMida_ML'	-0.000784813	0	'MWFa_RL'	0	8.04E-05
									'MWMida_FL'	0	0	'MWFa_mWFa'	0	0
									'MWMida_MidL'	0	0	'MWFa_mWRa'	0	0
									'MWMida_RL'	0.001473441	0	'MWFa_AMWMida'	0	0
									'MWMida_mWFa'	0	0	'MWFa_AMWRa'	-5.75E-05	0
									'MWMida_mWRa'	0	0	'MWFa_AWFc'	9.48E-05	-0.000361706
									'MWMida_AMWFa'	0	0	'MWFa_AWRc'	0	0
									'MWRa_AFc'	0	0	'MWFa_A_ML'	0	0
									'MWRa_AMidc'	9.00E-07	0	'MWFa_AMidL'	0	0
									'MWRa_ARc'	0	0.00E+00	'MWFa_ARL'	0	0
									'MWRa_AT2'	0	0	'MWFa_AmWFa'	0	0
									'MWRa_WFc'	0	0	'MWFa_AmWRa'	0	0
									'MWRa_WRc'	-0.000588855	0	'MWFa_MR'	0	-0.001298116
									'MWRa_ML'	0	0	'MWMida_MWRa'	0	0
									'MWRa_FL'	-0.000263473	0	'MWMida_AMidc'	7.14E-07	0
									'MWRa_MidL'	-0.000360402	0	'MWMida_ARc'	0	0
									'MWRa_RL'	0	0	'MWMida_AT2'	0	0
									'MWRa_mWFa'	0.001202679	0	'MWMida_WFc'	0.001200307	0
									'MWRa_mWRa'	0.00073192	0	'MWMida_WRc'	0	0
									'MWRa_AMWFa'	0	0	'MWMida_ML'	0	0
									'AFc_ARc'	9.38E-10	0	'MWMida_FL'	0	0
									'AFc_AT2'	0	0.00E+00	'MWMida_MidL'	0	0
									'AFc_WFc'	-4.61E-07	0	'MWMida_RL'	0	-0.000603253
									'AFc_WRc'	0	0.00E+00	'MWMida_mWFa'	0	0
									'AFc_ML'	0	0	'MWMida_mWRa'	0	0
									'AFc_FL'	1.72E-06	0.00E+00	'MWMida_AMWFa'	0	0
									'AFc_MidL'	0	0	'MWMida_AMWMida'	-0.000193881	0
									'AFc_RL'	0	0	'MWMida_AMWRa'	0	0
									'AFc_mWFa'	0	0	'MWMida_AWFc'	-9.50E-05	0
									'AFc_AMWFa'	-3.09E-06	0.00E+00	'MWMida_AWRc'	0	0
									'AMidc_ARc'	0	0	'MWMida_A_ML'	0	0
									'AMidc_AT2'	-2.57E-09	0	'MWMida_AFL'	0	0
									'AMidc_WFc'	-2.87E-06	0.00E+00	'MWMida_AMidL'	0	0
									'AMidc_WRc'	0	0.00E+00	'MWMida_AmWFa'	0	0
									'AMidc_ML'	2.01E-06	0	'MWMida_AmWRa'	5.91E-05	0
									'AMidc_FL'	0	-8.63E-07	'MWMida_MR'	0	0
									'AMidc_MidL'	0	0	'MWRa_AFc'	0	0
									'AMidc_RL'	1.47E-06	0	'MWRa_AMidc'	1.24E-06	0
									'AMidc_mWFa'	0	0.00E+00	'MWRa_ARc'	3.45E-07	0
									'AMidc_mWRa'	0	0	'MWRa_AT2'	0	0
									'AMidc_AMWFa'	0	0	'MWRa_WFc'	0.000772091	0
									'ARc_AT2'	6.04E-10	0	'MWRa_WRc'	0	0
									'ARc_WFc'	0	-3.21E-06	'MWRa_ML'	0.000666996	0
									'ARc_WRc'	-3.11E-06	1.94E-06	'MWRa_FL'	0	0
									'ARc_ML'	0	0.00E+00	'MWRa_RL'	0.000419501	0
									'ARc_FL'	0	0	'MWRa_mWFa'	0.000340222	0
									'ARc_MidL'	-1.39E-06	0	'MWRa_mWRa'	0	0
									'ARc_RL'	0	0.00E+00	'MWRa_AMWFa'	0	0
									'ARc_mWFa'	2.51E-06	0	'MWRa_AMWMida'	0	0
									'ARc_mWRa'	3.41E-06	0.00E+00	'MWRa_AWFc'	0	0
									'ARc_AMWFa'	0	0.00E+00	'MWRa_AWRc'	0	0
									'AT2_WFc'	1.36E-06	0	'MWRa_A_ML'	0	0
									'AT2_WRc'	0	0	'MWRa_AFL'	0	0
									'AT2_ML'	2.96E-07	1.73E-07	'MWRa_AMidL'	0	0
									'AT2_FL'	-1.44E-06	0.00E+00	'MWRa_ARL'	0	0
									'AT2_MidL'	0	0.00E+00	'MWRa_AmWFa'	0	0
									'AT2_RL'	-5.94E-07	0	'MWRa_mWRa'	0	0
									'AT2_mWFa'	-4.81E-07	3.44E-07	'MWRa_MR'	-0.002234351	0
									'AT2_mWRa'	0	0.00E+00	'AFc_AMidc'	0	0
									'AT2_AMWFa'	0	0	'AFc_ARc'	1.24E-06	0
									'WFc_WRc'	-0.000572216	0	'AFc_AT2'	0	0
									'WFc_ML'	0	0	'AFc_WFc'	0	0
									'WFc_FL'	0	0	'AFc_WRc'	0	0
									'WFc_MidL'	0.00091 4369	0	'AFc_ML'	0	0
									'WFc_RL'	0	0	'AFc_FL'	0	0
									'WFc_mWFa'	0.001294128	0	'AFc_MidL'	1.59E-06	0
									'WFc_mWRa'	0.001430156	0	'AFc_RL'	-8.54E-07	0
									'WFc_AMWFa'	0	0.000698496	'AFc_mWFa'	1.75E-06	0
									'WRc_ML'	0	0.001059569	'AFc_mWRa'	0	0
									'WRc_FL'	0	0	'AFc_AMWFa'	0	0
									'WRc_MidL'	0	0	'AFc_AMWMida'	2.78E-07	0
									'WRc_RL'	0.000822802	0	'AFc_AMWRa'	0	0
									'WRc_mWFa'	0	0	'AFc_AWRc'	0	0
									'WRc_mWRa'	0	0	'AFc_A_ML'	0	0
									'WRc_AMWFa'	0	-0.002427514	'AFc_AFL'	0	0
									'ML_FL'	0	0	'AFc_ARL'	0	1.10E-06
									'ML_MidL'	0	0	'AFc_AmWFa'	0	0
									'ML_RL'	0	0	'AFc_AmWRc'	0	0
									'ML_mWFa'	0	0	'AFc_MR'	9.21E-07	0
									'ML_AMWFa'	0	0	'AMidc_ARc'	0	0
									'FL_MidL'	0.000382015	0	'AMidc_AT2'	-2.24E-09	0
									'FL_RL'	0.000473021	0	'AMidc_WRc'	-9.25E-07	0
									'FL_mWFa'	0.000865418	0	'AMidc_WRc'	1.45E-06	0
									'FL_AMWFa'	-0.000359676	0	'AMidc_ML'	0	0
									'MidL_RL'	0	0	'AMidc_FL'	-2.66E-06	0
									'MidL_mWFa'	0	0	'AMidc_MidL'	0	0
									'MidL_mWRa'	0	0	'AMidc_RL'	0	0
									'MidL_AMWFa'	-0.000674005	0	'AMidc_mWFa'	0	0
									'RL_mWFa'	-0.001139455	0	'AMidc_mWRa'	0	0
									'RL_mWRa'	-0.001440112	0	'AMidc_AMWFa'	0	0
									'RL_AMWFa'	0	0	'AMidc_AMWMida'	0	0
									'mWFa_AMWFa'	-0.002174795	0	'AMidc_AMWRa'	1.81E-07	0
									'mWFa_AMWFa'	0	-0.00021062	'AMidc_AWFc'	-4.65E-08	0
									'mWRa_AMWFa'	0	0	'AMidc_AWRc'	0	0
												'AMidc_A_ML'	0	0
												'AMidc_AFL'	0	0
												'AMidc_AMidL'	0	-1.69E-05
												'AMidc_ARL'	0	0
												'AMidc_AmWFa'	-1.47E-07	0
												'AMidc_AmWRa'	0	0
												'AMidc_MR'	6.18E-06	0
												'ARc_AT2'	5.31E-10	0
												'ARc_WFc'	0	0
												'ARc_WRc'	0	0
												'ARc_ML'	0	0
												'ARc_FL'	-1.23E-06	0
												'ARc_MidL'	0	0
												'ARc_RL'	0	-4.05E-07
												'ARc_mWFa'	0	0
												'ARc_mWRa'	0	0
												'ARc_AMWFa'	0	0
												'ARc_AMWMida'	0	0
												'ARc_AWFc'	0	0
												'ARc_AWRc'	0	0
												'ARc_A_ML'	0	0
												'ARc_AFL'	0	0
												'ARc_AMidL'	-6.78E-06	0
												'ARc_AmWFa'	0	0
												'ARc_AmWRa'	0	0
												'ARc_MR'	0	0
												'AT2_WFc'	0	0
												'AT2_WRc'	-1.76E-07	0
												'AT2_ML'	0	0
												'AT2_FL'	0	0
												'AT2_MidL'	-1.07E-06	0
												'AT2_mWFa'	-4.15E-07	1.86E-07
												'AT2_mWRa'	0	0
												'AT2_AMWFa'	0	0
												'AT2_AMWMida'	0	0
												'AT2_AWFc'	0	0
												'AT2_AWRc'	0	0
												'AT2_A_ML'	0	0
												'AT2_AFL'	0	0
												'AT2_AMidL'	1.99E-06	0

Label	Value 1	Value 2
'AT2_ARL'	0	0
'AT2_AmWFa'	0	0
'AT2_AmWRa'	0	0
'AT2_MR'	0	0
'WFc_WRc'	-0.001192223	0
'WFc_FL'	0	0
'WFc_ML'	-0.000187407	0
'WFc_MidL'	0	0
'WFc_RL'	0	0
'WFc_mWFa'	0	0
'WFc_mWRa'	0	0
'WFc_AMWFa'	0	0
'WFc_AMWMida'	-0.000116601	0
'WFc_AMWRa'	0	0
'WFc_AWFc'	0	0.000415924
'WFc_AWRc'	0	0
'WFc_A_ML'	0	0
'WFc_AFL'	0	0
'WFc_AMidL'	0	0
'WFc_ARL'	0	0
'WFc_AmWFa'	0	0
'WFc_AmWRa'	0	0
'WFc_MR'	0	0
'WRc_ML'	0	8.15E-05
'WRc_FL'	0.000787534	0
'WRc_MidL'	0	0
'WRc_RL'	0	0
'WRc_mWFa'	0	0
'WRc_mWRa'	0	0
'WRc_AMWFa'	0	0
'WRc_AMWMida'	0.000215512	0
'WRc_AMWRa'	0	0
'WRc_AWFc'	0	0
'WRc_AWRc'	0	0
'WRc_AFL'	0	0
'WRc_AMidL'	0	0
'WRc_ARL'	0	0
'WRc_AmWFa'	0	0
'WRc_AmWRa'	0	0
'WRc_MR'	0	0
'ML_FL'	0	0
'ML_MidL'	0	0
'ML_RL'	0	0.00010015
'ML_mWFa'	0	0
'ML_mWRa'	0	0
'ML_AMWFa'	0	0
'ML_AMWMida'	-5.87E-05	0
'ML_AMWRa'	0	0
'ML_AWFc'	0	0
'ML_AWRc'	0	0
'ML_A_ML'	0	0
'ML_AFL'	0	0
'ML_AMidL'	0	0
'ML_ARL'	0	0
'ML_AmWFa'	0	0
'ML_AmWRa'	0	0
'ML_MR'	-0.000306809	0
'FL_MidL'	0.000358512	0
'FL_RL'	0.000741997	0
'FL_mWFa'	-0.000474848	0
'FL_mWRa'	0	0
'FL_AMWFa'	0	0
'FL_AMWMida'	0	0
'FL_AMWRa'	4.51E-05	0
'FL_AWFc'	0	0
'FL_AWRc'	0	0
'FL_A_ML'	0	0
'FL_AFL'	0	0
'FL_ARL'	0	0
'FL_AMidL'	0	0
'FL_AmWFa'	0	0
'FL_AmWRa'	0	0
'FL_MR'	0	0
'MidL_RL'	0	0
'MidL_mWFa'	0	0
'MidL_mWRa'	0	0
'MidL_AMWFa'	0	-3.53E-05
'MidL_AMWMida'	0.000103016	0
'MidL_AMWRa'	0	0
'MidL_AWFc'	0	0
'MidL_AWRc'	0	0
'MidL_A_ML'	0	0
'MidL_AFL'	0	0
'MidL_ARL'	0	0
'MidL_AMidL'	0	0
'MidL_AmWFa'	0	0
'MidL_AmWRa'	0	0
'MidL_MR'	-0.000309587	0
'RL_mWFa'	0	0
'RL_mWRa'	0	0
'RL_AMWFa'	0	0
'RL_AMWMida'	0	0
'RL_AMWRa'	0	0
'RL_AWFc'	0	0
'RL_AWRc'	0	0
'RL_A_ML'	0	0
'RL_AFL'	0	0
'RL_AMidL'	0	0
'RL_ARL'	0	0
'RL_AmWFa'	0	0
'RL_AmWRa'	0	0
'RL_MR'	0	0
'mWFa_mWRa'	0	0
'mWFa_AMWFa'	0	0
'mWFa_AMWMida'	0	0
'mWFa_AMWRa'	-5.77E-05	0
'mWFa_AWFc'	0	0
'mWFa_AWRc'	0	0
'mWFa_A_ML'	0	0
'mWFa_AFL'	0	0
'mWFa_AMidL'	0	0.006686792
'mWFa_ARL'	0	0
'mWFa_AmWFa'	0	0
'mWFa_AmWRa'	0	0
'mWFa_MR'	0	0
'mWRa_AMWFa'	0	0
'mWRa_AMWMida'	0	0
'mWRa_AMWRa'	0	0
'mWRa_AWFc'	0	0
'mWRa_AWRc'	0	0
'mWRa_A_ML'	0	0
'mWRa_AFL'	0	0
'mWRa_AMidL'	0	0
'mWRa_ARL'	0	0
'mWRa_AmWFa'	0	0
'mWRa_AmWRa'	0	0
'mWRa_MR'	0	0
'AMWFa_AMWMida'	0	0
'AMWFa_AMWRa'	0	0
'AMWFa_AWFc'	0	0
'AMWFa_AWRc'	0	0
'AMWFa_A_ML'	0	0
'AMWFa_AFL'	0	0
'AMWFa_AMidL'	0	0
'AMWFa_ARL'	0	0
'AMWFa_AmWFa'	0	0.000116459
'AMWFa_AmWRa'	0	0
'AMWFa_MR'	0	0
'AMWMida_AMWRa'	0	0
'AMWMida_AWFc'	0	0
'AMWMida_AWRc'	-3.51E-05	-0.000255403
'AMWMida_A_ML'	0	0
'AMWMida_AFL'	0	0
'AMWMida_AMidL'	-0.000763882	0
'AMWMida_ARL'	0	0
'AMWMida_AmWFa'	0	0
'AMWMida_AmWRa'	0	0
'AMWMida_MR'	0	0
'AMWRa_AWFc'	0	0
'AMWRa_AWRc'	0	0
'AMWRa_A_ML'	0	0
'AMWRa_AFL'	0	0
'AMWRa_AMidL'	0.006684201	0
'AMWRa_ARL'	0	0
'AMWRa_AmWFa'	0	0
'AMWRa_AmWRa'	0	0
'AMWRa_MR'	0	0
'AWFc_AWRc'	-2.73E-05	0
'AWFc_A_ML'	0	0
'AWFc_AFL'	0	0
'AWFc_AMidL'	0	0
'AWFc_ARL'	-0.000335758	-0.009977449
'AWFc_AmWFa'	0	0
'AWFc_AmWRa'	0	0
'AWFc_MR'	0	0
'AWRc_A_ML'	0.00236078	0.0070035116
'AWRc_AFL'	-0.00032855	0
'AWRc_AMidL'	-0.002276591	-0.008692122
'AWRc_ARL'	-0.000418847	0
'AWRc_AmWFa'	0	0
'AWRc_AmWRa'	0	0
'AWRc_MR'	0	0
'A_ML_AFL'	0	0
'A_ML_AMidL'	0	0
'A_ML_ARL'	0.014155638	0
'A_ML_AmWFa'	0	0
'A_ML_AmWRa'	0	0
'A_ML_MR'	0	0
'AFL_AMidL'	0	0
'AFL_ARL'	0	0
'AFL_AmWFa'	0	0
'AFL_AmWRa'	0	0
'AFL_MR'	0	0
'AMidL_ARL'	-0.023789653	0
'AMidL_AmWFa'	0	0
'AMidL_AmWRa'	0	0
'AMidL_MR'	0	0
'ARL_AmWFa'	0	0
'ARL_AmWRa'	0	0
'ARL_MR'	0	0
'AmWFa_AmWRa'	0	0
'AmWFa_MR'	0	0
'AmWRa_MR'	0	0

*MR = MLRho

APPENDIX E

An important model closely related to this study is the standard growth curve for pigs bred for their meat. The growth of pigs relative to their age and weight is shown in Table 64 and Figure 157.

Table 64: Standard Growth of Pigs Produced for their Meat Obtained from Carr (1998)

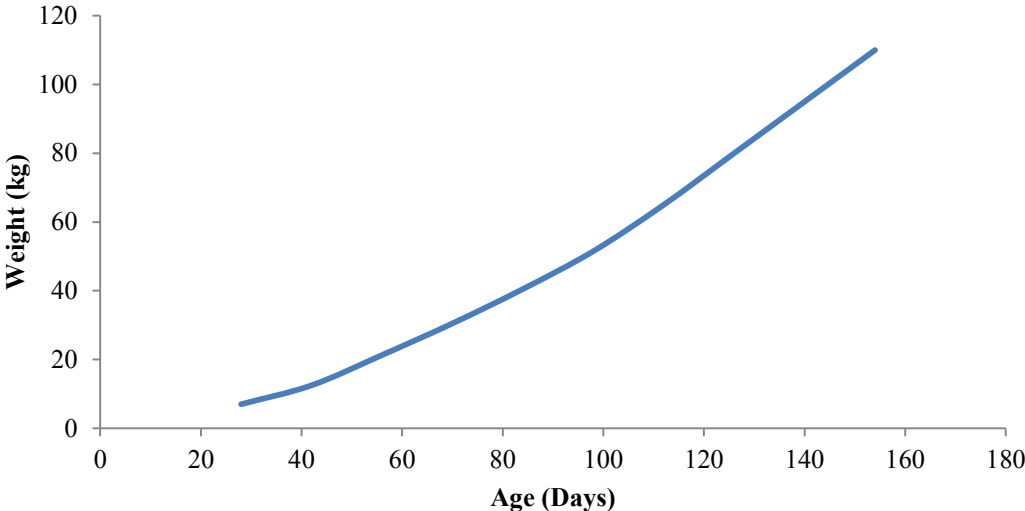| Age Weeks	Day	Weight (kg)
4	28	7
6	42	12.5
8	56	21.3
10	70	30.5
12	84	40.5
14	98	51.5
16	112	65
18	126	80
20	140	95
22	154	110

Figure 157: Standard Growth Curve for Pigs Bred for their Meat According to Carr (1998)

This curve can be approximated by the following power equation;

$$Weight = 0.0293Age^{1.6337}$$ **Equation 4: Standard Growth Curve Equation**

This standard growth curve can be used as a reference over the grower-finisher growth phases, between 30 and 120 kg live weight (LW). A grower pig generally weighs between 30 and 60 kg and a finisher pig generally weighs between 60 and 120 kg. Different diets are usually supplemented in these different stages of growth.

APPENDIX F

In order to manipulate the base image to enhance segmentation or improve the visual appearance many different convolution filters can be used. A convolution filter can be visualised as a mask which when applied to an original image **F** will transform the image into a new image **G.** Where **G** is an image that has greater chance of identifying any targeted feature compared to the image **F**. Depending on the application these filters can be used to smooth, sharpen, blur or determine the edge within the filter area. Although only examples of filters with of dimensions 3x3 are shown in Table 65 below a filter structure can take on any shape or size such as a circle, diamond, square or any polygon for that matter. Changing the filter structural element to one other than a square or rectangle gives rise to the additional challenge of keeping the filter within the image dimensions and covering all pixels within the image without biasing or excluding some pixels from the manipulation. Some common filters with their coefficients are listed below along with their function. The coefficients are either applied directly to the intensity values or the intensity values within the filter are used in combination to perform the manipulation.

Table 65: Various Convolution Filters

Filter Type	Combination	Function	Example
Gradient	$\begin{array}{ccc} a & -b & c \\ b & x & -d \\ c & d & -a \end{array}$	Direction specific edge detection ($x = 0$) and Texture enhancement ($x = 1$) The larger the filter size the thicker the edges	$\begin{array}{ccc} 0 & 1 & 1 \\ -1 & 0 & 1 \\ -1 & -1 & 0 \end{array}$
Laplacian	$\begin{array}{ccc} a & -b & c \\ b & x & -d \\ c & d & -a \end{array}$	Omni directional edge detection if $x = 2(|a| + |b| + |c| + |d|)$ and Texture enhancement if $x > 2(|a| + |b| + |c| + |d|)$ The larger the filter size the thicker the edges	$\begin{array}{ccc} -1 & -1 & -1 \\ -1 & 8 & -1 \\ -1 & -1 & -1 \end{array}$
Smoothing	$\begin{array}{ccc} a & b & c \\ b & x & d \\ c & d & a \end{array}$ $a, b, c, d \geq 0$	Blur and Remove detail The larger the filter size the greater the smoothing Strong blur ($x = 0$) Weak blur ($x = 1$)	$\begin{array}{ccc} 0 & 1 & 0 \\ 1 & 0 & 1 \\ 0 & 1 & 0 \end{array}$
Gaussian	$\begin{array}{ccc} a & b & c \\ b & x & d \\ c & d & a \end{array}$ $x > 1$	Values a, b, c, d are integer approximations of the Gaussian curve	$\begin{array}{ccc} 1 & 2 & 1 \\ 2 & 4 & 2 \\ 1 & 2 & 1 \end{array}$

Median	<table><tr><td>a</td><td>b</td><td>c</td></tr><tr><td>d</td><td>x</td><td>e</td></tr><tr><td>f</td><td>g</td><td>h</td></tr></table>	Noise removal without blurring edges reduces detail $$x = median(a,b,c,d,e,f,g,h)$$
Sigma	<table><tr><td>a</td><td>b</td><td>c</td></tr><tr><td>d</td><td>x</td><td>e</td></tr><tr><td>f</td><td>g</td><td>h</td></tr></table>	Highlights edges based on determining if the pixel at location x is significant or insignificant in respect to its neighbourhood $y = [a,b,c,d,e,f,g,h]$ (neighbourhood) $x = mean(y)$ if $x < mean(y) - k \times std(y)$ or $$x > mean(y) + k \times std(y)$$ Where k is a threshold value for the acceptable deviation range from the mean
Mean	<table><tr><td>a</td><td>b</td><td>c</td></tr><tr><td>d</td><td>x</td><td>e</td></tr><tr><td>f</td><td>g</td><td>h</td></tr></table>	Blurs edges and reduces detail $$x = mean(a,b,c,d,e,f,g,h)$$

One commonly used spatial technique is to apply a median filter to the image region which is effective at minimising image noise. Other local neighbourhood processing techniques include edge detection which highlights the large steps between different levels of light intensity. An example is in (McFarlane and Schofield, 1995) who devise a segmentation algorithm that uses a differencing between a median background and an edge detection method using a laplacian filter before identifying the object based on shape.